Effect of an engineer species on the diversity and functioning of benthic communities : the Sabellaria Alveolata reef habitat

Auriane Jones

UNIVERSITE BRETAGNE LOIRE / SCIENCES DE LA MER ET DU LITTORAL

Thèse préparée à l'Université de Bretagne Occidentale

pour obtenir le diplôme de DOCTEUR délivré de façon partagée par
L'Université de Bretagne Occidentale et l'Université de Bretagne Loire

Spécialité: Ecologie marine

École Doctorale Sciences de la Mer et du Littoral

présentée par

Auriane Jones

Effect of an engineer species on the diversity and functioning of benthic communities: the *Sabellaria alveolata* reef habitat

Thèse soutenue le 14 décembre 2017
devant le jury composé de:

Erik BONSDORFF
Professor of marine biology, Åbo Akademi University / *Rapporteur*

Sébastien LEFEBVRE
Professeur des universités, Université de Lille 1 sciences et technologies / *Rapporteur*

Ruth CALLAWAY
Senior lecturer, Swansea University / *Examinatrice*

Fred JEAN
Professeur des universités, Université de Bretagne Occidentale / *Examinateur*

Pierre-Guy SAURIAU
Chercheur CNRS, CR1-HDR, UMR LIENSs, La Rochelle / *Examinateur*

Stanislas DUBOIS
Chercheur Ifremer, Cadre de recherche HDR, Centre Bretagne / *Directeur de thèse*

Jérôme FOURNIER
Chercheur CNRS, CR1-HDR, UMR BOREA, Staion de Biologie Marine de Concarneau / *Directeur de thèse*

Nicolas DESROY
Chercheur Ifremer, Cadre de recherche HDR, LERBN / *Encadrant scientifique, membre invité*

UBO Université de Bretagne Occidentale

Ifremer

Le travail de préparation de cette thèse de doctorat a été financé par l'Ifremer et la Région Bretagne et soutenu par le projet français LabexMer (ANR-10-LABX-19-01) et le programme du gouvernement français « Investissements d'Avenir ». Ce travail de thèse a également bénéficié d'une bourse EC2CO DRIL (CNRS).

The work for the preparation of this PhD thesis was funded by Ifremer and the Region of Brittany along with the French project LabexMer (ANR-10-LABX-19-01) and by the French government under the program "Investissements d'Avenir". This PhD work was also funded by an EC2CO DRIL (CNRS) grant.

Remerciements

Et voilà, trois ans (et un gros mois) de recherches sur un petit ver marin dont peu de personnes ont entendu parlé s'achève et je dois dire que cette petite fin d'un monde rempli d'hermelles me rend sentimentale. Au départ, je viens d'un monde peuplé de requins et accessoirement d'un peu de blé, de maïs, de vaches et de cochons, mais mon cœur a toujours été dans la mer. Et voilà que je me retrouve dans ce monde qu'est l'estran, ni vraiment mer ni vraiment terre, vers lequel les gens partent en tracteurs !!! comme quoi le monde agricole n'est jamais bien loin ! En cette fin de l'an 2017 de l'hermelle (très important signe astrologique chinois, il faut le savoir), je pense pouvoir dire que cette thèse a été un catalyseur de relations humaines et de découverte des autres. Et je vais tenter, sans trop m'étendre (mais à ce niveau je ne peux vous apporter aucune garantie de brièveté, car certains diront que j'aime bien parler, voire que je suis pipelette…) de remercier de manière exhaustive, toutes et je dis bien toutes (enfin je vais essayer) les personnes qui ont, de près ou de loin, contribuer à l'accomplissement de ma thèse !

Tout d'abord, je tiens à remercier les membres du jury qui ont accepté d'évaluer ma thèse :

- Pr Erik Bonsdorff, Abo Akademi
- Pr Sébastien Lefebvre, Université de Lilles
- Pr Fred Jean, Université de Bretagne Occidentale
- Dr Ruth Callaway, Swansea University
- Dr Pierre-Guy Sauriau, CNRS

Ensuite, je tiens à vivement remercier mes trois encadrants de thèse. Mon co-directeur de thèse Jérôme Fournier, qui a toujours su trouver les mots justes avec moi, pour m'aider à continuer et à toujours aller plus loin et plus haut. Je n'avais jusque-là jamais rencontré une personne avec autant de culture scientifique et humaine à la fois. Il m'a donné envie de repousser sans arrêt les limites de ma connaissance, tout en remettant en question mes idées préconçues et mes impressions. Je n'aurais pu espérer plus grand soutien tout au long de ma thèse. Malheureusement, les hermelles ne sont pas son seul sujet de prédilection et l'appel de l'Antarctique ne lui permettra pas d'être à ma soutenance, ce que je regrette énormément. En prévision de son absence, il a déjà pensé au pot d'après-thèse, ce qui nous permettra de trinquer à sa santé ! Je tiens à chaudement remercier THE Monsieur Hermelle et mon autre co-directeur de thèse, Stanislas Dubois, sans qui cette thèse n'aurait jamais vu le jour. Il a su me faire aimer dès le premier coup d'œil ce petit ver marin (même si j'ai bien cru mourir la première fois que je suis allée sur le récif de Sainte-Anne avec lui) et tout ce qu'il change autour de lui. Je pense que ce ver est un peu son bébé scientifique, et il a su me guider au début pour ensuite me laisser voler de mes propres ailes, et me forger ma propre opinion de chercheur. Je tiens également à le remercier énormément pour son soutien de A à Z dans la rédaction de ce manuscrit, et les corrections qu'il a faites

dessus à des heures impossibles ! Et voilà que j'arrive à Nicolas Desroy, mon encadrant scientifique. Je crois que Nico avait encore plus hâte que moi que cette thèse se termine pour pouvoir enfin m'appeler Docteur Jones en zozotant comme Demi-Lune ! Je me dois de souligner sa précieuse aide au cours de ma thèse notamment sur le terrain et au labo. Il faut savoir que la détermination de polychètes et moi, ça fait au moins 40 000, Thibault peut confirmer ma nullité absolue dans ce domaine. Nico a passé des heures (mêmes des semaines voire des mois) à déterminer des polychètes riquiquis et autres invertébrés étranges pour ma thèse. Sans lui et son bateau, la première campagne de ma thèse aurait été très compromise, et en plus il est venu sur le terrain en ayant la grippe !!

Je tiens également à remercier toutes les autres personnes qui m'ont aidée durant ma thèse et sans lesquelles je n'aurais jamais réussi à arriver jusqu'à ce manuscrit. Je pense tout d'abord aux très très nombreuses personnes qui se sont faites embarquer sur le terrain de manière plus ou moins volontaire. Comme la veille pour le lendemain, quand je réalisais que la marée n'était que de 85 et que je n'allais jamais réussir à faire tous mes prélèvements, alors un grand merci à Cécile, Lilou et Seb de la station de Dinard. Et Ludo, le compagnon de mes sorties mensuelles sur le terrain sans qui rien de tout ça n'aurait été possible ! Je dois avouer que les sacs à dos ne devaient pas peser tout à fait le même poids…Un grand merci à Claire Rollet, la big boss de la station Ifremer de Dinard, qui a toujours été là pour moi, sur le terrain, lors de mon déménagement, pour me dire de rentrer chez moi, merci Claire pour ta gentillesse ! Merci aussi à Julien (pour la table basse aussi), Julia (« Sur la plage abandonnée, coquillages et crustacés », pendant des heures et des heures de tri de sédiment !), René, Aurélie, Aurore, François, Françoise, Daniel (une pensée toute particulière pour Daniel qui m'a mise en contact avec des pêcheurs à pied de la Baie du Mont), bien sûr Patrick pour son aide au labo, sur le terrain, sa bonne humeur et pour avoir partagé plein d'histoires avec moi ! Merci également à Priscilla, membre de mon comité de thèse et précieuse aide sur le terrain, et à ses fidèles compagnons nantais, Laurent et Pierre de la guilde du NDVI ! Merci aussi à Anthony de la réserve de Saint-Brieuc pour son aide sur les terrains de février et septembre, et son efficacité combinée avec Nico ! Merci aussi à Pompon pour les nombreux allers-retours à dos de tracteur en Baie du Mont ! Merci à la team carottes benthiques et flux biogéochimiques : Lionel Denis et Gwendoline Duhong pour leur bonne humeur sur le terrain et leur soutien psychologique post-terrain aussi ! Merci aussi beaucoup à Julien Cucherousset, l'autre membre de mon comité de thèse, d'avoir toujours été présent pour m'épauler, répondre à mes questions, et vérifier que tout allait bien, tout ça même en étant loin. Anik merci beaucoup pour tes corrections de dernière minute, ton soutien et ta gentillesse.

Je remercie aussi chaudement toutes les personnes (uniquement au féminin) qui ont participé, par des stages ou des formations continues à la collecte et à l'analyse de données pour ma thèse ; les filles vont avez fait un boulot de malade: Ségolène Jambut, Flavie Delanzy (que j'ai encore embêté récemment au sujet de la production secondaire !), Louise Lanrivain, Anne Verdurmen (merci pour les moments supplémentaires passés à analyser les sucres !), Célia Bellengier (qui a peut-être ouvert un resto depuis la dernière fois), Angelica Navarro (pour toutes ses très nombreuses heures sup !), Sarah

Gouge et Nolwenn Lescop (merci pour les centaines de boulettes !). Un grand merci aussi à Delphine, ma copine dinardaise pour tous les bons moments passés au boulot, à la plage, une bière à la main…

Après la petite station de Dinard, j'ai débarqué dans le grand centre Bretagne et même s'il pouvait paraître impressionnant à première vue, toutes les personnes de Dyneco m'ont fait me sentir comme chez moi ! Vous êtes une belle bande de joyeux lurons, amoureux de la mer, et ça fait chaud au cœur ! Même si je ne faisais pas toujours les pauses café, quand c'était le cas vous rendiez toujours ce moment joyeux, convivial et ressourçant ! Alors un grand merci à Antoine (alias Carlito), Aline, Philippe, Claire, Jacques, Yohann, Cédric, Jean-Do, Xavier, Mickael et une pensée toute particulière pour Touria qui a toujours été là pour moi dans les moments durs, merci pour le super pack anti déprime, les petits gâteaux et les dattes ! Un grand merci aussi à Jacqueline pour ces gentilles paroles et son soutien sans faille dans les problèmes administratifs. Un immense merci à Martin aussi, nous avons eu beaucoup de discussions scientifiques très intéressantes et stimulantes, merci aussi pour son aide en stats et sur R, merci aussi pour le soutien psychologique de fin de thèse.

Maintenant place aux remerciements des BOYS comme dirait Thibault ! J'ai eu l'immense chance et le privilège de partager mon bureau brestois avec une bande de mecs fantastiques : un Grec mystérieux, Nikos (et nos discussions très sérieuses sur la vie et les livres !), un joyeux roux Thibault (et ses talents de décorateur d'intérieur et de cuisto !) et mon BRO Bastien (surtout pour les soirées bières, bières game of Thrones, bière volley… ! je nous fais passer pour des poches ;-) .et je sais qu'au fond tu aimes bien les Bourguignons ;-)) ! Les gars vous m'avez vraiment fait rêver, sans vous cette thèse n'aurait vraiment pas eu la même saveur ! La liste de choses pour lesquelles je pourrais vous remercier est super longue et je ne vais jamais réussir à l'écrire en entier, donc juste un ENORME MERCI POUR TOUT !! Pierre, tu n'as pas la chance d'appartenir au monde du benthos, toi ton truc se sont les organismes microscopiques de la colonne d'eau, mais tu es aussi un geek de la diversité fonctionnelle et je te remercie pour toute ton aide, en stats, sur R, sur des questions de diversité fonctionnelle, et pour les nombreuses discussions très sérieuses et intéressantes que nous avons eues (et aussi pour les soirées bières ☺) ! Carole, une grosse pensée pour toi et tes gentils textos de soutiens, merci pour les sorties, les apéros et les nouvelles rencontres ! Gabriel, merci encore pour Tulipe (la Tulipe de Bastien) c'est trop cool que tu sois passé, et merci pour ta gentillesse à la fin de ma thèse ! A special international thanks to the volley ball team !! Danke schon, Muchos gracias !! You guys helped me so much not to become crazy towards the end ! It was such a nice break to come play with you.

Et bien sûr j'ai presque failli les oublier les PICPUCIENS : ma magnifique bande de potes du lycée qui ont tous réclamé mon premier article, qui m'ont encouragé jusqu'au bout, je vous aime les copains ! alors merci beaucoup à Manon, Romain, Jérôme et Antoine !! Et un big up en plus aux Guystouquettes, les casseurs loveurs de l'Agro à l'énorme cœur !! Merci infiniment les gars !!

Il est temps maintenant pour moi de remercier la personne qui compte le plus pour moi, je pense qu'elle se reconnaîtra. Tu es dans ma vie depuis un bon bout de temps maintenant, et tu as su m'épauler

sans jamais faillir, pour m'aider à poursuivre mon rêve de gamine de faire de la biologie marine ! Jusqu'à la fin de cette thèse tu as été là à m'aider, à discuter d'écologie avec moi à une heure du matin pour m'aider à écrire ma conclusion générale ! Tu es vraiment une personne formidable avec un cœur immense et un cerveau tout aussi gros, et tu as une grande et belle intelligence humaine ! Sans toi cette thèse serait probablement très différente, car nos discussions ont souvent fait germer des idées nouvelles !

Enfin, je souhaite remercier du fond du cœur TOUTE ma famille avec une pensée pour mes cousines qui m'ont envoyé des messages de soutien pendant la rédaction. Maman, merci beaucoup d'avoir toujours été là pour écouter mes plaintes, mes problèmes, pour ton soutien sans faille jusqu'au bout ! Papa, merci de m'avoir donné cet amour de la biologie et de la mer, c'est vraiment le top ! et d'avoir été à 100% au cours de la publication de mon premier papier. Une pensée pour François qui m'aide à garder les pieds sur terre et à voir au-delà de mon récif d'hermelles !

J'espère très sincèrement n'avoir oublié personne, et si c'est le cas, je m'en excuse et on ira boire un verre ☺

Résumé détaillé

L'objectif de ce travail de thèse était de comprendre (1) l'impact d'un ingénieur structural de l'écosystème sur la diversité et le fonctionnement des communautés benthiques et (2) l'impact de perturbations sur le fonctionnement de l'habitat construit par l'espèce ingénieur. Pour y répondre, nous avons considéré l'habitat récifal construit par le polychète grégaire *Sabellaria alveolata* comme cas d'étude, et plus particulièrement, le récif de Sainte-Anne, localisé en Baie du Mont-Saint-Michel (Bretagne, France). Une zone caractérisée par des sédiments meubles (sable fin à vaseux), éloignée de 1.5 km et localisée sur le même niveau bathymétrique que le récif de Sainte-Anne a représenté le site contrôle, non influencé par l'espèce ingénieur.

Dans un premier temps, cet ingénieur physique de l'écosystème induit une profonde modification structurale puisqu'elle transforme un sédiment meuble en une structure tridimensionnelle dure et élevée relative au substrat initial. L'étude préliminaire a révélé que la présence d'un récif à *S. alveolata* augmente le stock de biomasse chlorophyllienne (*e.g.* microphytobenthos) présent localement dans le sédiment meuble ainsi que la richesse spécifique et l'abondance de macrofaune présente dans les structures biogéniques, formant un assemblage original d'espèces. La modification des conditions environnementales locales induites par ces structures biogéniques (granulométrie et contenu en matière organique) influence également la mise en place d'un assemblage faunistique particulier aux sédiments meubles sous leur influence directe. L'habitat récifal apparait comme un point chaud de biodiversité.

Par ailleurs, l'implantation de *S. alveolata* a des conséquences fonctionnelles importantes en termes de structure du réseau trophique et d'interactions alimentaires, estimées grâce aux isotopes stables du carbone et de l'azote. En effet, cet ingénieur de l'écosystème augmente le pool local de ressources alimentaires (macroalgues, microalgues et tapis bactérien) par des changements structuraux, abiotiques et biotiques. Ces ressources alimentaires locales sont consommées dans les structures biogéniques par de nombreuses espèces aux régimes alimentaires spécialisés, à la différence des sédiments meubles avoisinants où ces ressources alimentaires sont consommées par quelques espèces généralistes. De manière générale, *S. alveolata* conduit à une augmentation de la niche trophique des communautés benthiques (aire totale et ellipse standard) et du couplage benthique-pélagique à travers la forte abondance d'espèces suspensivores associées (*e.g. Magallana gigas*, *Mytilus* cf. *galloprovincialis*). En même temps, la compétition trophique potentielle entre l'ingénieur et les autres consommateurs primaires est très limitée comme révélée par des modèles de mélange.

De plus, le cycle de la matière organique et des nutriments (flux biogéochimiques) est favorisé par l'installation de *S. alveolata*, un effet positif principalement lié à l'espèce ingénieur elle-même qui structure linéairement les flux mesurés (*e.g.* demande en oxygène). Néanmoins, un niveau de diversité fonctionnelle intermédiaire, mesuré par la dispersion fonctionnelle, maximise le fonctionnement

biogéochimique, soulignant l'influence positive que les espèces associées peuvent avoir sur le fonctionnement du récif via leurs traits biologiques.

Finalement, le long d'un gradient de perturbation, j'ai observé un remplacement de la macrofaune associée et une augmentation de son abondance ainsi que son homogénéisation. Au niveau du fonctionnement du récif, l'utilisation des ressources trophiques (niche isotopique) et le fonctionnement biogéochimique global sont tous les deux maximaux pour un niveau de perturbation intermédiaire du récif, estimé par la densité de *S. alveolata* adulte. De manière générale, nos résultats révèlent l'importance de (1) la facilitation (*i.e.* interactions spécifiques positives) dans le fonctionnement de cet habitat ingénieuré, (2) limiter les activités anthropiques qui perturbent les structures biogéniques et (3) considérer ces structures en association avec les sédiments meubles adjacents au sein d'une définition élargie de ce qu'est un récif. Enfin, ce travail indique un effet global positif de *S. alveolata* sur tous les flux et fonctions mesurés, et l'utilisation d'un gradient de perturbations pointe vers un nouvel objectif de conservation pour ces habitats ingénieurés où leur capacité de résilience pourrait être optimale.

Extended abstract

The goal of this PhD was to understand (1) the effect of a structural ecosystem engineer on the diversity and functioning of benthic communities and (2) the impact of disturbances on the functioning of the habitat built by the engineer species. In this context, we used the reef habitat built by the gregarious polychaete *Sabellaria alveolata* as a case study, and more precisely, the Sainte-Anne reef, located in the Mont-Saint-Michel Bay (Brittany, France). A zone characterized by soft sediments (fine to muddy sand), 1.5 km from the Sainte-Anne reef and on the same bathymetric level, represented the control site, non-influenced by the engineer species.

First, this physical ecosystem engineer induces a very strong structural change since it transforms a soft sediment into hard three-dimensional structures elevated above the seabed. The preliminary study revealed that the presence of a *S. alveolata* reef increases the stock of benthic chlorophyll biomass (*e.g.* microphytobenthos) in the local soft sediments and increases the species richness and macrofauna abundance, forming an original assemblage of species. The biogenic structures, via the modification of the local environmental conditions (grain-size distribution and organic matter content), also lead to the formation of an original community in the soft sediments under its direct influence. The reef habitat constitutes a biodiversity hotspot.

Furthermore, the establishment of *S. alveolata* has important functional consequences in terms of food web structure and trophic interactions, estimated using carbon and nitrogen stable isotopes. Indeed, this ecosystem engineer increases the local pool of trophic resources (macro and microalgae, bacterial mats) through structural, abiotic and biotic changes. The locally produced trophic resources are consumed in the biogenic structures by a diverse community of trophic specialists, while in the adjacent soft sediments, they are consumed by a few trophic generalists. Overall, *S. alveolata* leads to an increase in the trophic niche of benthic communities (convex hull and standard ellipse) and of the benthic-pelagic coupling via the strong abundance of associated suspension-feeders (*e.g. Magallana gigas*, *Mytilus* cf. *galloprovincialis*). At the same time, the potential trophic competition between the engineer and the other primary consumers is very low as revealed using mixing models.

In addition, the organic matter and nutrient cycling (biogeochemical fluxes) are enhanced by the establishment of *S. alveolata*, a positive effect mainly linked to the engineer itself, which linearly structures the measured fluxes (*e.g.* oxygen demand). Notwithstanding, an intermediate functional diversity measured as the functional dispersion, maximizes the biogeochemical functioning; stressing the positive influence the associated species can have on the reef functioning via their biological traits.

Finally, along a disturbance gradient, I observed a replacement (turn-over) and an abundance increase of the associated macrofauna along with its homogenization. Regarding the reef functioning, the resource use (isotopic niche) and the global biogeochemical functioning appeared maximal where

the reef was intermediately disturbed, estimated by the density of adult *S. alveolata*. Overall, our results reveal the importance of (1) facilitation (*i.e.* positive species interactions) in the functioning of this engineered habitat, (2) limiting direct anthropogenic disturbances to the biogenic structures and (3) considering the actual engineered structures in association with the adjacent soft sediments, under an enlarged definition of a reef. In addition, this work indicates an overall positive effect of *S. alveolata* on all the measured fluxes and functions, while the use of a disturbance gradient hints towards a new conservation goal for these engineered habitats where their resilience capacity could be optimal.

Publications presented in this manuscript

1. **Jones A G**, Dubois S F, Desroy N, Fournier J. Interplay between abiotic factors and species assemblages mediated by the ecosystem engineer *Sabellaria alveolata* (Annelida: Polychaeta). Estuarine Coastal and Shelf Science in press. Doi: 10.1016/j.ecss.2017.10.001

2. **Jones A G**, Dubois S F, Brind'Amour A, Fournier J., Bajjouk A, Lerouxel A, Desroy N, Gernez P, Laurent B. What can habitat complexity and food source heterogeneity tell us about fine-scale isotopic compositions? (in preparation, will be submitted to PlosOne)

3. **Jones A G**, Dubois S F, Desroy N, Fournier J. Effect of habitat engineering species on food web structure and community isotopic niches (in preparation, will be submitted to Food Webs)

4. **Jones A G**, Denis L, Fournier J, Desroy N, Duhong G, Dubois S F. Linking multiple facets of biodiversity and ecosystem function in a coastal engineered habitat (ready to be submitted to Oikos)

5. **Jones A G**, Dubois S F, Desroy N, Fournier J. Ecological niche estimated with functional and isotopic community-wide metrics: complementary or redundant pictures when investigating marine engineered habitat? (in preparation, will be submitted to Functional Ecology)

Oral communications

1. Jones A G*, Dubois S F, Desroy N, Lerouxel A, Gernez P, Barillé L, Fournier J. Small scale isoscapes for marine benthic habitats. Isotope mapping of the honeycomb worm *Sabellaria alveolata*. International Conference on Application of Stable Isotope Techniques to Ecological Studies, April 3-8 2016, Tokyo, Japan

2. Jones A G*, Dubois S F, Desroy N, Fournier J. Biological traits analysis to assess changes in the functional structure associated with an ecosystem engineer, International Temperate Reefs Symposium, June 26-30 2016, Pisa, Italy

3. Jones A G*, Dubois S F, Desroy N, Fournier J. Habitat disturbance and beta diversity: the *Sabellaria alveolata* reef case. Benthic Ecology Meeting, April 12-16 2017, Myrtle Beach, South Caroline, USA

4. Jones A G*, Dubois S F, Desroy N, Fournier J. From structural to functional diversity investigated through the eyes of a reef builder, the honeycomb worm *Sabellaria alveolata*. Monthly seminar organized by Louise Firth, 04/05/2017, Plymouth University, UK

Table of contents

List of figures

List of tables

General introduction

1. Ecosystem engineering

1.1. The original concept of ecosystem engineering

Until the mid 1990's, the main interactions studied by ecologists as drivers of the distribution and abundance of species, where intra- and inter-specific competition for abiotic and biotic resources, predation, parasitism and mutualism (Ricklefs 1984). The role many organisms play in the creation, modification and maintenance of habitats via non-trophic interactions was known but lacked generality and a clear definition distinguishing it from other processes (Naiman 1988). In this context, Jones et al. (1994) introduced the term ecosystem engineering and the species responsible for this process were termed ecosystem engineers. They were defined as "organisms that directly or indirectly modulate the availability of resources (other than themselves) to other species, by causing physical state changes in biotic and/or abiotic material. In so doing they modify, maintain and/or create habitats (Jones et al. 1994)". This intial definition explicitly excluded trophic interactions such as the provision or consumption of tissue (Berke 2010). In this regards, it is different from the keystone species concept developed by Paine (1969, 1966), which focuses on species that play an overwhelming role in determining community structure compared to their relative abundance or biomass, often via trophic links. If keystone species of an ecosystem are removed, the ecosystem is predicted to be drastically modified as described in the trophic cascade between sea-otter decline, urchin increase and the disappearance of kelp beds (urchin barrens) (Estes and Palmisano 1974). Most importantly, keystone species focus on outcome while ecosystem engineering focuses on states and their change.

Two types of ecosystem engineers were initially described: autogenic and allogenic engineers (Jones et al. 1994). Autogenic engineers change the environment via their own physical structure (their living and dead tissues) while allogenic engineers change the environment by transforming living or non-living materials from one physical state to another, via mechanical or other means. The effects ecosystem engineers can have on their environment were classified into five categories linked to autogenic or allogenic engineering, with the mention that for some ecosystem engineers their effects can be described using a combination of two or more of these cases. These categories are presented in figure 1 with some examples. The idea behind these different categories is that, once transformed by the body or the biological activity of the engineer, the material is susceptible of affecting the flux of one or multiple resources, either directly or indirectly, if the modified flux affects a major abiotic parameter. Beavers (*e.g. Castor* sp.) are a classic example of case 2b allogenic engineering (Figure 1). Indeed, they transform a living material (a tree) into a physical barrier (cut trees in a dam) which retains water, creating ponds and generating important wetlands (Wright et al. 2002). The autogenic equivalent of beavers are trees in a forest (Case 2a) (Jones et al. 1994). Overall many organisms could be considered as ecosystem engineers, like cows, which transform grass into cowpats. Indeed, a diverse invertebrate community can end up colonizing these pats, relying on them for food and shelter. Nonetheless, the

interesting question to ask is whether recognizing the engineering dimension can increase our understanding of ecological interactions and processes (Jones et al. 1994, Hastings et al. 2007, Berke 2010). In this regards and according to Berke (2010), "ecosystem engineering allows us to treat the effects organisms have on the environment as a coherent suite of interactions, rather than a collection of unrelated case studies".

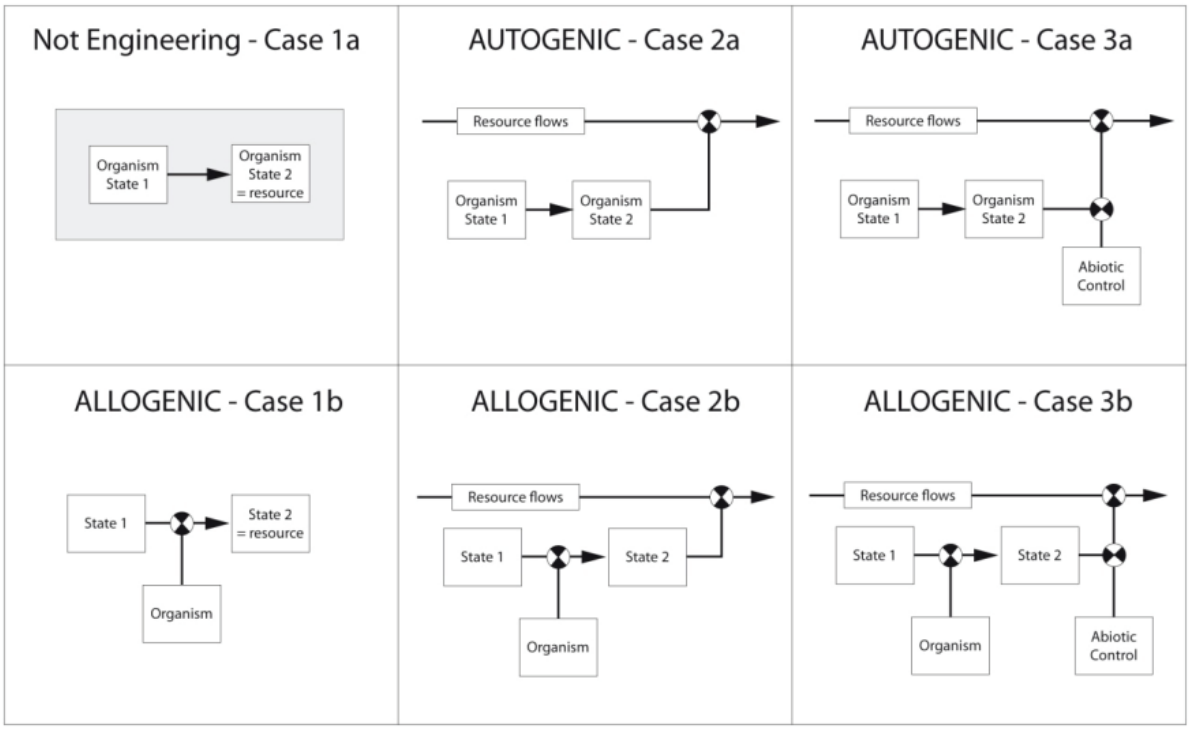

Figure 1. Conceptual models of autogenic and allogenic engineering by organisms as proposed by Jones et al. (1994). The white and black circle indicates points of modulation. Case 1a represents the direct provision of resources by one species to another and is not engineering, since it does not involve modulation of resource flows. Rabbits and badgers that dig extensive burrows occupied by other species are examples of case 1b allogenic engineers. In this case, the resource is actually the structure created by the species and constitutes a new habitat for other species. Bog moss (*Sphagnum* spp.) and submerged macrophytes (*e.g. Zostera marina*), case 2a autogenic engineers, respectively create raised bogs and meadows, which modifies the local hydrology, pH and topography (bog moss) or attenuates light and enhances sedimentation (macrophytes). Prairie dogs (*Cynomys* sp.) and marine burrowing macrofauna, case 2b allogenic engineers, continuously disrupt the soil or the sediments, changing the physical-chemical properties of the soil (prairie dogs) or increasing oxygenation of the sediments, stimulating microflora and increasing decomposition rates (marine burrowing macrofauna). Cases 3a (autogenic) and 3b (allogenic) are examples where the ecosystem engineer combines elements of other cases. Crustose coralline algae are examples of case 3a. They overgrow and cement together detritus on outer barrier reefs, decreasing hydrodynamic forces via their own body and the cement they secrete. Ribbed mussels are an example of case 3b. These organisms build dense mussels beds with their own body and using byssal threads, preventing salt marsh physical erosion and disturbance.

1.2. Physical ecosystem engineering

Using the example of a tree and the diverse ecological effects it can have on other organisms via change in physical state or condition (*e.g.* intact tree vs tree with holes) or via changes to the local environment (*e.g.* tree debris), Jones et al. (1997) refined the concept of ecosystem engineering by adding the term physical. This new definition presents physical ecosystem engineers as "organisms that directly or indirectly control the availability of resources to other organisms by causing physical state changes in biotic or abiotic materials. The process of physical ecosystem engineering by organism is the physical modification, maintenance or creation of habitats. The ecological effects of engineering on other species occur because the physical state changes directly or indirectly control resources used by these other species." In Jones et al. (1997), the direct provision of living space by the structure of an organism becomes part of physical engineering while it was not originally included in the concept of ecosystem engineering (Jones et al. 1994).

The introduction of physical ecosystem engineering by Jones et al. (1997) paved the way to the development of a conceptual framework with the goal of gaining a general understanding of this process and predicting engineering effects (Jones et al. 2010). This framework is based on four cause/effect relationships linking four components: the engineer and the associated structural, abiotic and biotic changes (Figure 2). First, a new structural state arises when the physical ecosystem engineer establishes (structural change), leading to environmental modifications (abiotic change). Both structural and abiotic changes can in turn lead to biotic modifications (biotic change) and these three types of change can all feedback to the engineer. This framework connects the ecosystem engineering process and the associated abiotic dynamics, with the biotic consequences of this process for other species and the engineer. An important part of this framework is the definition of a baseline, corresponding to the unmodified state before the establishment of the engineer and the formation of new structural/abiotic/biotic states. Furthermore, structural changes are often accompanied by changes in the distribution of material fluids and solids like in the case of coral reefs that attenuate wave action leading to an increase sedimentation in the back reef. Structural and/or abiotic changes can lead to many kinds of biotic responses at the organism level (*e.g.* growth and reproduction), at the species level (*e.g.* abundance and distribution changes, inter-specific interactions like competition) and at the ecosystem level (*e.g.* processes like biogeochemical process rates and primary productivity). In the end, biotic changes vary in magnitude (weak, strong or no effect) and direction (positive or negative) (Jones et al. 1997, Wright et al. 2004). When one or several of the aforementioned pathways affects the activity and/or density of the engineer, both positive and/or negative engineer feedbacks can occur, happening on the same or different time scales (Jones et al. 2010).

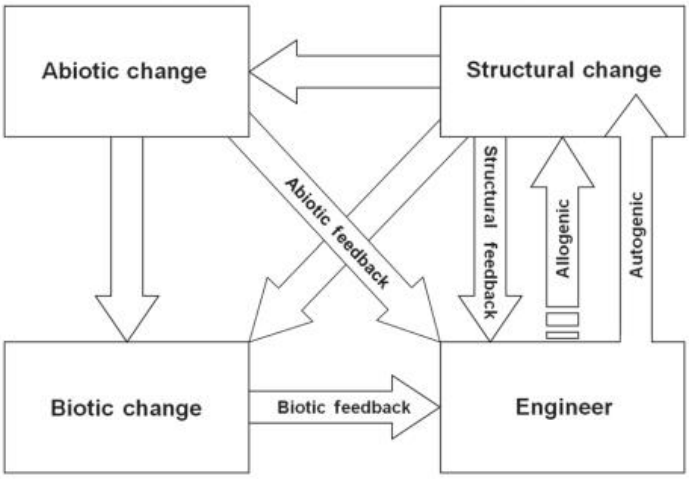

Figure 2. Physical ecosystem engineering by organisms as conceptualized by Jones et al. (2010) and presenting the cause/effect relationships taking place in an engineered system. The solid arrow for autogenic engineering represents the physical manifestation of the engineer in the environment. The striped arrow for allogenic engineering represents the action of the engineer on other living and non-living structure.

1.3. Ecosystem engineers and biodiversity

The physical state changes caused by ecosystem engineer control the availability of resources on which other species depend, hence ecosystem engineering can have positive or negative ecological consequences depending on the species of interest (Jones et al. 1997). When considering physical ecosystem engineers and the creation of engineered habitats, it could appear at first sight they would have a mostly positive effect on other species (Hacker and Gaines 1997). Nonetheless, the engineered habitat can be beneficial for a large number of species for which it represents a new adequate living space but it also disrupts the initial local conditions, eliminating entirely some species from the engineered environment or making others much rarer. A good example are species that rework the sediment commonly called bioturbators (Reise 2002). From the Devonian onwards, fossil records show a decline in the diversity of immobile suspension-feeders living in soft marine sediments, as mobile taxa diversified. These major changes in the structure of marine benthic communities were attributed by Thayer (1979) to the evolution of the so-called 'biological bulldozers' or bioturbators (Volkenborn et al. 2009), that destabilize the sediment, fouling, overturning and burying immobile suspension feeders, now largely confined to hard substrata. Hence, the question of whether a physical ecosystem engineer has a positive or negative effect, will depend on the level of organization (*e.g.* a particular species, a group of species like primary producers or suspension-feeders or the overall species richness and abundances) under investigation (Streitberger et al. 2017) along with the temporal and spatial scale of interest (Jones et al. 1997, Hastings et al. 2007). For example, if one considers a landscape with a diversity of habitats such as engineered, non-engineered and formerly engineered patches, this increase

in habitat diversity linked to the effect of engineering will almost certainly enhance the regional species richness (Jones et al. 1997, Wright et al. 2004).

Focusing on how engineers influence ecosystems and the resulting diversity of mechanisms and pathways, Berke (2010) proposed a new way to classify these species based on their functional diversity. In this classification, the emphasis was placed on how ecosystem engineers modulate the availability of resources to other organisms and four none exclusive functional classes of ecosystem engineers were distinguished: structural engineers, bioturbators, chemical engineers and light engineers (Table 1).

Table 1 Summary of the four engineer functional classes as proposed by Berke (2010), with examples of ecosystem-level effects and associated marine, aquatic and terrestrial ecosystem engineers.

Engineer class	Ecosystem effects	Marine and aquatic examples	Terrestrial examples
Structural engineers	Create living space Reduce disturbance Alter hydrodynamics Alter sedimentation Alter diversity / richness (usually enhance)	Corals Bivalves Tube-building invertebrates Seagrasses, aquatic plants and macroalgae Mangroves	Most plants Mound-building insects Beavers
Bioturbators	Enhance disturbance Mix sediment Alter biogeochemistry Alter (usually reduce) diversity / richness	Burrowing infauna (polychaetes, bivalves, crustaceans, echinoderms, nemerteans, fish) Excavators (sediment-biting fish, skates and rays, gray whales, crabs, horseshoe crabs, echinoderms)	Burrowing vertebrates (e.g. fossorial rodents, mammals, lizards) Burrowing invertebrates (e.g. earthworms, ants, termites) Excavators (e.g. porcupines, skunks)
Light engineers	Alter light intensity, penetration, scatter Alter turbidity	Zooplankton Phytoplankton Filterers (e.g. bivalves, ascidians)	Overlaps with structural engineers; anything casting shade, most plants
Chemical engineers	Create biogeochemical gradients (physically or physiologically)	Microbes Seagrasses and aquatic plants Macroalgae Many burrowers (e.g. lugworms)	Most plants Mycorrhizal fungi Nutrient vectors (e.g. seabirds, bears)

Structural engineers appear as the most obvious class because these organisms often create new habitats, like forests, beaver dams, termite mounds in the terrestrial realm or like coral reefs, mussel beds, tube mats, macroalgae meadows or seagrass forests in the aquatic realm. In this regards, structural engineers could be considered as a particular type of physical ecosystem engineers (Jones et al. 1997). According to Berke (2010), "structural engineers operate through similar processes and have similar types of effects "(Table 1), hence understanding the functioning of the habitat built by one structural

engineer, hereafter called an engineered habitat (Jones et al. 1997), is likely to be relevant to many others. In general, structural engineers provide new living space for other organisms where physical disturbances are reduced (Bruno et al. 2003). They also alter abiotic forces like waves, current and wind influencing processes like sedimentation (González-Ortiz et al. 2014). Overall, they generally enhance diversity and richness (Gutiérrez et al. 2003, Bouma et al. 2009).

Furthermore, feedbacks to the engineer can occur when the change in the physical state either positively or negatively affects it. Regarding negative feedbacks, it has been shown that mussels via the creation of mussel beds in dynamic subtidal soft sediments, limit hydrodynamic stress thus facilitating their own predator, a sea star (Agüera et al. 2015). Differently, beavers via dam building, create ponds in which they live, feed while avoiding predators, an example of a positive feedback (Jones et al. 1997). Cases where the engineered habitat has a direct and positive effect on the fitness of the engineer, are examples of 'extended phenotype' (Dawkins 1982, Jones et al. 1997). Ecosystem engineering appears very important where environmental conditions are extreme, and such conditions seem to have favored the selection of engineers with these 'extended phenotypes' through enhanced survival of the engineer and the cohabiting fauna (Jones et al. 1997).

2. Ecosystem engineering, facilitation and the niche

First defined by Grinnell (1917) and Elton (1927), the niche concept is a key concept in ecology. Hutchinson (1957) refined it and distinguished the realized from the fundamental niche. The Grinellian niche or the 'habitat niche' refers to what determines the presence of a species in a given location in terms of environmental conditions (habitat and resources) and is linked to the principle of competitive exclusion, where species exclude others because of similar 'habitat niches' (Gause, 1935). The Eltonian niche or the 'functional niche' refers to the role of a species in a system and is often linked to the species' position in the food web. The niche according to Hutchinson (1957) is defined as a hypervolume in which each dimension represents a resource (*e.g.* food, material, space) or an environmental condition (*e.g.* temperature, humidity, pH, salinity, sediment grain-size). In this regard, the fundamental niche corresponds to the range of requirements of a species without considering biotic interactions. Inside this range, the species can live indefinitely since there are no negative interspecific interactions such as competition, predation or parasitism. Differently, the realized niche is commonly considered as the modification of the physical space actually occupied by a species after exclusion by competitors and other enemies, hence the realized niche is classically viewed as being included in the fundamental niche. The fundamental and realized niches, as classically defined, are based on negative interactions between organisms that shape the distribution of species and natural communities. In this context, including facilitation (*i.e.* positive species interactions) into niche theory leads, as developed by Bruno et al. (2003), to "the paradox that the spatial extent of the realized niche of a species can be larger than the spatial range predicted by the fundamental niche". Indeed, facilitation can lead to the survival of species

in niche space they could not occupy if they were alone and not benefiting from positive interspecific interactions.

Many intertidal structural engineers like oysters, macroalgae or cordgrass, create complex habitats that reduce local pressures such as predation or thermal stress, all examples of facilitation (Bertness and Callaway 1994, Bruno et al. 2003, Bouma et al. 2009). Ultimately, these favorable environmental changes can lead to a larger realized niche compared to the fundamental niche, as reported for mussels and barnacles in *Ascophyllum nodosum* canopies by Bertness et al. (1999). Different mechanisms can be considered under the global term of facilitation such as habitat amelioration, predation refuge, resource and recruitment enhancement (Figure 3) and all these mechanisms can take place in engineered habitats. For example, saltmarshes decrease hydrodynamic disturbances, represent a new source of food and favor benthic recruitment (Eckman 1983, Bertness and Callaway 1994, Bruno 2000). In the end, the creation of new habitats by structural engineers and the biodiversity increase that often results is directly linked to the process of facilitation.

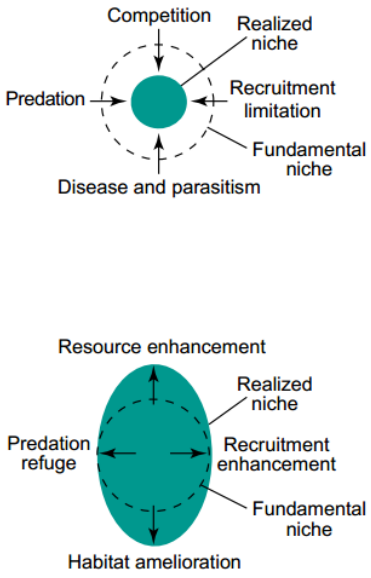

Figure 3. The niche concept with (bottom) and without (top) facilitation as presented by Bruno et al. (2003). When facilitation is considered, the realized niche (green circle) can be larger than the spatial range predicted by the fundamental niche (dashed line). Incorporating facilitation into the niche concept recognized processes that can expand the amount of space that meets the requirements of the fundamental niche (*e.g.* predation refuge) and can mitigate the effects of niche-shrinking factors (*e.g.* predation).

3. Integrating ecosystem engineering into food webs

3.1. Interaction webs

In the initial definition of ecosystem engineering, trophic interactions in the form of provision or consumption of tissue is explicitly excluded (Jones et al. 1994, Berke 2010). Nevertheless, to move towards the understanding of nature in all its complexity, ecosystem engineering and trophic ecology must be considered together (Gharajehdaghipour et al. 2016). Indeed, there is no reason why processes driven by engineering should not be coupled to the rich diversity of trophic linkages to create interaction webs that more accurately reflect interactions in communities and ecosystems (Jones et al. 1997). Engineering and trophic relations can interact in a number of ways, with the most obvious being the control ecosystem engineer can have on the distribution and abundance of trophic resources for other species, via the creation of physical structures, and the direct consumption of the engineer by other species. This second interaction is very close to the negative feedback to the engineer mentioned earlier, the difference lying on whether the species consuming the engineer is present because of the engineering effects (negative feedback) or is independent from the engineering effects.

A decade ago, researchers started investigating the coupling of non-trophic and trophic interactions into more global interaction webs (Olff et al. 2009, Bascompte 2010, Golubski and Abrams 2011, Kéfi et al. 2012) and Sanders et al. (2014) specifically addressed the question of integrating ecosystem engineering into food web studies. In a food web, engineer species can affect nodes by changing species richness, abundance and biomass and they can affect links by changing predator-prey interaction strength via the creation of prey refuges or predator rich habitats (Grabowski and Powers 2004, Sanders et al. 2014, Agüera et al. 2015). Engineers modulate the food web nodes and links according to three non-exclusive pathways, acting more or less strongly on these pathways (Sanders et al. 2014, van der Zee et al. 2016). These pathways are (1) altered abiotic conditions like temperature, wind or sediment deposition, (2) consumable abiotic resources like light and nutrients and (3) non-trophic resources like predator- or competitor-free space. The modification of consumable abiotic resources like nutrients can result in the addition of new primary producers or alter primary producer biomass, which may then propagate to higher trophic levels (Sanders et al. 2014). Ecosystem engineers can affect the entire food web or parts of it (Figure 4). They can also have varying trophic positions, either being top predators (*e.g.* Arctic fox (Gharajehdaghipour et al. 2016)), intermediate consumers (*e.g.* termites, prairie dogs, reef-building mollusks, lugworms (Gutiérrez et al. 2003)) or primary producers (*e.g.* trees, bog moss, macrophytes and seagrass (Bos et al. 2007)). Since structural engineers create *de novo* an entirely new habitat, they illustrate as put by Sanders et al. (2014), "the situation where the engineer has a 'global' impact on the food web by creating the elemental structure" (Figure 4D). In this regard, many marine autotrophs and invertebrates like corals, seagrass and a diverse range of suspension-feeders (*e.g.* bivalves, polychaetes, amphipods) that build reef-type structures, belong to this

category. In this context, it could be tempting to focus on the engineered habitat food web, "forgetting" these food webs unlikely function in isolation. Many studies have demonstrated the strong connection engineered habitats can have with other engineered habitats and/or with adjacent non-engineered habitats (Gillis et al. 2014, van der Zee et al. 2016), stressing the importance of integrating the engineered habitat food web in the global landscape (Polis et al. 1997, Hyndes et al. 2014).

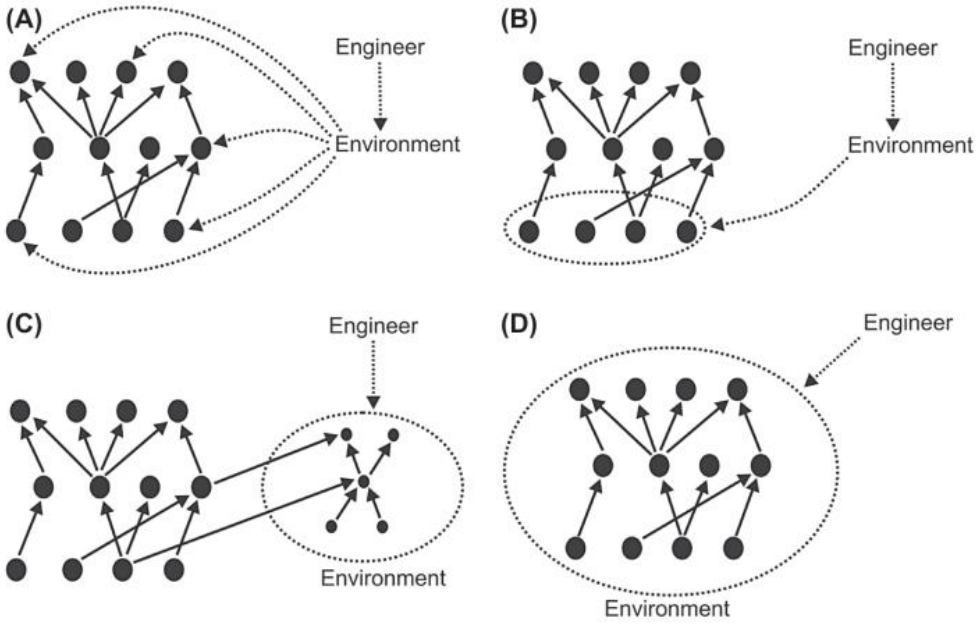

Figure 4. Ecosystem engineering can affect different parts of a food web as presented by Sanders et al. (2014). It can affect (A) a sub-set of species at different trophic levels; (B) one trophic level; (C) a food web compartment or (D) all species in a food web by for example creating the entire environment in which the food web occurs.

3.2. Investigating trophic transfers and food web functioning

Trophic transfers and food web functioning are important aspects of the global functioning of an ecosystem (Duffy et al. 2007, Rigolet et al. 2015) and this trophic component of functionality is often considered when evaluating the impact of natural and anthropogenic disturbances on ecosystems (Layman et al. 2007a, Nordström et al. 2015, Quillien et al. 2016, Nordström and Bonsdorff 2017). Indeed, 'pristine' and 'degraded' ecosystems often differ by their respective food web complexity, the presence and abundance of large top predators and food source heterogeneity, bringing either stability to the system or making it more vulnerable to disturbances (Neutel et al. 2007, Rooney et al. 2008). Furthermore, habitat diversity and spatial heterogeneity, which can be caused by ecosystem engineers, influence the distribution and diversity of autotrophic and heterotrophic organisms (Kraan et al. 2009), leading to changes in trophic interactions (Larkin et al. 2008). In this regards, studying the trophic

functioning of engineered habitats, the trophic links they have with adjacent habitats and how they can be modified when the habitat is increasingly disturbed, are fundamental research questions (Suykerbuyk et al. 2012, van der Heide et al. 2014).

Originally, trophic links between species were studied by analyzing the stomach contents of consumers, but this technique presents a number of methodological difficulties and informs on the ingested diet of the species rather than on its assimilated diet. In this context, stable isotopes (especially of carbon and nitrogen) have proven to be powerful tools to trace pathways of energy among sources and consumers, inside ecosystems and at various spatial and temporal scales (West et al. 2009, Rascher et al. 2012, Hyndes et al. 2014, Christianen et al. 2017). Carbon (^{13}C / ^{12}C) isotope ratios, reported as $\delta^{13}C$, are often used to understand the origin of organic matter fueling food webs (Fry and Sherr 1989). Indeed, primary producers have distinct $\delta^{13}C$ linked to their physiology, their size and their environment (France 1995, Hemminga and Mateo 1996, Hemminga et al. 1999). The $\delta^{13}C$ of consumers is usually similar to that of their source of organic matter (~1‰ trophic shit (DeNiro and Epstein 1978)), informing on their diet (Fry et al. 1978). Differently, nitrogen (^{15}N / ^{14}N) isotope ratios, reported as $\delta^{15}N$ are often used as an indicator of the trophic position of an organism in the food web (Post 2002). The coupled use of carbon and nitrogen stable isotopes can inform on the contribution of different food sources to the diet of an organisms, using mixing models (Phillips 2001, 2012). Recently, a more functional use of stable isotopes has been developed via a set of indices (Bearhop et al. 2004, Layman et al. 2007a, Jackson et al. 2011) that quantify and measure different aspects of the trophic structure of communities (*e.g.* diversity of basal resources, food web length, trophic diversity and redundancy).

4. Integrating diversity and ecosystem engineering into the functioning of ecosystems

4.1. Diversity and the functioning of ecosystems

The title of the May 2017 editorial of Nature is "Why function is catching on in conservation?" (Nature 2017) and it points out how "the standard definition of biodiversity focuses too heavily on counting the number of different species, when perhaps it should concentrate on what each of those species contributes to the ecosystem." This editorial stresses the need for a more functional approach of nature. The classic approach in conservation is considering that communities with an equal number of species deserve equal attention, while they could be characterized by a set of species that perform very different functions either individually or collectively. The distribution and range of what organisms do in a system is called functional diversity (Tilman 2001) and it is being increasingly considered to set priorities and determine how conservation resources are allocated (Bremner 2008, Devictor et al. 2010, González-Ortiz et al. 2014, Riemann et al. 2017). This new vision of conservation turned towards

functional diversity, brings up the question of why conservationists are considering this form of diversity.

The answer is directly linked to the increasing disturbances ecosystems worldwide are experiencing (*e.g.* habitat fragmentation and modification, organic matter enrichment of rivers, lakes and coastal waters, ocean acidification), directly or indirectly caused by human activities (Rockström et al. 2009, IPCC 2014). The most visible advert effect these disturbances have on terrestrial and aquatic systems is biodiversity loss, classically measured as species richness (Sala et al. 2000, Hooper et al. 2005), but other forms of diversity can be lost such as genetic or functional diversity. In the wake of the realization that the 6th mass extension was on its way (Ceballos et al. 2015), the global scientific community started investigating in the 1990's, the links between biodiversity and ecosystem functioning (Schulze and Mooney 1994, Kunin and Lawton 1996), known as BEF studies (Tilman and Downing 1994). Indeed, natural ecosystems perform a broad range of functions such as primary and secondary production, organic matter recycling, water filtering (*e.g.* oyster reefs) and extreme weather event buffering (*e.g.* coral reefs and tsunamis). Some also have high patrimonial (*e.g.* sacred lands and animals) and economical value (*e.g.* eco-tourism) (Costanza et al. 1997). Hence, understanding how disturbances affects the overall functioning of ecosystems and the different functions they perform has become of the utmost importance. In this context, biodiversity can be seen as a direct measurement of ecosystem functioning or as reacting to various disturbances, hence helping to predict the effects disturbances could have on ecosystem functioning.

Traditionally, BEF studies have focused on species richness in the context of terrestrial autotrophic ecosystems. These original BEF studies revealed that a decline in plant species richness leads to a decrease in functions like carbon and nutrient cycling, or production and decomposition (Balvanera et al. 2006, Cardinale et al. 2011). Only measuring species richness, implicitly means that all species are considered equal, which is obviously not true especially if we think about structural ecosystem engineer or keystone species. In addition, only considering species richness limits our ability to detect early on the effects disturbances can have on ecosystem functioning (Mouillot et al. 2013a). Indeed, before disturbances are strong enough to lead to the local extinction of a species, other diversity changes with implications on the functioning of ecosystems can happen. Hence, considering other forms of diversity like functional diversity can provide valuable information on ecosystem functioning (Lavorel and Garnier 2002, Díaz et al. 2007, Cadotte et al. 2011) and on community response to disturbances (Bremner et al. 2006, Paganelli et al. 2012, Belley and Snelgrove 2017). For example, Mouillot et al. (2011) demonstrated that functional identity of species and functional diversity among grassland species, rather that species diversity per se, together promote key ecosystem functions such as decomposition and primary productivity.

4.2. Measuring functional diversity

There are many ways of measuring functional diversity and all of them depend on the use of functional traits (Lavorel and Garnier 2002) which are considered as either determining a given ecosystem function or process (*i.e.* effect traits) or as responding to environmental factors such as resources or disturbances (*i.e.* response traits). In the case of plant and fish functional diversity, functional traits are measured on organisms sampled in the ecosystem under investigation (Mokany et al. 2008, Villéger et al. 2010) and can be directly linked to functions like leaf surface area to primary production (Lavorel and Garnier 2002) or the ratio of gut length to standard length to fish trophic status (Kramer and Bryant 1995). In benthic communities, the diversity of organisms (*e.g.* mollusks, polychaetes, crustacean) and the lack of straightforward measurable functional traits, except size and/or biomass, leads to the use of biological traits often taken from the literature and completed using expert knowledge (Bremner 2008). The set of biological traits considered in a study depends on the question under investigation like the effects of a food pulse (Belley and Snelgrove 2017) or the natural environmental variability characterizing estuaries (van der Linden et al. 2016). Nevertheless, the majority of biological traits used in benthic studies can be linked to ecosystem functioning (effect traits) as well as responding to ecosystem changes (response traits). Using these biological traits, Bremner et al. (2003, 2006) developed Biological Trait Analysis (BTA), a method which considers that the functional roles of species are determined by their biological traits (*i.e.* life history traits, morphological and behavioral characteristics) and hence uses these traits to link a community to the ecological processes it performs.

Based on species' traits, many functional diversity indices have been proposed over the years like the FD by Petchey and Gaston (2002), the variance in characters weighted by the abundance (FDvar) by Mason et al. (2003), the community-weighted mean (CWM) by Garnier et al. (2004), the functionality regularity index (FRO) as a measure of functional evenness by Mouillot et al. (2005), the three complementary indices developed by Villéger et al. (2008) (FRic, FDiv and FEve) and the functional dispersion (FDis) by Laliberté and Legendre (2010). These different indices either consider a single trait (FDvar, FRO and CWM), hence focusing on the particular function(s) estimated by the trait or consider multiple traits, hence providing a synthetic vision of functional diversity. In this regards, Villéger et al. (2008) proposed a flexible framework linking functional richness (FRic), functional evenness (FEve) and functional divergence (FDiv) to ecosystem properties or to environmental variables (Figure 5). Overall, no consensus has been reached over the "perfect" association of functional indices (Petchey and Gaston 2006) and every study uses a particular set of traits and indices, making their comparison hard.

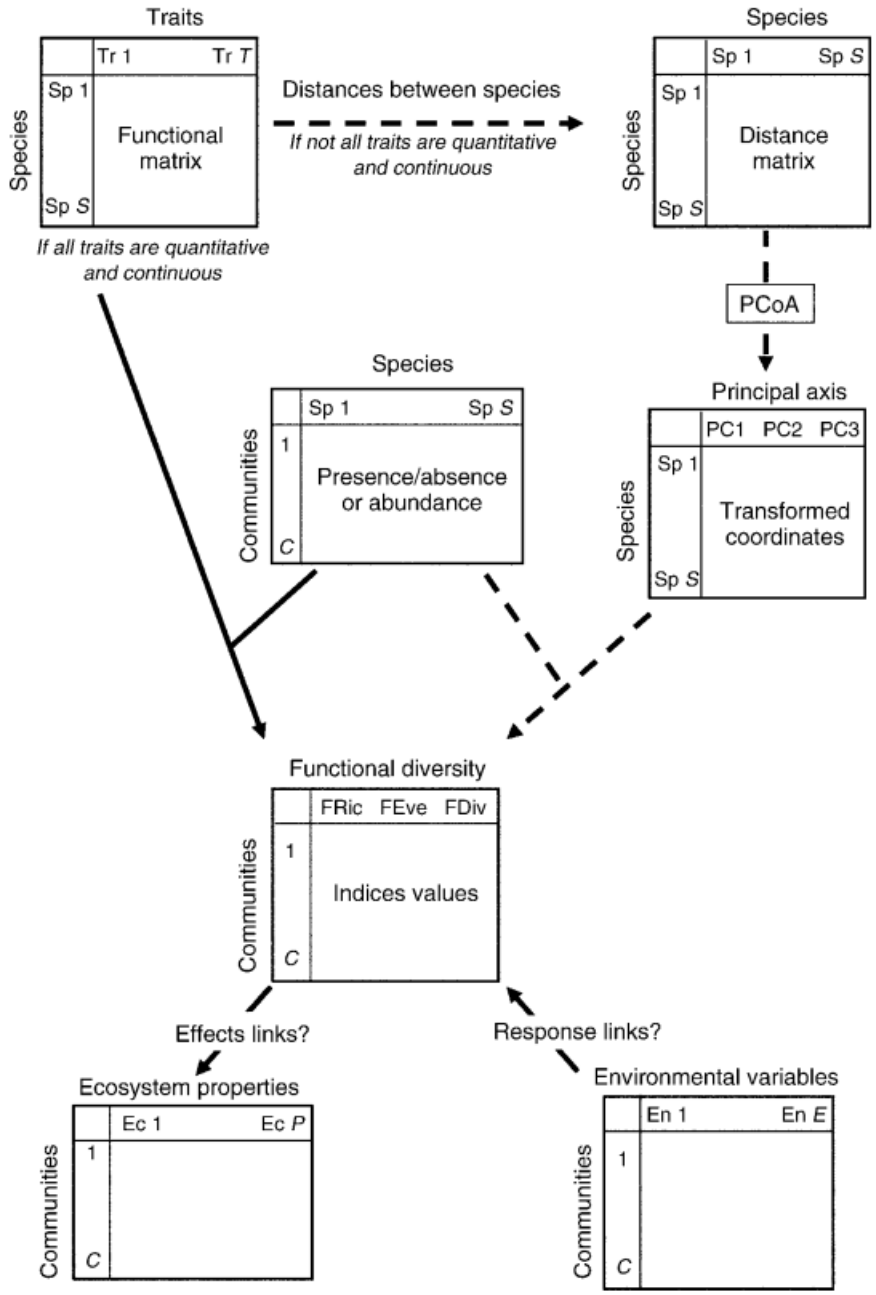

Figure 5. General framework proposed by Villéger et al. (2008) to study the effect of environmental conditions on functional diversity or the effect of functional diversity on ecosystem properties.

4.3. Using engineered habitats in biodiversity-ecosystem functioning studies

Many engineered habitats are actors in key ecosystem functions like forests and trees in primary production and carbon dioxide sequestration (Pan et al. 2011) or oyster reefs in bentho-pelagic coupling, water filtration and coastal protection (Kellogg et al. 2013). Indeed, ecosystem engineers modulate resources used by other species like energy, materials, space, food or a combination of these resources (Jones et al. 1997) and the modulation of these different resources affect fluxes of energy, materials and organisms inside the engineered habitat (Jones et al. 2006) and between the focal habitat and adjacent habitats. These fluxes represent the different functions an engineered habitat performs. Many engineered

habitats are threatened worldwide like coral reefs by high temperature, sedimentation and modified top-down control (Bellwood et al. 2004, Fabricius 2005), tropical forests by logging and agricultural land reclamation (Houghton 1990) or many temperate reefs (bivalves and polychaetes) by direct harvesting, coastal modification and trampling (Beck et al. 2011, Plicanti et al. 2016). Hence, it is becoming increasingly important to understand the functioning of engineered habitats and how it is affected by disturbances. In this context, understanding the link between ecosystem functioning (*e.g.* primary production, biogeochemical fluxes, trophic functioning) and diversity (taxonomic and functional) at the scale of an engineered habitat and how these two components of BEF studies change in an increasingly disturbed engineered habitat are interesting research questions. Such questions have been addressed in terrestrial ecosystems but examples are very scare in the marine realm (Denslow 1995, Mouillot et al. 2013a, Eldridge et al. 2016).

5. The reef-builder *Sabellaria alveolata* as a biological model

Sabellaria alveolata is a sedentary suspension-feeding polychaete from the Sabellariidae family. This family of polychaetes presents many species that build more or less extensive reef structures. These reef-building species are from the genus *Sabellaria*, *Phragmatopoma*, *Gunnarea* and *Idanthyrsus* and occur worldwide (Achary 1974, Pawlik 1988a). The largest reef structures are present on the Equatorial (*Idanthyrsus pennatus*), Californian (*Phragmatopoma lapidosa* previously known as *P. caudata*), South African (*Gunnarea capensis*) and French (*Sabellaria alveolata*) coasts. *S. alveolata* is a sedentary polychaete commonly found along the European coastline from Scotland and Ireland to Morocco (Atlantic coast) (Muir et al. 2016) and more anecdotally in the Mediterranean Sea where it used to be abundant in some areas like Marseille (France). The structures built by this species can present two forms: hummocks or veneers on rocky substratum in the upper-littoral zone where they rarely exceed 50 cm in height for a few hundreds of square meters (Figure 6) and much more imposing structures up to 2 m in height and extending over tens of hectares (Figure 7) (Gruet 1972, Schlund et al. 2016). These actual reefs are much rarer and occur in sandy environments in the lower intertidal zone. A hard substratum is necessary for the initial establishment of *S. alveolata* like a shellfish bed or old rock-built fisheries (Gruet 1972). If the structures develop into large biogenic reefs, than the initial hard substratum is no longer visible, hence the reefs end up occurring in an entirely soft sediment area. Such extensive reefs occur in two zones along the French coasts, in the Bourgneuf Bay (Gruet 1972) and in the Mont-Saint-Michel Bay (Audouin and Milne-Edwards 1832, Lucas and Lefevre 1956, Caline et al. 1988).

Figure 6. Examples of *S. alveolata* growing on a rocky shore as hummocks (left) and veneers (right). These pictures were taken in the Champeaux reef along the Normandy coast (France). Photos taken by A G Jones.

Figure 7. Example of *S. alveolata* growing on soft sediments in the Champeaux reef along the Normandy coast (France). The pictures presented in Figure 6 were taken along the cliffs visible in the back of the left picture. Photos taken by A G Jones.

Figure 8. Example of an individual from the species *S. alveolata* on its dorsal side. The head (white part) is composed of an opercular crown with tentacular filaments that the polychaete uses to feed and collect sediment particles to build its tube. Photo taken by A Guerin

This 3cm-long polychaete (Figure 8) lives in a tube it builds using sediment particles (Figure 9). The sediment particles are collected by the polychaete using tentacular filaments and selected depending on their nature, shape and diameter by the building organ located close to the mouth (Gruet 1984). This species has a preference for sediments of a bioclastic origin (shell fragments) as shown by Fournier et al. (2010) and Le Cam et al. (2011). The tube-building process is continuous as long as the building material is available in the local environment and the hydrodynamic conditions (waves and currents) strong enough to remobilize the sand grains making them available to the polychaete (Gruet 1972). This continuous tube-building activity is one of the mechanisms leading to the formation of high biogenic structures. One of the mechanisms leading to the formation of extensive biogenic reefs is the positive chemotaxis displayed by the pelagic larva for the L-dopa present in the organic cement produced by the adult worms for their tube-building activity (Pawlik 1988b). The association of this gregarious behavior, of a continuous tube-building activity and of favorable environmental conditions (*i.e.* grain-size structure, hydrodynamic processes, food availability and water temperature) can lead to the development of large biogenic reefs (Holt et al. 1998) as observed in the Mont-Saint-Michel Bay. Cold temperatures can lead to massive die-offs of the organisms jeopardizing the reefs they build (Crisp 1964) while sediment movements and winter storms can also have drastic consequences on these structures by causing their smothering or their erosion (Gruet 1972) (Figure 10).

Figure 9. Tubes of the polychaete *S. alveolata* of different diameters linked to the size of the individual. Note the large tube openings where live adult polychaetes and the small tube openings where live newly recruited juveniles. Photo taken by A G Jones

Figure 10. Example of a *S. alveolata* veneer presenting a visible erosion pattern. This erosion was probably caused by a strong physical force like tidal waves or waves generated by a storm. Photo taken by A G Jones

Gruet (1972) described the different evolutionary stages of a *S. alveolata* reef present in a predominantly soft sediment area (La Sennetière reef in the Bourgneuf Bay, France), from the primary establishment to the destruction of the structures. In the primary stage, the polychaete establishes on pebbles or any other hard substrata (*e.g.* empty shells). Then, individual tubes can become coalescent giving rise to isolated ball-shaped structures, which can end up forming barriers and platforms, representing the climactic growth stages. Any of these structural types can be damaged by various disturbances giving rise to a degraded or disturbed reef. Many disturbances can affect this biogenic habitat such as direct natural disturbances (sediment movement, storms and cold winters), direct anthropogenic disturbances (trampling) and indirect anthropogenic disturbances through shellfish farming and coastal modification (Gruet 1972, Dubois et al. 2006a, Desroy et al. 2011, Plicanti et al. 2016). Indeed, these reefs are well-known fishing grounds and many anglers come to collect bivalves attached to the biogenic structures like mussels (*Mytilus edulis*) and Japanese oysters (*Magallana gigas*) (Figure 11). This anthropogenic activity damages the reef via the extraction of these bivalves growing on the reef and via the associated trampling (Desroy et al. 2011, Plicanti et al. 2016). Overall, these disturbances lead to a gradual modification of the reef visible through disaggregation, fragmentation, decrease in height and decrease in ecosystem engineer density (Dubois et al. 2002, Desroy et al. 2011). The recovery of a disturbed reef and the overall resilience of these engineered habitats largely depends on the input of pelagic larvae and larval recruitment. Despite a weak synchronism in spawning, there are two major spawning events

corresponding to the two pelagic production peaks in temperate waters: a principal spawning event in April and a secondary one in September (Dubois et al. 2007a). The input of larvae to the reefs largely depend on the local hydrodynamics and even more so, on the meteorological conditions which can modify the larval distribution and dispersion (Ayata et al. 2009).

Figure 11. Example of the overall aspect of a disturbed *S. alveolata* reef (top) and of a close-up where we can see that the tube density is very low compared to figures 9 and 10 (bottom). Here the disturbed reef is mainly colonized by the Japanese oyster *Magallana gigas*. Photos taken by A G Jones

6. Objectives

Sabellaria alveolata is a common physical ecosystem engineer present along the European coasts where it builds more or less extensive biogenic structures in the intertidal zone. Many studies have investigated the macrofauna living in association with *S. alveolata* reefs and found that these engineered habitats are home to an original species assemblage and constitute biodiversity hotspots (Dias and Paula 2001, Dubois 2003, Porta and Nicoletti 2009, Schlund et al. 2016). Overall, *S. alveolata* plays a number of important roles through the creation of a new three-dimensional habitat that increases the physical complexity of the initial substrate, enhances the local biodiversity, limits coastal erosion and represents recreational fishing grounds. These habitats are subject to multiple disturbances both natural (*e.g.* storms) and anthropogenic (*e.g.* trampling). These disturbances modify the physical structure of the reef and can lead to epibiont colonization (*e.g.* oyster and green macroalgae) modifying the associated macrofauna in terms of richness, abundance and composition (Dubois et al. 2002, 2006a, Plicanti et al. 2016) (Figure 11). Overall, little is known about the actual ecological consequences disturbances have on the reef habitat, except that counterintuitively, species richness and macrofauna abundance are higher in degraded reefs than in non-degraded reef forms like platforms and ball-shaped structures (Dubois et al. 2002).

Trophic interactions are a key aspect of the functioning of a habitat (Cucherousset and Villéger 2015, Rigolet et al. 2015) and until now, no study as investigated the food web of this engineered habitat. Nevertheless, previous studies have looked into the temporal variability of the diet of several co-occurring suspension-feeders, including *S. alveolata,* in a rocky shore environment and in macrotidal systems. These studies revealed the important contribution of autochthonous food sources like benthic microalgae (Lefebvre et al. 2009) and green macroalgae (Dubois and Colombo 2014) to the diet of *S. alveolata*. Field observations of two *S. alveolata* reefs present on soft sediment, the Sainte-Anne and Champeaux reefs (Mont-Saint-Michel Bay, France) have revealed the presence of large mudflats colonized by benthic microalgae in the back reef zone. Mud colonized by microalgae is also present at finer scales, such as behind reef patches or between *S. alveolata* tubes (Figure 12). Furthermore, green macroalgae can grow on *S. alveolata* reefs, representing a potential food source for grazers, and once fragmented through the microbial loop, for suspension- and deposit-feeders. Hence, *S. alveolata* creates an entire environment where new trophic interactions take place and where two basal nodes seem to be affected relative to a non-engineered soft sediment. These basal nodes are benthic microalgae (probable biomass increase) and green macroalgae (new food source), which could be consumed by the engineer species, as the 'gardening hypothesis' states (Hylleberg 1975) and/or by the macrofauna present in the actual biogenic structures (engineered sediment) or in the adjacent soft sediments where the microalgae grow (associated sediment). In this context, carbon and nitrogen stable isotopes are relevant tools to investigate the basal resources fueling the reef food web (engineered and associated sediments) and the overall trophic functioning of the engineered and associated sediments.

Figure 12. Local mud accumulation behind the biogenic structures where benthic microalgae grow. Photo taken by A G Jones

As stated earlier, the ecological consequences of disturbances on the reef have only been studied using classic taxonomic indices like species richness or Hill's indices, providing limited information. In this context, functional diversity indices could be interesting complementary tools to investigate the link 1) between a measured function of the reef and the reefs diversity, as in biodiversity-ecosystem functioning (BEF) studies (Mokany et al. 2008, Mouillot et al. 2011) and 2) between diversity and disturbance, as in the framework developed by Mouillot et al. (2013). In this context, the main goal of this study is to understand the effect of an engineer species, in this case *S. alveolata*, on the diversity and functioning of benthic communities. More specifically, *S. alveolata* engineered habitats will be used as a biological model to address five questions, corresponding here to five articles (Figure 13). 1) What are the structural, abiotic and biotic changes caused by the establishment of a *S. alveolata* reef and how are they linked? 2) What can habitat complexity and local benthic food source heterogeneity tell us about the fine-scale isotopic compositions of the ecosystem engineer and an associated suspension-feeder? 3) How important are autochthonous resources (benthic microalgae and green macroalgae) in the overall functioning of the reef food web? 4) What can the application of the BEF framework tell us about the effect of increasing disturbances on the biogeochemical fluxes of the engineered sediments, an example

of a key ecosystem function in benthic ecosystems? 5) In the case of an engineered habitat, how do functional and isotopic diversity indices change along a disturbance gradient and what information can they provide on the estimation of the ecological niche of a community?

The first chapter can be seen as a preliminary study (article 1). Indeed, this published work replaces different previously known aspects of the engineering effect of *S. alveolata* in a more formal framework. In this study, three types of sediment are considered: a control sediment, representing the original state before the establishment of the engineer, the engineered sediments corresponding to the actual biogenic structures build by the engineer and the soft sediments present around the reef structures and considered as being influenced by the engineered sediments. In this context, we investigated how the establishment of the engineer modified the grain-size distribution of the engineered and associated sediments along with a number of sediment characteristics (*e.g.* sediment grain-size, organic matter and chlorophyll *a*). Then, the biotic effects of *S. alveolata* on benthic communities was investigated by looking at the taxonomic diversity and species assemblages of the three sediment types. We addressed the link between these different changes and the consequences they could have on the reef functioning, as a global entity considering both the engineered and the associated sediments. The second part of this paper focuses on the engineered sediments and on the effects of a continuous and increasing disturbance on the associated macrofauna using beta diversity indices.

The second chapter focuses on trophic interactions and food web functioning using carbon and/or nitrogen stable isotopes. The first part (presented as a manuscript, article 2) looks into the interactions between habitat complexity, food source heterogeneity and spatial scales in explaining the carbon isotopic ratio variations of the engineer and an associated suspension-feeder at the scale of the most extensive *S. alveolata* reef: the Sainte-Anne reef. In this work, we coupled several methodological tools to explain the spatially explicit variations of the isotopic composition of *S. alveolata* and *M.* cf. *galloprovincialis*, as done with isoscapes (West et al. 2009). We used multispectral images of the reef and the calculation of the normalized vegetation index to estimate the biomass of benthic microalgae in the associated sediments and of green macroalgae on the engineered sediments. Landscape ecology metrics were calculated to describe the engineered sediment physical complexity, which can affect the presence and abundance of the different basal resources, their redistribution at the habitat scale and their dietary availability. The two tools were associated with classic field surveys to estimate the cover of potential trophic competitors. To investigate the different spatial scales of variations, Moran Eigenvector Maps were built using the 75 x 75 m grid used for the sampling of the two suspension-feeders. The second part (article 3) moves away from particular suspension-feeders and looks into how the establishment of an engineer species modifies local food webs using convex hull area and standard ellipse area. In addition, we address the place of autochthonous (benthic microalgae and green macroalgae) vs allochthonous (phytoplankton) food sources in the trophic functioning of the engineered and non-engineered habitat using mixing models. The mixing models outputs allows the evaluation of the trophic competition between the main suspension feeders living in the engineered sediment.

In the last two chapters, I address the functioning of the engineered habitat either through direct measurements or through the use of integrative functional and isotopic diversity indices. First (article 4), we measured biogeochemical fluxes taking place in engineered and non-engineered soft sediments, to evaluate how the establishment of a structural engineer modified these key functions of benthic habitats. Then, focusing on the engineered sediments, the links between diversity measured using species or biological traits and the measured ecosystem functions were investigated. This allowed the evaluation of the effects increasing disturbances to the engineered sediments can have on its functioning. Second (article 5), we investigated the complementary and/or redundancy of a set of functional and isotopic diversity indices in the context of an increasingly disturbed engineered habitat. According to the framework developed by Devictor et al. (2010a), the functional diversity indices and the isotopic diversity indices were considered as proxies of respectively, the fundamental and realized ecological niches of the engineered habitat. In this context, the combined use of these two types of indices provided use information on processes shaping the engineered habitat.

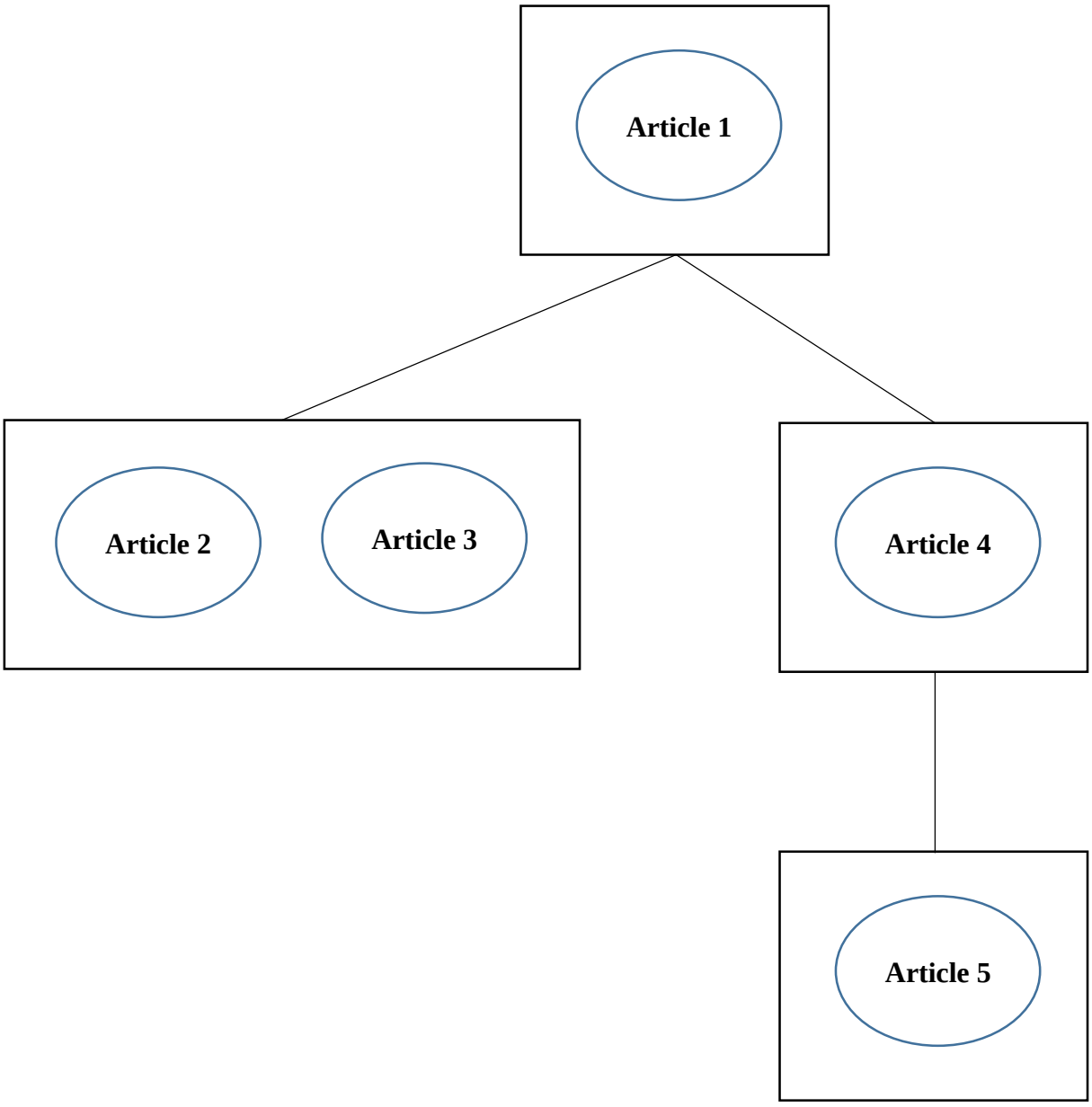

Figure 13. Global framework presenting the organization of this study into four different chapters (black boxes). The first, third and fourth chapters are each composed of one article (blue ellipses) while the second chapter is composed of two articles.

7. Sampling strategy

Articles 1, 3 and 5 are based on the same two sampling campaigns that took place in late February (further identified as winter) and late September (further identified as summer) 2015 (Table 3). Article 2 is based on an independent two-day sampling campaign that took place in April 2015 (one

day) and May 2015 (one day). Finally, article 4 is based on a last batch of independent samples gathered in April 2015 (two days), September 2015 (two days) and February 2016 (two days) in the Sainte-Anne reef area, to perform benthic core incubations (Table 2). I was involved in all the aforementioned sampling campaigns.

Table 2 Articles presented in this manuscript and corresponding sampling campaign.

	"winter and summer" sampling	"isoscape" sampling	"benthic fluxes" sampling
Article 1	**X**		
Article 2		**X**	
Article 3	**X**		
Article 4			**X**
Article 5	**X**		

Table 3 Samples collected for the first article which correspond to the "winter and summer" sampling campaign.

Sampling dates	2 dates: late February 2015 (winter) and late September 2015 (summer)		
Sampling area	Control	Sainte-Anne reef	
Stations	10	10 coupled stations (one associated sediment station and one engineered sediment station)	
Sediment type	Control sediment	Associated sediment	Engineered sediment
Environmental parameters	**n° of replicates / station of each sediment type**		
Grain size distribution	3 cores (19 cm², 5 cm depth)	3 cores (19 cm², 5 cm depth)	3 samples (collection of small parts, 8x3 cm)
Organic matter content	3 cores (57 cm², 1 cm depth)	3 cores (57 cm², 1 cm depth)	No samples
Chlorophyll a and pheopigment concentrations	3 cores (57 cm², 1 cm depth)	3 cores (57 cm², 1 cm depth)	No samples
Soluble and insoluble carbohydrate concentration	3 cores (57 cm², 1 cm depth)	3 cores (57 cm², 1 cm depth)	No samples
Macrofauna taxonomic diversity	**n° of replicates / station of each sediment type**		

Macrofauna > 1mm	3 cores (269 cm², 15 cm depth)	3 cores (269 cm², 15 cm depth)	3 cores (269 cm², 15 cm depth)
Macrofauna > 5mm	3 quadrats (1 m², 5 cm depth)	3 quadrats (1 m², 5 cm depth)	3 quadrats (1 m², hand sampling)

The second article (chapter 2 part 1) is based on the independent "isoscape" sampling campaign (Table 4). Here, only one sampling area was considered, the Sainte-Anne reef area and the sampling was performed according to a regular 75 x 75 m grid covering all the engineered sediments and representing 283 stations.

Table 4 Independent and explanatory variables along with the corresponding raw data and sampling dates ("isoscape" sampling), considered in the second article.

Raw data	Sampling date	Final data for each station	Independant variable	Explanatory variable
3 to 10 adult *Sabellaria alveolata* individuals	May 2015 (one day)	Mean *S. alveolata* carbon isotopic composition (3 pooled individuals)	X	
1 to 5 *Mytilus* cf. *galloprovincialis* individuals	May 2015 (one day)	Mean *M.* cf. *galloprovincialis* carbon isotopic composition (1 to 3 pooled individuals)	X	
Reef health state survey	April 2015 (one day)	Mean *M.* cf. *galloprovincialis* cover (3 replicates)		X
		Mean *Magallana gigas* cover (3 replicates)		X
Multispectral image of the reef	September 2015 (one day)	Engineered sediment mean normalized difference vegetation index (NDVI) value (proxy for *Ulva* spp. biomass)		X
		Associated sediment mean NDVI value (proxy for microphytobenthos biomass)		X
Aerial photography of the reef	August 2014 (one day)	Set of landscape ecology metrics calculated using FRAGSTAT software		X

The third article (chapter 2 part 2) is based on a monthly survey (January 2015 to February 2016) of the primary producers at the base of the food webs and on the « winter and summer » sampling campaign during which the consumers were sampled in the control and Sainte-Anne reef areas (Table 5, 6 and 7).

Table 5 Sampling dates of the primary producers and consumers along with the sampling area (control and reef), with in grey the months when the sampling took place and the cross indicating that the sample was used to calculate the mean and standard deviations of the carbon and nitrogen isotopic compositions of the primary producers. These values are used in the mixing models and displayed on the isotopic biplots (see article 3). For the particulate organic matter (POM), the sampling took place just before high tide seaward of the Sainte-Anne reef. We considered it to be distributed homogeneously at the scale of the central part of the MSMB and consequently to have the same isotope composition at the reef and control sites. POM : particulate organic matter, MPB : microphytobenthos, SOM : sediment organic matter.

Sampling months	01-15	02-15	03-15	04-15	05-15	06-15	07-15	08-15	09-15	10-15	11-15	12-15	01-16
POM	x	x	x	x		x				x	x	x	x
MPB reef				x	x	x	x	x	x				
MPB control													
SOM reef													
SOM control													
***Ulva* spp. reef**		x	x	x	x	x	x	x	x	x			x
Consumers reef													
Consumers control													

Table 6 Primary producer sampling (except the particulate organic matter which was sampled in the subtidal zone in front of the Sainte-Anne reef and considered to supply both the Sainte-Anne reef area and the control area) campaign implemented in the third article. MPB: microphytobenthos, SOM: sediment organic matter**.**

Area	**Control**	**Sainte-Anne reef**	
Sampling dates	Late February and late September 2015 (cf. chapter 1)	Once every month from January 2015 to January 2016	
Stations (every month except February and September 2015)	No samples	2 stations : one in the undisturbed reef part and the other in the disturbed reef part	
Stations (February and September 2015)	10 stations (cf. chapter 1)	10 coupled stations (one associated sediment station and one engineered sediment station) cf. chapter 1	
Sediment type	Control sediment	Associated sediment	Engineered sediment
	n° of replicates / station of each sediment type		
MPB	3 cores (57 cm², 1 cm depth)	3 cores (57 cm², 1 cm depth)	No samples
SOM	3 cores (57 cm², 1 cm depth)	3 cores (57 cm², 1 cm depth)	No samples
***Ulva* spp.**	No samples	No samples	1 sample

Table 7 Consumer sampling campaign implemented in the third article.

Sampling dates	2 dates: late February 2015 (winter) and late September 2015 (summer)		
Sampling area	Control	Sainte-Anne reef	
Stations (cf. chapter 1)	10	10 coupled stations (one associated sediment station and one engineered sediment station)	
Sediment type	Control sediment	Associated sediment	Engineered sediment
	n° of replicates / station of each sediment type		
Macrofauna > 1mm for biomass estimation (cf. chapter 1)	3 cores (269 cm², 15 cm depth)	3 cores (269 cm², 15 cm depth)	3 cores (269 cm², 15 cm depth)
Macrofauna > 1mm for isotopic compositions	1 core (269 cm², 15 cm depth)	1 core (269 cm², 15 cm depth)	1 core (269 cm², 15 cm depth)
Macrofauna > 5mm for biomass estimation (cf. chapter 1) and isotopic compositions	3 quadrats (1 m², 5 cm depth)	3 quadrats (1 m², 5 cm depth)	3 quadrats (1 m², hand sampling)
Mobile megafauna > 20mm for biomass estimation and isotopic compositions	6 fyke nets in the control area placed for 24h (estimated sampled surface 6869 m²)	6 fyke nets in the Sainte-Anne reef area placed for 24h (estimated sampled surface 6869 m²)	

The fourth article (chapter 3) is based on an independant sampling campaign performed in the Sainte-Anne reef area and at three different dates. This sampling was explicitely done to measure different biogeochemical fluxes in engineered and non-engineered sediments.

Table 8 "Benthic fluxes" sampling campaign implemented in the fourth article.

Sampling area	**Sainte-Anne reef area**			
Sampling dates	3 dates: April 2015 (spring), September 2015 (summer) and February 2016 (winter)			
Sediment type	Muddy sediment (soft sediment)	Sandy sediment (soft sediment)	Undisturbed engineered sediment	Disturbed engineered sediment
N° of sampled cores for incubations	4 cores (15 cm diameter, depth 30 cm)	4 cores (15 cm diameter, depth 30 cm)	4 cores (15 cm diameter, depth 30 cm)	4 cores (15 cm diameter, depth 30 cm)
Biogeochemical fluxes (independent variables)	Sediment oxygen demand, ammonium, nitrates and nitrites			
Macrofauna (explanatory variables)	After the incubation, all the macrofauna > 1mm present in each core was collected for calculation of structural and functional diversity indices and abundance and biomass estimation			

The fifth article (chapter 4) is based on data gathered during the "winter and summer" sampling campaign.

Table 9 Data from the "winter and summer" sampling campaign used in the fifth article.

Sampling area	**Sainte-Anne reef area**
Sampling dates	2 dates: late February 2015 (winter) and late September 2015 (summer)
Stations	10 stations composed of two coupled associated and engineered sediment stations (cf. chapter 1)
Sediment type	Associated and engineered sediment
***Sabellaria alveolata* adult density**	Calculated using the mean density (mean of three replicates, see chapter 1) and opercular diameter to identify the adults
Functional diversity indices	Calculated using the mean biomass (mean of three replicates, see chapter 1) and biological traits of each species
Isotopic diversity indices	Calculated using the mean biomass (mean of three replicates, see chapter 1) and the mean isotopic composition (see chapter 2 part 2) of each species

Chapter I

The first chapter of this manuscript replaces the reef-builder *Sabellaria alveolata* in the general framework of physical ecosystem engineering. This part is composed of one article published in 2017 in Estuarine Coastal and Shelf Science.

This chapter presents a comparison between a control soft sediment considered as the baseline state before the establishment of the engineer (control sediments), the hardened sediments in which the engineer lives (engineered sediments) and the soft sediments present around these engineered sediments and considered as being potentially influenced by the engineer (associated sediments). First, this comparison focuses on environmental parameters like the grain-size distribution, the organic matter content and the chlorophyll *a* concentration. Then, the macrofaunal changes are investigated using classic taxonomic indices (species richness, abundance, Hill's indices) and by looking into the macrofauna assemblages (PCoA). The link between the environmental and biotic changes is studied using a distance based redundancy analysis. The last part focuses on a disturbance gradient at the engineered sediment scale and looks into the beta diversity along this gradient.

This study demonstrates that *S. alveolata* is a highly structuring species since it modifies the overall local environment (engineered and associated sediments) and the species assemblage, creating a biodiversity hotspot and an original macrofauna assemblage. The beta diversity measures highlight the role of the reef as an important recruitment zone, a role enhanced by disturbance.

Article 1 - Interplay between abiotic factors and species assemblages mediated by the ecosystem engineer *Sabellaria alveolata* (Annelida: Polychaeta)

Auriane G. Jones [a,b,c], Stanislas F. Dubois [a], Nicolas Desroy [b], Jérôme Fournier [c,d]

Article published in Estuarine Coastal and Shelf Science

[a] IFREMER, Laboratoire Centre de Bretagne, DYNECO LEBCO, 29280 Plouzané, France

[b] IFREMER, Laboratoire Environnement et Ressources Bretagne nord, 38 rue du Port Blanc, BP 80108, 35801 Dinard cedex, France

[c] CNRS, UMR 7208 BOREA, 61 rue Buffon, CP 53, 75231 Paris cedex 05, France

[d] MNHN, Station de Biologie Marine, BP 225, 29182 Concarneau cedex, France

Abstract

Sabellaria alveolata is a gregarious polychaete that uses sand particles to build three-dimensional structures known as reefs, fixed atop rocks or built on soft sediments. These structures are known to modify the local grain-size distribution and to host a highly diversified macrofauna, altered when the reef undergoes disturbances. The goal of this study was to investigate the different sedimentary and biological changes associated with the presence of a *S. alveolata* reef over two contrasting seasons (late winter and late summer), and how these changes were linked. Three different sediments were considered: the engineered sediment (the actual reef), the associated sediment (the soft sediment surrounding the reef structures) and a control soft sediment (*i.e.* no reef structures in close proximity). Univariate and multivariate comparisons of grain-size distribution, soft sediment characteristics (organic matter content, chlorophyll *a*, pheopigments and carbohydrate concentrations) and macrofauna were conducted between the different sediment types at both seasons and between the two seasons for each sediment type. A distance-based redundancy analyses (dbRDA) was used to investigate the link between the different environmental parameters and the macrofauna assemblages. Finally, we focused on a disturbance continuum of the engineered sediments proxied by an increase in the mud present in these sediments. The effects of a continuous and increasing disturbance on the associated fauna were investigated using pairwise beta diversity indices (Sørensen and Bray-Curtis dissimilarities and their decomposition into turnover and nestedness). Results showed a significant effect of the reef on the local sediment distribution (coarser sediments compared to the control) and on the benthic primary production (higher in the associated sediments). At both seasons, *S. alveolata* biomass and sediment principal mode were the environmental parameters which best differentiated the engineered, associated and control sediment assemblages. These two parameters are under the ecosystem engineer's influence stressing its importance in structuring benthic macrofauna. Furthermore, in late summer but not in late winter, presence/absence and abundance-based beta diversity were positively correlated to our disturbance proxy (mud content) a tendency driven by a species replacement and a rise in the associated fauna density. Our first set of results highlight the importance of *S. alveolata* reefs as benthic primary production enhancers via their physical structure and their biological activity. The results obtained using beta diversity indices emphasize the importance of recruitment in structuring the reef's macrofauna and – paradoxically – the ecological value of *S. alveolata* degraded forms as biodiversity and recruitment promoters.

1. Introduction

Ecosystem engineers are organisms capable of modifying their local environment through their physical presence (*i.e.* autogenic engineers) and/or their biological activity (*i.e.* allogenic engineers), "directly or indirectly modulating the availability of resources to other species" (Jones et al., 1994). Ultimately, these species maintain, modify, create or even destroy habitats (Bouma et al., 2009; Jones et al., 1994). The abiotic modifications caused by ecosystem engineers can lead to facilitation for some organisms (Hacker and Gaines, 1997) and inhibition through negative species interaction for others (Bouma et al., 2009; Jones et al., 1997). Nonetheless, bioengineered habitats are often reported to host a more diverse species assemblage than the adjoining non-engineered habitats (Ataide et al., 2014; De Smet et al., 2015; Jones et al., 1997; Stachowicz, 2001). Physical ecosystem engineering appears to be particularly important where the environment is extreme (*e.g.* thermic, hydrodynamic and/or hydric stress), like in temperate intertidal areas (Bouma et al., 2009; Jones et al., 1997). Indeed, according to Jones et al. (1997, 1994), these extreme conditions might have favored the selection of "extended phenotype engineers" through enhanced survival of the engineer and the cohabiting fauna (Dawkins, 1982). These engineer species create complex habitats that reduce local pressures such as predation or thermal stress, whilst increasing biodiversity (Bouma et al., 2009). Ultimately, such favorable environmental changes can lead to an interesting paradox where "the spatial extent of the realized niche of a species can be larger than the spatial range predicted by the fundamental niche" as described by Bruno et al. (2003) and reported for mussels and barnacles in *Ascophyllum nodosum* canopies by Bertness et al. (1999).

Temperate coasts host a striking number of ecosystem engineering species, spanning from mollusks (for a review see Gutiérrez et al. (2003)) and polychaetes (*e.g. Lanice conchilega* (De Smet et al., 2015)) to canopy-forming algae (*e.g. Ascophyllum nodosum* (Bertness et al., 1999)). Along the European coastline, a particular ecosystem engineer has the ability to build three-dimensional structures on top of sediments qualified as reefs (Holt et al., 1998). This species is a common gregarious tubiculous polychaete called *Sabellaria alveolata* (Linnaeus, 1767), a.k.a. the honeycomb worm. It generally lives in the intertidal zone from mid to low tide levels and can be found from Scotland and Ireland to Morocco (Muir et al., 2016). *Sabellaria alveolata* uses sand particles remobilized by waves and tidal action to build the tube in which it lives (Le Cam et al., 2011). Since the pelagic larvae are attracted by the L-dopa present in the organic cement produced by the adult worms for their tube-building activity, they will tend to settle on existing reefs (Pawlik, 1988b; Wilson, 1968). This phenomenon coupled with favorable environmental conditions (*i.e.* grain-size structure, hydrodynamic processes, food availability and water temperature) can lead to the development of large biogenic reefs (Holt et al., 1998). These structures are commonly found on rocky substrata as veneers or hummocks where they rarely exceed 50 cm in height for a few tens of square meters but in some rare instances, they can be found in soft bottom areas where they can grow up to two meters in height and several hectares in size (Holt et al.,

1998; Noernberg et al., 2010). The largest of these formations, which is also the largest biogenic habitat in Europe, is located in the Mont Saint-Michel Bay (MSMB) in France (Desroy et al., 2011; Dubois et al., 2002).

The research around this species has mainly focused on its physiology (*i.e.* reproduction, fecundity, feeding mode) (Dubois et al., 2003, 2005, 2006a, 2009) and its tube building activity (Fournier et al., 2010; Le Cam et al., 2011). Other studies have looked into the ecology of reefs with a particular interest on the associated fauna (Dias and Paula, 2001; Porta and Nicoletti, 2009; Schlund et al., 2016) and factors influencing it such as the reef's different growth stages (Dubois et al., 2002), epibionts (Dubois et al., 2006b), human trampling (Plicanti et al., 2016) and ecological status (Desroy et al., 2011). A large part of these studies has focused on *Sabellaria alveolata* reefs on rocky substrata and not on soft sediment. Reefs developing on soft sediment are far less frequent along the European coast (*i.e.* MSMB and Bourgneuf Bay in France) (Holt et al., 1998). Nonetheless, they constitute exceptional locations composed of two distinct entities: the actual three-dimensional reef structures (engineered sediment), which is spatially discontinuous and the soft sediment present between the reef structures (associated sediment) (Desroy et al., 2011). Several kilometers separate them from the nearest rocky shore which signifies, in contrast to the veneer form of *S. alveolata* structures, complete isolation from most of the juvenile and adult fauna inhabiting these rocky shores. Furthermore, their physical borders are easy to visualize against the surrounding soft sediment. These sites give us the chance to study different components of *S. alveolata*'s engineering effect (Passarelli et al., 2014; Wright et al., 2006). This engineering effect can be seen from both an environmental and a biological perspective by looking at how the ecosystem engineer modifies the local sedimentary characteristics and how the biodiversity changes between a control sediment, the associated and the engineered sediments. The control soft sediment represents the baseline or the unmodified state before the honeycomb worms start building reefs, hence representing a new structural state (Jones et al., 2010).

This biogenic habitat is not structurally homogenous, mainly due to multiple disturbances; direct natural disturbances such as storms and cold winters, direct anthropogenic disturbances such as trampling and indirect anthropogenic disturbances through shellfish farming and coastal engineering. These disturbances lead to a gradual modification of the reef visible through disaggregation, increasing fine sediments, decreasing ecosystem engineer density and increasing epibiont cover, causing a number of changes in the associated fauna (Dubois et al., 2006b, 2002; Plicanti et al., 2016). Modifications of the associated fauna have been investigated in several categorical ways but never along a disturbance continuum (Dubois et al., 2006b, 2002; Plicanti et al., 2016). To understand the changes in the associated fauna along this continuum, we chose to focus on the beta diversity seen as "the extent of change in community composition" as defined by Whittaker (1960) and on an abundance-based dissimilarity measurement using the Bray-Curtis dissimilarity. Analyzing beta diversity in a *S. alveolata* reef can help us understand the functioning of this biogenic habitat and give more relevant information to decision makers regarding conservation issues. First, taking into account the three previously defined sediment

types (control, associated and engineered sediments), we tested in a categorical way, the following hypotheses: (1) the engineered sediment affects the different sedimentary characteristics of the associated sediment, especially grain-size, organic matter content and microphytobenthos and (2) the diversity and species composition of both the engineered and the associated sediments are different from the control sediment. We also looked into potential changes between late winter and late summer, regarding sediment composition and macrofauna assemblages for each sediment type. Then, using beta diversity and dissimilarity measurements, we tested the following hypothesis: an increasing disturbance of the engineered sediment promotes (1) beta diversity and more specifically species turnover and (2) abundance-based dissimilarity and more specifically abundance gradients.

2. Materials and methods

2.1. Study area

This study took place in the central part of the MSMB where the largest bioconstruction in Europe is located; the Sainte-Anne reef (48°38'700N and 1°40'100W), built by the honeycomb worm *Sabellaria alveolata* (Desroy et al., 2011). This reef is situated in the lower intertidal zone (*i.e.* between the - 2 and the - 4 m isobaths (Noernberg et al., 2010)), parallel to the coast and to the dominant tidal currents and also near important blue mussel (*Mytilus edulis*) cultures. In 2014, the maximal dimensions of the Sainte-Anne reef were 2.5 km in length for 1 km in width and the engineered sediment represented about 32 ha for about 128 ha of associated sediment (unpublished results). The area located in the central part of the bay and along the same isobath as the reef is characterized by medium to muddy sands (Bonnot-Courtois et al., 2009) and by a species poor "*Macoma balthica* community" (Dubois et al., 2002).

2.2. Sampling design and laboratory analyses

Two sampling areas were defined; the Sainte-Anne reef area and a control area. The reef area was composed of two sediment types, the engineered and the associated sediments (Figure 14). The control area was a soft sediment zone located 1.5 km North-East of the reef area and on the same bathymetric level. It was characteristic of the medium to muddy sands found in this part of the bay (Bonnot-Courtois et al., 2009). Sampling took place over a two-day period in late winter (late February) and late summer (late September). These two seasons were chosen because they are highly contrasted environmentally (*e.g.* hydro-sedimentary features) and biologically (*e.g.* recruitment patterns, species turnover, growth rates). Indeed, winter is a period of low biological activity and high environmental pressures (cold temperatures, wind and storms) while late summer is a post-recruitment period with a higher biological activity (Arbach Leloup et al., 2008; Cugier et al., 2010). Hence, sampling at these

two seasons helps us to have a more complete picture of the dynamics happening in our different study zones.

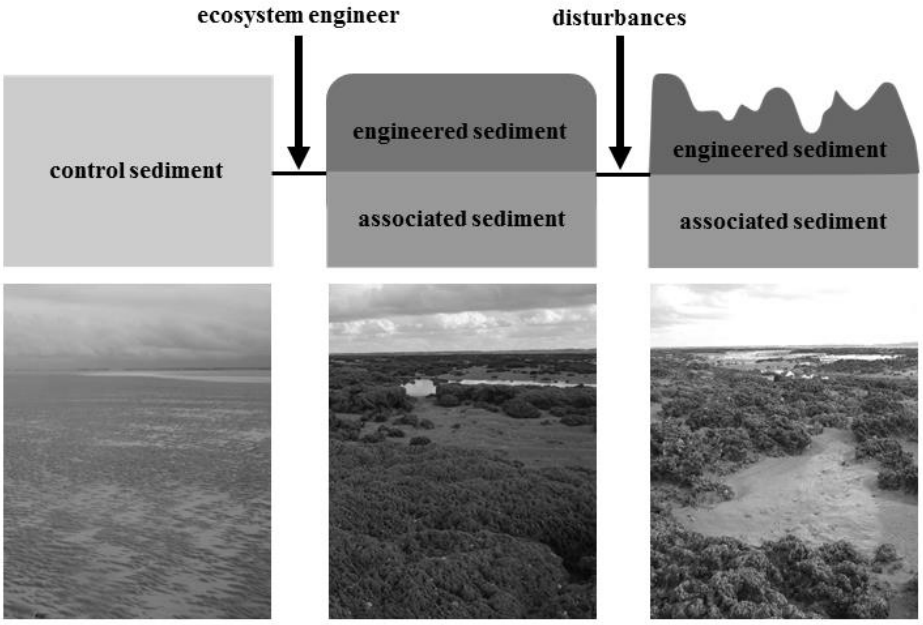

Figure 14. Schematic overview presenting the habitat modifications caused by (1) the establishment of an ecosystem engineer and (2) disturbances of the engineered sediment. Recruitment of *S. alveolata* leads to the formation of a biologically modified sediment (engineered sediment) and to a soft sediment under the influence of the engineered sediment (associated sediment). Engineered sediment then face direct (*e.g.* trampling, storms) and/or indirect disturbances (*e.g.* shellfish farming) which can lead to a gradual alteration.

To investigate the effects of *S. alveolata* on diversity and species composition, we compared the macrofauna associated with the three different sediment types: the *S. alveolata* reefs, the sediments present around these structures and the control soft sediments. For each sediment type (*i.e.* engineered, associated and control sediment, Figure 14), ten stations were sampled. Every engineered sediment station was paired with an associated sediment station, in order to investigate how the reef structures modify the adjoining soft sediment. The stations were at least 75 m apart and at each station, six samples separated by at least 5 m were randomly taken at low tide. The first three samples were done using a 18.5 cm side corer (269 cm^2) to a depth of 15 cm (core samples). For engineered sediments, this depth corresponds to the layer where *Sabellaria alveolata* and more than 90% of all species live (Dubois et al., 2002). The other three samples were done using a 1 m^2 quadrat in order to estimate the over dispersed macrofauna, mainly composed of bivalves and gastropods (quadrat samples). All engineered sediment samples (core and quadrat samples) were taken at least 1 m from the reef edge to avoid a known border effect on the macrofauna diversity (Gruet, 1972), while the associated sediment samples (core and quadrat samples) were taken at least 1 m away from the reef structures. The soft sediment core samples were sieved through a 1-mm square mesh on site while the engineered sediment core samples were taken

back to the laboratory where they were broken apart under water and the fauna retained on a 1-mm square mesh was collected. Associated and control quadrat samples were done by sieving on site the first 5 cm of sediment through a 5-mm square mesh. For the engineered quadrat samples, we sampled by hand all the visible macrofauna located on the reef and inside the reef interstices. All core and quadrat samples were fixed in a 5% formaldehyde solution, after which all the macrofauna was sorted, counted and identified to the species or genus level (except for nemerteans, oligochaetes and nematodes) and finally preserved in a 70% ethanol solution. For each engineered sediment core sample, all the *Sabellaria alveolata* were weighted (total wet weight).

To look at how the ecosystem engineer modifies its environment, we randomly collected three sediment samples for grain-size distribution, total amount of organic matter (TOM), pigment concentration (*i.e.* chlorophyll *a* and pheopigments) and total carbohydrate concentration (*i.e.* soluble and insoluble carbohydrates), at each associated and control sediment station. For the grain-size distribution, the first 5 cm of sediments were sampled using a small plastic core (19 cm^2). For all the other sedimentary characteristics, only the first centimeter of sediment was sampled using a plastic petri dish (57 cm^2). Additional samples were collected in order to characterize the sediments constituting the *Sabellaria alveolata* tubes as well as the sediments potentially trapped within the biogenic structure. These consisted in randomly collecting three small reef parts (about 8 x 3 cm) in each engineered sediment station. Sediment grain-size distribution was obtained by mechanical sieving using AFNOR calibrated sieves (from 25 mm to 63 µm) and granulometric parameters were estimated using the 'G2Sd' package in R v. 3.3.0 (Fournier et al., 2014). Prior to mechanical sieving, the engineered sediments were cautiously broken into their original elements, *i.e.* mostly bioclasts as evidenced in Le Cam et al. (2011). For all the other analyses, the sediments were first freeze-dried in order to work on dry matter. TOM was determined as the difference between the weight of freeze-dried sediment and the weight after 4 hours at 450° (Aminot and Kerouel, 2004). Pigment concentrations ($\mu g.g^{-1}$ dry sediment) were estimated using the monochromatic technique (Lorenzen, 1967) described in Aminot and Kerouel (2004). The chlorophyll *a* (Chl *a*) concentration was used as a proxy for microphytobenthos (MPB) biomass (Jeffrey et al., 1997) while pheopigments (Pheo) concentration gave us information about the amount of degraded photoautotrophs. Soluble carbohydrates (Sol) present in the sediment were extracted by hydrolysis (100°C for 45 min), after which the pellets were treated with sulfuric acid (H_2SO_4) and placed 4 hours at 100°C in order to obtain the insoluble carbohydrates (Ins). Sol and Ins concentrations ($\mu g.g^{-1}$ dry sediment) were then estimated by colorimetric phenol sulfuric dosage (Dubois et al., 1956). Sol were considered as being an important labile source of carbon for consumers living in the sediment such as bacteria and deposit-feeding invertebrates (Bellinger et al., 2009) while the insoluble carbohydrates to soluble carbohydrates ratio (Ins/Sol) was used as a proxy for the C/N ratio and as a TOM degradation index (Delmas, 1983).

2.3. Data analysis

2.3.1. Biological and environmental engineering effects

Since macrofauna was sampled using two different techniques (cores and quadrats), densities of species were estimated using the catch-per-unit-effort (CPUE) method, *i.e.* the ratio between the total catch and the total amount of effort used to harvest the catch (Skalski et al., 2005). At one sampling location, when a species was only collected by core or quadrat, its density was estimated using the corresponding sampling surface. However, when a species was sampled by both methods, cumulated abundances were divided by the sum of each gear's CPUE. This estimation method was used for 17 species in late winter and 15 in late summer, taking into account all three sediment types. Species' densities were calculated using the formula:

$$\text{density}_{\text{A}}\ (\text{ind.}\,\text{m}^2) = \frac{(\text{abundance}_{\text{Aq}} + \text{abundance}_{\text{Ac}})}{(\text{CPUE}_{\text{q}} + \text{CPUE}_{\text{c}})}$$

where $density_A$ is species' A abundance per m², $abundance_{Aq}$ is species' A abundance using the quadrat, $abundance_{Ac}$ is species' A abundance using the core, $CPUE_q$ is the quadrat's catch-per-unit-effort (1 m²) and $CPUE_c$ is the core's catch-per-unit-effort (0.0269 m²).

To assess the effect of *Sabellaria alveolata* on the associated macrofauna and validate our *a priori* grouping into engineered, associated and control sediments, Principal Coordinates Analysis (PCO) were performed for the late winter and late summer data sets. Analyses were performed on a Bray-Curtis similarity matrix calculated from log-transformed densities after *S. alveolata* was removed from the matrix, in order to take into account only the species associated with this sediment type. Indeed, because of its high abundance (*i.e.* on average, 63% of the total abundance), the single presence of *S. alveolata* would automatically cause a strong grouping of engineered sediment samples. Species present in only one sample (*i.e.* in less than 2% of all samples) were excluded from the initial matrix. To identify species typifying each sediment, species that correlated more than 60% with one of the first two axes (*i.e.* Spearman correlations) were plotted on each PCO. In parallel, a one-way univariate permutational ANOVA (permanova) was performed on the same species density matrices as for the PCOs, in order to evaluate if there was a significant difference in the species composition of each sediment type.

Finally, the macrofauna diversity of each replicate (core and associated quadrat) sampled in late winter and late summer, was assessed using Hill's indices; N0 (number of species), N1 (exp (H') where H' is the Shannon-Winner diversity ($\log_e$)) and N2 (1/D where D is the Simpson's dominance index (Hill, 1973)) as recommended by Gray (2000) and the total macrofauna density. These indices inform how the total abundance is partitioned between the different species (Gray, 2000; Whittaker, 1972 for details). Densities calculated using the CPUE method and for 1 m² as previously detailed, were used to calculate N1 and N2. For each replicate, N0 was calculated as the sum of the species richness recorded in the core and the species richness recorded in the associated quadrat. For N0, N1 and N2, *S. alveolata*

was either kept or removed from the initial data in order to investigate how this species influences the partitioning of the associated fauna abundance.

To test for significant differences between the three sediment types for the different grain size and macrofauna descriptors and because none of the descriptors fulfilled normality of distribution and homogeneity of variance, permanovas were performed, with sediment type considered as a fixed factor. We used Euclidian distance as a distance measure and ran 9999 permutations for each test. If the main test was significant, pairwise tests were performed. Effect of the presence of the engineered sediment on soft sediment environmental parameters (TOM, Chl *a*, Pheo and Ins/Sol) was investigated by comparing these parameters between associated and control sediments, also using permanovas. Prior to performing permanovas, we tested for homogeneity of dispersions using the PERMDISP PRIMER routine (Anderson et al., 2008). When raw data presented significantly different dispersions between the three sediment types ($p < 0.05$), it was log transformed (in late winter: principal mode, TOM, Chl *a*, Pheo, macrofauna density with and without *S. alveolata*, N0 with and without *S. alveolata* and N2 with *S. alveolata*, in late summer: macrofauna density with and without *S. alveolata*, N0 with and without *S. alveolata* and N1 without *S. alveolata*). When log transformation did not lead to homogenous dispersions (in late winter:% mud,% sand and Sol, in late summer: TOM, Chl *a*, Sol, N1 and N2 calculated with *S. alveolata*), non-parametric statistical tests were performed (Kruskal-Wallis test for the granulometric and macrofauna parameters and Wilcoxon-Mann-Whitney for the other environmental parameters).

In order to evaluate if the different environmental and macrofauna parameters were significantly different between late winter and late summer for each sediment type, one-factor permanovas were performed, with season considered as a fixed factor. We chose to perform one-factor rather than two-factor univariate analysis of variance (in this case with sediment type and season as fixed factors), because we lacked replication inside each season for our different sediment types (Underwood, 1997). As previously mentioned, permanovas (9999 permutations) were used rather than t-tests because none of the investigated variables were normally distributed. Homogeneity of dispersions was also tested (PERMDISP) and data was transformed when necessary (square-root transformation for TOM in the associated sediments, log transformation for macrofauna density with *S. alveolata* in the control sediments and for macrofauna density without *S. alveolata* in the engineered sediments). The Permanovas, PERMDISP routines and PCOs were performed using the PRIMER v6 software with the PERMANOVA+ add-on (Anderson et al., 2008). *Post-hoc* Kruskal-Wallis tests were performed with the 'kruskalmc' function from the 'pgirmess' package (Giraudoux, 2016) using R version 3.3.0 (R Core Team, 2016).

2.3.2. Linking environmental and biological engineering effects

The relationship between the environmental characteristics and the macrofauna present in the three sediment types was investigated using distance-based linear models (DistLM). In line with

Legendre and Anderson (1999) and McArdle and Anderson (2001), DistLM models were coupled to a distance-based redundancy analysis (dbRDA) to define the best fitted model in a multi-dimensional space in a way similar to a constrained PCO. DistLM models were built using the Bayesian Information Criterion (BIC) to identify "good" models and the 'best' procedure to select the variables according to the BIC. Prior to the DistLM and dbRDA analysis, the environmental parameters were displayed using Draftsman plots and the ones presenting an important skewness were transformed to approach normality (Anderson et al., 2008). If two predictor variables were strongly correlated ($r^2 > 0.80$), one of them was removed from the analysis in order to avoid multi-collinearity (Dormann et al., 2013). Except for the grain-size data, environmental parameters used to characterize an engineered sediment sample were the same as for its corresponding associated sediment sample. For late winter, the final predictor data set contained the% sand, Pheo (both square-root transformed),% mud, TOM, *S. alveolata* biomass (all three fourth-root transformed), principal mode and Ins/Sol (both log transformed). For late summer, the final predictor data set was the same as for late winter, except the% sand which was removed (absolute correlation with% mud > 0.8). *S. alveolata* biomass was used rather than abundance because this parameter provides more information about ecosystem functioning (Cardinale et al., 2013). *S. alveolata* biomass was considered as a predictor variable since it physically modifies its environment and it was consequently removed from the macrofauna data set. The DistLM models and dbRDA analysis were performed using the PRIMER v6 software with the PERMANOVA+ add-on (Anderson et al., 2008).

2.3.3. Disturbances and biological engineering effect

At its climax, a *S. alveolata* reef is formed by 100% honeycomb worm tubes, leaving virtually no space for infaunal organisms. When natural or anthropogenic disturbances (*e.g.* storms, trampling) physically damage the reef, tubes are destroyed, freeing up space. This new available space can be filled either with other organisms such as the oyster *Magallana gigas* (formerly known as *Crassostrea gigas*) or by fine particles. Fine particles accumulate from suspended sediments, or from the feces and pseudofeces of *S. alveolata* and other bivalves (biodeposition) (Dubois et al., 2006b). In either case, this fine sediment can end up trapped inside the *S. alveolata* reefs. Consequently, the increased deposition of mud inside the engineered sediments is the result of several different and often concomitant disturbances. Fine sediment deposition has previously been recognized as a significant disturbance to stream macroinvertebrates (Mathers et al., 2017) and benthic habitats (Balata et al., 2007; Mateos-Molina et al., 2015; Miller et al., 2002). Similarly, we chose to consider mud content as a proxy for disturbance. This proxy was also chosen because it is independent from *Sabellaria alveolata* population dynamics and physiological state. Finally, using the mud content makes the two seasons readily comparable.

Beta diversity was calculated using pairwise multivariate distances since they are independent of sample size and regional diversity (gamma diversity) allowing accurate potential comparisons among regions (Bennett and Gilbert, 2016). We chose to use the presence/absence based indices presented by

Baselga (2010) in order to partition total beta diversity, expressed by Sørensen dissimilarity (β_{sor}), into the turnover (β_{sim}) and nestedness (β_{nes}) components. In this case, $\beta_{sor} = \beta_{sim} + \beta_{nes}$. Under conditions of equal species richness, $\beta_{sor} = \beta_{sim}$ and $\beta_{nes} = 0$, while under conditions of unequal species richness, β_{sim} and β_{nes} vary between 0 and β_{sor}. Sørensen dissimilarity varies between 0 and 1, with 0 indicating that two samples have identical species list and 1 indicating no common species (Baselga, 2010). For β_{sim}, 0 indicates complete nestedness, and a maximal value of 1 can be found if in one of the two considered samples, there are no species recorded and in the other, the number of species is maximal (Koleff et al., 2003). To have a complementary vision of how disturbance affected the associated fauna abundance, the abundance-based dissimilarity (Bray-Curtis dissimilarity, d_{BC}) was also partitioned into balanced changes in abundance ($d_{BC\text{-}bal}$) and abundance gradients ($d_{BC\text{-}gra}$), which are closely related to turnover and nestedness components respectively (Baselga, 2013). These indices were computed after removing *S. alveolata* from the presence/absence and density matrices. They were calculated using the pairwise measures in order to have the beta diversity and the dissimilarities for each pair of samples (*i.e.* 435 pairs). Then, using Euclidian distance, all the mud content pairwise differences were calculated. Finally, using the different pairwise measures, we performed Mantel tests (9999 permutations) for late winter and late summer data, to test the null hypothesis of no relationship between the mud content distance matrix and each beta diversity matrix. A p-value below 0.05 indicates a significant correlation between the two investigated distance matrices, with the sign of the r-value indicating if the two matrices are positively or negatively associated. The beta diversity indices were computed using the 'beta.pair' function, and the Bray-Curtis dissimilarity indices using the 'bray.part' function, both from the 'betapart' R package (Baselga, 2013). The Mantel tests were performed using the 'mantel.rtest' function from the 'ade4' R package (Dray and Dufour, 2007).

To test the link between the macrofaunal assemblages based on their respective beta diversity and dissimilarity indices and the disturbance parameter (*i.e.* mud content), non-metric multidimensional scaling ordinations (nMDS) were successively performed for each index (β_{sor}, β_{sim}, β_{nes}, d_{BC}, $d_{BC\text{-}bal}$ and $d_{BC\text{-}gra}$) and at each sampling period (late winter and late summer) using the 'metaMDS' function of the 'MASS' R package (Venables and Ripley, 2002). Then, the 'envfit' function ('vegan' R package) was used to test if the mud content was significantly correlated with each ordination (Oksanen et al., 2016). When a correlation was significant, the mud contents were fitted and plotted on the given nMDS using the 'ordisurf' function of the 'vegan' R package (Oksanen et al., 2016). All these analyses were performed using R version 3.3.0 (R Core Team, 2016).

3. Results

3.1. Environmental engineering effect

Mean values of grain-size distribution parameters measured within each sediment type are reported in Table 10a. Analyses revealed significant differences between the sediment types for all tested metrics in late winter ($p < 0.001$) and for all but one in late summer (mud content). At both periods, there was a strong engineering effect on the principal mode marked by a significantly coarser sediment in the engineered and associated sediments than in the control sediments (Table 10a). In late winter, the sorting index S_0 was significantly lower in the engineered and associated sediments than in the control and mud content was significantly lower in the associated sediments than in the other two sediment types. Finally, the sand content was significantly higher in the engineered sediment relative to the other sediment types. In late summer, associated sediments had a higher sorting index than the engineered sediments and one comparable to the control sediments. Although associated sediments were also characterized by a higher mud content in late summer compared to late winter (permanova: $p = 0.0051$), no significant difference was observed between the three sediment types. For all grain-size parameters, the control sediments showed no significant changes between late winter and late summer (permanova: p(principal mode) = 0.23 , $p(S_0) = 0.60$, p(mud) = 0.37 and p(sand) = 0.42). The pattern was similar for the engineered sediments (permanova: p(principal mode) = 0.059 , $p(S_0) = 0.78$, p(mud) = 0.78 and p(sand) = 0.39). The associated sediments showed significant changes in their grain-size distribution between late winter and late summer. In late winter, they were much more homogenous than in late summer (Table 10) and they became significantly muddier between the two sampling campaigns (permanova: $p = 0.0051$) leading to a significant decrease in the principal mode (permanova = 0.025).

The comparison of sedimentary parameters revealed a strong engineering effect at both periods regarding TOM, Chl *a* and Sol (Table 10b, $p < 0.005$). In both seasons, TOM was consistently twice as high in the engineered environment than in the control zone. Organic matter content also showed a significant decrease between late winter and late summer in the reef zone (permanova: $p = 0.029$) and no significant temporal change in the control sediments (permanova: $p = 0.29$). Similarly, Chl *a* concentration was ten times higher in the soft sediments adjacent to the engineered structures than in the control and did not display any significant temporal changes in either the control (permanova: $p = 0.29$) or the associated sediments (permanova: $p = 0.72$). Sol concentration was also consistently four times higher in the reef environment than in the control and displayed a temporal stability similar to the Chl *a* (permanova: p(control) = 0.87 and p(associated) = 0.82). In late winter, the Pheo concentration was significantly higher in the control than in the associated sediments while in late summer, there was no significant difference. In both sediment types, Pheo concentrations did not show significant changes between the two sampling campaigns (permanova: p(control) = 0.10 and p(associated) = 0.11). Finally, Ins/Sol was not significantly different between associated and control sediments in late winter and late

Table 10 Mean values (± standard errors) for (a) the grain-size parameters of the three sediment types (engineered, associated and control) and (b) the environmental parameters for the associated and the control sediments. Significant differences ($p < 0.05$) of the one-way ANOVAs are in bold and for (a), post-hoc results are designated by superscript letters indicating homogenous groups of samples. TOM: total organic matter content, Chl a: chlorophyll a concentration, Pheo: pheopigments concentration, Sol: soluble carbohydrates concentration, Ins/Sol: ratio of the concentration of insoluble carbohydrates on soluble carbohydrates.

(a)	Late winter				Late summer			
	Engineered	*Associated*	*Control*	*p-value*	*Engineered*	*Associated*	*Control*	*p-value*
Principal mode (µm)	688 ± 35^{a}	1010 ± 118^{a}	186 ± 8^{b}	< **0.001**	618 ± 8^{a}	692 ± 74^{a}	201 ± 9^{b}	< **0.001**
Sorting index (S_0)	1.71 ± 0.05^{a}	1.72 ± 0.05^{a}	2.97 ± 0.34^{b}	< **0.001**	1.69 ± 0.05^{a}	2.98 ± 0.45^{b}	2.70 ± 0.37^{b}	**0.018**
Mud (%) (< 63 µm)	10.00 ± 0.83^{a}	1.84 ± 0.44^{b}	27.38 ± 3.62^{a}	< **0.001**	9.59 ± 1.22^{a}	20.47 ± 5.37^{a}	21.61 ± 5.23^{a}	0.106
Sand (%) (63-200 µm)	87.19 ± 0.83^{a}	76.74 ± 1.40^{b}	71.69 ± 3.53^{b}	< **0.001**	85.77 ± 1.40^{a}	65.11 ± 4.09^{b}	76.79 ± 5.17^{ab}	**0.001**

(b)	Late winter			Late summer		
	Associated	*Control*	*p-value*	*Associated*	*Control*	*p-value*
TOM (%)	6.96 ± 0.72	2.70 ± 0.30	**<0.001**	4.91 ± 0.59	2.26 ± 0.28	**<0.001**
Chl *a* (µg.g^{-1} sediment)	12.21 ± 2.49	2.83 ± 0.58	**0.0022**	13.39 ± 2.24	3.92 ± 0.88	**0.002**
Pheo (µg.g^{-1} sediment)	14.54 ± 0.36	16.18 ± 0.36	**0.0014**	15.56 ± 0.53	15.41 ± 0.29	0.826
Sol (µg.g^{-1} sediment)	442 ± 72	113 ± 25	**0.0027**	467 ± 78	120 ± 25	**<0.001**
Ins/Sol	8.59 ± 2.29	8.63 ± 0.37	0.9998	5.96 ± 0.43	6.32 ± 0.33	0.5175

summer, and was significantly higher in late winter compared to late summer for the control sediments (permanova: $p = 0.0001$). This temporal pattern was not detected in the associated sediments (permanova: $p = 0.28$) probably because of the important variability in late winter (Table 10).

3.2. Biological engineering effect

In late winter, 9244 organisms belonging to 121 different taxa were sampled in the cores and 8478 organisms belonging to 26 different taxa were sampled with the quadrats (see the Appendix for a complete list of species). Comparatively, in late summer more organisms and taxa were sampled with the cores (23463 organisms/125 taxa) while fewer organisms and more taxa were sampled with the quadrats (4677 organisms/30 taxa). For all sediment types, total species richness was consistently higher in late summer than in late winter but this difference was significant only for the control and engineered sediments (permanova: p(control) = 0.039, p(associated) = 0.071 and p(engineered) = 0.0001).

PCOs and one-way permanovas performed on density matrices indicated that the three sediment types significantly differed ($p < 0.05$) in their associated fauna at both sampling periods, confirming our *a priori* sediment type grouping (Figure 15 and Figure 16). PCO axis 1 explained in late winter and late summer, respectively 26.1 and 30.3% of the total variation present in the resemblance matrix and clearly separated the engineered samples from the control samples. PCO axis 2 explained in late winter and late

summer, respectively 14.6 and 14.8% of the total variation and discriminated the engineered and control samples from the associated samples. In both seasons, engineered samples were highly clustered compared to the more scattered associated and control sediments samples. In late winter, the control and associated sediments were well separated while there was a small overlap between the associated and engineered sediments (Figure 15). In late summer, there was an overlap between the associated and control sediments (Figure 16). This overlap was mostly due to bivalves like *Limecola balthica* or *Cerastoderma edule* and to the polychaete *Nephtys hombergii* (Figure 16 and Appendix). Finally, engineered sediments were characterized by a much greater number of species correlated at more than 60% with each PCO axis (11 in late winter and 17 in late summer) than the associated (3 in late winter and 1 in late summer) and the control sediments (3 in late winter and 6 in late summer).

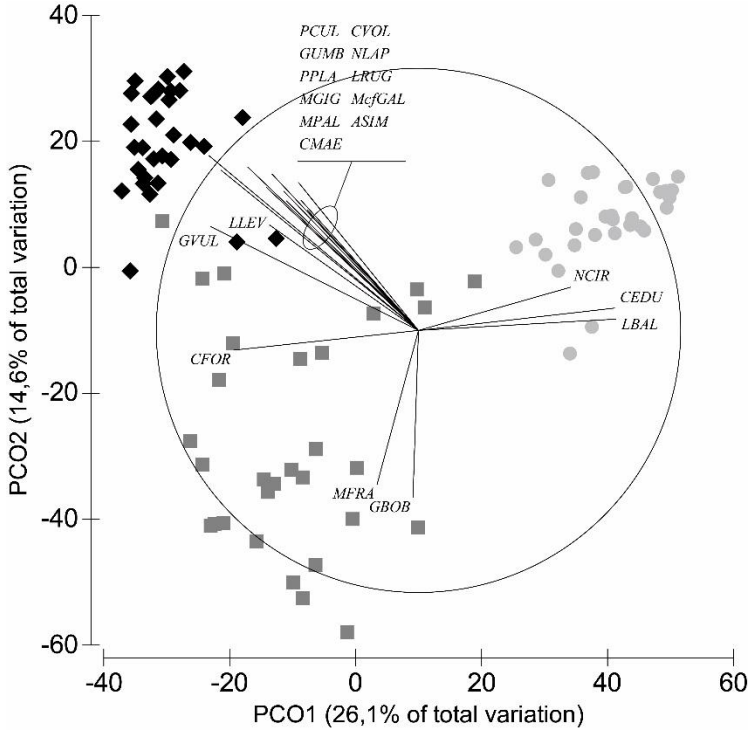

Figure 15. PCO analysis of macrobenthos associated with the three sediment types in late winter. The analysis is based on Bray-Curtis similarities of log transformed density data. The black diamonds, the grey squares and the light grey circles represent the engineered, the associated and the control sediment samples respectively. Vectors represent species correlating more than 60% with one of the first two PCO axes. The correlations are based on Spearman coefficients. ASIM: *Achelia simplex*, CEDU: *Cerastoderma edule*, CFOR: *Crepidula fornicata*, CMAE: *Carcinus maenas*, CVOL: *Corophium volutator*, GBOB: *Goniadella bobrezkii*, GUMB: *Gibbula umbilicalis*, GVUL: *Golfingia vulgaris*, LBAL: *Limecola balthica*, LLEV: *Lekanesphaera levii*, LRUG: *Lekanesphaera rugicauda*, McfGAL: *Mytilus* cf. *galloprovincialis*, MFRA: *Mediomastus fragilis*, MGIG: *Magallana gigas*, MPAL: *Melita palmata*, NCIR: *Nephtys cirrosa*, NLAP: *Nucella lapillus*, PCUL: *Perinereis cultrifera*, PPLA: *Porcellana platycheles*. .

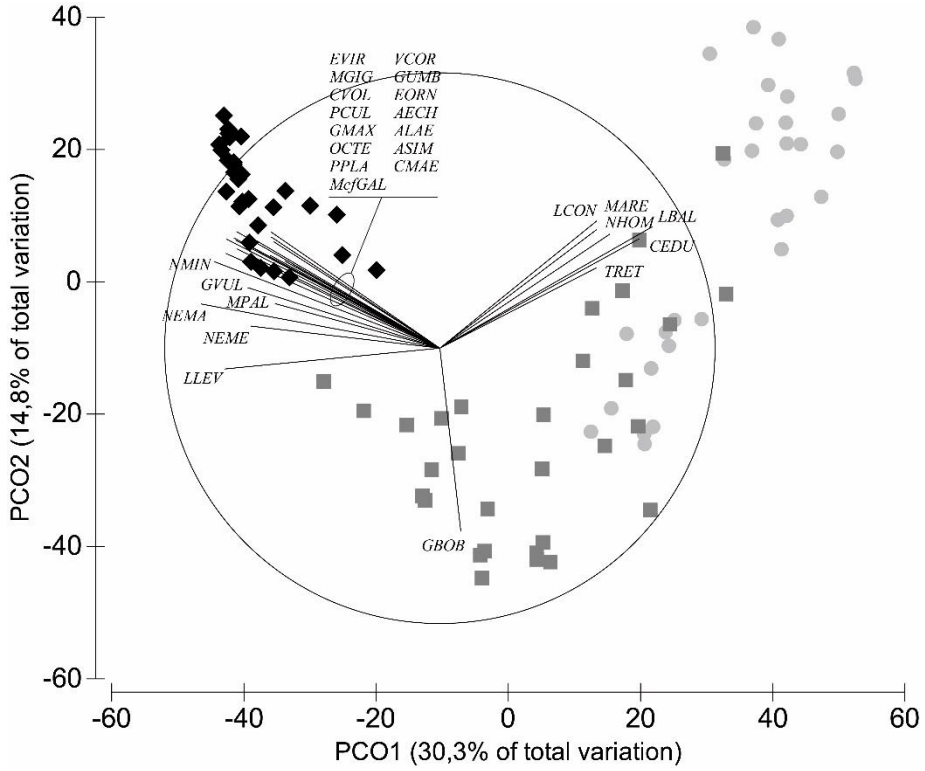

Figure 16. PCO analysis of macrobenthos associated with the three sediment types in late summer. The analysis is based on Bray-Curtis similarities of log transformed density data. The black diamonds, the grey squares and the light grey circles represent the engineered, the associated and the control sediment samples respectively. Vectors represent species correlating more than 60% with one of the first two PCO axes. The correlations are based on Spearman coefficients. AECH: *Achelia echinata*, ALAE: *Achelia laevis*, ASIM: *Achelia simplex*, CEDU: *Cerastoderma edule*, CMAE: *Carcinus maenas*, CVOL: *Corophium volutator*, EORN: *Eulalia ornata*, GBOB: *Goniadella bobrezkii*, GMAX: *Gnathia maxillaris*, GUMB: *Gibbula umbilicalis*, GVUL: *Golfingia vulgaris*, LBAL: *Limecola balthica*, LCON: *Lanice conchilega*, LLEV: *Lekanesphaera levii*, LRUG: *Lekanesphaera rugicauda*, MARE: *Malmgrenia arenicolae*, McfGAL: *Mytilus* cf. *galloprovincialis*, MFRA: *Mediomastus fragilis*, MGIG: *Magallana gigas*, MPAL: *Melita palmata*, NCIR: *Nephtys cirrosa*, NEMA: *Nematoda* spp., NEME: *Nemerte* sp., NHOM: *Nephtys hombergii*, NLAP: *Nucella lapillus*, NMIN: *Nephasoma minutum*, OCTE: *Odontosyllis ctenostoma*, PCUL: *Perinereis cultrifera*, PPLA: *Porcellana platycheles*.

Mean macrofauna diversity indices and densities were calculated within each sediment type and for each sampling campaign (Table 11a and Table 11b). At the sediment type scale, one-way permanovas showed significant differences between engineered sediments on the one hand and associated and control sediments on the other, for all the diversity measurements and densities at both periods. There were two exceptions regarding N1 and N2 calculated in late summer with *S. alveolata* taken into account. In these cases, there were no significant differences between the three sediment types. When *S. alveolata* was taken into account, total macrofauna density was 20 times higher in the engineered sediments at both periods. This difference was maintained even after *S. alveolata* was removed from the data set but it was reduced to an average 5-fold difference. The engineered sediment was also home to significantly more species (mean species richness N0) than the associated and control sediments and this, whatever the situation.

Table 11 Mean values (± standard errors) for the total macrofauna density (number of individuals.m^{-2}), N0, N1 and N2 with (a) Sabellaria taken into account and (b) Sabellaria excluded, for the three sediment types (engineered, associated and control) and at both sampling periods (late winter and late summer). N0 represents the species richness, N1 the exponential of the Shannon-Winner diversity and N2 the inverse of the Simpson dominance index. Significant differences ($p < 0.05$) of the one-way ANOVAs are in bold and post-hoc results are designated by superscript letters indicating homogenous groups of samples.

	Late winter				Late summer			
(a) Macrofauna (*Sabellaria* included in the analyses)								
	Engineered	*Associated*	*Control*	*p-value*	*Engineered*	*Associated*	*Control*	*p-value*
Density	10067 ± 841^{a}	585 ± 102^{b}	629 ± 109^{b}	**<0.001**	23911 ± 2530^{a}	1029 ± 156^{b}	1403 ± 351^{b}	**<0.001**
N0	17 ± 1^{a}	7 ± 1^{b}	8 ± 1^{b}	**<0.001**	26 ± 1^{a}	9 ± 1^{b}	10 ± 1^{b}	**<0.001**
N1	2.92 ± 0.37^{a}	4.46 ± 0.50^{b}	4.54 ± 0.37^{b}	**0.013**	6.01 ± 0.65^{a}	4.61 ± 0.38^{a}	5.22 ± 0.28^{a}	0.229
N2	1.87 ± 0.23^{a}	3.75 ± 0.40^{b}	3.60 ± 0.28^{b}	**<0.001**	3.93 ± 0.44^{a}	3.44 ± 0.30^{a}	4.04 ± 0.25^{a}	0.315
(b) Macrofauna (*Sabellaria* excluded from the analyses)								
	Engineered	*Associated*	*Control*	*p-value*	*Engineered*	*Associated*	*Control*	*p-value*
Density	2385 ± 518^{a}	538 ± 91^{b}	629 ± 109^{b}	**<0.001**	11066 ± 1814^{a}	981 ± 137^{b}	1403 ± 351^{b}	**<0.001**
N0	16 ± 1^{a}	7 ± 1^{b}	8 ± 1^{b}	**<0.001**	25 ± 1^{a}	9 ± 1^{b}	10 ± 1^{b}	**<0.001**
N1	7.73 ± 0.51^{a}	4.30 ± 0.49^{b}	4.54 ± 0.37^{b}	**<0.001**	9.00 ± 0.52^{a}	4.51 ± 0.37^{b}	5.22 ± 0.28^{b}	**<0.001**
N2	5.63 ± 0.42^{a}	3.64 ± 0.39^{b}	3.60 ± 0.28^{b}	**<0.001**	5.82 ± 0.38^{a}	3.36 ± 0.30^{b}	4.04 ± 0.25^{b}	**<0.001**

Regarding macrofauna density, N1 and N2, associated and control sediments presented similar temporal patterns when comparing late winter and late summer. Their respective macrofauna density increased significantly between the two campaigns (permanova: p(control) = 0.023 and p(associated) = 0.018) while N1 and N2 showed non-significant differences (permanova: p(control-N1) = 0.15, p(control-N2) = 0.25, p(associated-N1) = 0.83 and p(associated-N2) = 0.53). Between late winter and late summer, the engineered sediments presented a significant increase in the total macrofauna density (permanova: p(density with *S. alveolata*) = 0.0001) only driven by a significant increase in the associated fauna density (permanova: p(density without *S. alveolata*) = 0.0001 and p(*S. alveolata* density) = 0.54). They also showed a significant increase in the case of N1 and N2 calculated with *S. alveolata* (permanova: p(N1) = 0.0007 and p(N2) = 0.0001), a change which was not significant once the engineer species was removed (permanova: p(N1) = 0.089 and p(N2) = 0.73).

3.3. Linking environmental and biological engineering effects

DistLM and dbRDA analysis were performed in late winter (Figure 17a) and late summer (Figure 17b) with *S. alveolata* biomass considered as an environmental parameter. In both seasons, *S. alveolata* biomass was the parameter which best explained the relationship between environmental parameters and macrofauna assemblages (18.0% in late winter and 24.8% in late summer). In late winter,

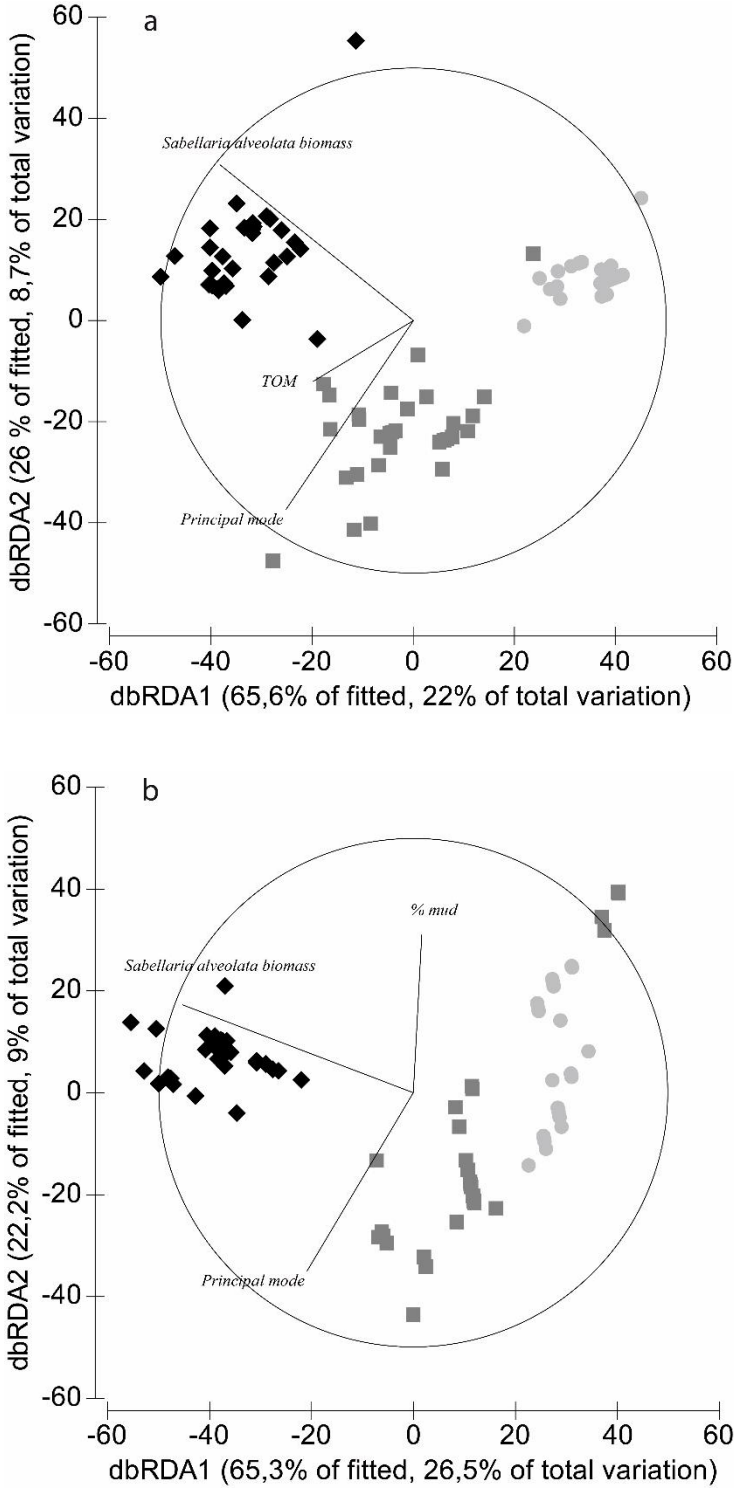

Figure 17. dbRDA plots based on a) the late winter data set and b) the late summer data set and representing the three sediment type macrofauna composition as explained by the set of environmental parameters composing the most parsimonious explanatory model. Vectors represent the environmental parameters selected by the DistLM routine. The black diamonds, the grey squares and the light grey circles represent the engineered, the associated and the control sediment samples respectively.

the most parsimonious model, explaining 33.6% of the total variation in species assemblages, was defined by (1) *Sabellaria* biomass (square-root transformed, 18.0%), (2) principal mode (log transformed, 13.2%) and (3) total organic matter content (fourth-root transformed, 10.7%, Figure 17a). The first two axes explained 91.6% of the fitted variation and 30.7% of the total variation. Species assemblage were structured according to two gradients. The first was driven by *S. alveolata*, and separated engineered sediments from the two other types. The second was driven by the sediment principal mode and the total organic matter content and separated the associated from the control sediments (Figure 17a). In late summer, the most parsimonious model explained 40.7% of the total variation in species assemblages. It was defined by the same first two variables as for late winter: *Sabellaria* biomass (square-root transformed, 24.8%) and principal mode (log transformed, 16.9%). The third selected variable differed from late winter since it was the mud content (fourth-root transformed) and it explained only a very small part of the total variation (0.079%). The first two axes explained 87.5% of the fitted variation and 35.6% of the total variation. Again, species assemblages were structured according to two gradients but they did not separate the different sediment types as clearly as in late winter. *S. alveolata* still defined the first gradient and clearly separated the engineered sediments from the two soft sediments. The opposition between the principal mode and the mud content defined the second gradient. Along this gradient, the distinction associated/control sediments was not well defined. Indeed, there were three associated sediment samples characterized by high mud contents and isolated from the rest of the associated sediment samples (Figure 17b).

3.4. Disturbances and biological engineering effect

Consistent mean values in late winter (10%) and late summer (9.59%), confirm the choice of the mud content as a suitable 'disturbance parameter' (Table 10a). Indeed, these values did not significantly vary between the two contrasted seasons we sampled (permanova: $p = 0.78$). In contrast, the mean *S. alveolata* density almost doubled between late winter (7682 ± 3312 ind.m^{-2}) and late summer (12844 ± 14262 ind. m^{-2}), with a very high summer variability, leading to no significant change (permanova: $p = 0.54$). Oppositely, the mean *S. alveolata* biomass by surface unit significantly decreased between late winter (646 ± 317 g. m^{-2}) and late summer (318 ± 211 g. m^{-2}) (permanova: $p = 0.0001$).

Mantel tests performed between the mud content distance matrix and the different beta diversity matrices showed a clear temporal difference between late winter and late summer. The tests were not significant when performed using the late winter data sets ($p > 0.05$, Table 12), while they revealed a significant and positive correlation between the mud content distance matrix and β_{sor} ($p < 0.001$, $r = 0.24$), β_{sim} ($p = 0.0066$, $r = 0.15$), d_{BC} ($p < 0.001$, $r = 0.38$) and $d_{BC\text{-}gra}$ ($p < 0.001$, $r = 0.29$) (Table 12) using the late summer data sets. These results indicate that in late winter, an increase in mud content, used as a proxy for disturbance, does not lead to beta diversity changes but in late summer, it leads to (1) an increase in beta diversity driven by a species replacement and (2) an increase in abundance-based

dissimilarity driven by an abundance gradient. Ordination plots of similarities (nMDS) of macrofaunal assemblages based on β_{sor}, β_{sim}, β_{nes}, d_{BC}, $d_{BC\text{-}bal}$ and $d_{BC\text{-}gra}$ indices were performed in late winter and late summer (Figure 18 and Figure 19). In late winter, the correlation between the mud content and the different nMDS plots was significant for β_{sor} ($p = 0.008$), β_{nes} ($p = 0.023$), d_{BC} ($p = 0.019$) and $d_{BC\text{-}gra}$ ($p = 0.027$). The mud content explained 30.67% of the ordination based on β_{sor} and 24.54% of the ordination based on β_{nes}. Similarly, 26.93% and 24.51% of the ordination based on d_{BC} and $d_{BC\text{-}gra}$ respectively where explained by the mud content. In late summer, the correlation between the mud content and the different nMDS plots was significant and much higher for all the indices; β_{sor} ($p = 0.001$), β_{nes} ($p = 0.036$), β_{sim} ($p = 0.001$), d_{BC} ($p = 0.001$), $d_{BC\text{-}gra}$ ($p = 0.002$) and $d_{BC\text{-}bal}$ ($p = 0.006$). Indeed, the mud content explained over 50% of the ordination based on β_{sor} ($r^2 = 53.07\%$) and d_{BC} ($r^2 = 52.76\%$), around 40% of the ordination based on β_{sim} ($r^2 = 39.23\%$) and $d_{BC\text{-}gra}$ ($r^2 = 41.33\%$), and between 20 and 30% of β_{nes} ($r^2 = 21.25\%$) and $d_{BC\text{-}bal}$ ($r^2 = 29.56\%$). When the correlation was significant, the fitted mud contents were plotted on the corresponding nMDS plots (Figure 18 and Figure 19). The correlation between the disturbance proxy and the different nMDS plots showed a pattern similar to the one revealed by the late summer Mantel test, with beta diversity changes mainly driven by a species turnover and an abundance gradient.

Table 12 Results of the Mantel tests between (a) the different beta diversity matrices and the mud content distance matrix and (b) the different abundance-based dissimilarity matrices and the mud content distance matrix at both sampling periods (late winter and late summer). β_{sor} is the Sørensen pairwise dissimilarity and accounts for the total beta diversity, β_{sim} is the Simpson pairwise dissimilarity and accounts for the turnover component of the total beta diversity, β_{nes} is the nestedness-resultant dissimilarity and accounts for the nestedness component of the total beta diversity; $\beta_{sor} = \beta_{sim} + \beta_{nes}$. d_{BC} is the Bray-Curtis index of dissimilarity and accounts for the total abundance-based dissimilarity, $d_{BC\text{-}bal}$ is the balanced variation in abundances component of the Bray-Curtis dissimilarity and is equivalent to an abundance-based turnover, $d_{BC\text{-}gra}$ is the abundance gradient component of Bray-Curtis dissimilarity and is equivalent to an abundance-based nestedness; $d_{BC} = d_{BC\text{-}bal} + d_{BC\text{-}gra}$. Significant simulated p-values ($p < 0.05$) and associated observed correlation are in bold.

	Late winter		**Late summer**	
	Observed correlation r	*Simulated p-value*	*Observed correlation r*	*Simulated p-value*
(a) Beta diversity indices				
β_{sor}	0.13	0.070	**0.24**	**<0.001**
β_{sim}	0.066	0.23	**0.15**	**0.0066**
β_{nes}	0.032	0.33	0.077	0.094
(b) Abundance-based dissimilarity indices				
d_{BC}	0.14	0.052	**0.38**	**<0.001**
$d_{BC\text{-}bal}$	0.050	0.28	0.058	0.18
$d_{BC\text{-}gra}$	0.046	0.28	**0.29**	**<0.001**

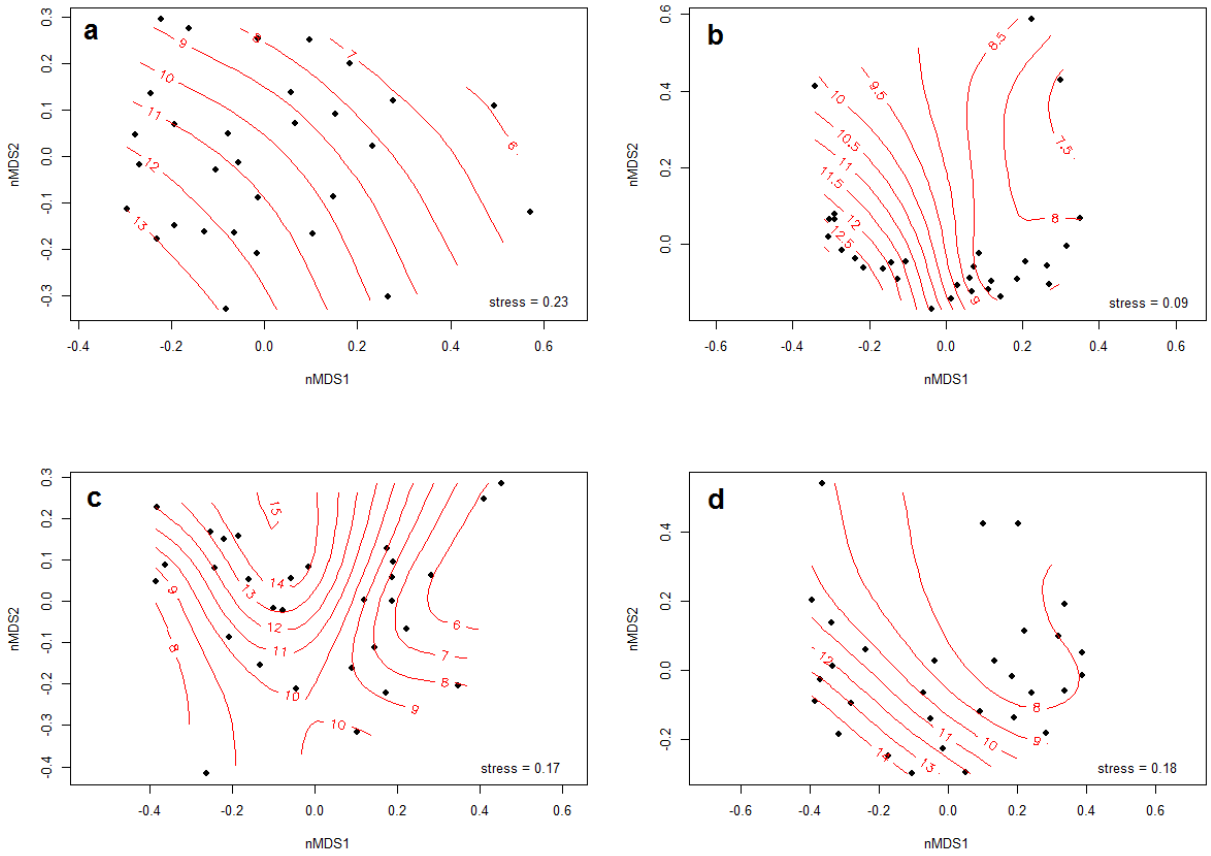

Figure 18. Late winter nMDS ordination plots of the benthic macrofauna assemblages based on a) the Sørensen total beta diversity, b) the nestedness component of the total beta diversity, c) the Bray-Curtis index of dissimilarity and d) the abundance gradient component of the Bray-Curtis dissimilarity. The stress value of the nMDS is indicated on each plot. The lines indicate the different fitted mud contents obtained using the 'ordisurf' function.

4. Discussion

4.1. Engineered structures cause grain-size distribution changes

Environmental engineering effects are composed of two types of changes, structural and abiotic changes, structural changes being caused by ecosystem engineers and inducing abiotic changes (Jones et al., 2010). *S. alveolata* is capable of biologically modifying soft sediments by selectively gluing together bioclastic sand particles, in order to build its tube (Fournier et al., 2010). This leads to the transformation of an initial soft sediment into a three-dimensional hard substratum with a long lasting resistance to physical loading via the secreted organic cement (Le Cam et al., 2011). *Sabellaria alveolata* can therefore be considered as a "structural engineer" according to Berke (2010). Structural changes caused by physical ecosystem engineers result in a variation in the distribution of fluid and solid material termed abiotic changes (Jones et al., 2010). In the case of *S. alveolata*, a direct abiotic engineering effect observable through the engineered sediments and an indirect one, observable through the associated sediments, were detected. Engineered and associated sediments presented, at both sampling periods, a coarser texture than the control sediments, confirming the impact Sabellariidae polychaetes have on the local sediment's texture by selecting sand particles of a specific size to build their tubes

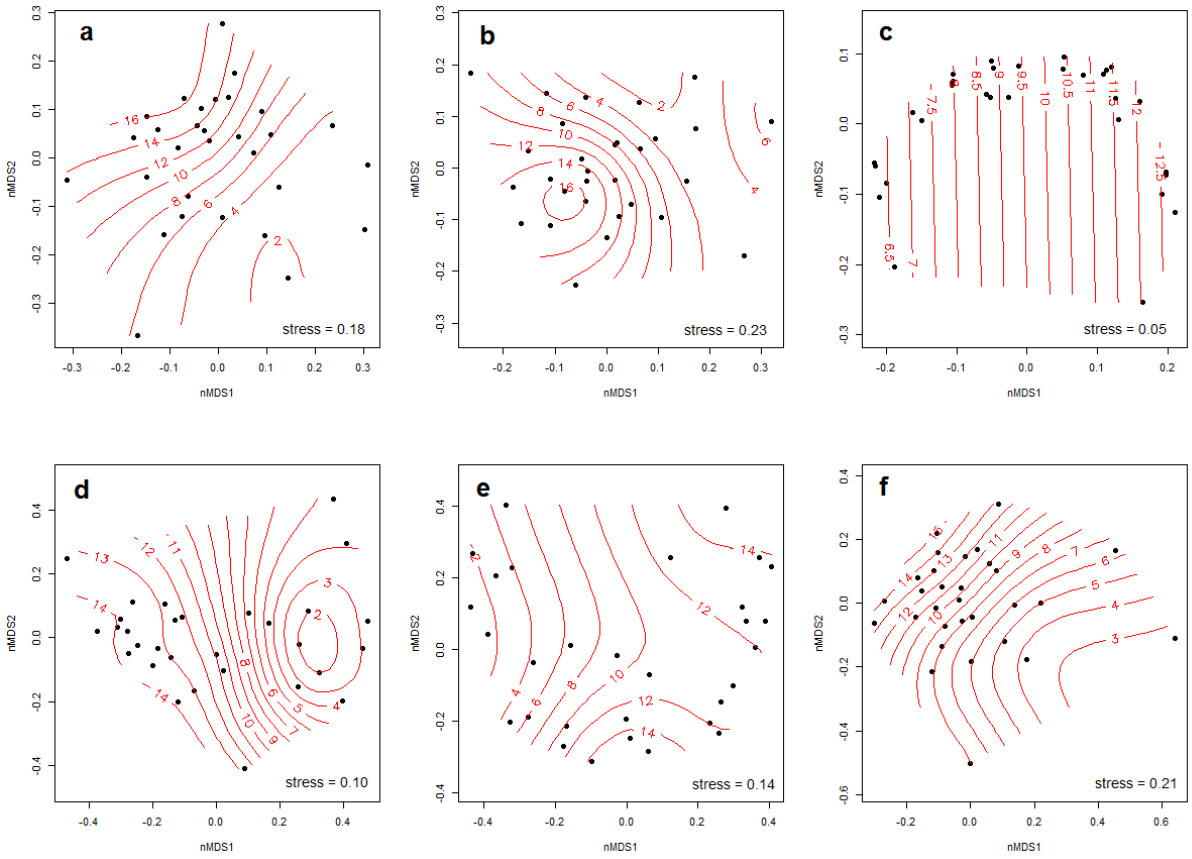

Figure 19. Late summer nMDS ordination plots of the macrofauna benthic assemblages based on a) the Sørensen total beta diversity, b) the turnover component of the total beta diversity, c) the nestedness component of the total beta diversity, d) the Bray-Curtis index of dissimilarity, e) the abundance gradient component of the Bray-Curtis dissimilarity and f) the balanced variation in abundances component of the Bray-Curtis dissimilarity. The stress value of the nMDS is indicated on each plot. The lines indicate the different fitted mud contents obtained using the 'ordisurf' function.

(*Phragmatopoma caudata* (= *P. lapidosa*) (Gram, 1968; Kirtley and Tanner, 1968; Main and Nelson, 1988), *Sabellaria vulgaris* (Wells, 1970), *Sabellaria nanella* (Bremec et al., 2013)). Ultimately, these bioconstructing Sabellariidae species create reefs characterized by a grain-size distribution different from the local soft sediments. The case of the associated sediments raises the question of the definition of a reef habitat. In Europe, "reefs" are recognized as a marine habitat to be protected and are listed under Annex I of the EC Habitats Directive (Council Directive EEC/92/43 on the Conservation of Natural Habitats and of Wild Fauna and Flora) under the designation of Special Areas of Conservation (SACs). They are defined as "submarine or exposed at low tide, rocky substrates and biogenic concretions". In the light of our findings, we can very well consider the engineered and the associated sediments as the same sediment but under two different forms, a consolidated (engineered sediments) and an unconsolidated form (associated sediments). Hence, we propose to widen the definition of a "reef" to include the non-engineered sediments under its direct influence.

The main difference between the engineered and associated sediments concerns their mud content. At both seasons, the engineered sediments have a mean mud content around 10%, as previously observed by Le Cam et al. (2011). *Sabellaria wilsoni* veneers have also been reported to present consistent silt and clay contents across two contrasting seasons (rainy and dry seasons in Ataide et al., 2014) indicating that Sabellariidae polychaetes build new habitats presenting stable sedimentary conditions. The mud present in the engineered sediments is located in small cracks and crevices protected from the main hydrodynamic processes (*i.e.* winter storms, tidal currents and swell). Conversely, the associated sediments are characterized by a steep and significant increase in mud content between winter (2%) and summer (21%). As shown by Caline et al. (1988) for the Sainte-Anne reef (MSMB), localized mud depositions are linked to hydrodynamic and associated hydro-sedimentary processes induced by the presence of the reef itself and of the mussel farms (bouchots) in front of the reef (McKindsey et al., 2011). These mud depositions are observed behind reef structures important enough to act as physical barriers (Caline et al., 1988), where they are generally superficial and consequently easily eroded by strong wave action, limiting their presence in winter.

4.2. Engineered structures enhance benthic primary production and potentially microbial activity

As reported by Jones et al. (2010), abiotic changes induced by physical engineering activity can themselves cause biotic changes. Our results clearly show that at both seasons, associated sediments have a higher organic matter content compared with the control sediments. At both seasons, high levels of organic matter were associated with high chlorophyll *a* concentrations, indicating that part of the organic matter present in the associated sediments is the consequence of MPB development. The high benthic primary production promoted by the Sainte-Anne reef, compared to a generally lower benthic production in the MSMB as measured by Davoult et al. (2008) and Migné et al. (2009), confirms its important biotic engineering effect. Similar results were found for the invading intertidal reef-forming polychaete *Ficopomatus enigmaticus* (Bruschetti et al., 2011), for shallow oyster reefs (*Crassostrea virgina*, Newell et al., 2002) and for intertidal mussel beds (Engel et al., 2017). According to Berke (2010), "structural engineers operate through similar processes and have similar types of effects". Consequently, the creation of benthic primary production hotspots by reef-building structural engineers could be a general property of these marine species. Nonetheless, this phenomenon was observed at the scale of the largest and probably oldest *S. alveolata* reef in Europe (Audouin and Milne-Edwards, 1832) and the study by Engel et al. (2017) highlighted the importance of the size and age of the bioconstruction in promoting local benthic microalgae. Hence, further studies are needed to confirm the general role of *S. alveolata* reefs as "biological power stations" (Engel et al., 2017).

Furthermore, the high chlorophyll *a* concentrations measured in late winter and late summer indicate that *S. alveolata* reefs promote an important benthic primary production all year round, that could be a relevant food source for deposit- (Kanaya et al., 2008) and suspension-feeders (Lefebvre et

al., 2009) through resuspension processes (Hylleberg, 1975; Ubertini et al., 2015). In the associated sediments, MPB often grows on small accumulations of pure mud and is consequently easily eroded and available to consumers. Such benthic primary production may have a trophic importance during the winter months (Lefebvre et al., 2009), when the phytoplankton production is typically low (Arbach Leloup et al., 2008; Cugier et al., 2010). Filter feeding mollusks are known to stimulate MPB growth (Engel et al., 2017; Newell et al., 2002) via inorganic nutrient release (*i.e.* carbon, nitrogen and phosphorus (van Broekhoven et al., 2014)) and bacterial remineralization of their biodeposits (van Broekhoven et al., 2015). Similarly, *S. alveolata* produces large amounts of feces and pseudofeces visible on the sediment (Dubois et al., 2005), that could favor MPB growth. Primary production could also be enhanced by the presence of other suspension-feeders living in the engineered sediments, such as *Magallana gigas,* which can reach densities of 100 ind.m^{-2} as measured in the disturbed engineered sediments using the quadrats. As already observed in *Ficopomatus enigmaticus* reefs (Bruschetti et al., 2011), *S. alveolata* reefs probably increase the bentho-pelagic coupling by linking pelagic organic matter to the benthic compartment via their suspension-feeding activity and biodeposition.

In late winter and late summer, associated sediments had consistently higher soluble carbohydrate concentrations than the control sediments. Carbohydrates are the components of the mucus coating the pseudofeces produced by *S. alveolata* and other suspension-feeders (van Broekhoven et al., 2015). Hence, when these pseudofeces are deposited on the associated sediments, it could increase their concentration in soluble carbohydrates. Soluble carbohydrates also compose the extracellular polymeric substances produced by benthic diatoms (Bellinger et al., 2009) and are an important source of organic carbon, rapidly consumed by heterotrophic microorganisms present in the sediment (Bhaskar and Bhosle, 2005; Goto et al., 2001). Consequently, *S. alveolata* presence could support all year round an important bacterial activity through the soluble carbohydrates excreted by the diatoms and present in the mucus coating the biodeposits. This organic carbon can either be used by the bacteria for their growth (bacterial biomass production) or be remineralized (bacterial respiration) as showed by Hubas et al. (2006). In the first case, the bacteria can be a source of food for infaunal organisms such as nematodes and become an important trophic link in structuring energy fluxes in the community (Pascal et al., 2009, 2008). In the second case, the bacteria release inorganic nutrients such as carbon (Jiao et al., 2010), which can then be used by photoautotrophs present in the sediment (*e.g.* diatoms) or in the water column (*e.g.* phytoplankton) further maintaining the local primary production.

Furthermore, according to Delmas (1983), an insoluble/soluble carbohydrate ratio (Ins/Sol) ranging between 6 and 8 indicates a low degradation rate of the organic matter, while a ratio varying between 10 and 30 reflects a high degradation rate. Delmas (1983) also suggests using the Ins/Sol ratio as a proxy for the C/N ratio. Mean Ins/Sol ratios were not significantly different between the associated and control sediments with values around 8.6 in late winter, and 6.0 in late summer, indicating that *S. alveolata* does not affect the organic matter degradation rate in soft sediments; it is consistently of good quality and weakly degraded. Nonetheless, in late summer, the organic matter present in the control and

associated sediments appears less degraded and more easily incorporable in the food web than in late winter, probably in response to a higher biological activity of photoautotrophs and bacterial communities (Hubas et al., 2006).

4.3. Engineered structures create an original macrofauna assemblage linked to the sedimentary changes

In addition to promoting the local benthic production, *S. alveolata* strongly modifies the macrofauna assemblages present in the engineered and associated sediments compared to the control sediments and this difference is present at both sampling seasons. Consequently, *S. alveolata* engineers two original species assemblages, one associated with the actual bioconstructions and the other associated with the sediments surrounding these structures. In late winter and late summer, the environmental parameter primarily responsible for macrofauna differences between the three sediment types is the ecosystem engineer via its biomass. Studies on other ecosystem engineers have demonstrated a similar structuring effect of the engineer on the macrofauna, for example *via Haploops nirae* density in subtidal mats (Rigolet et al., 2014b) and *Lanice conchilega* density in intertidal beds (De Smet et al., 2014). The benthic macrofauna is secondarily structured by the principal mode and the organic matter content of the sediments, two environmental parameters reported to structure soft sediment macrofauna communities in a large diversity of sites such as the intertidal flats of the Schelde estuary (Ysebaert and Herman, 2002) and over multiple spatial scales in Portuguese transitional water systems (Veiga et al., 2016). In our case, these two parameters are influenced by *S. alveolata*, indicating the importance of this engineer species in structuring the local benthic macrofauna.

Structural diversity analyses indicate that assemblages present in the associated and control sediments are similarly structured in late winter and late summer. Dominant species are mainly polychaetes (*e.g. Goniadella bobrezkii*) and mollusks species (*e.g. Crepidula fornicata*) in the associated sediments and the mollusks *Limecola balthica* and *Cerastoderma edule* in the control sediments, with a consortium of less abundant species. Furthermore, the benthic fauna present in the associated sediments appears as a combination of species living in the two other sediment types, enriched by polychaete species such as *Glycera tridactyla*, *Protodorvillea kefersteini* and *Saccocirrus papillocercus*. These three polychaete species are either carnivore-scavengers or surface deposit-feeders, with important movement capacities, key biological traits in organic matter rich and variable environments (Rigolet et al., 2014b) like the associated sediments. The overlapping observed between the control and associated sediments is much more pronounced in late summer, after the recruitment period (Thorin et al., 2001) and is caused by a few species (*e.g. Cerastoderma edule*, *Limecola balthica* or *Nephtys hombergii*). *Cerastoderma edule* recruitment and settlement of macrozoobenthos larvae is known to be enhanced coastward of mussel beds due to a decrease in hydrodynamic forces caused by these bioengineered habitats (Commito et al., 2005; Donadi et al., 2014, 2013). Similarly, *S. alveolata* reefs act as natural

breakwaters limiting hydrodynamic energy, which could lead to an enhanced recruitment of macrobenthic species like *Cerastoderma edule* and *Limecola balthica*. This phenomenon is a lot less visible in winter maybe indicating that these species do not survive the variable environmental conditions characterizing the associated sediments or the winter temperatures. Indeed, locals repeatedly come to the Sainte-Anne reef to dig up bivalves like cockles (*Cerastoderma edule*) and Japanese carpet shells (*Ruditapes philippinarum*) enhancing small-scale spatial heterogeneity and potentially leading to changes in the macrofauna of the associated sediments (Watson et al., 2017). We also recorded inside the associated sediments some species generally present in the engineered sediments, like *P. cultrifera* or *G. vulgaris*. This can be caused by the presence of broken reef parts in the associated sediments, because of the variable sedimentary preferences of some species (*e.g. G. vulgaris*) or because of the use of the associated sediments by some species to move between reef patches (*e.g. Perinereis cultrifera*).

Species richness and associated macrofauna density were always highest in the engineered sediments than in the two soft sediments, stressing *S. alveolata*'s role in enhancing local biodiversity and abundance. Our results confirm previous studies on *S. alveolata* reefs (Dias and Paula, 2001; Dubois et al., 2002; Holt et al., 1998) and agree with a large body of literature reporting positive effects of tubiculous polychaete species (De Smet et al., 2015), reef-building polychaetes (McQuaid and Griffiths, 2014) and bivalves (Gutiérrez et al., 2003; Lejart and Hily, 2011; Norling and Kautsky, 2007) on species richness and associated fauna abundances. Intertidal engineers like *S. alveolata* create new complex habitats that reduce pressures such as thermal and hydric stress and increase the number of primary producers (*i.e.* MPB and ulva), potentially extending trophic niches and overall leading to a biodiversity increase (Bouma et al., 2009; Jones et al., 1997; Stachowicz, 2001). New environmental conditions created by *S. alveolata* also lead to the paradox mentioned by Bertness et al. (1999), and facilitate the colonization of intertidal zones by subtidal species, like the polychaete *Spirobranchus lamarcki* or the gastropod *Crepidula fornicata*.

Structural diversity indices calculated for the engineered sediments (considering *S. alveolata*) and the beta diversity analysis both reveal a change between late winter and late summer in how the macrofauna is structured. In late winter, N1 and N2 are both significantly lower than in the two other sediment types while in late summer, macrofauna density in the engineered sediments is distributed similarly than in the associated and control sediments. Consequently, during winter *S. alveolata* dominates more strongly the engineered sediments than the dominant species present in the associated and control sediments, a result similar to the *Haploops nirae* habitats in summer (Rigolet et al., 2014b). Differently, in late summer *S. alveolata* does not affect the community structure in a different way than other abundant species do in the associated (*Crepidula fornicata*, *Cirriformia tentaculata*, *Mediomastus fragilis*, *Goniadella bobrezkii*) and control sediments (*Cerastoderma edule*, *Limecola balthica*, *Lanice conchilega*, *Malmegrenia arenicolae* and *Nepthys spp.*). Regarding beta diversity, it significantly increases along the disturbance gradient in late summer but not in late winter. These observed contrasts between the two seasons can have two causes, probably acting in synergy: a low *S. alveolata* recruitment

and an important recruitment of associated species. This last argument was also suggested by Mateo-Ramirez et al. (2015) to explain the increase in decapod abundance associated with *Posidonia oceanica* meadows, between winter-spring and summer-autumn. In the MSMB, the recruitment success of *S. alveolata* is known to be strongly year-to-year variable depending on the synchrony between favorable environmental conditions (tidal and meteorological conditions) and main reproductive periods (Ayata et al., 2009), and 2015 seemed to be a year characterized by low settlement rates (pers. obs.). A weak *S. alveolata* recruitment leads to a decrease in spatial competition between the engineer and other macrofauna species favoring recruitment of associated species. Indeed, between winter and summer, many other benthic species recruit in the MSMB (Thorin et al., 2001) and biogenic habitats like *Mytilus edulis* and *Crepidula* spp. beds, are known to favor recruitment of pelagic larvae (Berke, 2010) by affecting boundary-layer flow (Eckman, 1983). Consequently, a low *S. alveolata* recruitment associated with the upraised position of the reef in a soft bottom environment and the absence of neighboring hard substratum, one exception being the off-bottom mussel farms, lead to an important recruitment of benthic larvae to the Sainte-Anne reef. The hard nature of the engineered sediments can also act as either a support for egg capsules (*e.g. Nucella lapillus*) or an attractant for pelagic larvae of rocky shore species like *Gibbula umbilicalis* or *Eulalia viridis* (Kingsford et al., 2002). When *S. alveolata* is excluded, N1 and N2 values are systematically higher in the engineered sediments, a pattern unaffected by season. *Sabellaria alveolata* associated macrofauna shows a structuration similar to *Lanice conchilega* intertidal beds (De Smet et al., 2015) when compared to non-engineered sediments. De Smet et al. (2015) also recorded the lack of a temporal effect on N1 and N2. Consequently, despite its strong dominance, *S. alveolata* creates a species-rich habitat where individuals are overall equitably distributed between taxa.

4.4. Engineered sediment disturbance and mechanisms linked to beta diversity changes

S. alveolata reefs are subject to various disturbances causing changes in species richness and composition (Dubois et al., 2006b, 2002; Plicanti et al., 2016) but not in diversity indices (Dubois et al., 2002). According to Clarke and Gorley (2006), diversity indices are unable to detect subtle changes in complex communities like *S. alveolata* reefs. Hence, using beta diversity and abundance-based dissimilarity along a continuum can help us detect these changes and better understand how disturbances affect the macrofauna associated with the reef. The Mantel tests indicate that in summer the beta diversity increases along the disturbance gradient, driven by a species turnover and an increase in species abundances. Differently, the multidimensional ordinations based on Sørensen and Bray-Curtis dissimilarities, are at both seasons significantly correlated with the mud content. Consequently, mud appears as a driver of beta diversity changes all year round but its importance increases between late winter and late summer.

All year round, mud can act directly as an environmental filter for some benthic species present inside the reef and lead to a beta diversity increase (Baselga, 2010). Indeed, mud could play the same environmental filter role in the engineered sediments as it does in soft sediments (Anderson, 2008;

Ysebaert and Herman, 2002). Disturbances to the reef also increase its structural complexity and frees space creating new microhabitats. The increase in the engineered sediment's complexity and heterogeneity, linked to our disturbance proxy, lead to an increase in species richness and beta diversity (Ellingsen and Gray, 2002) by mechanisms like the provision of refuges from predation and physical stressors (Margiotta et al., 2016). Finally, disturbed engineered sediments are more fragmented than their undisturbed counterparts. The important spatial continuity characterizing platform reefs (Dubois et al., 2002) and engineered sediments in "good ecological status" (Desroy et al., 2011) lead to an increase in the dispersal potential of mobile predators like decapods (*e.g. Carcinus maenas*), gastropods (*e.g. Ocenebra erinaceus*) and errant polychaetes (*e.g. Eulalia viridis*). In an experimental microbial landscape, dispersal had a negative effect on local community, metacommunity and landscape beta diversity (Sørensen dissimilarity) mainly because of predation by generalist predators (Cadotte and Fukami, 2005). Consequently, all year round, negative biotic interactions are probably acting in synergy with environmental sorting and habitat complexity to shape the observed beta diversity changes.

Between late winter and late summer, many benthic species recruit. The recruitment of benthic species to soft bottom sediments is known to be under the influence of biotic factors like organic content and food supply (Snelgrove and Butman, 1994). In spring-summer, the mud present in the disturbed engineered sediments is probably richer in organic matter, presenting a better quality compared to winter, as suggested by the associated sediment results. Multiple facts go in this direction. First, part of the spring phytoplankton bloom is known to sediment, potentially enriching the mud in fresh organic matter (Cugier et al., 2010). Second, during spring and summer green algae develop on the reef (Dubois et al., 2006b) enriching the mud in fresh detritus. Finally, in spring and summer *S. alveolata* and other suspension-feeders (*Magallana gigas* and *Mytilus cf. galloprovincialis*) increase their metabolic rates (Gillooly et al., 2001) and consequently produce more feces and pseudofeces, which could further enrich the mud in organic matter. In the end, changes in abiotic factors (topographic complexity, spatial competition and presence of microdepositional environments (small gapes in the reef filled with fine sediments, Snelgrove et al., 1993)) associated with changes in trophic factors (trophic competition, trophic cues (green algae and MPB present on and around the tubes – pers. obs.)) probably act in synergy and cause the recruitment of a richer and different assemblage of species in the disturbed reef parts compared to the undisturbed ones. Indeed, our results show an increase settlement of opportunistic and deposit-feeding species, like *Capitella capitata*, *Cirriformia tentaculata*, *Parathelepus collaris* and *Tharyx killariensis*, and of species presenting a high affinity for mud (*Corophium volutator*) in the more disturbed reefs. In the same time, the release in spatial and trophic competition linked to a decrease in the engineer density, favors the settlement of suspension-feeding species like *Magallana gigas* and *Porcellana platycheles*. In late summer, some of these species are present in very high densities like *P. platycheles* (up to 9000 ind.m^{-2}), *Achelia* spp. (up to 7000 ind.m^{-2}) or *Corophium volutator* (up to 5000 ind.m^{-2}), while the others are less abundant. In the end, the interplay between recruitment and the engineered sediments dynamics seem responsible for the observed species turnover and abundance

increase along the disturbance gradient. In addition, other factors linked to an increasing disturbance, like a higher oyster cover (*Magallana gigas*) probably also structure the associated fauna as shown by Dubois et al. (2006). Indeed, oyster shells provide a suitable substratum for many sessile species and are known to enhance species richness and abundance (Lejart and Hily, 2011).

Finally, the late winter and late summer multidimensional ordinations also show that at both seasons, mud rates above 10-12% induce a homogenization of the species composition, congruently with results of Balata et al. (2007). They reported that in subtidal rocky reefs structured by the coralline algae *Lithophyllum* spp., the sedimentation "reduced the dissimilarity between assemblages overriding the influence of inclination of the substratum on beta diversity". The packing of samples ordinated by d_{BC} is also greater for mud contents above 12% indicating that high mud contents not only streamline the species composition but also their absolute abundances.

Conclusion

Our results illustrate the need to protect a system in its integrity and not just parts of it. In our case, future conservation plans should consider *S. alveolata* reefs and associated sediments as an ecological entity. These habitats are in theory targeted by the European Union's Habitats Directive 92/43/EEC (habitat type 1170 'Reef') but in practice, very few reefs are protected. In the Sainte-Anne reef, a local legislation prohibits the harvesting of bivalves in the associated soft sediments (*e.g. Ruditapes philippinarum*) but not on the engineered sediments (*e.g. Magallana gigas*) increasing anthropogenic disturbances to the reef. In this context, prohibiting such practices until interactions between *S. alveolata* and *M. gigas*, particularly regarding benthic primary production and trophic competition, are clearly elucidated, should be considered.

Furthermore, the biogenic habitat created by *S. alveolata* is home to an original species assemblage presenting a high richness and density all year round, a case similar to many other structural engineers (Berke, 2010; Jones et al., 1994). These habitats are subject to numerous environmental and anthropogenic disturbances leading to changes in their physical structuration and complexity. In the MSMB, these changes are associated with the establishment of mud inside the engineered sediments, the increase in microhabitat availability and more diversified food sources. All year round, these differences act as environmental filters for post-recruits and juveniles. During the summer recruitment period, these differences act as cues for settling larva, leading to an enhanced recruitment inside the more disturbed reefs. In the end, during the spring-summer period, an increasing disturbance leads to an increase in species richness, a change in the species present in the engineered sediments (turnover) and to higher abundances (abundance gradient). This species turnover pleads for a recognition of the ecological value the "degraded" *S. alveolata* reefs have, as biodiversity and recruitment promoters.

Finally, our results are in contradiction with a study reporting that increasing disturbances to mussel beds increased patchiness and in the end reduced the diversity of the associated macrofauna (Díaz et al., 2015), highlighting the variable response fauna associated to structural engineers can have to disturbances. These different results also stress the importance of spatial and temporal scale on evaluating the impact disturbances have on biodiversity, as reported by Lepori and Hjerdt (2006) for aquatic systems.

Appendix

Mean densities (number of individuals.m^{-2}) of species present in each sediment type (CS: control, AS: associated and ES: engineered) at the two sampling seasons (late winter and late summer). The mean densities were calculated using the ten stations sampled in each sediment type and at each season.

Species	**Late winter**			**Late summer**		
	CS	**AS**	**ES**	**CS**	**AS**	**ES**
Polychaete						
Acromegalomma vesiculosum	0	0	0	0	0	2.48
Ampharete baltica	0	0	0	0	1.24	0
Aonides oxycephala	0	1.24	0	0	0	0
Aonides paucibranchiata	0	0	0	0	6.20	0
Armandia polyophthalma	1.24	0	0	0	0	0
Capitella capitata	6.20	0	0	1.24	0	1.24
Caulleriella alata	0	0	0	1.24	0	0
Cirriformia tentaculata	0	35.96	0	0	42.16	4.96
Dipolydora flava	0	0	0	0	0	4.96
Eteone flava	0	0	0	1.24	0	0
Eteone longa	0	0	0	3.72	3.72	0
Eulalia aurea	0	0	3.72	0	0	0
Eulalia clavigera	0	0	9.92	0	0	1.24
Eulalia ornata	0	0	1.24	0	0	93.01
Eulalia viridis	0	0	22.32	0	0	27.28
Eumida arctica	0	0	0	0	0	1.24
Eumida sanguinea	12.40	1.24	16.12	14.88	0	47.12
Eunereis longissima	0	0	0	3.72	0	0
Glycera alba	3.72	4.96	2.48	13.64	13.64	1.24
Glycera tridactyla	0	1.24	0	0	1.24	0
Goniadella bobrezkii	1.24	228.17	0	14.88	189.73	11.16
Lanice conchilega	62.00	0	0	602.67	8.68	0
Lepidonotus squamatus	0	0	2.48	0	0	0
Magelona johnstoni	1.24	0	0	1.24	0	0
Malacoceros fuliginosus	1.24	0	0	3.72	0	0
Malmgrenia arenicolae	6.20	3.72	0	142.61	2.48	0
Mediomastus fragilis	6.20	65.72	6.20	13.64	280.26	44.64
***Myrianida* sp.**	0	2.48	0	0	0	0
Mysta picta	1.24	0	0	0	0	0

Nephtys cirrosa	59.52	0	0	54.56	8.68	0
Nephtys hombergii	17.36	0	0	55.80	38.44	0
***Nephtys* sp.**	1.24	0	0	0	0	0
Notomastus latericeus	16.12	2.48	1.24	48.36	2.48	48.36
Odontosyllis ctenostoma	0	1.24	12.40	0	0	271.57
Odontosyllis gibba	0	1.24	29.76	0	0	0
Parathelepus collaris	0	0	0	0	1.24	49.60
Perinereis cultrifera	0	7.44	164.93	0	1.24	146.33
Pholoe inornata	0	0	1.24	1.24	0	7.44
Phyllodoce laminosa	0	0	2.48	0	0	11.16
Phyllodoce mucosa	0	0	0	11.16	0	0
Polycirrus aurantiacus	0	3.72	0	0	0	0
***Polycirrus* sp.**	0	0	7.44	0	0	0
Protodorvillea kefersteini	0	1.24	0	0	6.20	0
Pseudopolydora pulchra	0	1.24	0	0	0	0
Pseudopotamilla reniformis	0	0	0	0	0	3.72
Pygospio elegans	4.96	0	0	0	0	6.20
Sabellaria alveolata	0	47.12	7682.22	0	48.36	12844.62
Saccocirrus papillocercus	0	1.24	0	0	13.64	0
Scalibregma celticum	0	1.24	0	0	0	0
Scolelepis (Parascolelepis) tridentata	1.24	0	0	0	0	0
Scolelepis (Scolelepis) cantabra	0	0	0	0	2.48	0
Scoloplos (Scoloplos) armiger	14.88	0	0	4.96	0	0
Sphaerosyllis bulbosa	0	0	0	0	14.88	7.44
***Sphaerosyllis* sp.**	0	1.24	0	0	0	0
Spio martinensis	6.20	0	0	0	0	0
Spio symphyta	0	0	0	2.48	0	0
Spirobranchus lamarcki	0	22.32	24.80	0	14.88	68.20
Spirobranchus triqueter	0	0	1.24	0	0	0
Sthenelais boa	0	0	1.24	0	0	0
Syllis garciai	0	1.24	0	0	2.48	3.72
Syllis gracilis	0	0	2.48	0	1.24	11.16
Tharyx killariensis	126.49	2.48	0	1.24	2.48	1.24
Thelepus setosus	0	0	0	0	1.24	28.52
Websterinereis glauca	0	0	0	1.24	1.24	0
Crustacea						
***Anapagurus* sp.**	0.04	0	0	0	0	0
Athanas nitescens	0	1.24	1.24	0	0	1.24
Bathyporeia elegans	0	0	0	7.44	0	0
Bathyporeia guilliamsoniana	34.72	0	0	0	0	0
Bathyporeia nana	0	0	0	1.24	0	0
Bathyporeia pelagica	1.24	0	0	4.96	0	0
Bathyporeia pilosa	0	0	0	2.48	0	0
Bodotria pulchella	0	0	0	0	1.24	0
Bodotria scorpioides	1.24	0	0	0	1.24	0
Cancer pagurus	0	0	2.48	0	0	1.24
Carcinus maenas	2.48	0	29.76	7.44	1.24	89.28
Cleantis prismatica	0	1.24	0	4.96	0	0

Corophium arenarium	3.72	0	18.60	0	0	29.76
Corophium volutator	0	0	64.48	0	0	403.02
Crangon crangon	0.08	0	0	0	0	0
Cumopsis goodsir	1.24	0	0	62.00	1.24	0
Diogenes pugilator	0.11	0	0	0.11	0	0.04
Eocuma dollfusi	6.20	0	0	6.20	0	1.24
Ericthonius punctatus	0	0	0	0	0	2.48
Eurydice pulchra	0	0	0	2.48	0	0
Gammaropsis nitida	0	0	4.96	0	0	2.48
Gnathia maxillaris	0	0	9.92	0	0	90.52
***Hemigrapsus* sp.**	0	1.24	1.24	0	0	0
Jaera (Jaera) albifrons	1.24	0	0	1.24	0	0
Jassa ocia	0	0	26.04	0	1.24	60.76
Lekanesphaera levii	8.68	13.64	171.13	12.40	47.12	358.38
Lekanesphaera rugicauda	3.72	3.72	79.36	9.92	9.92	49.60
***Leptocheirus* sp.**	0	0	1.24	0	0	0
Liocarcinus holsatus	0	0	0	0.12	0	0
Melita palmata	0	9.92	161.21	1.24	6.20	117.81
***Microdeutopus* sp.**	0	0	1.24	0	0	0
Nymphon brevirostre	0	0	0	0	0	2.48
Orchomene humilis	0	0	0	1.24	0	0
Phtisica marina	0	0	0	1.24	0	0
Porcellana platycheles	0	2.48	711.80	0	1.24	2679.79
Portumnus latipes	1.24	0	0	0.31	0	0
Pseudocuma (Pseudocuma) longicorne	3.72	0	0	0	0	0
Pseudomystides limbata	0	0	4.96	0	0	0
Siphonoecetes (Centraloecetes) kroyeranus	1.24	0	0	11.16	0	0
Thia scutellata	0.12	0	0	0	0	0
Tryphosites longipes	0	0	0	1.24	0	0
Urothoe brevicornis	2.48	0	0	2.48	0	0
Urothoe elegans	0	0	0	1.24	0	0
Urothoe poseidonis	3.72	0	0	12.40	0	1.24
Urothoe pulchella	23.56	0	0	24.80	0	0
***Urothoe* sp.**	2.48	0	0	0	0	0
Mollusca						
Abra alba	0.19	0.06	0	1.26	0.07	0
Acanthochitona crinita	0	0	4.96	0	0	0
Aeolidia papillosa	0	0	1.24	0	0	0
Buccinum undatum	0	0	1.24	0	0	0
Cerastoderma edule	70.95	0.12	0.11	18.39	0.20	0.06
Crepidula fornicata	0.64	25.11	26.76	0	15.54	7.11
Gibbula cineraria	0	0	0.23	0	0	0.12
Gibbula umbilicalis	0	0.15	26.02	0	0	39.53
Lacuna pallidula	0	0	0	0	0	1.24
Limecola balthica	89.00	0.12	0.03	187.04	3.97	0
Littorina littorea	0	0	3.16	0	0	1.40
Littorina saxatilis	0	0	0.04	0	0	0
Macomangulus tenuis	0.27	0	0	0.52	0.03	0

Magallana gigas	0	0	17.60	0	0.12	23.31
Modiolula phaseolina	0	0	0	0	0	21.08
***Modiolus* sp.**	0	0	0	0	0	14.88
Mytilus* cf. *galloprovincialis	1.24	0.31	5.13	0.76	0.20	10.91
Nucella lapillus	0	0.04	6.21	0	0	8.10
Ocenebra erinaceus	0	0.03	0.52	0	0.08	0.25
Ostrea edulis	0	0	0.04	0	0	0.04
Phorcus lineatus	0	0	0	0	0	0.04
Polititapes aureus	0	0	2.48	0	0	0
Polititapes rhomboides	0	0.04	0.07	0	0	0
Ruditapes decussatus	0	0.04	0.03	0	0.11	0.03
Ruditapes philippinarum	0.24	0.39	0.25	0.28	0.99	0.10
Scrobicularia plana	0	0	0	1.24	0	0
Spisula elliptica	0	0	0	0	2.48	0
Spisula solida	0.04	0.41	0	0.91	0.16	0
Tritia reticulata	6.73	0.08	0.24	3.61	0.35	0.10
Venerupis corrugata	0.12	0.54	0.81	0.16	0.23	1.62
Venus verrucosa	0	0	0	0	0.04	0
Ascidiacea						
Microcosmus claudicans	0	0	0	0	0	9.92
***Molgula* sp.**	0	0	0	0	1.24	7.44
Phallusia mammillata	0	0	0	0	0	1.24
Polycarpa fibrosa	0	0	0	0	0	14.88
Polyclinum aurantium	0	0	11.16	0	0	0
Pyura microcosmus	0	0	7.44	0	0	0
Styela clava	0	0	7.44	0	0	16.12
Anthozoa						
Actinia equina	0	0	0	0	0.03	0.04
Anemona sp.	0	0	0	0	0	1.24
Cereus pedunculatus	2.48	9.92	64.48	0	2.48	58.28
Urticina felina	0	0	0	0	0	0.04
Pycnogonida						
Achelia echinata	0	1.24	54.56	0	4.96	1311.99
Achelia laevis	0	0	8.68	0	1.24	261.65
Achelia simplex	0	1.24	95.49	0	2.48	962.29
Anoplodactylus virescens	0	0	0	0	0	17.36
Sipuncula						
Golfingia (Golfingia) elongata	0	3.72	6.20	0	0	57.04
Golfingia (Golfingia) vulgaris vulgaris	0	24.80	192.21	0	8.68	130.21
Nephasoma (Nephasoma) minutum	0	22.32	62.00	0	16.12	626.23
Phascolion (Phascolion) strombus strombus	0	1.24	0	0	0	0
Echinodermata						
Acrocnida spatulispina	1.24	0	0	1.24	0	0
Amphipholis squamata	0	2.48	0	0	2.48	49.60
Other						
Nematoda	1.24	6.20	9.92	1.24	102.93	2368.53
Nemertea	0	11.16	69.44	6.20	47.12	184.77
Oligochaeta	0	0	1.24	0	33.48	38.44

Insecta						
Axelsonia littoralis	0	0	79.36	0	0	13.64
***Hydrogamasus* sp.**	0	0	14.88	0	0	8.68
Vertebrata						
Lipophrys pholis	0	0	0.04	0	0	0.12

Chapter II

The second chapter of this manuscript looks into the trophic functioning of the reef according to different spatial scales and focusing either on specific species or considering the entire macrofauna community. This part is composed of two articles in preparation. The first should be submitted to PlosOne and the second to Food Webs.

The first article presents the carbon isobitat, a habitat-scale isoscape, for two abundant suspension-feeders: the engineer *Sabellaria alveolata* and *Mytilus* cf. *galloprovincialis*. The spatial variation observed using these isobitats were explained by a set of abiotic (physical structure of the engineered sediments), biotic (local primary producer abundance and abundance of potential trophic competitors like oysters) and spatial variables (Moran Eigenvector Maps). This study demonstrates the low habitat-scale intra-specific variability regarding the carbon isotope ratios of two suspension-feeder and it highlights the need to consider spatial heterogeneity of benthic primary production in the context of food web studies along with different spatial scales.

The second article uses carbon and nitrogen stable isotope ratios measured for the entire macrofauna community to compare the trophic functioning of the control, associated and engineered sediments. Overall, the reef community presents a larger trophic niche than the control community linked to the presence of the three-dimensional biogenic structures and the increased local primary production. This article further reveals the low trophic competition between abundant suspension-feeders present in the engineered sediments, especially between the engineer, the Japanese oyster and the porcellanid crab.

Article 2 - What can habitat complexity and food source heterogeneity tell us about fine-scale isotopic compositions?

Article in preparation (submission toPlosOne)

Auriane G. Jones [a,b,c], Stanislas F. Dubois [a], Anik Brind'Amour [d], Jérôme Fournier [c,e], Touria Bajjouk [b], Lerouxel Astrid [f], Nicolas Desroy [b], Gernez Pierre [f], Laurent Barillé [f]

[a] IFREMER, Centre de Bretagne, DYNECO LEBCO, 29280 Plouzané, France

[b] IFREMER, Laboratoire Environnement et Ressources Bretagne nord, 38 rue du Port Blanc, BP 80108, 35801 Dinard cedex, France

[c] CNRS, UMR 7208 BOREA, 61 rue Buffon, CP 53, 75231 Paris cedex 05, France

[d] IFREMER, Centre Atlantique, Unité Ecologie et Modèles pour l'Halieutique, Rue de l'Ile d'Yeu, BP 21105, 44311 Nantes Cedex 03, France

[e] MNHN, Station de Biologie Marine, BP 225, 29182 Concarneau cedex, France

[f] UNIVERSITE DE NANTES, Laboratoire Mer Molécules Santé, 2 rue de la Houssinière, 44322 Nantes Cedex 03, France

1. Introduction

Food web structure and trophic interactions are key aspects of an ecosystem's functioning (Duffy et al. 2007, Rigolet et al. 2015) along with structural and functional diversity (Tilman et al. 2014). These trophic components of functionality are often considered when evaluating the impact of natural and anthropogenic disturbances on ecosystems (Layman et al. 2007b, Nordström et al. 2015, Quillien et al. 2016, Nordström and Bonsdorff 2017). Indeed, 'pristine' and 'degraded' ecosystems often differ by their respective food web complexity, the presence and abundance of large top predators and food source heterogeneity, bringing either stability to the system or making it more vulnerable to disturbances (Neutel et al. 2007, Rooney et al. 2008). Habitat diversity and spatial heterogeneity influence the distribution and diversity of autotrophic and heterotrophic organisms (Pittman et al. 2004, Kraan et al. 2009), leading to changes in trophic interactions (Larkin et al. 2008). In this context, stable isotopes have proven to be powerful tools to trace pathways of organic matter among sources and consumers at various spatial and temporal scales (West et al. 2009, Rascher et al. 2012, Hyndes et al. 2013, Christianen et al. 2017). Indeed, temporal and spatial patterns of isotopic composition variations are mapped and studied at the scale of continents, or over the geographical range of a species, as isotope landscapes or isoscapes (West, 2005). These isoscapes help reconstruct migration patterns over large spatial scales like North America and across multiple generations (Hobson and Wassenaar 1997, Hobson 2005, Flockhart et al. 2013). In the marine realm, isoscapes are often applied at regional or larger spatial scales to retrace movements and foraging behaviors of wide ranging consumers (Graham et al. 2010) like marine mammals (Newsome et al. 2010) and fish (MacKenzie et al. 2011, Carlisle et al. 2012).

Carbon (^{13}C / ^{12}C) and nitrogen (^{15}N / ^{14}N) isotope ratios, reported as $\delta^{13}C$ and $\delta^{15}N$, are often used to investigate basal sources of organic matter (Fry and Sherr 1989), assimilated diet (Ben-David et al. 1997, Phillips 2001, 2012) and consumer trophic position (Post 2002), at the population-, community- and habitat-scale. Primary producers have distinct $\delta^{13}C$ linked to their physiology, their size and their environment (France 1995, Hemminga and Mateo 1996, Hemminga et al. 1999) and $\delta^{13}C$ of consumers are usually similar to that of their source of organic matter (~1‰ trophic shit ;DeNiro and Epstein, 1978), directly informing on their diet (Fry et al. 1978). Small-scale spatial variability in the stable isotope ratio of primary producers and consumers is being increasingly acknowledged and investigated in coastal marine ecosystems such as intertidal oyster farms (Dubois et al. 2007b), coastal lagoons (Carlier et al. 2009, Como et al. 2012) and tidal marshes (Larkin et al. 2008, Wang et al. 2015). Many environmental factors have been identified as drivers of these spatial variations, such as hydrodynamic processes (*e.g.* tidal cycles (Hill et al. 2008)), habitat characteristics (*e.g.* topographic heterogeneity (Larkin et al. 2008)), mud content and elevation (Dubois et al. 2007b), terrestrial organic matter inputs (Carlier et al. 2009) and salinity (Prado et al. 2014). These environmental factors directly or indirectly affect the presence, biomass, availability and stable isotope ratios of the primary producers at the base of the food webs, affecting in turn consumer's stable isotope composition (Richoux and Froneman 2007,

Stokes et al. 2011, Ubertini et al. 2012). These studies have highlighted the importance of quantifying intra-specific variations at small spatial scales when using stable isotopes to characterize trophic pathways. Indeed, if intra-specific variability is not considered, erroneous conclusions can emerge on the contributions of different sources to assimilated diets of consumers (Barnes et al., 2008) and when using primary consumers to estimate the trophic position of higher order consumers (Post 2002, Hyndes et al. 2013). Nonetheless, many trophic studies using stable isotopes, continue to consider a very limited number of sampling locations while studying vast habitats (several hundreds of square meters), only sparsely considering potential intra-habitat variability (Vizzini and Mazzola 2006, Grall et al. 2006, Dubois et al. 2007b, Riera 2007, Rigolet et al. 2014a, De Smet et al. 2015a). This limited sampling can hinder the ability to detect different spatial patterns of $\delta^{13}C$ and/or $\delta^{15}N$ variations and potential drivers of these patterns. In this context, it is time to bridge the gap between large-scale isoscapes and habitat-scale trophic studies to understand habitat-scale patterns of variations in the isotopic compositions of food sources and consumers, as recently done by Christianen et al. (2017) in the Wadden Sea for benthic communities and (Rascher et al. 2012) in an autotrophic community invaded by an exotic N_2 fixing plant.

Intertidal habitats created by physical ecosystem engineers (Jones et al. 2010) like mussels (Engel et al. 2017), oysters (Echappé et al. 2017) or sessile polychaetes (Dubois et al. 2002) are good candidates to investigate the different spatial scales of variation of a consumer's isotopic composition. Since these habitats exist because the ecosystem engineer is present, it is possible to sample the engineer species according to different designs and over the entire extent of the habitat. Furthermore, the presence of these habitats on soft sediments makes their delimitation and mapping straightforward. Many physical ecosystem engineers are sessile primary consumers mostly feeding on suspended organic matter (*e.g. Mytilus edulis*, *Crassostrea virginica*, *Sabellaria alveolata*). Their living habit and feeding strategy restricts their food sources to suspended or resuspended particles locally available, hence limiting potential sources of variations. Indeed, mobile consumers such as coastal fish feed in multiple habitats (*e.g.* salt marshes, seagrass meadows and soft sediments in (Prado et al. 2014)) while deposit feeders use the diversified sources of organic matter present in the sediments (Como et al. 2012, Christianen et al. 2017), and are highly dependent on the spatial and temporal variability in those potential food sources. Several physical ecosystem engineers also promote local food sources such as intertidal and subtidal benthic microalgae, via the habitat they engineer and their biological activity (Rigolet et al. 2014a, Echappé et al. 2017, Engel et al. 2017, Jones et al. 2018). These locally produced food sources can then be used by the ecosystem engineer according to the 'gardening hypothesis' (Hylleberg 1975) and/or by other associated species.

Sabellaria alveolata a.k.a. the honeycomb worm is a European habitat-building and suspension-feeding ecosystem engineer (Gruet 1972, Dubois et al. 2005). This polychaete is commonly found in the intertidal zone along the Atlantic coast from Scotland and Ireland to Morocco (Muir et al. 2016), where it lives in tubes mainly composed of bioclastic sand particles resuspended by wave action (Lucas

and Lefevre 1956, Gruet 1972). It can build three-dimensional structures called reefs, veneers or hummocks, over several hundreds of square meters on hard surfaces like rocky shores, pebbles or oyster shells on soft sediments (Gruet 1972, Wilson 1974, Caline et al. 1988). The largest *S. alveolata* reef covered 225 ha in 2001 and it is a rare example of a reef built on soft sediments (Desroy et al. 2011), allowing an easy contouring of the bioconstructions (engineered sediments) against the neighboring soft sediments (associated sediments) (Noernberg et al. 2010, Desroy et al. 2011). At the scale of this reef, benthic microalgae production in the associated sediments is higher in late winter and late summer compared to control soft sediments uninfluenced by the reef (Jones et al. 2018) and once resuspended, they can represent part of the diet of suspension-feeders like *S. alveolata* (Dubois et al. 2007b). Green algae are also present on the engineered sediments (Dubois et al. 2006a) during spring, summer and autumn, potentially becoming a trophic resource for suspension-feeders once detached and fragmented (Dubois and Colombo 2014). At smaller spatial scales, field observations have shown that benthic microalgae (pers. obs.) and green macroalgae (Rollet et al. 2015) are heterogeneously distributed.

In this context, *S. alveolata* and an associated suspension-feeder *Mytilus* cf. *galloprovincialis* classically attached to the engineered bioconstructions, were hypothesized to 1) respond to basal resource small-scale spatial heterogeneity through changes in the proportion of benthic (microalgae and green algae) and pelagic (phytoplankton) food sources to their diet, which would be evidenced from their $\delta^{13}C$ (France 1995, Christianen et al. 2017). 2) Other parameters could alter the availability of these different sources for the suspension-feeders and consequently their $\delta^{13}C$, notably intra and inter-specific trophic competition and the engineered sediment's physical structure. Indeed, changes in physical habitat complexity (fragmentation and density) affects turbulent diffusion of food sources, altering their availability for suspension-feeders living in these biogenic habitats like bivalves in seagrass meadows (González-Ortiz et al. 2014). 3) Finally, $\delta^{13}C$ variations occurring at various spatial scales could be driven by the previously mentioned abiotic (physical habitat complexity) and biotic (basal resource heterogeneity and intra and inter-specific trophic competition) variables. To test these three hypotheses, a 75 m- resolution $\delta^{13}C$ isoscape (West et al. 2009) of *S. alveolata* and *Mytilus* cf. *galloprovincialis*, was built using systematic field sampling. This resolution can be considered as medium relative to the reef's extent (2.5 km long for 1 km wide); nonetheless, it is a fine scale when compared with previous benthic studies. First, potential variables explaining these two isoscapes were investigated at the global reef scale; biotic variables (proxies for benthic microalgae and green algae biomass, oyster and mussel cover) and abiotic variables (spatial structuration metrics). Then, using Moran's eigenvector maps (MEMs, (Dray et al. 2006)) to describe global to local $\delta^{13}C$ patterns of spatial variations, we tried to explain the different inherent $\delta^{13}C$ isoscapes with the same set of explanatory variables.

2. Materials and methods

2.1. Study site and reef state survey

Our study took place in the largest *S. alveolata* reef in Europe, the Sainte-Anne reef (48°38'700N and 1°40'100W) located in the Mont-Saint-Michel Bay (MSMB, France) between Brittany and Normandy and in the Western part of the English Channel (Desroy et al. 2011). This 225 ha reef (as measured in 2001) is one of three existing *S. alveolata* structures present exclusively on soft sediments (Holt et al. 1998). Hence, two types of sediments are visible: the sediment engineered by *S. alveolata* (engineered sediment, hereafter ES, 61.5 ha in 2001) commonly called reef and the soft sediments present around the structures (associated sediment, hereafter AS, 163.5 ha in 2001) (Noernberg et al. 2010). The Sainte-Anne reef is parallel to the coast and to the main tidal currents and located ca. 3 km from the coastline in the lower intertidal zone (*i.e.* between the -2 and the -4 m isobaths (Noernberg et al. 2010)). *S. alveolata* reefs are dynamic biogenic structures that expand and retreat over time following a general growth pattern. To study the reef's health state, (Dubois 2003) initiated a survey of the Sainte-Anne reef, based on a 75 x 75 m grid covering all the ES. The monitoring went on in 2007, 2011 and 2015 to investigate its evolution over time (Desroy et al. 2011). During these surveys, the operators gather a number of data at the grid scale such as qualitative indications on the dominant sediment type of the AS (mud, muddy sand, fine sand, medium sand, coarse sand). Using these qualitative indications, a semi-quantitative index between 1 and 5 representing mud abundance (1 = 100% coarse sand to 5 = 100% mud) was built. Inside each grid, the operators also estimated, using a 1 m² quadrat, the oyster (*Magallana gigas* formerly known as *Crassostrea gigas*) and the mussel (*Mytilus* cf. *galloprovincialis*, a mussel with a phenotype very close to *Mytilus galloprovincialis*) cover (3 replicates), indicated as cov_{MGIG} and cov_{McfGAL}. The 2015 health state survey took place in spring and covered 283 stations.

2.2. Suspension-feeder field sampling and stable isotope analysis

During one low tide in May 2015, between three and ten adult *S. alveolata*, were systematically collected in the 283 stations (75 x 75 m grid cells) of the spring 2015 reef state survey (Desroy et al. 2011). Between one and five *M.* cf. *galloprovincialis* individuals were also collected in every grid where we could find some (in 81% of the 283 stations that is 230 stations). Suspension-feeders were all collected ca. 50 cm above the sediment. *S. alveolata* individuals were carefully extracted from their tube using tweezers and only undamaged adults were kept. All the collected individuals were stored in ice during transport to the laboratory and then at -20°C until further processing. For stable isotope analysis, only immature adult *S. alveolata* were used, to limit potential ontogenetic diet changes (Hamilton et al. 2011) and physiological changes linked to gametogenesis that could affect trophic fractionation

(Blanchet-Aurigny et al. 2012, Lefebvre and Dubois 2016a). Similarly, mussels with a similar size (mean size = 34.4 ± 4.5 mm) were selected. To limit inter-individual variability, 3 individuals – unless less were collected – were pooled at each station (Barnes et al. 2008, Hyndes et al. 2013). The *S. alveolata* were prepared by removing their opercular crown, their caudal peduncle and the content of their digestive track. For the mussels, mantle was used. After dissection, all samples were rinsed with Milli-Q water before freeze-drying. Each pool of individuals was ground to a homogenous powder and 1 mg was weighted into a tin capsule. All the samples were analyzed using a Thermo Delta V isotope mass spectrometer coupled via a Conflo IV to a Carlo Erba NC2500 elemental analyzer (Cornell University Stable Isotope Laboratory). Isotopic ratios of carbon are reported using the standard δ notation as units of parts per thousand (‰) relative to the international reference standards:

$$\delta X = \left[\left(R_{sample}/R_{reference}\right) - 1\right] \text{ x } 1000 \quad (1)$$

where X = ^{13}C, and R = $^{13}C/^{12}C$. Vienna-Peed Dee Belemnite limestone was used a reference standard. The analytical precision was 0.09 ‰.

2.3. Estimation of benthic primary production

To measure the spatial heterogeneity of benthic primary production, normalized difference vegetation index (NDVI) was used as a proxy for MPB and *Ulva* spp. biomass (Rouse et al. 1974, Maxwell et al. 1982, Méléder et al. 2003). NDVI was calculated using a multispectral image taken on September 27, 2015 at 11h06 (UT) by the Pleiades-1 satellite sensor (Airbus Defense and Space). This image was corrected for atmospheric effects and calibrated in reflectance values (Matthew et al. 2000). In multispectral mode, the Pleiades radiometer covers four channels: a blue (430-550 nm), a green (490-610 nm), a red (600-720 nm) and a near-infrared (750-950 nm) (IGN 2015). The image covered the entire Sainte-Anne reef with a 2 meters spatial resolution after resampling (IGN 2015), hence the NDVI was calculated for each 2 x 2 m pixel. We only considered benthic microalgae associated with fine sediments (*i.e.* epipelic microalgae) since it can be easily resuspended by tidal currents (Ubertini et al. 2015) and potentially consumed by suspension-feeders (Ubertini et al. 2012). Consequently, before calculating the NDVI for each AS pixel, a first spectral mask to remove the ES was applied and a second one to remove coarse sands in the AS. NDVI was also calculated for each ES pixel as a proxy for the *Ulva* spp. biomass. For each AS and ES pixel, the NDVI was calculated using the red and the near-infrared channels with the following formula (Rouse et al. 1974, Maxwell et al. 1982):

$$\text{NDVI} = \frac{(R_{NIR} - R_{red})}{(R_{NIR} + R_{red})} \quad (2)$$

where R_{red} is the red reflectance value (600-720 nm) and R_{NIR} is the near-infrared reflectance value (750-950 nm). NDVI varies between -1 and +1 with positive values tending towards 1 reflecting higher photosynthetic activity (Maxwell et al. 1982). In the intertidal zone, water (white on Figure 20b and Figure 20c) has negative NDVI values, while positive values inform on the presence of photoautotroph organisms. On the ES, NDVI value were thresholded between 0 and 1 to take into account the dense

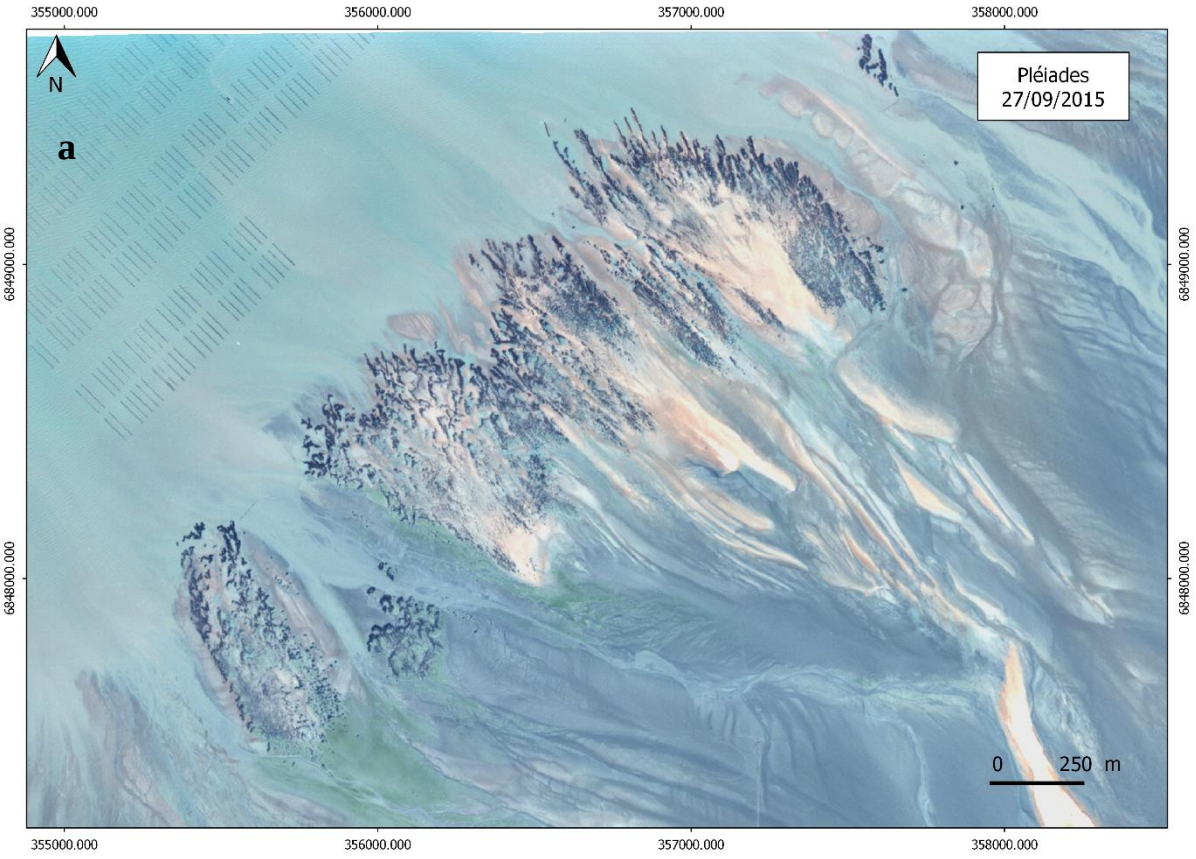
355000.000
356000.000
357000.000
358000.000
N
a
Pléiades
27/09/2015
6849000.000
6848000.000
0
250 m

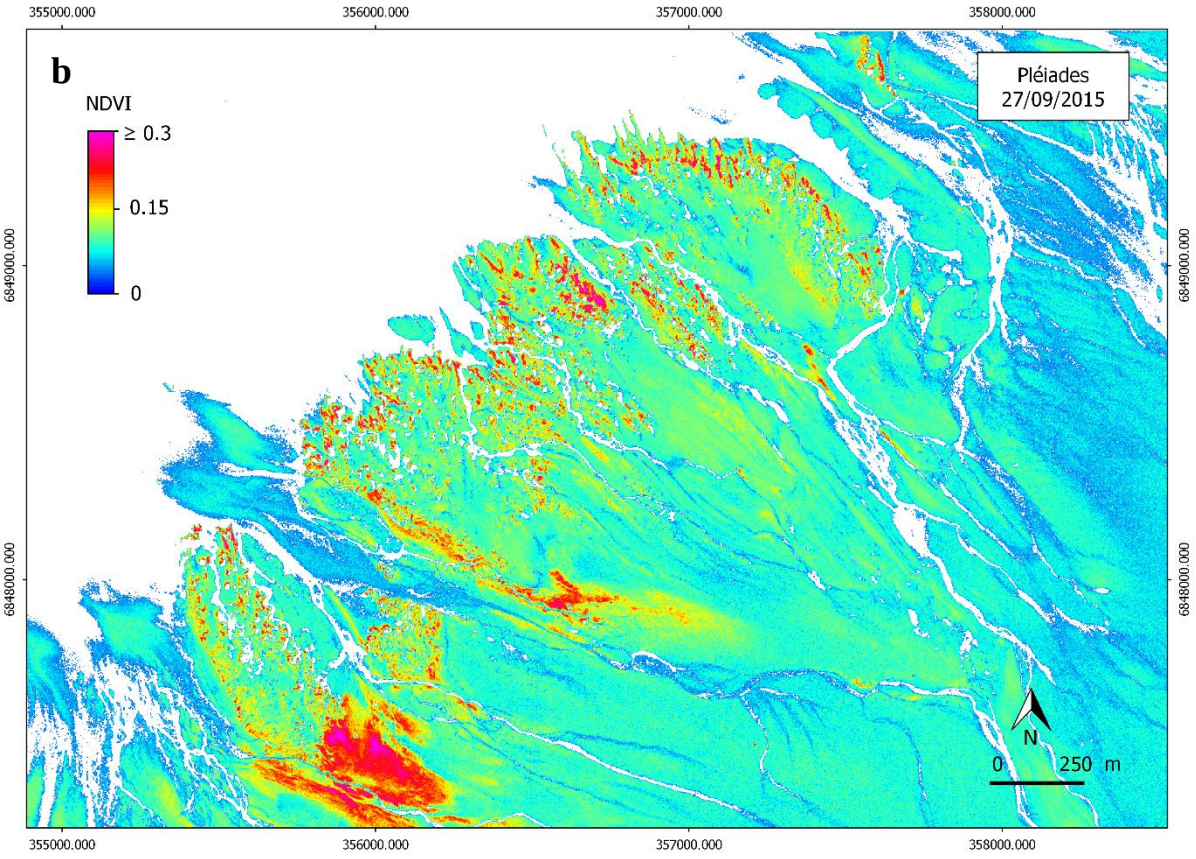
355000.000
356000.000
357000.000
358000.000
b
NDVI
≥ 0.3
0.15
0
Pléiades
27/09/2015
6849000.000
6848000.000
N
0
250 m

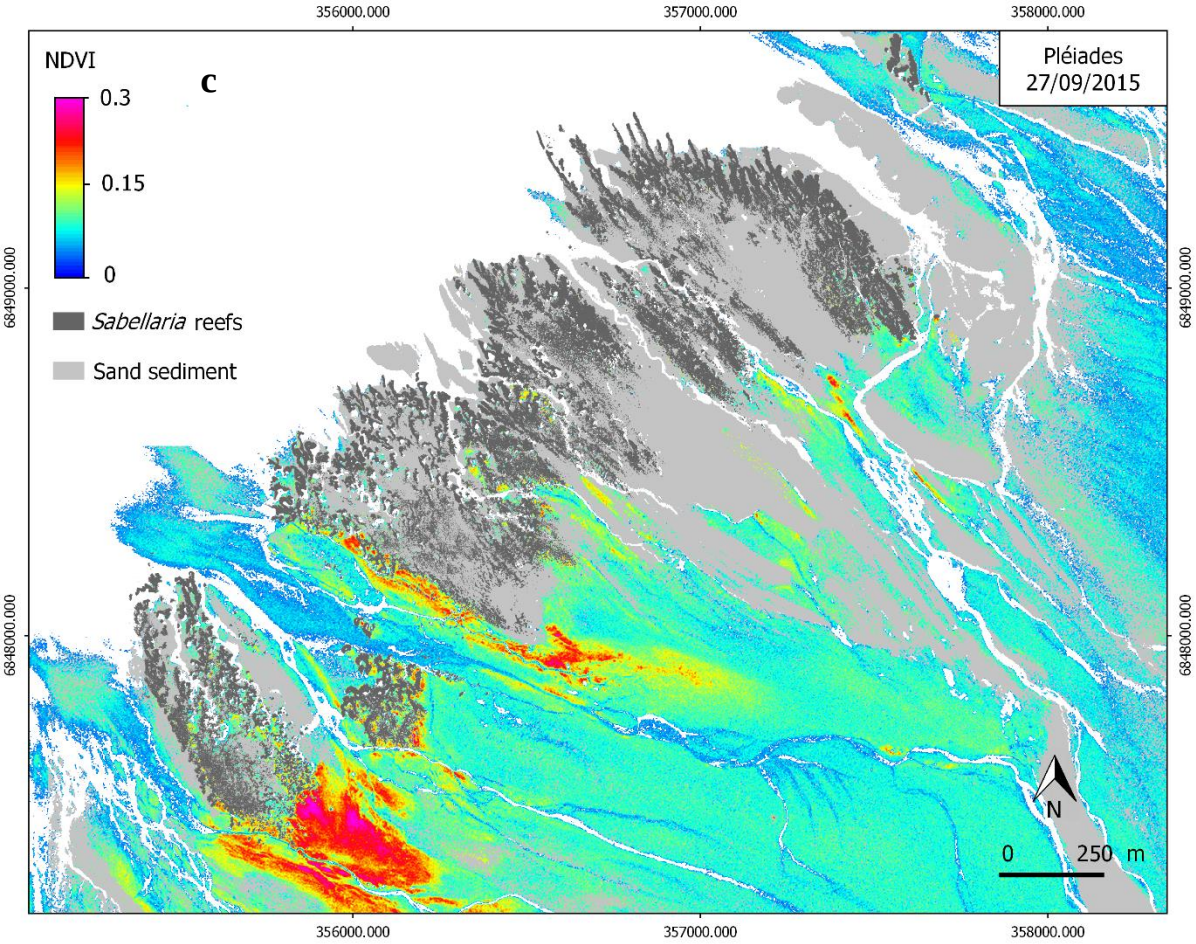
356000.000
357000.000
358000.000
NDVI
0.3
0.15
0
c
Pléiades
27/09/2015
Sabellaria reefs
Sand sediment
6849000.000
6848000.000
N
0
250 m

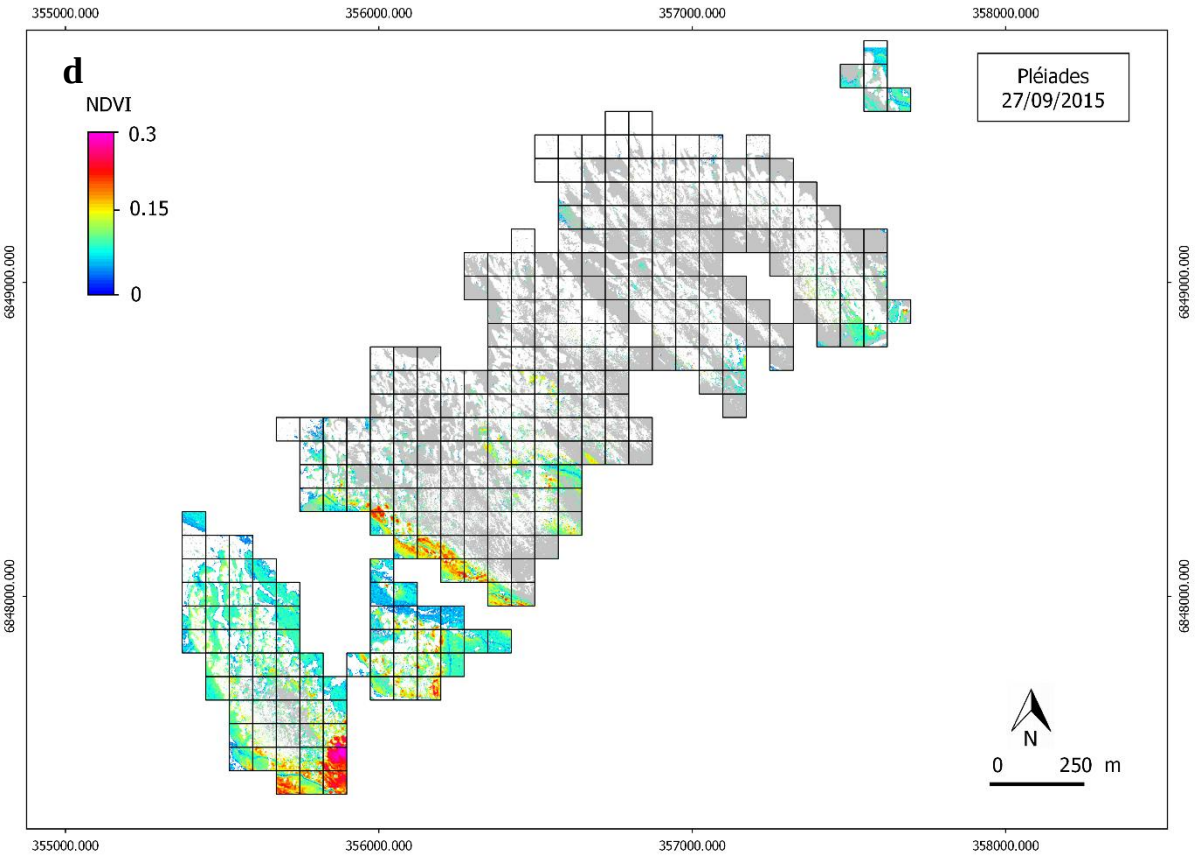
355000.000
356000.000
357000.000
358000.000
d
NDVI
0.3
0.15
0
Pléiades
27/09/2015
6849000.000
6848000.000
N
0
250 m

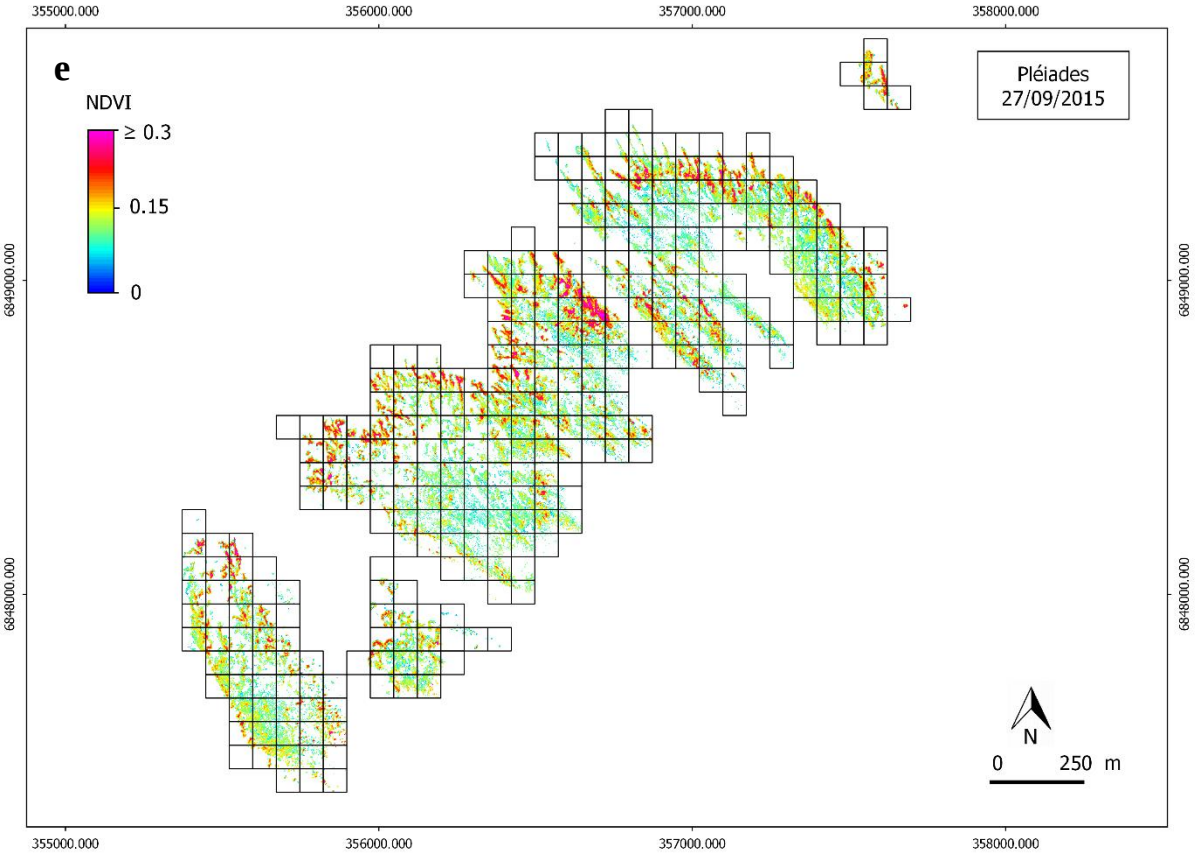

Figure 20. (a) False-color image of the Sainte-Anne reef zone acquired by the Pléiades satellite on September 9, 2015. Note the visible green color landward of the southwest sections of the reef sign of the presence of benthic microalgae, and the important sections of the associated sediments dominated by coarse sand and located in the central and northeast sections of the reefs. (b) Raw NDVI calculated for all the uncovered sediments (engineered and associated) using the same Pléiades image. Note the white color that corresponds to submerged sections like the seaward zone of the reef, tidal channels and small cuvettes located between the engineered sediments.(c) NDVI recalculated after applying two color-based masks to remove all the engineered sediments colonized by *Ulva* spp. and all the sandy associated sediments uncolonized by epipelic benthic microalgae. (d) NDVI map and grid used to extract the associated sediment NDVI considered as a proxy of MPB biomass. (e) NDVI map and grid used to extract the engineered sediment NDVI considered as a proxy of *Ulva* spp. biomass.

macroalgae which can have NDVI values superior to 0.3 (pink on Figures 20b and Figure 20c). On the AS, MPB was identified using NDVI values between 0 and 0.3 (blue to pink on Figure 20b and Figure 20c) (Méléder et al. 2003). Using the AS and the ES NDVI at the pixel resolution, a mean NDVI was calculated for each 75 x 75 m grid cell and for both sediment types (ES and AS). The mean engineered and associated sediment NDVI are indicated as $NDVI_{ES}$ and $NDVI_{AS}$.

2.4. Engineered sediment physical structuration

To quantify the physical structuration of the ES, landscape ecology metrics were used (McGarigal et al. 2012). On August 14, 2014 a high resolution (1 pixel = 15 x 15 cm) aerial photograph of the Sainte-Anne reef was taken (L'Europe vue du ciel) and displayed on a Geographical Information

System (GIS). Using the Supervised Image Classification tool in the Spatial analyst extension of ArcGIS©, a color analysis was performed to associate each pixel to ES or AS. Then, the resultant raster was manually corrected and a final map with the contour of the ES was obtained (Appendix S1). Using the final raster and the same 75 x 75 m grid used for the isoscapes, a set of spatial metrics was calculated, for the ES class and for each of 283 cells of the sampling grid using the public domain landscape ecology software FRAGSTATS version 4.2 (McGarigal et al. 2012). FRAGSTATS provides a large number of spatial metrics informing on both the geometry and the topology of the different landscape classes of interest and a subset of four metrics was selected (Table 13). These metrics were chosen because they informed on various aspects of the ES physical structuration (area, shape, proximity, contagion), were easy to interpret and corresponded to ecological realities of our study. A subset of uncorrelated metrics was used after testing the correlations (Spearman correlation). A threshold of |0.6| was deemed sufficient to considered them independent (see Appendix S2 for details). Finally, we verified that these metrics adequately measured fragmentation according to Wang et al., (2014). The independence between the different metrics and the engineered sediment abundance was also graphically checked (Appendix S3). Percentage of engineered sediments (pland), clumpiness index (clumpy) and perimeter-area fractal dimension (pafrac) are directly calculated at the grid scale while the Euclidian nearest neighbor distance (enn) is calculated at the ES patch scale. Its coefficient of variation (enn_{CV}) was used.

2.5. Spatial structuration of the $\delta^{13}C$

To take into account the structuration of *S. alveolata* and *M.* cf. *galloprovincialis* $\delta^{13}C$ at different spatial scales, Moran Eigenvector Maps (MEMs, Dray et al. (2006)) were built. MEMs are calculated based on the distances between the *n* sampling sites. They describe the variation associated with the position of the observations in space. MEMs represent a spectral decomposition of the spatial relationships among the sampling sites, which generates (*n*-1) eigenfunctions. MEMs are particular cases of Principal Coordinates of Neighbor Matrices (PCNMs, Borcard and Legendre, 2002) where the spatial autocorrelation is maximized regarding a spatial weighting matrix. They are obtained by eigenvalue decomposition of the spatial weighting matrix W computed as the cell-by-cell multiplication (Hadamard product) of a connectivity matrix B by a weighting matrix A (Dray et al. 2006, Legendre and Gauthier 2014). W indicates the strength of the potential interactions among the spatial units. The weighting matrix A was calculated as:

$$A = 1 - \left(\frac{D}{\max_{n} D}\right)^2 \text{ with } D = \text{Euclidian distance between the sampling points}$$

A varies between 0 when the Euclidian distance between two sampling stations is maximal and 1 when two sampling stations are neighbors (D = 0). For the connectivity matrix B, two grid cells were considered as connected if they were side or diagonal neighbors. To build the MEMs, all the stations for

Table 13 Class metrics used to quantify the physical structuration of the engineered sediments (from McGarigal et al., 2012)

Index	Type of index	Definition	Formula	Units	Range and interpretation
Percentage of landscape (pland)	Area metric	Sum of the areas (m^2) of all patches of the corresponding patch type, divided by total landscape area (m^2), multiplied by 100 to convert to a percentage	$\text{pland} = P_i = \frac{\sum_{j=1}^{n} a_{ij}}{A} * 100$ with P_i = proportion of the landscape occupied by patch type (class) i, a_{ij} = area (m^2) of patch ij and A = total landscape area (m^2), in our case A = 75x75 = 5625 m^2	Percent	0 < pland ≤ 100, approaches 0 when the engineered sediments become increasingly rare in the grid cell and pland = 100 when the entire grid cell consists of a single engineered sediment patch
Perimeter-area fractal dimension (pafrac)	Shape metric	2 divided by the slope of regression line obtained by regressing the logarithm of patch area (m^2) against the logarithm of patch perimeter (m)	$\text{pafrac} = 2 \Big/ \frac{\left[N \sum_{i=1}^{m}\sum_{j=1}^{n}(lnp_{ij} * lna_{ij}\right] - \left[\left(\sum_{i=1}^{m}\sum_{j=1}^{n}(lnp_{ij})\right)\left(\sum_{i=1}^{m}\sum_{j=1}^{n}(lna_{ij})\right)\right]}{\left(N \sum_{i=1}^{m}\sum_{j=1}^{n} lnp_{ij}^2\right) - \left(\sum_{i=1}^{m}\sum_{j=1}^{n} lnp_{ij}\right)^2}$ with p_{ij} = perimeter (m) of patch ii, a_{ij} = area (m^2) of patch ij and N = total number of patches in the grid cell	No unit	1 ≤ pafrac ≤ 2, equals 1 if the engineered sediment patch has a Euclidian shape like a square and increases as the engineered sediment patch form becomes more and more complex
Euclidian nearest neighbor distance: coefficient of variation (enn_{CV})	Isolation metric	Distance (m) to the nearest neighboring patch of the same type	enn = h_{ij} = distance (m) from patch ij to the nearest neighboring patch of the same class	Meters	Superior to 0 without limit, quantifies engineered sediment patch isolation
Clumpiness index (clumpy)	Contagion / interspersion metric	Proportional deviation of the proportion of like	given $G_i = \left(\frac{g_{ii}}{\left(\sum_{k=1}^{m} g_{ik}\right) - \min e_i}\right)$	No unit	-1 ≤ clumpy ≤ 1, equals -1 when the engineered sediment

adjacencies involving the corresponding class from that expected under a spatially random distribution	$$clumpy = \begin{bmatrix} \frac{G_i - P_i}{P_i} \; for \; G_i < P_i \; and \; P_i < 0.5 \; else \\ \frac{G_i - P_i}{1 - P_i} \end{bmatrix}$$ with g_{ii} = number of like adjencies between pixels of patch type i, g_{ik} = number of like adjencies between pixels of patch type i and k, $\min e_i$ = minimum perimeter (in number of cell surfaces) of patch type (class) i for a maximally clumped class and P_i = proportion of the landscape occupied by patch type (class) i	patches are maximally disaggregated, 0 when they are distributed randomly and approaches 1 when they are maximally aggregated

which we had a $\delta^{13}C$ value and all the explanatory variables were used. The reef patch located northeast of the main reef (Figure 20) was removed prior to the MEM building, because of its small size and isolation relative to the main reef zone. As a result, *S. alveolata* and *M.* cf. *galloprovincialis* were considered in 259 and 207 stations respectively, generating 258 and 206 MEMs. Only the MEMs corresponding to positive eigenvalues (*i.e.* positive autocorrelation) were retained (90 and 73 for *S. alveolata* and *M.* cf. *galloprovincialis,* respectively) as potential explanatory variables.

2.6. Data analysis

In a first step, we investigated the effect of (1) the abiotic variables (pland, pafrac, clumpy, enn_{cv}), (2) the biotic variables ($NDVI_{ES}$, $NDVI_{AS}$, cov_{MGIG} and cov_{McfGAL}) and (3) both the abiotic and biotic variables on the $\delta^{13}C$ of *S. alveolata* and *M.* cf. *galloprovincialis* with a multiple linear regression approach. Maps presenting the values of the biotic and abiotic explanatory variables at the scale of the entire reef are provided in Appendix S4. For (1), (2) and (3), a forward selection was performed to obtain the most parsimonious models that explained the $\delta^{13}C$ variations and each time, the potential multicollinearity among predictive variables was tested using the variance inflation factor (VIF). In all cases, the VIF was inferior to the common threshold value of 5 (Rogerson 2001). In order to avoid having an inflated type I error and overestimating the amount of explained variance, the modified forward selection method by Blanchet et al., (2008) was used. First, a global linear regression using all explanatory variables was carried out. If the global test was significant (p value < 0.1), then a forward selection (9999 permutations) was performed with two stopping criteria: a 0.1 alpha significance level and the adjusted R^2 obtained for each global linear regression.

In a second step, we looked into the different spatial scales of variations of the $\delta^{13}C$ of *S. alveolata* and *M.* cf. *galloprovincialis.* The positive MEMs described in part 2.6 were considered as potential explanatory variables for the $\delta^{13}C$ and using the forward selection method previously described (Blanchet et al. 2008), all the MEMs that significantly explained the $\delta^{13}C$ of both suspension-feeders were selected. These MEMs (4) represent the spatial scales at which the $\delta^{13}C$ was significantly structured. Then, to disentangle the relative effect of abiotic, biotic and spatial variables on the $\delta^{13}C$ variations, we followed the statistical framework developed in Mouillot et al., (2011). Three alternative nested models were built, using the four abiotic variables (pland, pafrac, clumpy, enn_{cv}), the four biotic variables ($NDVI_{ES}$, $NDVI_{AS}$, cov_{MGIG} and cov_{McfGAL}) and the significant MEMs. Each nested model was tested using generalized likelihood ratios to determine whether each type of explanatory variables (abiotic, biotic and spatial) had a significant additional contribution to the explanation of the $\delta^{13}C$. The parsimony of each model was assessed using the Akaike Information Criterion (AIC). The VIF was systematically inferior to 5 (Rogerson 2001). Finally, using the explanatory variables selected in (1), (2) and (4) we performed a variation partitioning of the $\delta^{13}C$ of *S. alveolata* and *M.* cf. *galloprovincialis* with respect to abiotic, biotic and spatial explanatory variables (Legendre et al. 2009, Legendre and Legendre 2012, Legendre and Gauthier 2014).

In a last step, we investigated which explanatory variables significantly influenced the $\delta^{13}C$ variations at each significant spatial scale. To do so, linear regressions between each selected MEM and the original $\delta^{13}C$, defining MEM sub-models, were performed. The fitted $\delta^{13}C$ predicted by each MEM sub-model represents the part of the original $\delta^{13}C$ explained by each spatial scale and it can be seen as the spatially explicit form of the response variable at the given MEM spatial scale. Using a forward selection (Blanchet et al. 2008), we obtained the abiotic (pland, pafrac, clumpy, enn_{cv}) and biotic variables ($NDVI_{ES}$, $NDVI_{AS}$, cov_{MGIG} and cov_{McfGAL}) that best explained the fitted $\delta^{13}C$ at the different spatial scales (Legendre and Gauthier 2014). All the statistical analysis were performed with R version 3.3.0 (R Core Team 2016). Package 'lmtest' was used for the log likelihood tests ('lrtest' function), package 'packfor' for the forward selection ('forward.sel' function) and package 'rms' for the VIF calculation ('vif' function). Finally, the 'vegan' package was used for the variance partitioning ('varpart' function).

3. Results

3.1. Local benthic primary production

Focusing on the AS, the NDVI obtained from the September 2015 satellite image (Figures 20 b, c, d and e), revealed a heterogeneous distribution of MPB and *Ulva* spp. biomass at the landscape scale. MPB biomass was lower in the northern sandy sediments compared to the southern muddy sediments. More locally, high NDVI was visible along a channel separating two reef sections and between engineered sediment patches. Using the semi-quantitative index representing mud abundance (1 = 100% coarse sand to 5 = 100% mud) derived from the reef health state survey data, a positive and significant correlation (Spearman, $r^2 = 0.53$, $p < 0.001$) was found between MPB biomass ($NDVI_{AS}$) and mud abundance (n = 251). Oyster ($r^2 = 0.49$ – Appendix S2) and mussel ($r^2 = 0.17$ – Appendix S2) cover were also significantly and positively correlated to the mean associated sediment NDVI. Seaward of the reef, the sediment was still underneath the water when the multispectral satellite image was taken. Hence, associated sediment NDVI (and the estimation of the MPB biomass) seaward of the reef could not be calculated.

In general, high *Ulva* spp. biomass was present in sections adjacent to the reef's borders and facing the open sea. Observation of green algae were scarce in sections surrounded by reef patches (Figure 20e). The Spearman correlation indicated that high *Ulva* spp. biomass was present where the engineered sediments covered a high percentage of the station (pland, $r^2 = 0.47$ – Appendix S2) and where the engineered sediment patches were highly aggregated (clumpy, $r^2 = 0.49$ – Appendix S2).

3.2. $\delta^{13}C$ variations without spatial structuration

The $\delta^{13}C$ of the two suspension-feeders had similar ranges, with values between -18.24 ‰ and -16.46 ‰ for *S. alveolata* and between -18.78 ‰ and -16.39 ‰ for *M.* cf. *galloprovincialis* (Figure 21). Figures 22a and Figure 22b represent the *S. alveolata* and *M.* cf. *galloprovincialis* isoscapes respectively. Overall, the two isoscapes do not display the same spatial structure with higher values concentrated in the southwest back reef in the mussel case while the *S. alveolata* show enriched values in various zones of the Sainte-Anne reef like in the northeast back reef and in some parts of the front reef.

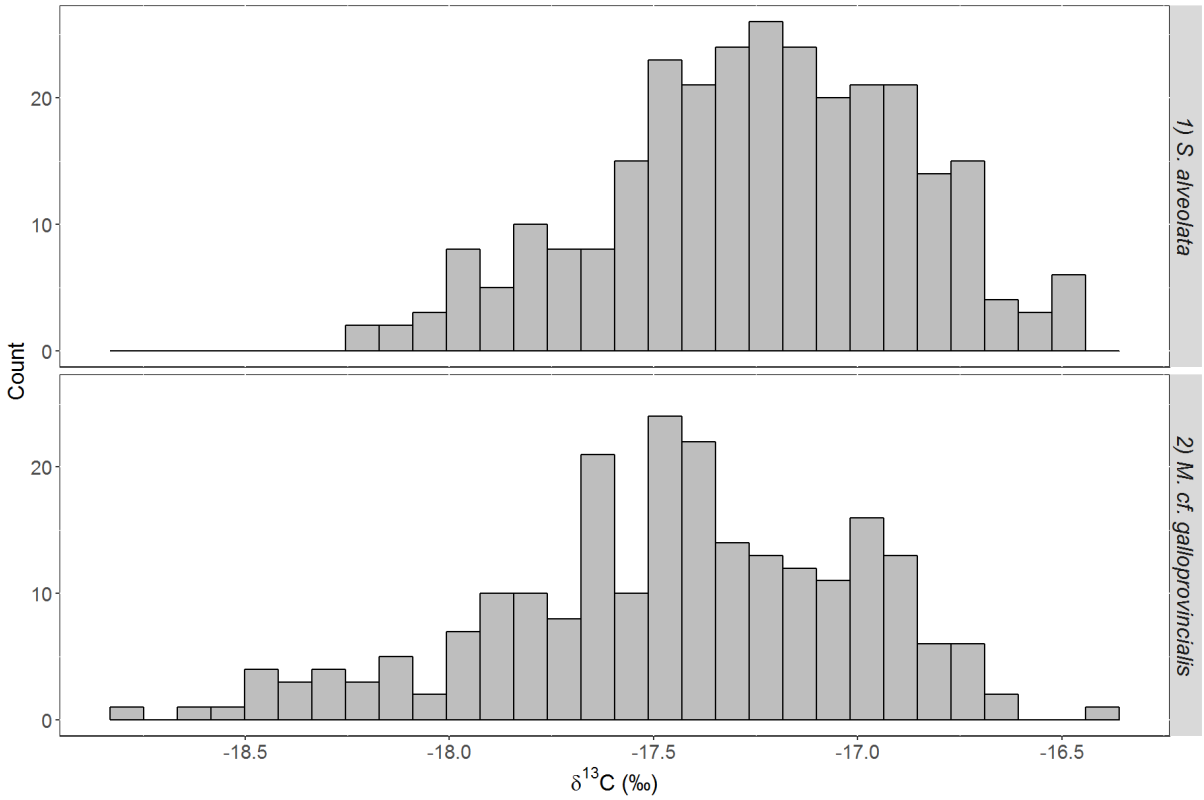

Figure 21. Histogram of the $\delta^{13}C$ for *Sabellaria alveolata* (n = 283) and *Mytilus* cf. *galloprovincialis* (n = 230).

Abiotic and biotic variables either considered separately or together explained less than 5% of the $\delta^{13}C$ variations of *S. alveolata* (R^2 = 0.012-0.037, Table 14) and up to 14% of the $\delta^{13}C$ variations of *M.* cf. *galloprovincialis* (R^2 = 0.036-0.14, Table 14). The model with all the variables or only the biotic variables always explained the highest amount of the total variance with an adjusted R^2 of 0.037 and 0.14 for and *M.* cf. *galloprovincialis* respectively (Table 14). In these cases and for both *S. alveolata* species, the mean NDVI of the associated sediments was the only selected variable and it always had a positive influence on the response variable. When only abiotic variables were considered in a model, the coefficient of variation of the Euclidian nearest neighbor distance was the only selected variable and

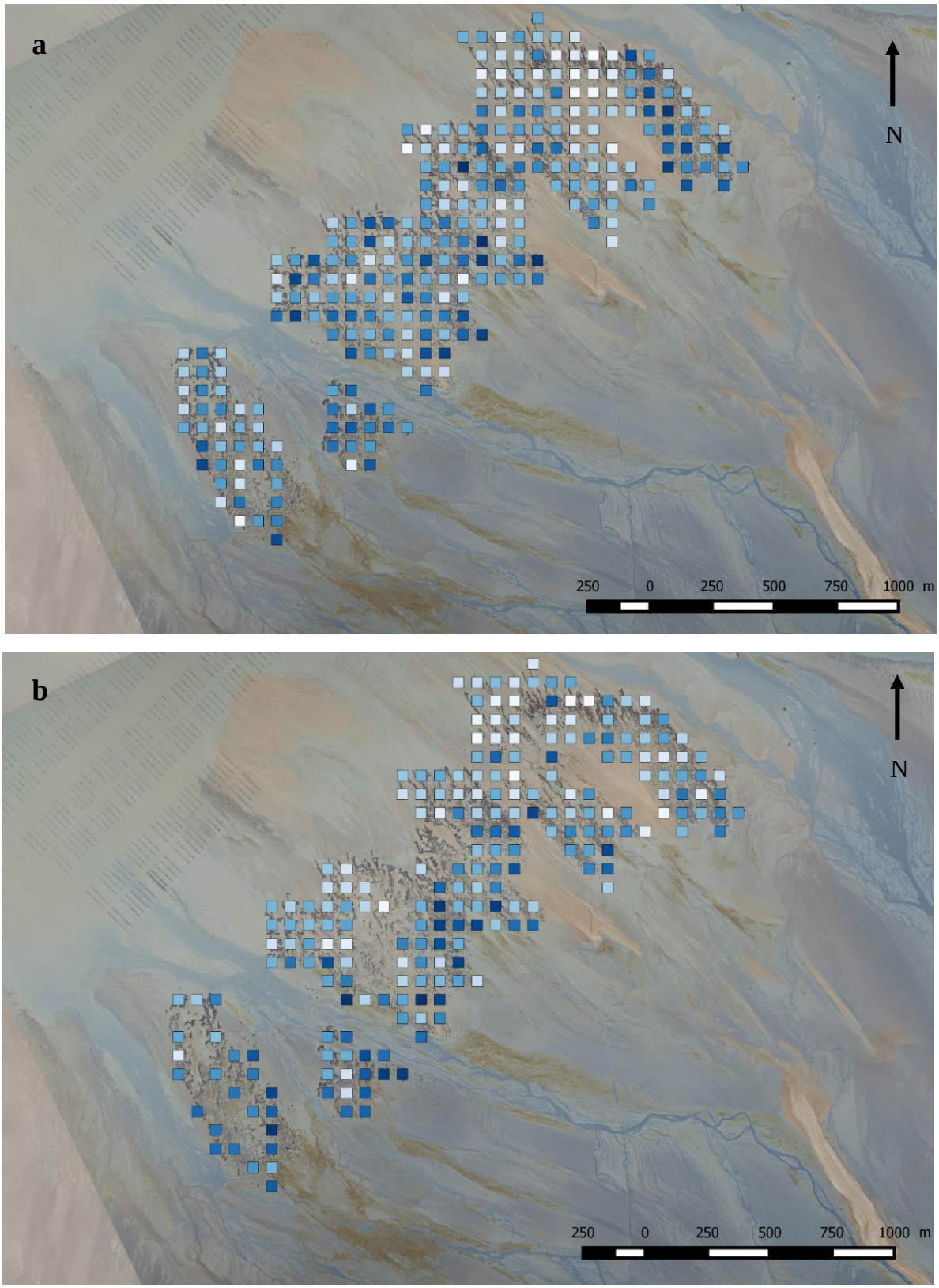

Figure 22. Carbon isoscape of (a) *S. alveolata* (n = 283) and (b) *M.* cf. *galloprovincialis* (n = 230). Darker colors represent more enriched $\delta^{13}C$ ratios. The *S. alveolata* isoscape ranges from -18.24 ‰ (white) to -16.46 ‰ (darkest blue) and the *M.* cf. *galloprovincialis* isoscape ranges from -18.78 ‰ (white) to -16.39 ‰ (darkest blue).

it had a significant and positive effect on the $\delta^{13}C$ of *S. alveolata*. For *M.* cf. *galloprovincialis*, the only abiotic variable selected was the perimeter-area fractal dimension and it had a significant and negative effect on the $\delta^{13}C$ of *M.* cf. *galloprovincialis.*

3.3. Spatial structuration of the $\delta^{13}C$

In a second part, Moran Eigenvector Maps (MEMs) were built using the sampling grid to look into the different spatial scales at which the $\delta^{13}C$ of the two suspension-feeders varied. The positive MEMs that best explained the response variable were selected. For *S. alveolata*, the forward selection identified six MEMs (n° 9, 4, 6, 32, 5 and 60) and together they explained 17.96% of the variability of the $\delta^{13}C$ of *S. alveolata*. For the mussel, the same procedure identified seven MEMs (n°28, 36, 30, 50, 19, 42, 07) and together they explained 13.85% of the variability of the $\delta^{13}C$ of *M.* cf. *galloprovincialis.* MEMs with high eigenvalues (low numbers) represent variations of the isotopic signal at a scale close to the entire sampling zone (*i.e.* the Sainte-Anne reef in our case) while MEMs with eigenvalues close to 0 (high numbers) represent local spatial scales of variations of the isotopic signal (*i.e.* scale close to 75 m). The part of the $\delta^{13}C$ of *S. alveolata* spatially structured is characterized by patterns of variations covering several hundred meters (Appendix S5) while in the case of *M.* cf. *galloprovincialis*, the part of the $\delta^{13}C$ explained by the MEMs is predominantly structured at smaller scales around a few hundred meters and lower (Appendix S6).

3.4. Contribution of the abiotic, biotic and spatial components to the $\delta^{13}C$

To disentangle the relative contribution of each type of variable (abiotic, biotic and spatial) to the $\delta^{13}C$ variations, four linear models for the $\delta^{13}C$ of each suspension-feeder were ran. The full model (A+B+MEM) included the four abiotic variables (A), the four biotic variables (B) and the six (*S. alveolata*) or seven (*M.* cf. *galloprovincialis*) significant MEMs (MEM). There were three nested models, either without the spatial component (A+B), without the biotic component (A+MEM) or without the abiotic component (B+MEM). The most parsimonious models, according to the AIC criteria, were the two models with the spatial component for *S. alveolata* (A+MEM and B+MEM) while for *M.* cf. *galloprovincialis,* it was the model without any abiotic component (B+MEM) (Table 15). The full model, the A+MEM and B+MEM models provided similarly high adjusted R^2 (0.18) for *S. alveolata* while for the mussel it was the B+MEM that provided the highest adjusted R^2 (Table 15). The likelihood tests indicated that for *S. alveolata*, only the spatial component made an additional contribution to the explanation of the $\delta^{13}C$ since the A+MEM and B+MEM models were not significantly outperformed by the full model (A+B+MEM). For *M.* cf. *galloprovincialis*, the spatial and biotic components made significant additional contributions to the explanation of the $\delta^{13}C$. The Venn diagrams illustrating the variance partitioning of the $\delta^{13}C$ of both suspension-feeders between abiotic, biotic and MEM (spatial) explanatory variables, indicated that between 82% (*S. alveolata*) and 77% (*M.* cf. *galloprovincialis*) of

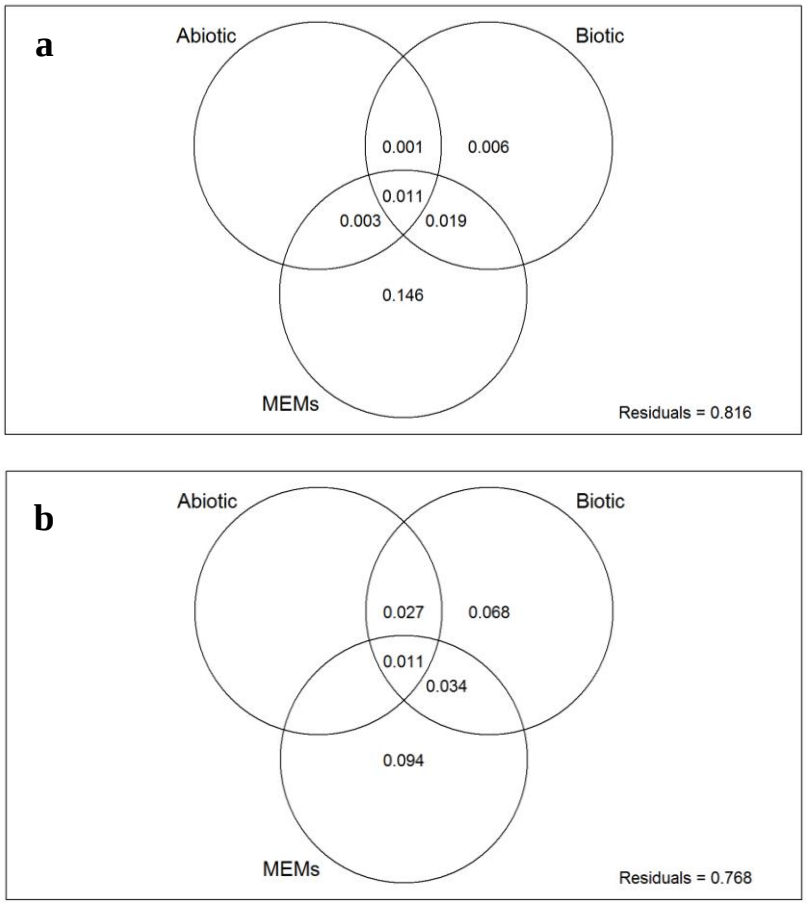

Figure 23. Venn diagram illustrating the result of variation partitioning of the $\delta^{13}C$ of (a) *S. alveolata* and (b) *M.* cf. *galloprovincialis* with respect to abiotic (Euclidian nearest neighbor distance for *S. alveolata* and perimeter-area fractal dimension for *M.* cf. *galloprovincialis*, top-left circle), biotic (mean NDVI of associated sediments for both species, top-right circle) and MEM explanatory variables (six selected MEMs for *S. alveolata* and seven selected MEMs for *M.* cf. *galloprovincialis*). The fraction of variation displayed in the diagram are computed from partial regressions. Values inferior to 0 are not shown.

the response variable was not explained by the set of variables we collected at the 75 m scale and above (Figure 23). For both species, MEMs uniquely explained the highest fraction of the adjusted R^2 (0.15 for *S. alveolata* and 0.094 for *M.* cf. *galloprovincialis*), followed by the biotic component (0.006 and 0.068) and lastly the abiotic component never explained alone a significant fraction of the adjusted R^2 ($adjR^2 < 0$ for both species). This evidences the importance of spatial structuration in explaining the $\delta^{13}C$ of suspension-feeders at scales superior to 75 m and indicates the importance of understanding which abiotic and biotic variables can explain the different spatial patterns.

3.5. Abiotic and biotic variables explaining the spatially structured $\delta^{13}C$

Each selected MEM represents a sub-model in which, the fitted $\delta^{13}C$ explained linearly by the given MEM, is considered as the new response variable. As previously, this new response variable was first explained using only the abiotic variables, then only the biotic variables and finally both type of

variables (Table 16). In some cases, the linear model with all the explanatory variables of a given type (all, abiotic or biotic) was not significant ($p > 0.1$) so we did not proceed to the forward selection (Blanchet et al. 2008). Hence, these cases are not presented in Table 16 since no variable significantly explained the fitted $\delta^{13}C$. This happened for *S. alveolata*, when all three combinations of explanatory variables were considered in the MEM60 sub-model. For *M.* cf. *galloprovincialis*, this happened when considering only abiotic explanatory variables in the MEM19 sub-model, and when all three combinations of explanatory variables were considered in the MEM28, 30, 36, 42 and 60 sub-models. Appendix S5 and S6 represent the maps of the fitted $\delta^{13}C$ of *S. alveolata* and *M.* cf. *galloprovincialis* respectively, obtained by linear regressions between each significant MEM and the original $\delta^{13}C$.

Abiotic and biotic variables - either considered separately or together - explained as much as 16% of the fitted $\delta^{13}C$ of *S. alveolata* at large spatial scales (MEM4) but explained a smaller portion of the fitted $\delta^{13}C$ of *M.* cf. *galloprovincialis* ($R^2 = 0.017\text{-}0.068$) whatever the spatial scale (Table 16). Generally, small but significant parts of the fitted $\delta^{13}C$ of species were accounted for at large spatial scales (MEMs inferior to 20) but it was no longer the case at more local scales. The *S. alveolata* fitted $\delta^{13}C$ was significantly and positively influenced by the Euclidian nearest neighbor distance (MEM4 and 6), the perimeter-area fractal dimension (MEM5), the mussel (MEM4) and oyster cover (MEM5 and 9). At a local scale (MEM32), the perimeter-area fractal dimension had a significant and negative influence on the fitted $\delta^{13}C$ of *S. alveolata*, while the clumpiness index and the mean NDVI of the ES had a negative influence on the fitted *S. alveolata* $\delta^{13}C$ at a larger scale (MEM9). The mean NDVI of the AS and the oyster cover had a negative effect on the fitted *S. alveolata* $\delta^{13}C$ at the MEM4 and 5 sub-models respectively. At one large spatial scale (MEM7), the fitted $\delta^{13}C$ of *M.* cf. *galloprovincialis* was significantly influenced by the clumpiness index (negative), the mussel cover (positive) and the oyster cover (negative). Finally, at a local scale (MEM19), the fitted $\delta^{13}C$ of *M.* cf. *galloprovincialis* was significantly influenced by biotic variables: the mean NDVI of the AS (positive), the mean NDVI of the ES (negative) and the oyster cover (positive).

4. Discussion

In this study, we mapped for the first time at a medium-resolution (75 m) the spatial variations in ^{13}C of a benthic ecosystem engineer and an associated potential competitor at the scale of a 150 ha biogenic habitat. Such isoscapes enabled an evaluation of the intra-habitat variability of the $\delta^{13}C$ of these two sessile suspension-feeders, an investigation of the different spatial scales of variations and an identification of abiotic and biotic variables linked to this variability.

4.1. Local benthic primary production

Heterogeneity in basal resources is at the base of the landscape food web theory developed by Rooney et al. (2008) and the Sainte-Anne reef is no exception (Figure 20). Firstly, the NDVI map

Table 14 Most parsimonious linear models (forward selection) that explained the $\delta^{13}C$ of (a) *S. alveolata* and (b) *M. cf. galloprovincialis* using all the explanatory variables (all), only abiotic variables (abiotic) and only biotic variables (biotic). The spatial structuration of the response variables is not taken into account and for each model, the adjusted R^2 (R^2) and the associated p-values (p) are presented. pland, percentage of the station covered by engineered sediments; pafrac, perimeter-area fractal dimension, enn_{cv}, coefficient of variation of the Euclidian nearest neighbor distance; clumpy, clumpiness index; $NDVI(AS)_{mean}$, mean NDVI of the associated sediment; $NDVI(ES)_{mean}$, mean NDVI of the engineered sediment; $mussel_{cov}$, *Mytilus cf. galloprovincialis* cover; $oyster_{cov}$, *Magallana gigas* cover. ***p < 0.001, ** 0.001 < p < 0.01 and * 0.01 < p < 0.05

(a)	**Explanatory variables**	**pland**	**pafrac**	**enn_{cv}**	**clumpy**	**$NDVI_{AS}$**	**$NDVI_{ES}$**	**cov_{McfGAL}**	**cov_{MGIG}**	**R^2**	**p**
Carbon	*all*					3.32**				0.037	0.001
isotope	*abiotic*			2.04*						0.012	0.04
ratio	*biotic*					3.32**				0.037	0.001
(b)	**Explanatory variables**	**pland**	**pafrac**	**enn_{cv}**	**clumpy**	**$NDVI_{AS}$**	**$NDVI_{ES}$**	**cov_{McfGAL}**	**cov_{MGIG}**	**R^2**	**p**
Carbon	*all*					5.87***				0.14	<0.001
isotope	*abiotic*		-2.93**							0.036	0.004
ratio	*biotic*					5.87***				0.14	<0.001

Table 15 (a) Multiple linear regressions between the $\delta^{13}C$ of *S. alveolata* or M. cf. galloprovincialis and all the explanatory variables (A+B+MEM), the abiotic and biotic explanatory variables (A+B), the abiotic explanatory variables and the significant MEMs (A+MEM), the biotic explanatory variables and the significant MEMs (B+MEM). The degree of freedom (df), Akaike Information Criterion (AIC), adjusted R^2 (R^2) and p-value (p) associated to each multiple linear regression is presented. The lowest AIC and the highest adjusted R^2 are in bold. (b) Results of the likelihood ratio tests comparing the nested models (χ^2) and the associated p-values (p). The significant differences between models ($p < 0.1$) are in bold.

	(a) Multiple linear regression					**(b) Likelihood ratio test**		
Response variable	**Model**	**df**	**AIC**	**R^2**	**p**	**Test**	**χ^2**	**p**
	A+B+MEM	244	188	0.18	< 0.001			
***S. alveolata* δ^{13}C**	*A+B*	250	223	0.041	0.018	*A+B+MEM vs. A+B*	47.28	**< 0.001**
	A+MEM	248	**184**	**0.18**	< 0.001	*A+B+MEM vs. A+MEM*	4.41	0.35
	B+MEM	248	**185**	**0.18**	< 0.001	*A+B+MEM vs. B+MEM*	4.83	0.30
	A+B+MEM	191	199	0.23	< 0.001			
***M.* cf. *galloprovincialis* δ^{13}C**	*A+B*	198	216	0.14	< 0.001	*A+B+MEM vs. A+B*	31.49	**< 0.001**
	A+MEM	195	213	0.16	< 0.001	*A+B+MEM vs. A+MEM*	22.54	**< 0.001**
	B+MEM	195	**193**	**0.24**	< 0.001	*A+B+MEM vs. B+MEM*	2.20	0.70

revealed a high biomass of benthic microalgae (NDVI up to 0.3) in the associated sediments landward of the reef (Figure 20b), confirming the importance of this engineered habitat in enhancing the local benthic primary production (Jones et al. 2018). Furthermore, high *Ulva* spp. and MPB biomass were concentrated in the central zone for green algae and southwest landward of the reef for MPB (Figure 20b). Green algae were generally present along the reef's borders while MPB was also detected along a major channel located in the South half of the reef, between engineered sediment patches and even in the sandy sediments present in the North sections. The asynchronous production in space detected for epipelic MPB was partly linked to the presence of mud and oysters while for *Ulva* spp. it was partly linked to the engineered sediments' physical structuration (Appendix S2). The significant positive correlation found between mud abundance and MPB biomass ($NDVI_{AS}$) agreed with previous results found in the macro-intertidal Baie des Veys in France (Orvain et al., 2012; Ubertini et al., 2012) and in several British and Dutch estuarine and coastal water bodies (Yallop et al. 2000). The mud present landward of the reef and behind relatively extended engineered sediment patches (pers. obs.) are large and small-scale direct consequences of the engineered sediment's barrier effect that reduces hydrodynamic forces and favors mud deposition in the resulting calmer zones (Caline et al. 1988, Dubois 2003, Desroy et al. 2011, González-Ortiz et al. 2014). This mud deposition (González-Ortiz et al. 2014) associated with the biological activity (feces and pseudo-feces) of *S. alveolata* (Dubois et al. 2005) and other bivalves (*M.* cf. *galloprovincialis* and *Magallana gigas* (van Broekhoven et al. 2015)) favors MPB development landward of the reef. Such a positive effect of engineered habitats on MPB development as previously been reported for mussel beds (Engel et al. 2017), oyster reefs (Echappé et al. 2017), oyster-farm structures (Orvain et al. 2012) and other polychaetes reefs (*Ficopomatus enigmaticus*, Bruschetti et al., 2011). The important role played by associated bivalves as MPB promoters was confirmed by the significant positive correlation between the oyster and mussel cover and the mean associated sediment NDVI (Appendix S2). For *Ulva* spp., an important continuous surface of engineered sediments favored an optimal growth leading to a high biomass. This result indicated that engineered sediments presenting a good health status were more exposed to *Ulva* colonization than more degraded reef sections, a conclusion in contradiction with Rollet et al. (2015). They emitted the hypothesis that green algae developed on engineered sediment patches in a bad health status by using the organic matter made available by the decaying *S. alveolata*.

4.2. Trophic importance of local benthic resources

Generally, suspension-feeders exhibit far less intra-specific variations compared to deposit-feeders (Carlier et al. 2009) because they have a selective assimilation of food (Dubois and Colombo 2014) and use a less variable pool of organic matter (*i.e.* only suspended or resuspended organic matter). At the scale of the reef, we only detected a 1.8 ‰ and 2.4 ‰ intra-specific variation in the $\delta^{13}C$ of respectively *S. alveolata* (range = -18.24 ‰ to -16.46 ‰) and the associated suspension-feeder *M.* cf. *galloprovincialis* (range = -18.78 ‰ to -16.39 ‰). These intra-specific variations were smaller

Table 16 Most parsimonious linear models (forward selection) that explained the spatial structuration of the carbon isotope ratio ($\delta^{13}C$) of (a) *S. alveolata* and (b) *M.* cf. *galloprovincialis* (fitted $\delta^{13}C$ predicted by each significant MEM model) using all the explanatory variables (all), only abiotic variables (abiotic) and only biotic variables (biotic). For each model, the adjusted R^2 (R^2) and the associated p-values (p) are presented. MEM, Moran Eigenvector Map; pland, percentage of the station covered by engineered sediments; pafrac, perimeter-area fractal dimension, enn_{cv}, coefficient of variation of the Euclidian nearest neighbor distance; clumpy, clumpiness index;, mean $NDVI_{AS}$, NDVI of the associated sediment; $NDVI_{ES}$, mean NDVI of the engineered sediment; cov_{McfGAL}, *Mytilus* cf. *galloprovincialis* cover; $cov_{MGIG,}$ *Magallana gigas* cover. In (a) all three MEM60 sub-models do not figure because the global models presented a p-value > 0.1 hence we did not perform the forward selection. For the same reason, in (b) the abiotic MEM19 sub-model and all three MEM28, 30, 36, 42 and 60 sub-models do not figure. ***p < 0.001, ** 0.001 < p < 0.01, * 0.01 < p < 0.05 and · 0.05 < p < 0.1

(a)	**Explanatory variables**	**pland**	**pafrac**	**enn_{cv}**	**clumpy**	**$NDVI_{AS}$**	**$NDVI_{ES}$**	**cov_{McfGAL}**	**cov_{MGIG}**	**R^2**	**p**
MEM4	*all*			5.3***		2.01*		2.24*	-2.61**	0.16	< 0.001
	abiotic			5.9***						0.12	< 0.001
	biotic					2.5*	2.3*	3.6***		0.10	< 0.001
MEM5	*all*		3.8***						2.7**	0.056	< 0.001
	abiotic		3.1**							0.032	0.002
	biotic					-2.68**			2.77**	0.031	0.007
MEM6	*all*			1.81.		2.09*				0.037	0.003
	abiotic			2.71**						0.024	0.0072
	biotic					2.90**				0.028	0.0040
MEM9	*all*						-2.6**		3.9***	0.076	< 0.001
	abiotic				-2.7**					0.024	0.007
	biotic						-2.6**		3.9***	0.076	< 0.001
MEM32	*all*		-2.8**							0.026	0.0057
	abiotic		-2.8**							0.026	0.0057
	biotic					2.77**				0.025	0.0061
(b)	**Explanatory variables**	**pland**	**pafrac**	**enn_{cv}**	**clumpy**	**$NDVI_{AS}$**	**$NDVI_{ES}$**	**cov_{McfGAL}**	**cov_{MGIG}**	**R^2**	**p**
MEM7	*all*				-3.3**			2.5*	-2.0*	0.068	< 0.001
	biotic							2.1*		0.017	0.034
MEM19	*all*					1.8.	-2.2*		1.8.	0.066	< 0.001
	biotic					1.8.	-2.2*		1.8.	0.066	< 0.001

compared to the suspension-feeding polychaete *Ficopomatus enigmaticus* in a subtidal coastal lagoon (-24.1 ± 0.2 ‰ to -21.5 ± 0.4 ‰, Como et al. (2012)), while they were in line with other suspension-feeders (*e.g. Cerastoderma glaucum, Mytilus galloprovincialis*) present in the Salses-Leucate lagoon (Carlier et al. 2009). Previous stable isotope analysis of filter-feeding mollusks from the eastern MSMB and the Sainte-Anne reef also collected after the phytoplankton bloom (spring) had $\delta^{13}C$ values around -20 ‰ suggesting a primary contribution of marine particulate organic matter (phytoplankton) to their diets (Riera, 2007). More specifically, the wild mussels from the Sainte-Anne reef sampled by Riera (2007) had $\delta^{13}C$ values depleted on average by 2 ‰ (range = -22.0 to -20.1 ‰) compared to our results, which conformed with the phytoplankton based diet generally admitted for mussels (Christianen et al. 2017). Comparing our 230 samples covering the entire reef with the 11 mussel samples collected at one sampling point by Riera (2007), the variation range is very similar. Differently, our results point towards a higher contribution of benthic sources to the diet of *M.* cf. *galloprovincialis* and *S. alveolata*, which is supported by other investigations in similar environments (Marín Leal et al. 2008, Dubois and Colombo 2014). The difference observed between our results and the values reported by Riera (2007) for bivalves sampled in spring 2003, could be linked to the establishment of new mussels farms North of the Sainte-Anne reef in 2003, creating a barrier between the open sea and the reef (Desroy et al. 2011). Indeed, these mussel farms modify the local currents (Salomon 2000) leading to the increased siltation observed by Desroy et al. (2011) and favoring the development of MPB, which can then be used by the local macrofauna. In addition, in the Western part of the MSMB Davoult et al. (2008) found that MPB biomass was high while productivity was low, suggesting that the MPB present is weakly exploited by primary consumers. This conclusion seems to be less true in the Sainte-Anne reef (not studied by Davoult et al. (2008)), indicating that this engineered habitat could be a "hotspot" regarding MPB contribution to the diet of local macrofauna. Furthermore, once detached and fragmented, macroalgae like *Ulva* spp. can also make up an important part of the assimilated diet of suspension-feeders (Dubois et al. 2007b, Dubois and Colombo 2014), which seems to be the case for the engineer species and *M.* cf. *galloprovincialis*.

4.3. $\delta^{13}C$ variations at the landscape scale

The $\delta^{13}C$ of the two suspension-feeders had a narrow range of variation limiting our ability to explain large portions of the total variability. Nonetheless, our first hypothesis stating that where the MPB biomass is higher, the suspension-feeders would have an enriched $\delta^{13}C$ because of a higher proportion of MPB in their diet was verified for both species. Indeed, without taking into account any spatial structuration, the mean NDVI of the associated sediments had a significant and positive influence on the $\delta^{13}C$ of *M.* cf. *galloprovincialis* and *S. alveolata* explaining a much higher fraction of the $\delta^{13}C$ variations of the first (14%) compared to the second (4%). These two suspension-feeders have different feeding mechanisms (*i.e.* external tentacular filaments and palps for *S. alveolata* and protected gills and labial palps for *M.* cf. *galloprovincialis*) leading to a stronger capacity of selection for the mussels

compared to *S. alveolata* (Dubois and Colombo 2014). Since benthic microalgae and by extent MPB have higher nutritional values than pelagic microalgae or green macroalgae, a suspension-feeder with the ability to select its food like mussels, could preferentially feed on MPB when available (Shumway et al. 1985, Mortillaro et al. 2014). A diet mainly based on sedimented organic matter, partially composed of benthic microalgae, was previously evidenced for exposed rocky shore blue mussels across the year (Dubois and Colombo 2014). In the same study, *S. alveolata* was shown to have a more diversified diet across the year with a dominance of *Ulva* in spring, an effect we did not detect at a global scale. Finally, the physical structuration of the engineered sediments never made a significant contribution in explaining the $\delta^{13}C$ variations and alone explained less than 4% of the total variability, stressing the prevalence of biotic factors in explaining the landscape scale diets of *S. alveolata* and *M.* cf. *galloprovincialis*.

4.4. Spatial patterns of variations

To take into account the multiscale spatial variation of the carbon isotopic signal, MEMs, (Dray et al. 2006), an approach very similar to PCNMs (Borcard and Legendre 2002), were used. This type of approach is commonly used to study the spatial and temporal distribution of communities (Legendre and Gauthier 2014) in terrestrial (Legendre et al. 2009), freshwater (Brind'Amour et al. 2005) and marine environments (Robert et al. 2014). In these different studies, the goal was to understand the relation between various aspects of community structure (*e.g.* species distribution, species richness, community composition, beta diversity) and environmental factors. Here, we applied this method designed for spatial ecology in the context of trophic ecology. The investigation of the different nested models and the variance partitioning revealed the importance of considering spatial patterns of variation when looking into habitat-scale $\delta^{13}C$ variations of consumers. Indeed, the spatial component explained between 14 and 18% of the total variability and all our results pointed towards the need to consider spatial patterns especially for *S. alveolata*. For *M.* cf. *galloprovincialis*, landscape scale biotic variables (*i.e.* associated sediment NDVI) made a significant contribution in explaining the $\delta^{13}C$ variations but considering the spatial component was also highly relevant. With our set of abiotic and biotic variables we were only able to explain large to medium spatial scales of variations of the $\delta^{13}C$, indicating other processes were shaping more local $\delta^{13}C$ patterns of variations (*i.e.* scale from 75 m to ~250 m, see Appendix S5 and S6). Even at large spatial scales, a very important part of the total variability remained unexplained.

Different factors could explain why we were not able to explain a large part of the total variability of the $\delta^{13}C$ patterns of variations, especially at more finer scales. A first explanation could be linked to small-scale biotic interactions, a second to small-scale variations in the $\delta^{13}C$ composition of benthic food sources and a third to the animal's individual physiology and diet-tissue fractionation, also called inherent variability (Barnes et al. 2008). Biotic interactions such as competition, predation and facilitation are key drivers of small-scale heterogeneity in trophic resources and species distribution

(Menge and Olson 1990) especially in complex habitats like *S. alveolata* reefs. In order to evaluate such inter- and intra-specific interactions and potentially link it to variations in the $\delta^{13}C$ composition of *S. alveolata* and *M.* cf. *galloprovincialis*, quantitative information on the presence and abundance of conspecifics and potential competitors (*Magallana gigas* and *Crepidula fornicata*) at a very high-spatial resolution (meter-scale) around where the animals were sampled, would have been necessary. In this regards, the information we had on oyster and mussel cover was not precise enough, nor at the most relevant spatial-scale. To try to limit the influence of such local interactions on the suspension-feeders' $\delta^{13}C$, several individuals were pooled prior to the stable isotope analysis. Nonetheless, the pooled individuals were often collected in close proximity (ca. 1-2 meters), not fully preventing meter-scale biotic interactions affecting their carbon isotopic composition. Furthermore, MPB can present variable carbon isotopic compositions as revealed by Christianen et al. (2017) at the scale of the Wadden Sea. In our case, the high spatial heterogeneity in the associated sediment's grain-size distribution could lead to the establishment of spatially distinct benthic microalgae communities (Underwood and Kromkamp 1999) presenting physiological differences and hence different $\delta^{13}C$ (France 1995). Since, we did not evaluate this source of variability, we cannot exclude it could explain part of the *S. alveolata* and *M.* cf *galloprovincialis* $\delta^{13}C$ variations. Finally, individual physiology and diet-tissue fractionation can explain very large parts of the intra-specific variability measured in wild populations (Barnes et al. 2008, Blanchet-Aurigny et al. 2012). Again, the pooling of individuals should have limited this inherent variability, hence focusing on the variability linked to diet but this source of intra-specific variability cannot be excluded.

Using MEMs to look into spatial patterns of $\delta^{13}C$ variation is a potentially fruitful new development. Here, each MEM sub-model accounts for a particular spatial pattern of enrichment or depletion of the $\delta^{13}C$. At large spatial scales, these patterns happen at scales over 300 m. At local spatial scales, the $\delta^{13}C$ variation patterns take place at the scale of a few adjacent station and even in some cases at the scale of one station (*e.g.* MEM 60 sub-model – Appendix S5). At each spatial scale, some sections of the reef do not present any particular pattern of enrichment or depletion (*e.g.* the South section of the reef in MEM4 sub-model – Appendix S5). The explanatory variables presented in Table 12 are the ones that significantly contribute to explaining a particular spatial pattern happening in one or several sections of the reef but never at the scale of the entire reef. At large spatial scales (MEM 4, 5 and 6 sub-models), the association of abiotic and biotic variables always explained the highest part of the fitted *S. alveolata* $\delta^{13}C$ variability. This result seems to point towards a complex interplay between resource abundance (MPB and *Ulva* spp.), physical structuration of the engineered sediments that can modify resource availability (González-Ortiz et al. 2014) and inter-specific interactions in explaining large-scale spatial patterns of *S. alveolata* $\delta^{13}C$ variations. In some cases, inter-specific interactions had a negative effect on the $\delta^{13}C$ of the engineer species probably through trophic competition (negative effect of oyster cover in MEM 4 sub-model). Indeed, *Magallana gigas* has a higher clearance rate (~2.3 $l.h^{-1}.g\ dmw^{-1}$ in Ropert and Goulletquer, 2000) than *S. alveolata* and is much more efficient at retaining small particles (4-5 µm)

than the engineer species (Dubois et al. 2003), leading to a potential decrease in resuspended MPB available to *S. alveolata* and a depleted $\delta^{13}C$. This result confirms the potential detrimental effect of the non-native pacific oyster regarding the availability of highly nutritional benthic microalgae to the engineer species but only in some reef sections. In MEM sub-model 4, the depleted zones correspond to zones previously identified as being under degradation between 2001 and 2007 (Desroy et al. 2011), which indicates that *Magallana gigas* colonization could be one of the causes of this long-term degradation. In other cases, inter-specific interactions had a positive effect on the isotopic composition probably caused by centimeter to meter-scale changes in boundary-layer flow that cause a retention of suspended particles like MPB close to the engineered sediments (Eckman 1983, Berke 2010). Such inter-specific interaction positively affecting resource availability is characteristic of facilitation, a common process shaping engineered habitats (Bruno et al. 2003).

The perimeter-area fractal dimension evaluates the average shape complexity taking into account all the engineered sediment patches present in a sampling station, meaning it does not consider the shape complexity of each engineered sediment patch (McGarigal et al. 2012). This parameter had a large-scale positive influence (MEM 4 sub-model) and a local negative influence (MEM 32 sub-model) stressing the multiscale interactions between ecological and physical processes that take place in self-organized habitats like mussel beds (van de Koppel et al. 2012) or *S. alveolata* reefs. We also detected a negative influence of *Ulva* on the $\delta^{13}C$ of both suspension-feeders at relatively large scales (MEM 9 and 19 sub-models) except for *S. alveolata* at the largest significant spatial scale (MEM 4 sub-model) where we detected a weak but positive influence. These algae act as a physical barrier to the settlement of *S. alveolata* larvae on the engineered sediments via their upright position over the reef (Dubois et al. 2006a) and a similar phenomenon could be limiting the availability of POM and resuspended MPB for suspension-feeders. When the reef is submerged, POM is always present in the water column while the peak of resuspended MPB concentration occurs shortly after the maximal current velocity (Koh et al. 2006), corresponding to the beginning of the rising tide (Salomon and Breton 2000). Consequently, suspension-feeders could benefit less from resuspended MPB in zones colonized by *Ulva*.

Conclusion

This study confirms the heterogeneous distribution of benthic microalgae and green macroalgae at the scale of a *S. alveolata* reef (Rooney et al. 2008) and highlights the importance of these locally produced food sources as key basal resource for suspension-feeders at the landscape scale. Indeed, the distribution of these different food sources explain part of the spatial patterns of variations of the $\delta^{13}C$ of *S. alveolata* and *M.* cf. *galloprovincialis*. In addition, inter-specific interactions (competition and facilitation) appear as important drivers of the $\delta^{13}C$ variations often in combination with the engineered sediment's physical structuration, stressing the diversity and complexity of the interactions happening at large and small spatial scales in this self-organized engineered habitat (van de Koppel et al. 2012).

Furthermore, we cannot exclude that the very strong tidal currents of the MSMB could cause the redistribution of the resuspended MPB at the landscape scale limiting the local variability in food sources available for suspension-feeders and consequently limiting their $\delta^{13}C$ variations. Finally, inherent physiological variability, meter-scale inter-specific interactions and the spatial variability in the $\delta^{13}C$ of the benthic food sources could also explain the important unexplained variability.

This study is a first and interesting step towards a more spatially explicit way of understanding trophic interactions at the scale of a habitat, which revealed a very low intra-habitat variability in the carbon isotopic composition of two abundant suspension-feeders. This result comforts "classic" sampling strategies used in trophic ecology, where primary consumers are collected in only a few points of an extensive habitat (several hectares), hence only covering a small part of it. Adopting this type of sampling strategy appears relevant when investigating the food-web of entire habitats, but much less relevant if the study goal is understanding particular inter- and/or intra-specific trophic interactions (competition or facilitation) happening at the habitat-scale. Finally, in the context of a heterogeneous and complex habitat like an engineered habitat, considering a spatial resolution inferior to 10 meters in a particular zone could be an interesting avenue to gain a more precise understanding of the mechanisms behind the variations in the isotope composition of primary consumers.

Appendix

Appendix S1. Treatments applied to the high resolution (1 pixel = 15 x 15 cm) aerial photograph of the Sainte-Anne reef taken on August 14, 2014: (a) original photograph, (b) original image with displayed on it the raster corresponding to all the engineered sediments in black (raster obtained using the Supervised Image Classification tool in the Spatial analyst extension of ArcGIS© and then manually corrected), (c) raster image of all the engineered sediments in black and (d) engineered sediment raster image with the sampling grid displayed on it (283 stations).

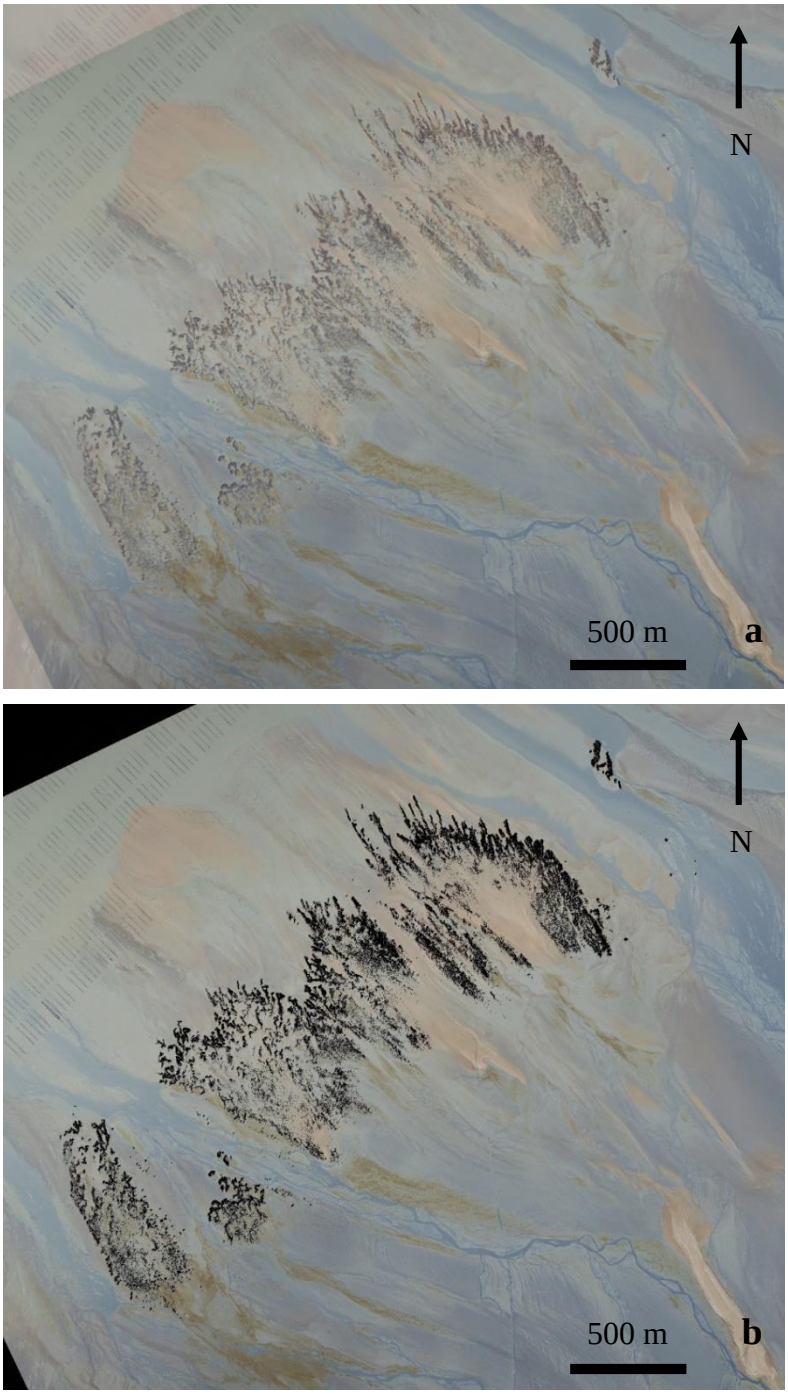

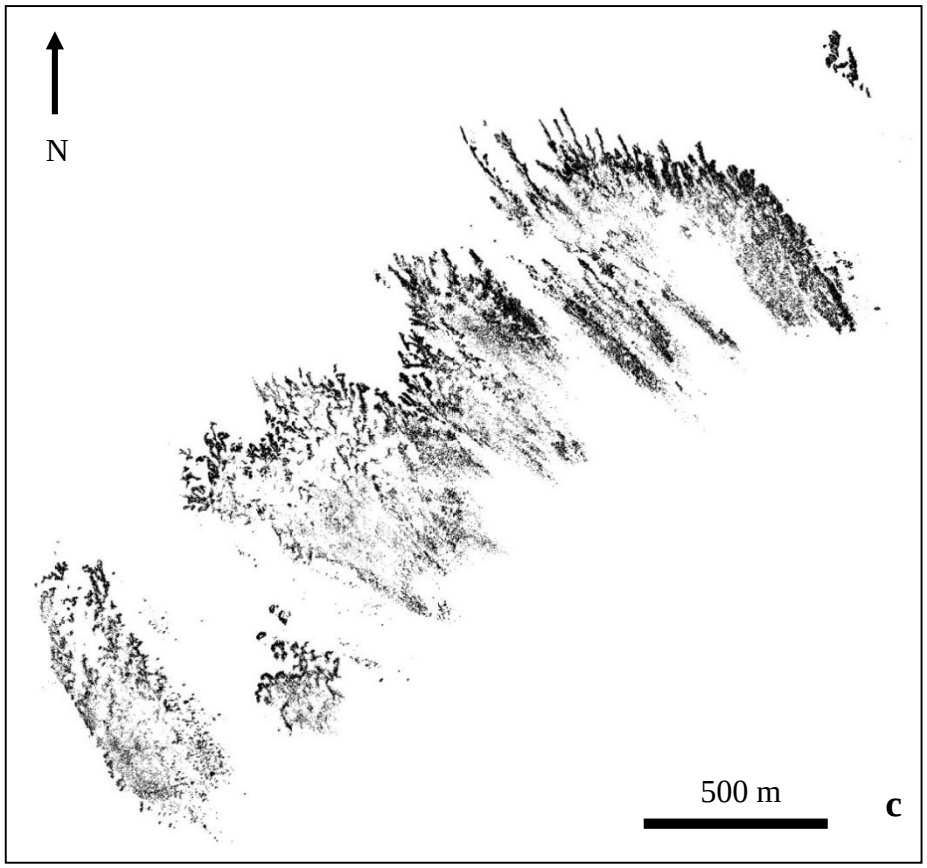
N
500 m
c

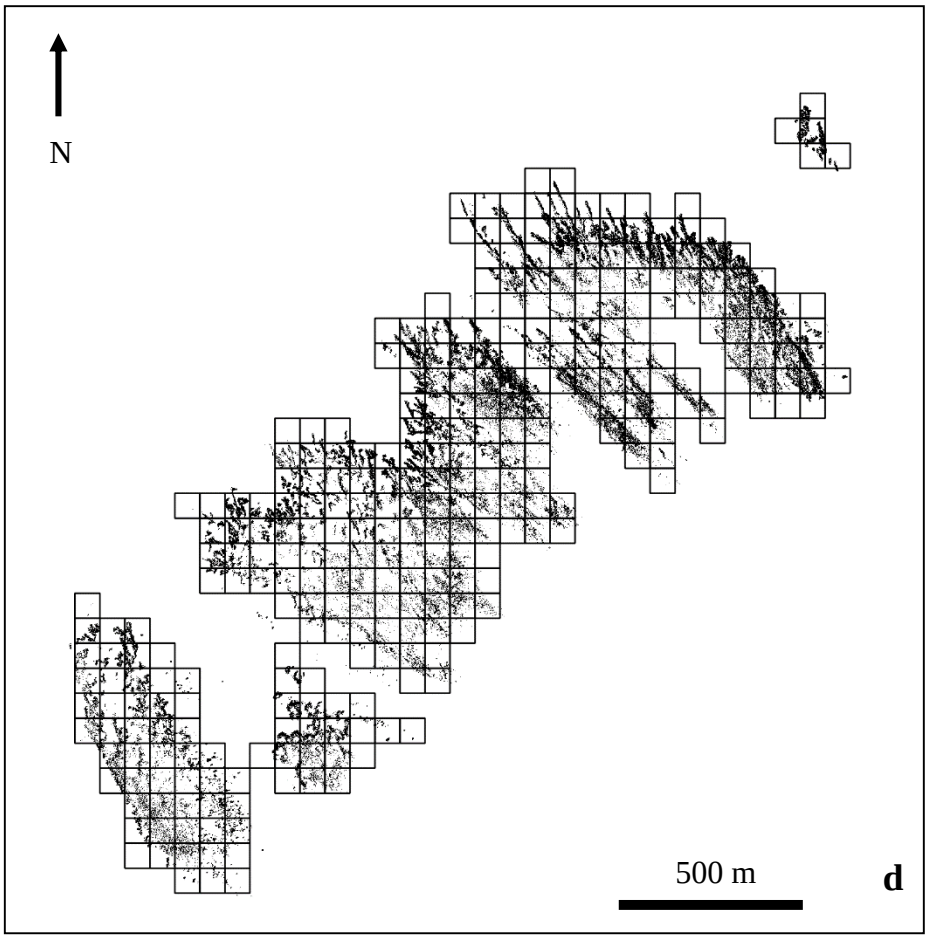
N
500 m
d

Appendix S2. Spearman correlation between all the explanatory variables (n = 259). ***p < 0.001, ** 0.001 < p < 0.01. Refer to the text for the acronyms.

	pland	**pafrac**	**enn$_{CV}$**	**clumpy**	**NDVI$_{AS}$**	**NDVI$_{ES}$**	**cov$_{MGIG}$**	**cov$_{McfGAL}$**
pland	1	0.33***	0.16	0.05	-0.17	0.47***	-0.02	-0.08
pafrac		1	**-0.52*** **	0.08	-0.39***	0.12	-0.30***	-0.08
enn$_{CV}$			1	-0.20**	0.35***	0.25***	0.35***	0.14
clumpy				1	-0.06	0.49***	-0.25***	0.21***
NDVI$_{AS}$					1	0.05	0.49***	0.17***
NDVI$_{ES}$						1	-0.08	0.10
cov$_{MGIG}$							1	-0.20***
cov$_{McfGAL}$								1

Appendix S3. Generalized additive models with a smooth fitting between (a) pafrac (n = 281), (b) enn_{CV} (n = 283) and (c) clumpy (n = 283) and the engineered sediment abundance (pland). Two stations had less than 10 engineered sediment patches resulting in non-defined pafrac (McGarigal et al. 2012), consequently they were removed before the GAM model was displayed.

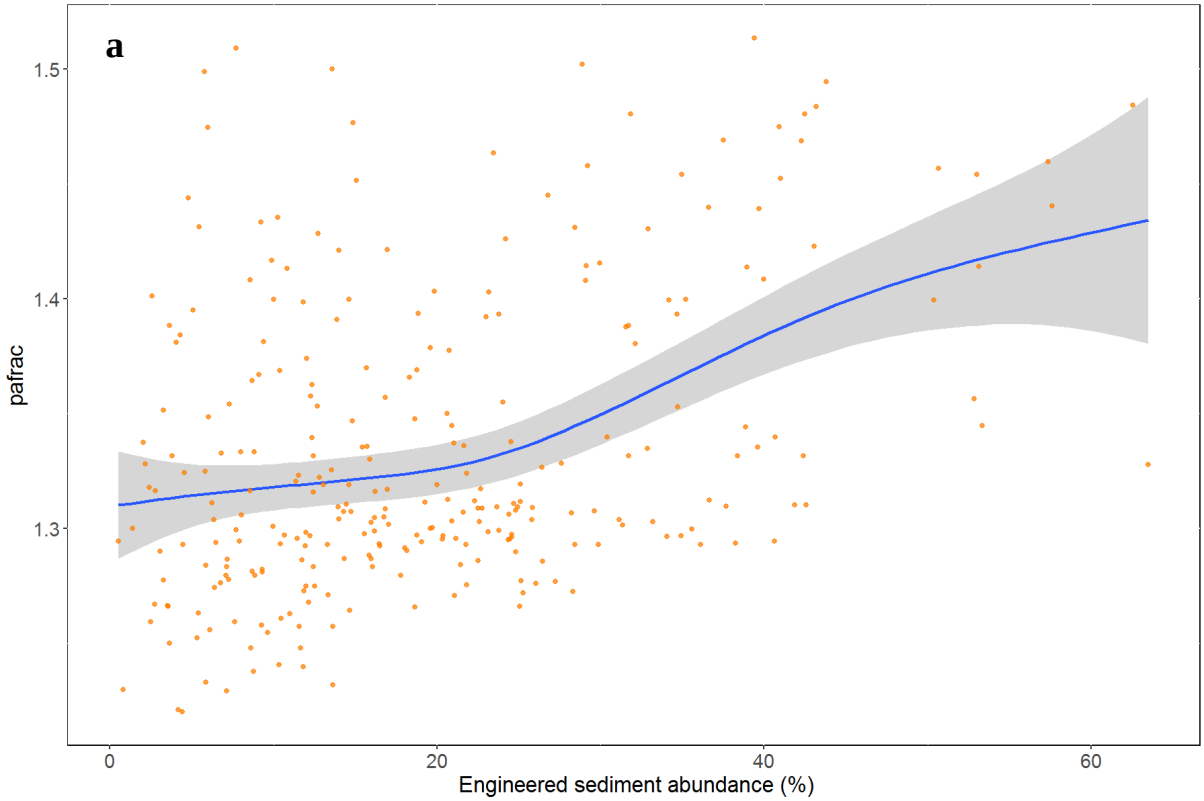

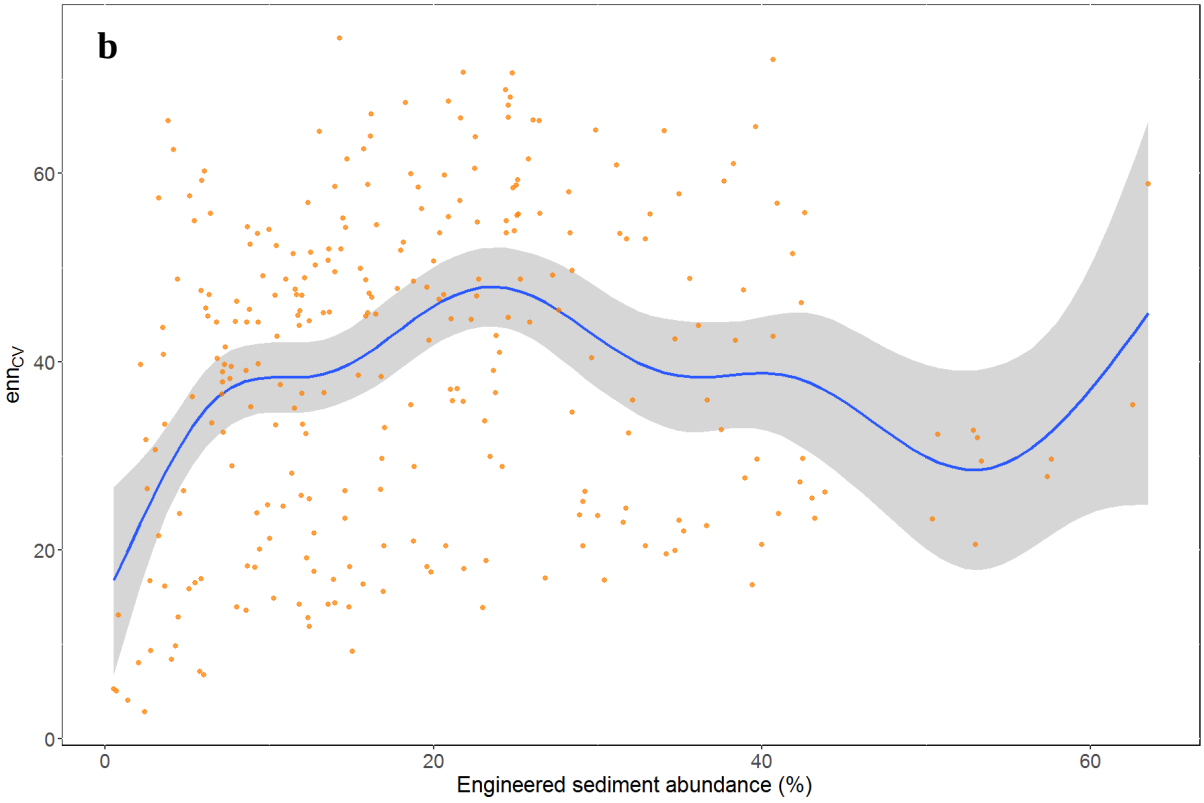

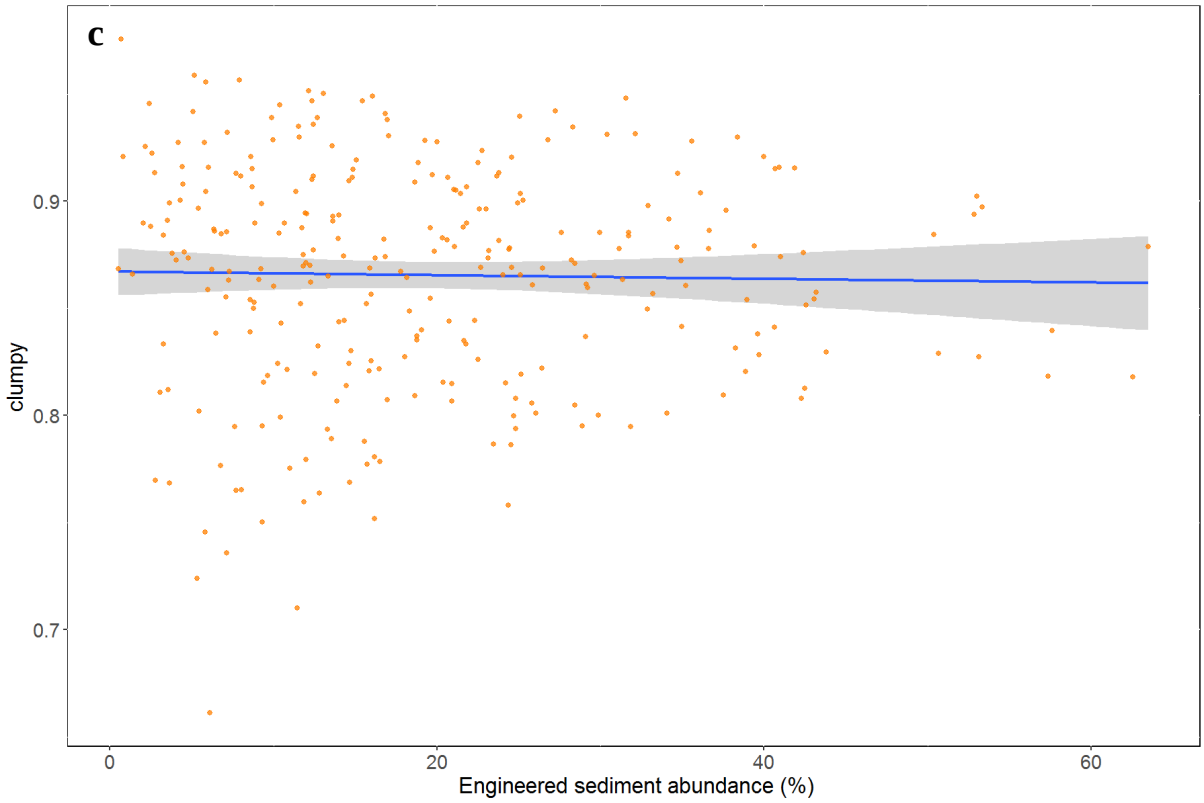
c
clumpy
0.9
0.8
0.7
0
20
40
60
Engineered sediment abundance (%)

Appendix S4. Maps of the biotic explanatory variables: (a) mean associated sediment NDVI (values from 0 to 0.16), (b) mean engineered sediment NDVI (values from 0.04 to 0.22), (c) oyster cover (values from 0 to 6.7), (d) mussel cover (values from 0 to 8.7), and of the abiotic variables: (e) engineered sediment cover percentage (values from 0.53 to 25.96), (f) perimeter-area fractal dimension (values from 1.22 to 1.51), (g) coefficient of variation of the Euclidian nearest neighbor distance (values from 2.80 to 74.36) and (h) clumpiness index (values from 0.66 to 0.98) for each 75 x 75 m sampling station. See Table 13 for the definition of each abiotic variable. Light colors represent low values of the variable and dark colors higher values of the variable.

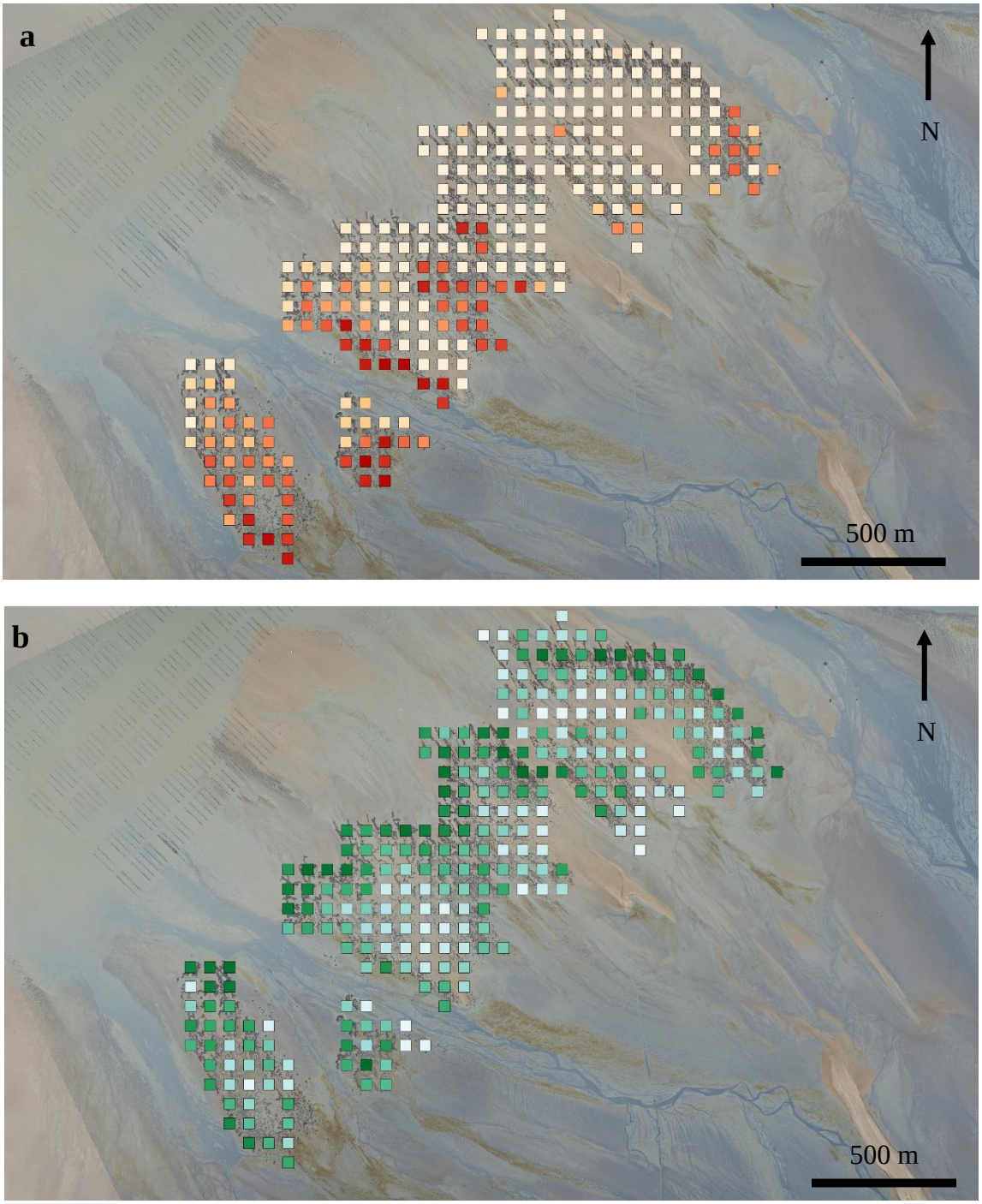

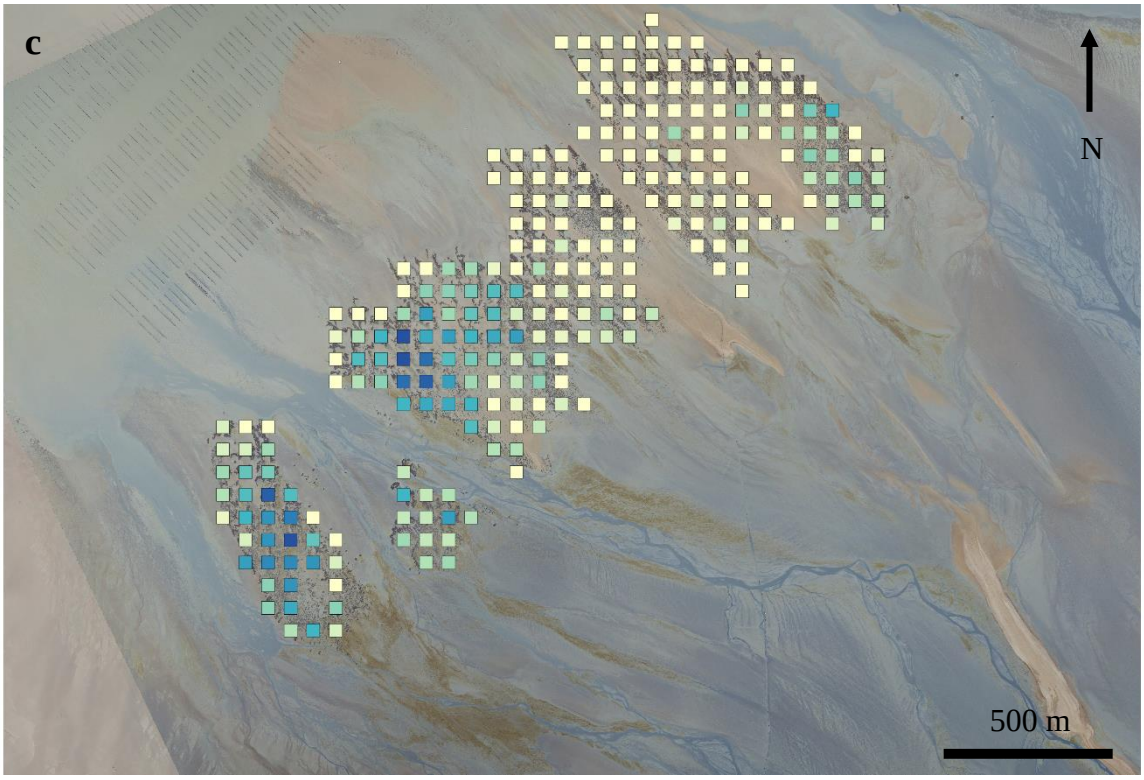
c
N
500 m

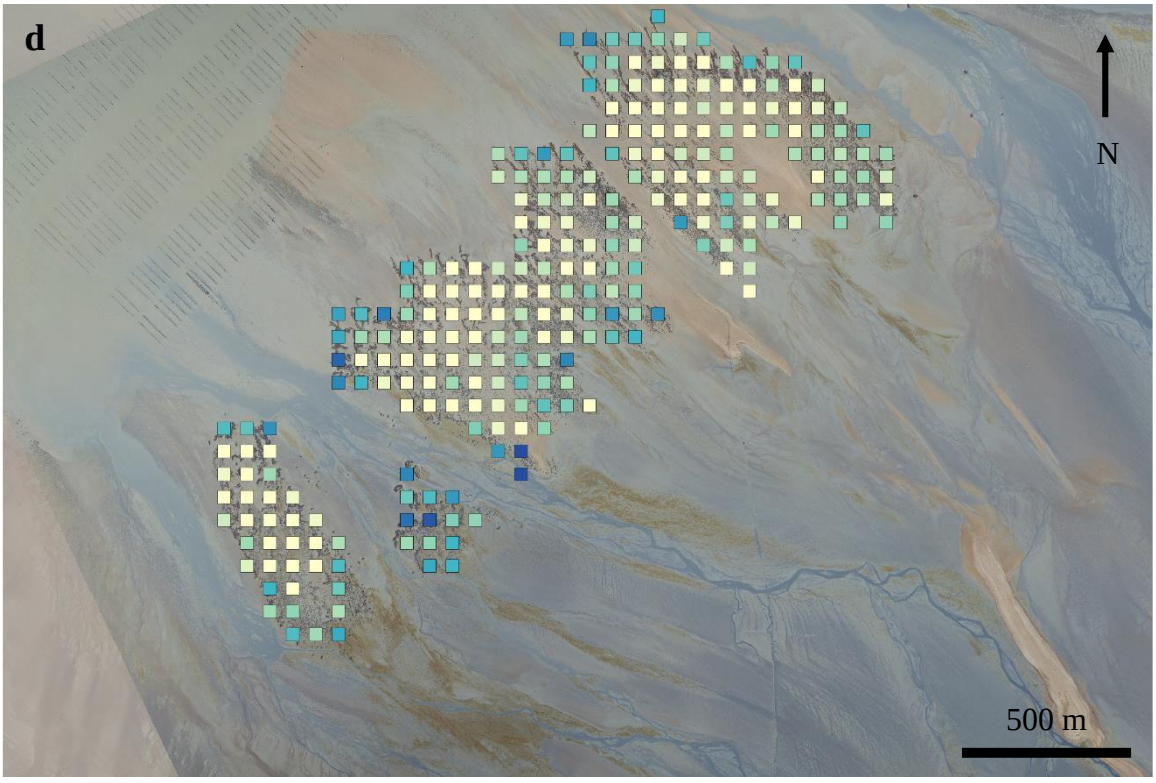
d
N
500 m

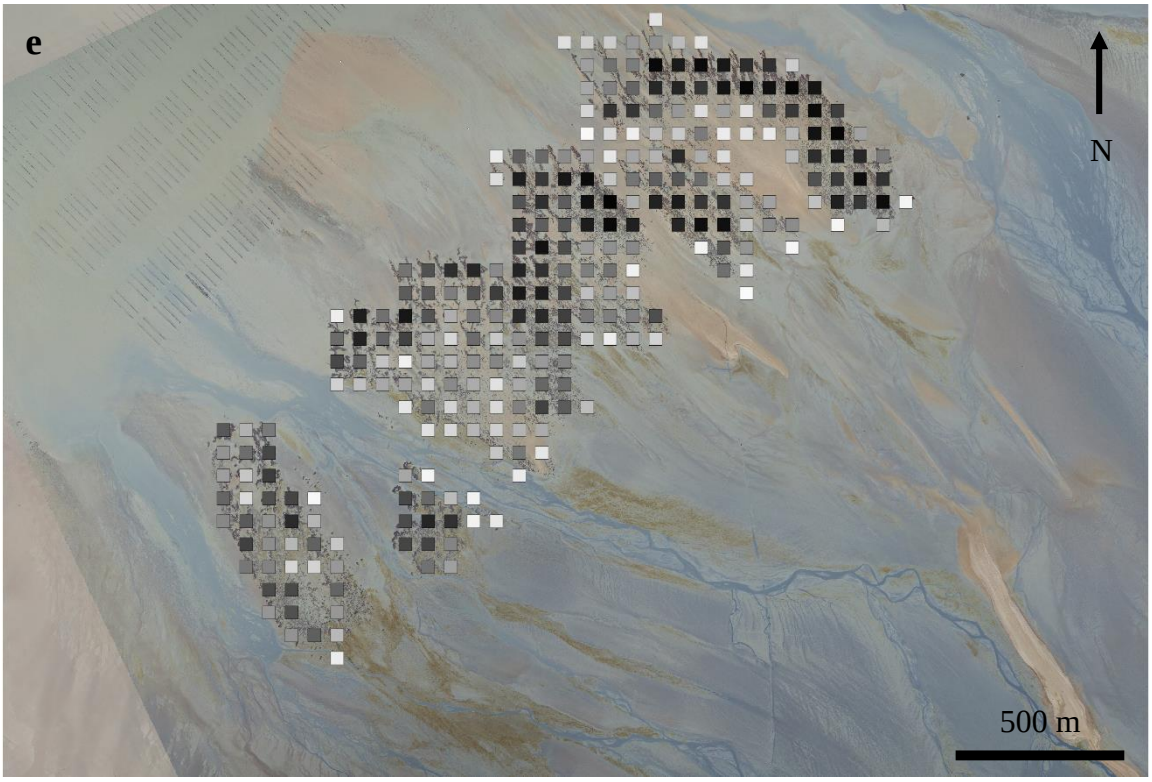
e
N
500 m

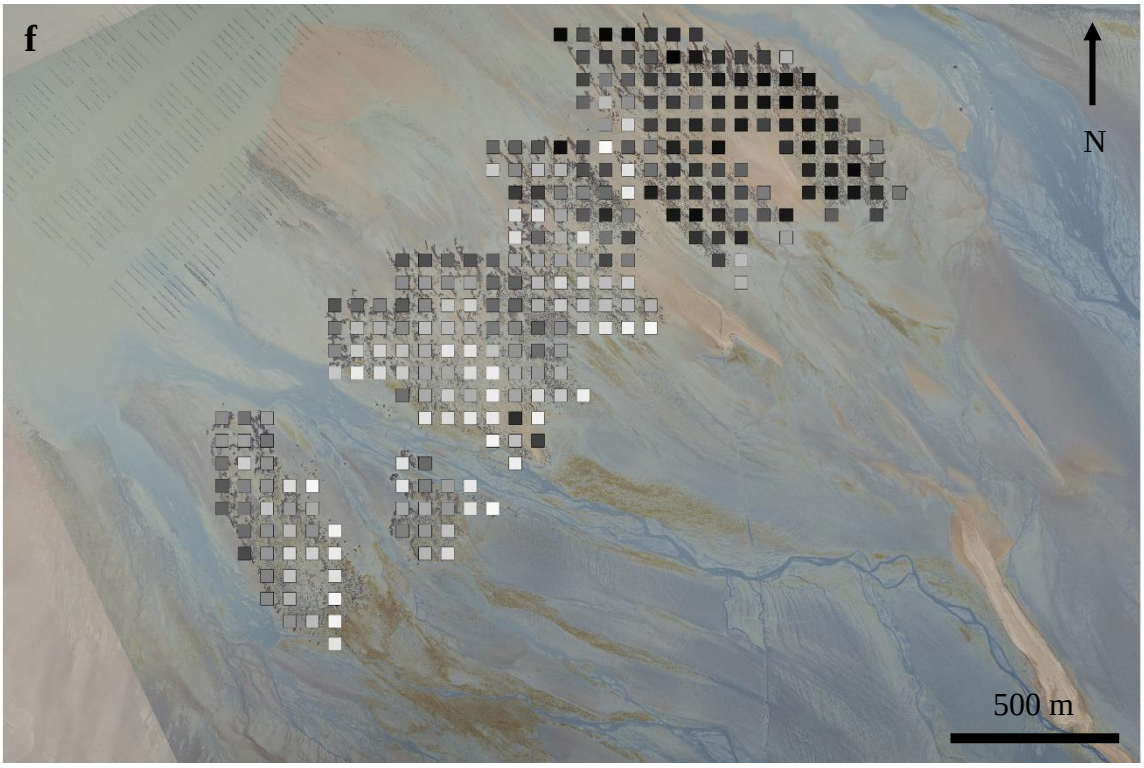
f
N
500 m

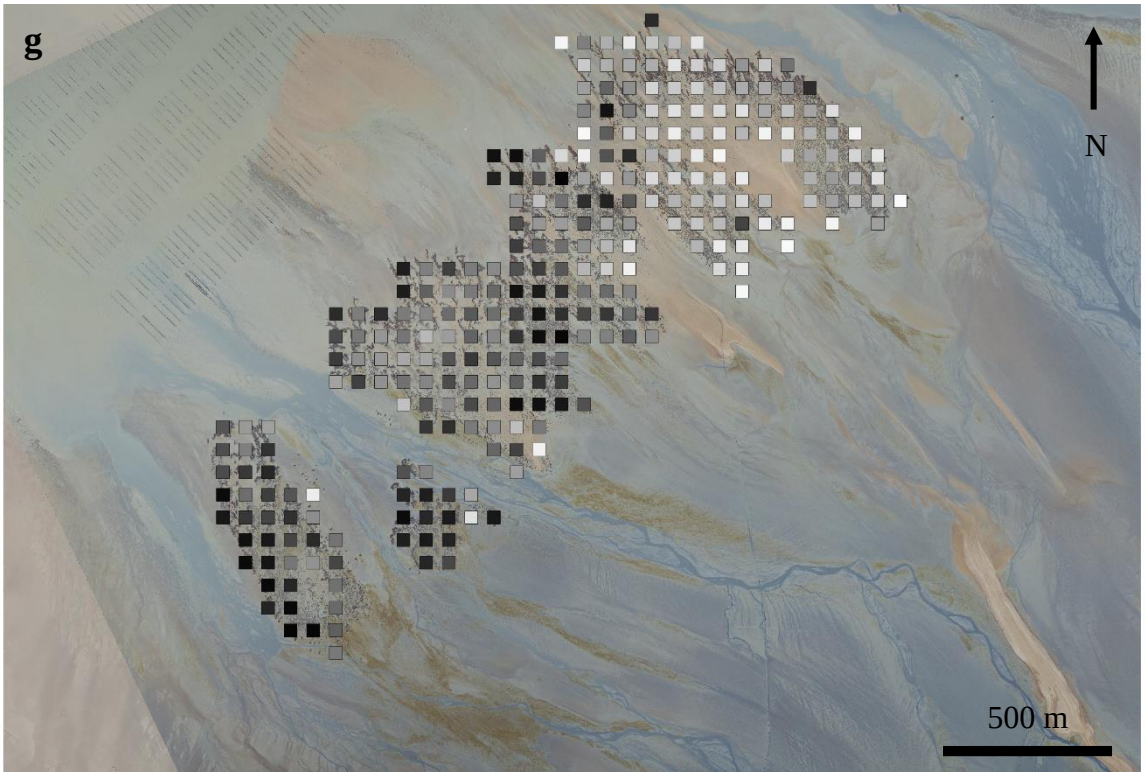
g
N
500 m

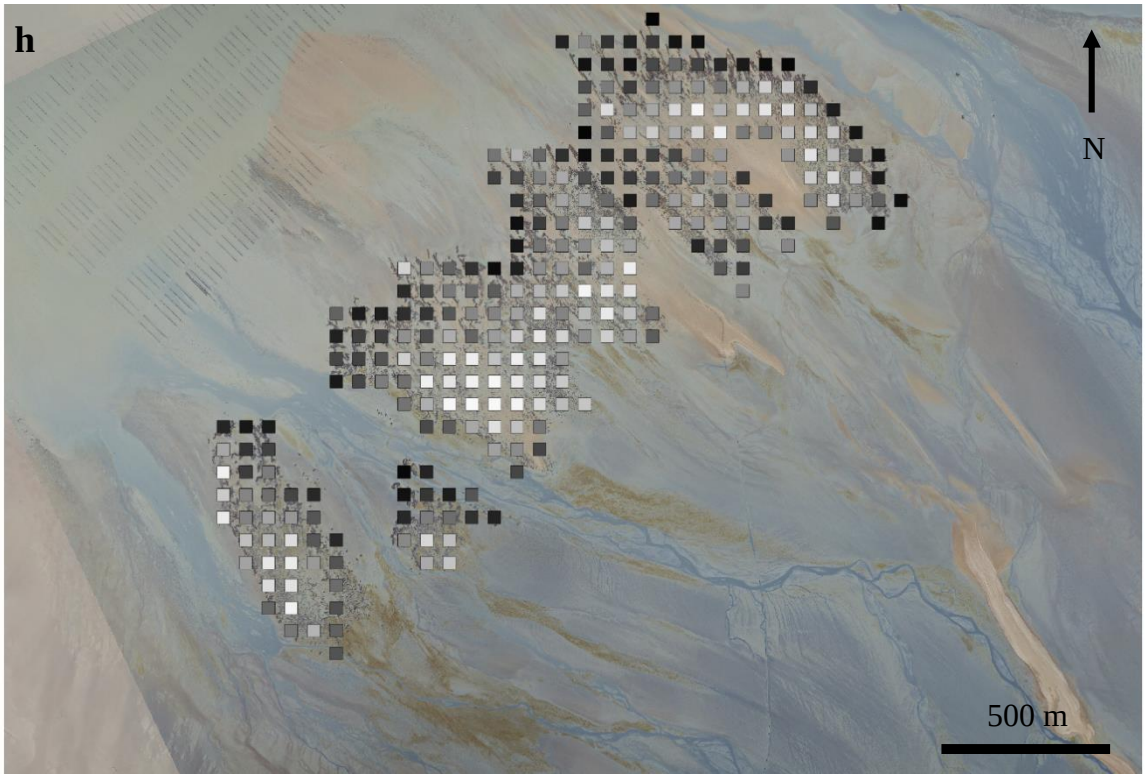
h
N
500 m

Appendix S5. Maps of the fitted $\delta^{13}C$ of *S. alveolata* obtained by linear regressions between each of the significant MEMs (4, 5, 6, 9, 32 and 60) and the original $\delta^{13}C$. The previous MEMs were selected as the ones that significantly explained the original $\delta^{13}C$.

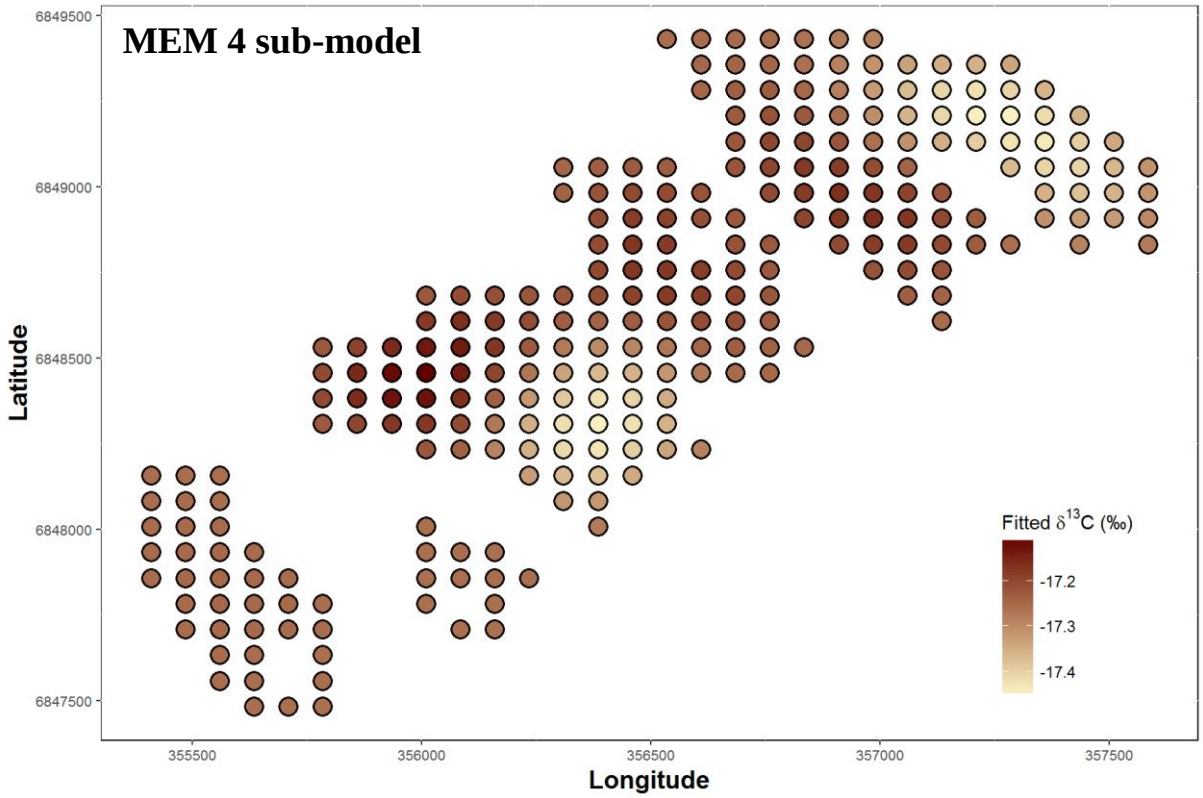

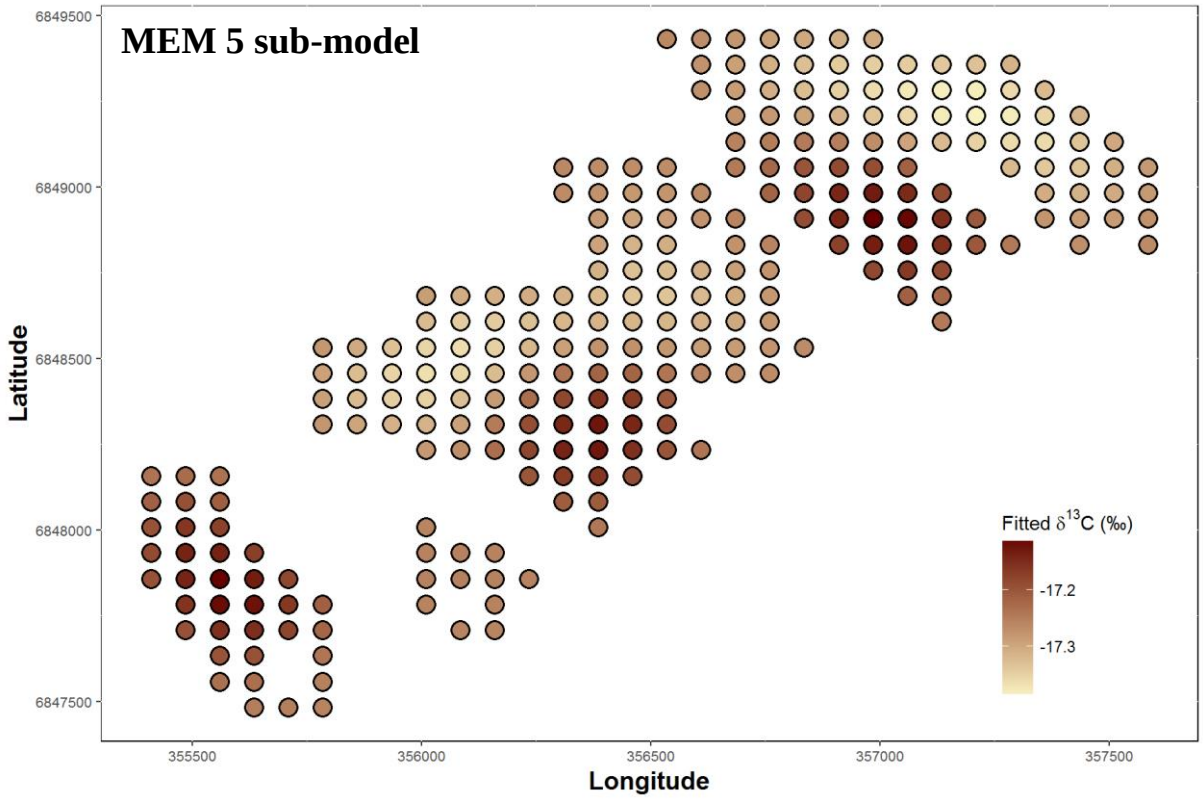

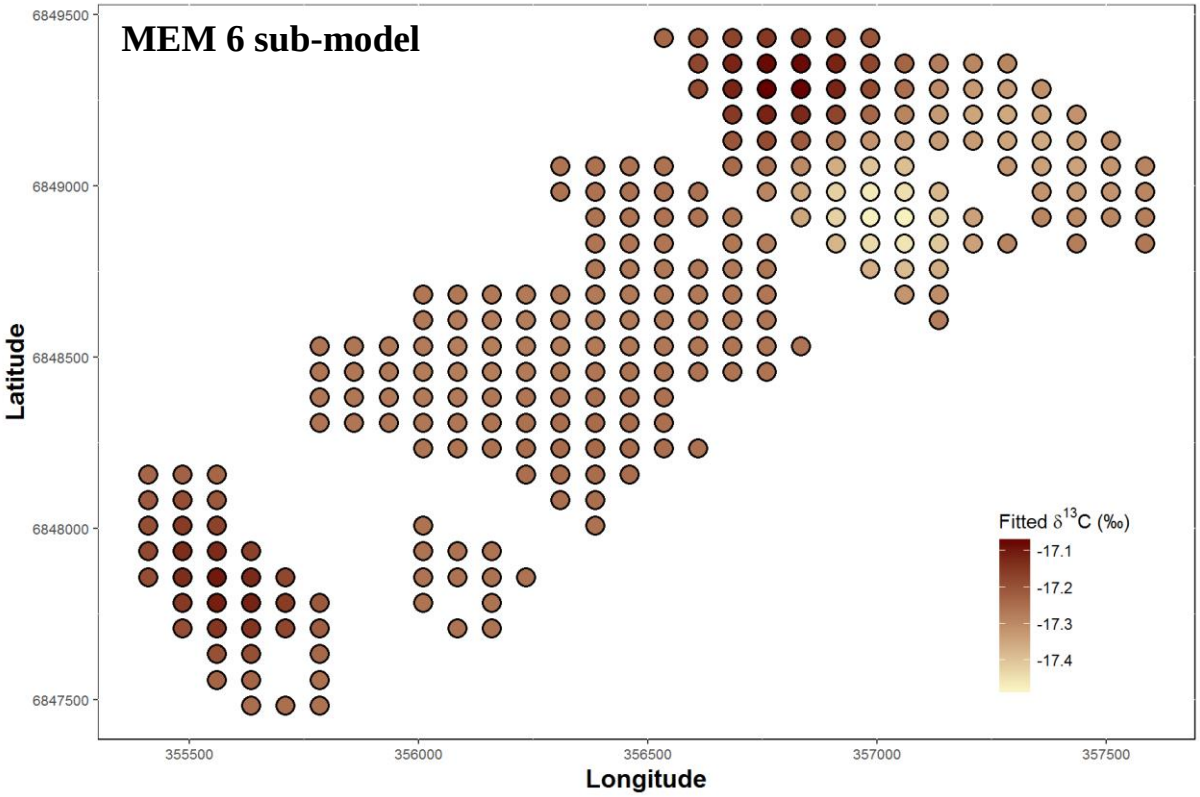
MEM 6 sub-model
Latitude
6849500
6849000
6848500
6848000
6847500
355500
356000
356500
357000
357500
Longitude
Fitted δ13C (‰)
-17.1
-17.2
-17.3
-17.4

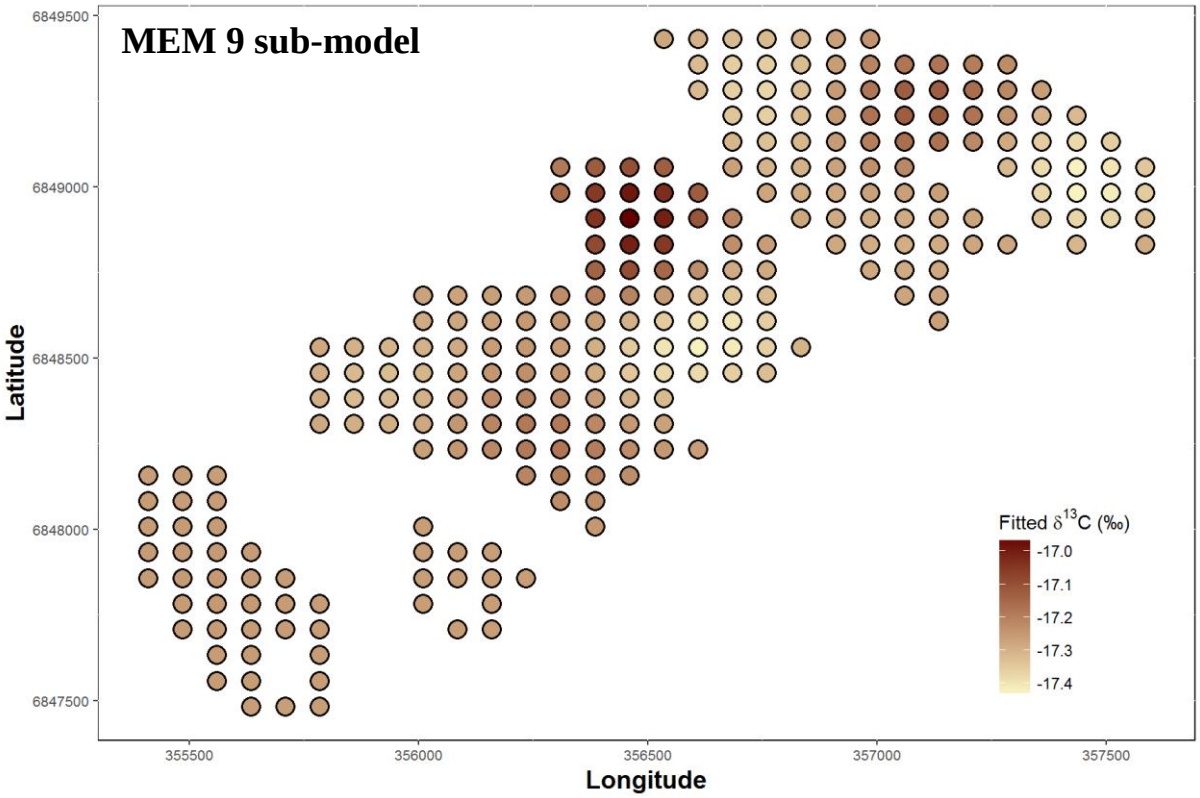
MEM 9 sub-model
Latitude
6849500
6849000
6848500
6848000
6847500
355500
356000
356500
357000
357500
Longitude
Fitted δ13C (‰)
-17.0
-17.1
-17.2
-17.3
-17.4

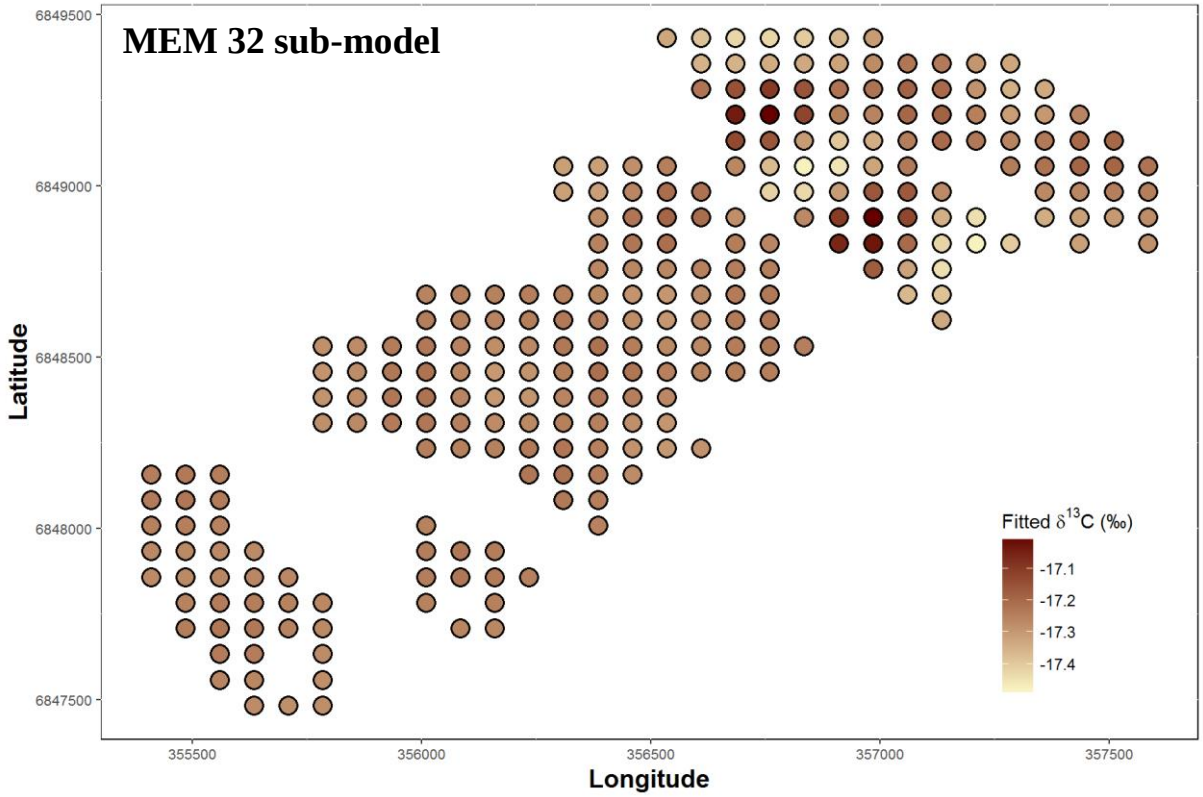
MEM 32 sub-model
Latitude
6849500
6849000
6848500
6848000
6847500
355500
356000
356500
357000
357500
Longitude
Fitted δ13C (‰)
-17.1
-17.2
-17.3
-17.4

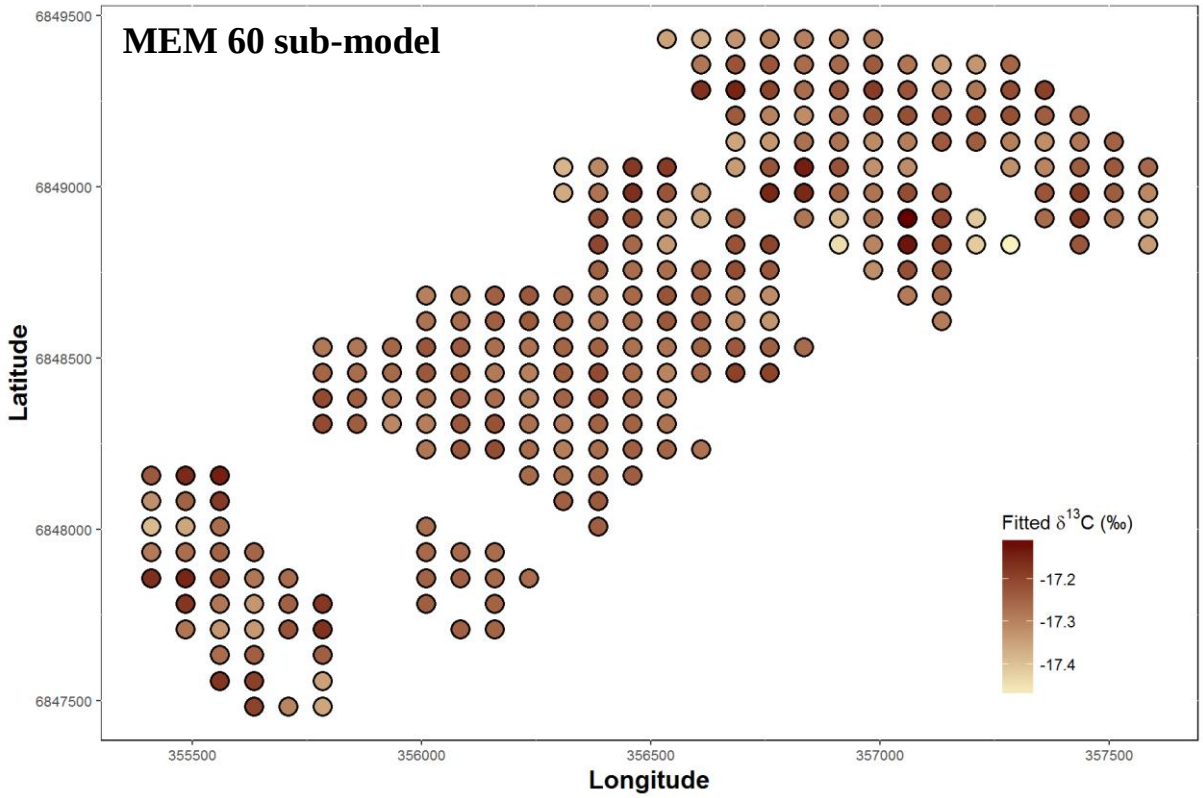
MEM 60 sub-model
Latitude
6849500
6849000
6848500
6848000
6847500
355500
356000
356500
357000
357500
Longitude
Fitted δ13C (‰)
-17.2
-17.3
-17.4

Appendix S6. Maps of the fitted $\delta^{13}C$ of *M.* cf. *galloprovincialis* obtained by linear regressions between each of the significant MEMs (7, 19, 28, 30, 36, 42 and 50) and the original $\delta^{13}C$. The previous MEMs were selected as the ones that significantly explained the original $\delta^{13}C$.

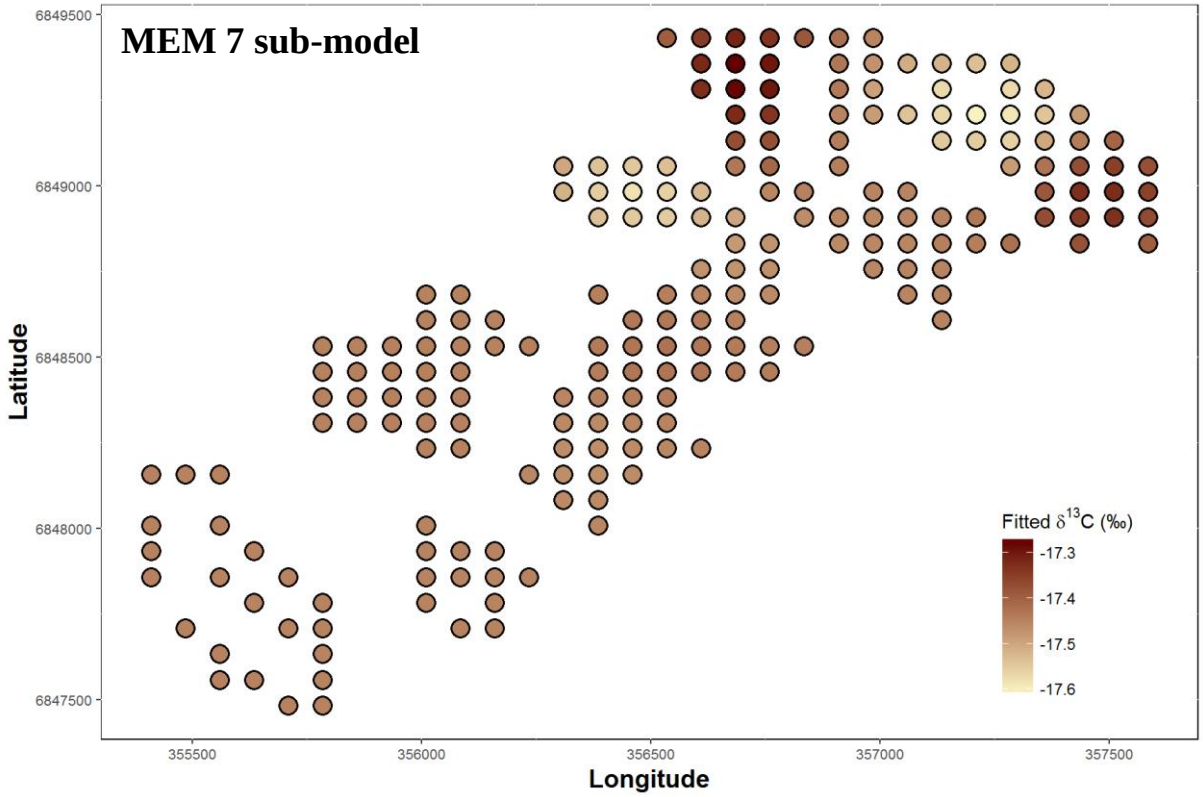

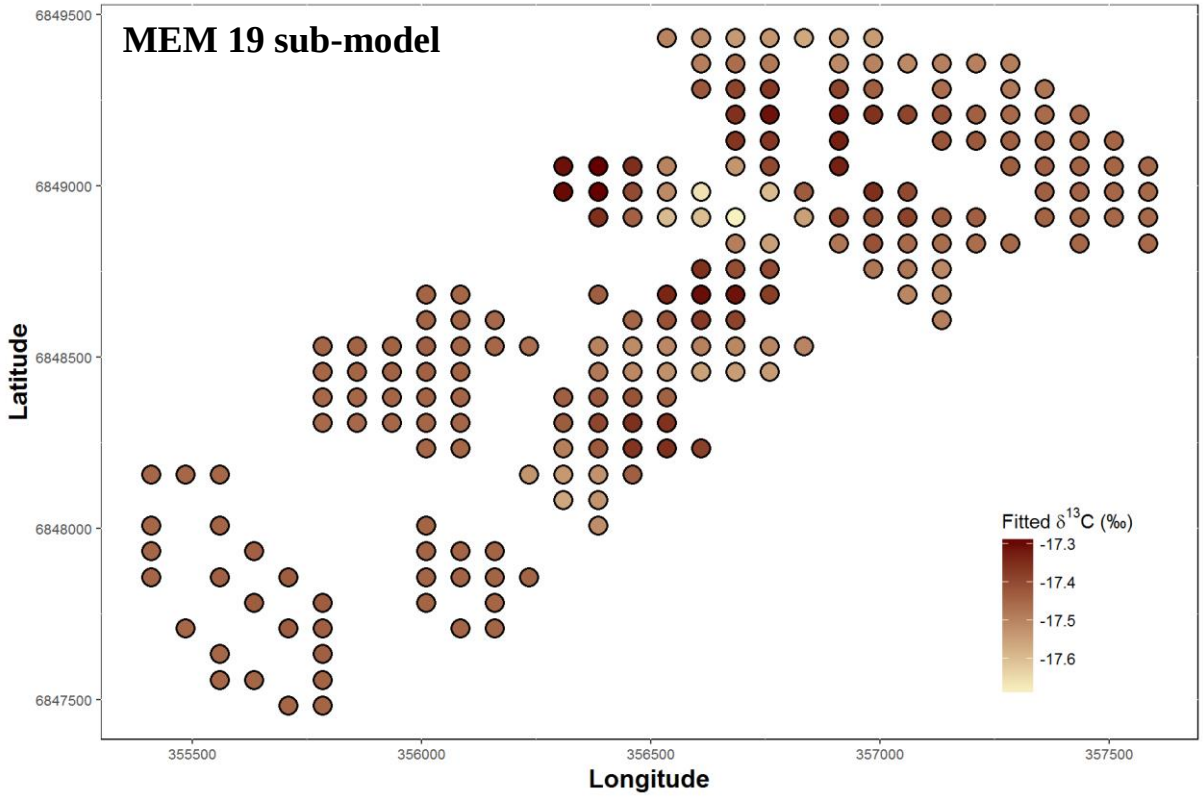

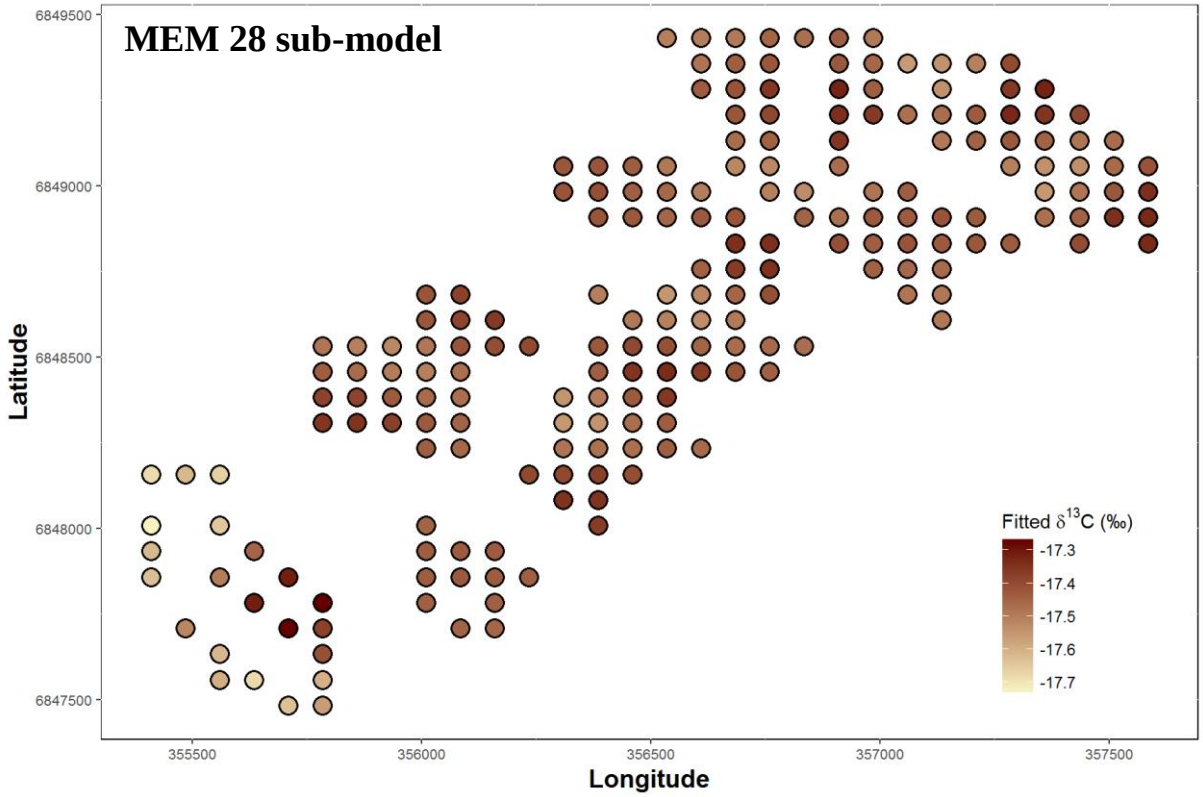
MEM 28 sub-model
Latitude
6849500
6849000
6848500
6848000
6847500
355500
356000
356500
357000
357500
Longitude
Fitted δ13C (‰)
-17.3
-17.4
-17.5
-17.6
-17.7

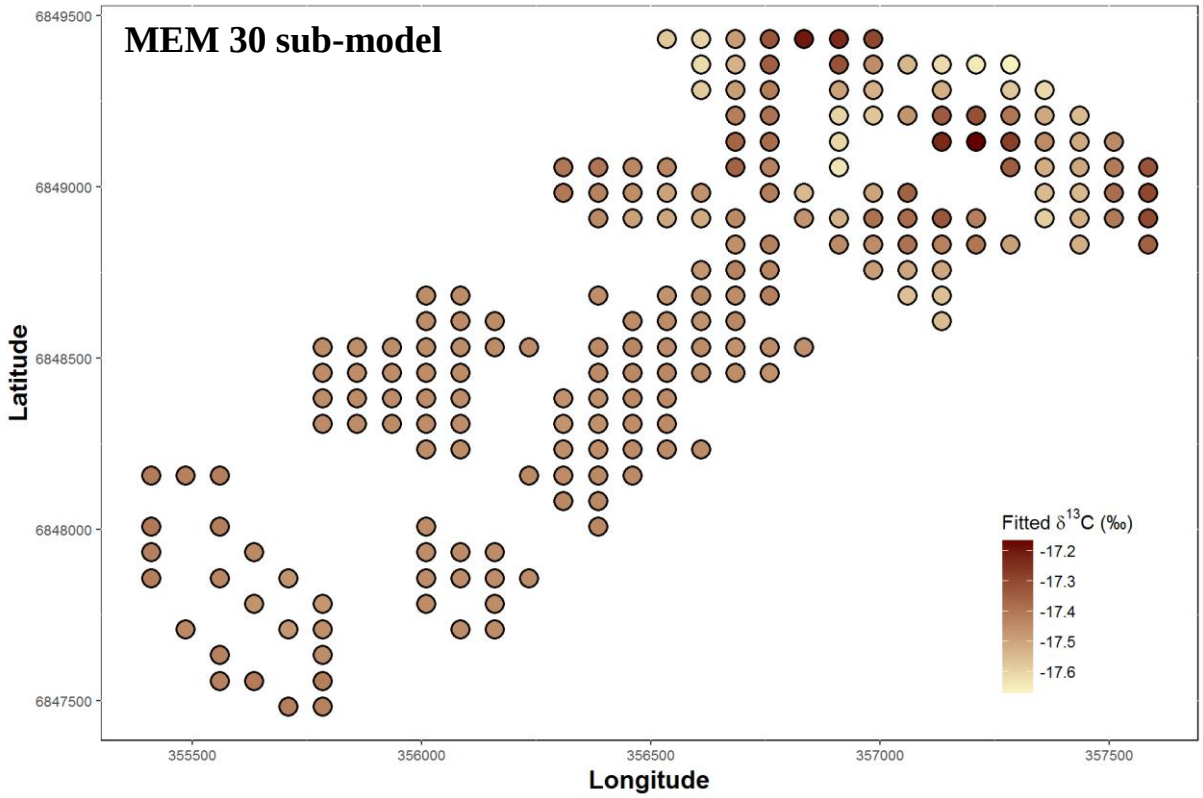
MEM 30 sub-model
Latitude
6849500
6849000
6848500
6848000
6847500
355500
356000
356500
357000
357500
Longitude
Fitted δ13C (‰)
-17.2
-17.3
-17.4
-17.5
-17.6

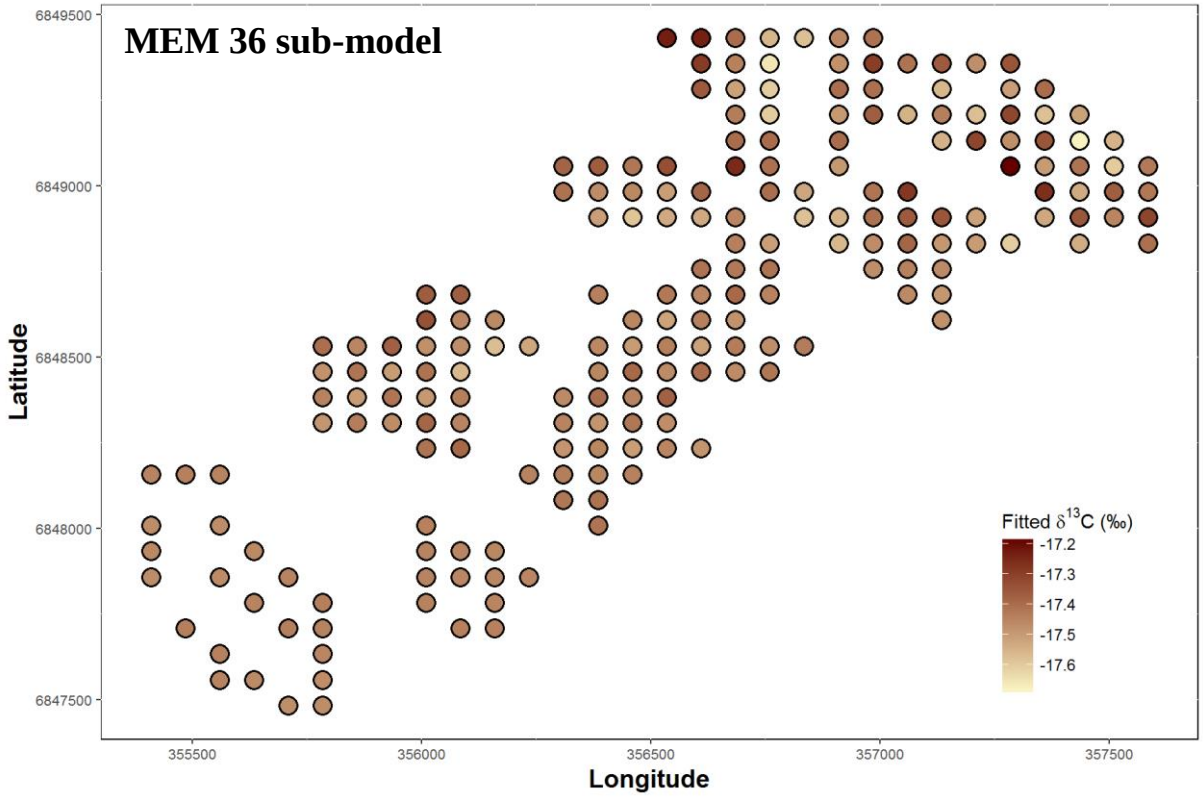
MEM 36 sub-model
Latitude
6849500
6849000
6848500
6848000
6847500
355500
356000
356500
357000
357500
Longitude
Fitted δ13C (‰)
-17.2
-17.3
-17.4
-17.5
-17.6

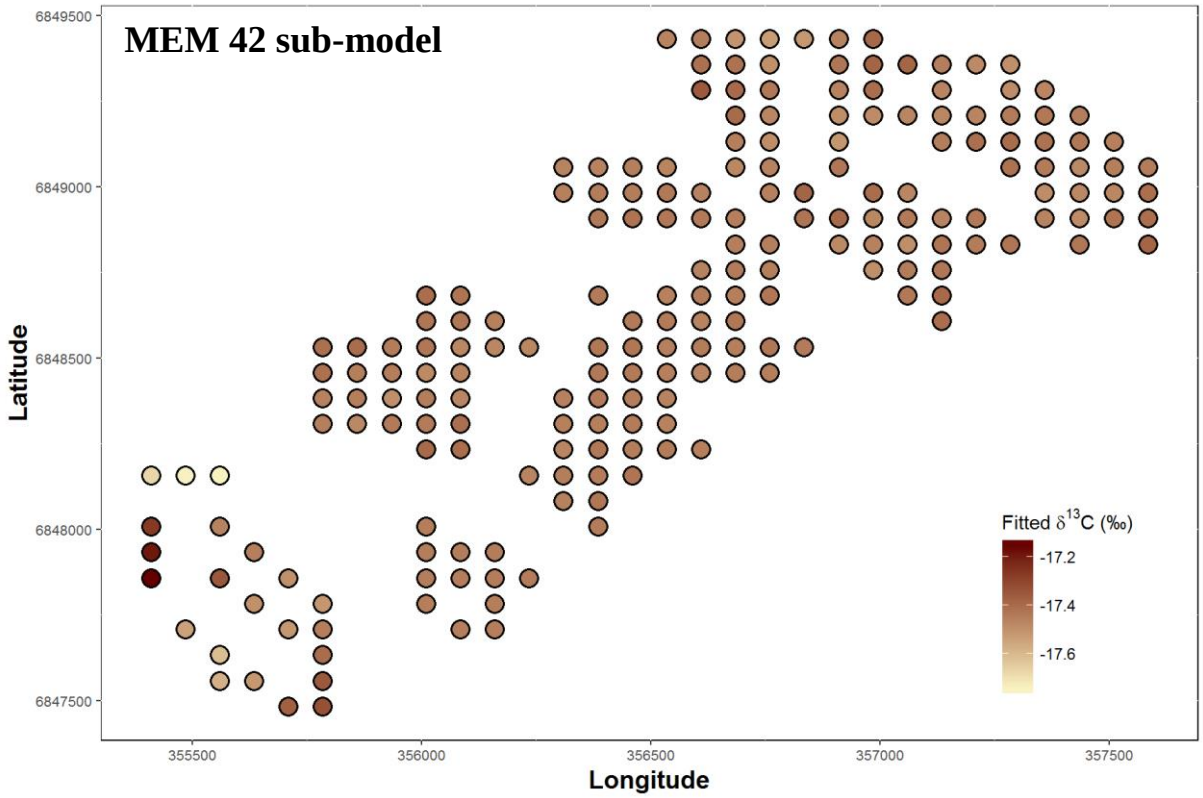
MEM 42 sub-model
Latitude
6849500
6849000
6848500
6848000
6847500
355500
356000
356500
357000
357500
Longitude
Fitted δ13C (‰)
-17.2
-17.4
-17.6

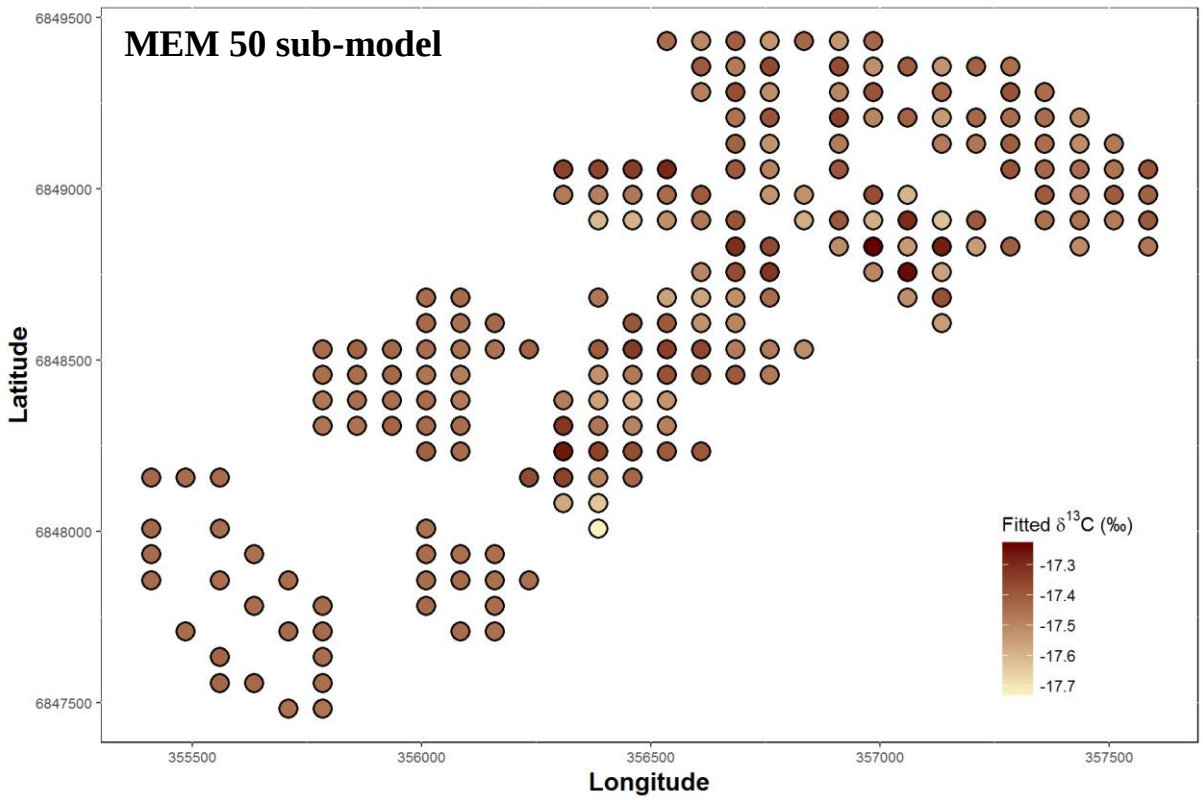
MEM 50 sub-model
6849500
6849000
6848500
6848000
6847500
Latitude
355500
356000
356500
357000
357500
Longitude
Fitted δ13C (‰)
-17.3
-17.4
-17.5
-17.6
-17.7

Article 3 - Effect of a habitat engineering species on food web structure and community isotopic niches

Auriane G. Jones [a,b,c], Stanislas F. Dubois [a], Nicolas Desroy [b], Jérôme Fournier [c,d]

Article in preparation (submission to Food Webs)

[a] IFREMER, Laboratoire Centre de Bretagne, DYNECO LEBCO, 29280 Plouzané, France

[b] IFREMER, Laboratoire Environnement et Ressources Bretagne nord, 38 rue du Port Blanc, BP 80108, 35801 Dinard cedex, France

[c] CNRS, UMR 7208 BOREA, 61 rue Buffon, CP 53, 75231 Paris cedex 05, France

[d] MNHN, Station de Biologie Marine, BP 225, 29182 Concarneau cedex, France

1. Introduction

Habitat heterogeneity is a common feature when considering both terrestrial and aquatic landscapes (McGarigal et al. 2012) and environmental factors such as geomorphology and physical disturbance are classically studied drivers of habitat heterogeneity (Burnett et al. 1998, Stallins 2006). In this context, Jones et al. (1994) introduced a new concept focusing on species which create such heterogeneity via their biological activity. These species are termed ecosystem engineers and this concept regroups organisms able to modulate directly or indirectly the availability of resources to other species, by modifying the physical properties of abiotic material (*e.g.* sediment, soil) or biotic material (*e.g.* trees in the case of beavers, Wright et al., 2002). Ultimately, via their biological activity, these organisms modify species assemblages and often create biodiversity hotspots (Jones et al. 1997, Bouma et al. 2009). Ecosystem engineering is a ubiquitous process (Wright and Jones 2006), continuously benefiting from theoretical and empirical developments regarding links with biodiversity changes (Wright et al. 2006), trophic ecology (Sanders et al. 2014, van der Zee et al. 2016), biogeochemical heterogeneity (Gutiérrez et al. 2003, Gutiérrez and Jones 2006) and spatial and temporal scales (Hastings et al. 2007).

Until recently, non-trophic interactions such as ecosystem engineering were not considered in ecological network research. A decade ago, researchers started investigating the coupling of non-trophic and trophic interactions into more global interaction webs (Olff et al. 2009, Bascompte 2010, Golubski and Abrams 2011, Kéfi et al. 2012) and Sanders et al. (2014) addressed the specific question of integrating ecosystem engineering into food web studies, using for example stable isotopes (van der Zee et al. 2016). In a food web, engineer species can affect nodes by changing species richness and biomass and they can affect links by changing predator-prey interaction strength via the creation of prey refuges or predator rich habitats (Grabowski and Powers 2004, Sanders et al. 2014). Ecosystem engineers modulate nodes and links according to three non-exclusive pathways and physical ecosystem engineers like *Zostera noltii*, can act more or less strongly on these three pathways (van der Zee et al. 2016), helping us to establish research priorities. These pathways are (1) altered abiotic conditions like temperature, wind or sediment deposition, (2) consumable abiotic resources like light and nutrients and (3) non-trophic resources like predator- or competitor-free space. The modification of consumable abiotic resources like nutrients can result in the addition of new primary producers or alter primary producer, which may then propagate to higher trophic levels (Sanders et al. 2014).

Physical ecosystem engineering is particularly present in stressful environments like deserts, intertidal zones or hydrothermal vents (Jones et al. 1997). Temperate coasts are home to many physical ecosystem engineers (Gutiérrez et al. 2012) both autotrophs like cordgrass (*Spartina* spp.), seagrass (*e.g. Zostera noltii*) and macroalgae (*e.g. Laminaria hyperborea*) and reef-building heterotrophs like mussels (*e.g. Mytilus edulis*) and oysters (*e.g. Crassostrea virginica*) (Goldberg 2013). Many reef-building polychaetes and bivalves promote local benthic microalgae via the structures they build and their

biological activity (Bruschetti et al. 2011, Echappé et al. 2017, Engel et al. 2017, Jones et al. 2018). These microalgae can be resuspended by tidal currents (Ubertini et al. 2015) making them available to the suspension-feeding ecosystem engineers and to the associated fauna (Dubois et al. 2007b, Ubertini et al. 2012). Consequently, reef-building ecosystem engineers can affect the presence and biomass of a food source (benthic microalgae) at the base of the local food web (node modulation) but is this local food source used by the ecosystem engineers and/or by other suspension-feeders living in the engineered habitat? Are the engineer species altruist or do they "garden" part of their food, as the 'gardening hypothesis' states for the lugworm *Abarenicola pacifica* (Hylleberg 1975)?

Sabellaria alveolata - a.k.a. the honeycomb-worm - is a gregarious intertidal polychaete, commonly found along the European coastline from Scotland and Ireland to Morocco (Muir et al. 2016). This sedentary polychaete lives in a tube it builds using mainly bioclastic sand particles glued together by an organic cement it produces (Gruet et al. 1987, Le Cam et al. 2011). This species transforms soft sediments into three-dimensional hard structures (engineered sediment), forming a new habitat (Dubois et al. 2002). These hard structures called reefs, are fixed atop rocks, pebbles and in rare cases, present in exclusively soft sediment zones (Holt et al. 1998, Desroy et al. 2011), covering surfaces from a few square meters to dozens of hectares. Previous studies have focused on the physiology of *S. alveolata* (Dubois et al. 2003, 2005, 2006b, 2009), on the macrofauna associated with this engineer (Dias and Paula 2001, Dubois et al. 2002, 2006a, Porta and Nicoletti 2009) and on the physical and sedimentary properties of the engineered reefs (Gruet 1984, Gruet et al. 1987, Fournier et al. 2010, Le Cam et al. 2011). In the last decade, the temporal and small-scale spatial variability of trophic relationships among co-occurring suspension-feeders including *S. alveolata*, have been investigated, in the context of shellfish culture (Dubois et al. 2007b, Lefebvre et al. 2009) and rocky shores (Dubois and Colombo 2014). At the scale of the largest *S. alveolata* reef in Europe, benthic microalgae biomass is higher in the soft sediments under the influence of the engineered sediments (associated sediments) than in soft sediments uninfluenced by the engineered sediment (control sediments) (Jones et al. 2018). Furthermore, green algae from the genus *Ulva* grow on the engineered sediments (Dubois et al. 2006a) where they can be consumed directly by grazers or indirectly, once detached and fragmented through the microbial loop, by suspension- and deposit-feeders. Consequently, via its engineering properties *S. alveolata* affects two nodes at the base of the local food web: the biomass of benthic microalgae also called microphytobenthos (MPB) and the presence of green algae (*Ulva* spp.). *S. alveolata* also affects the species composition present in both the engineered and the associated sediments, creating two distinct assemblages, both different from the control soft sediments species assemblage (Jones et al. 2018). In this context, we used an extensive sampling of the macrofauna and food sources present in the three sediment types (control, associated and engineered) coupled with stable carbon and nitrogen isotopic compositions to investigate several questions. (1) What is the contribution of autochthonous food sources (MPB and *Ulva* spp) to the diet of the main primary consumers present in the reef (engineered and associated sediments) compared to the control zone and does it change between winter

and summer? (2) How does the food web structure of an engineered sediment compare to a non-engineered soft sediment one and to what extent do the engineered and the associated sediments differentiate in terms of trophic functioning? While in terms of species composition, richness and abundance, the engineered and associated sediments are two distinct communities, one can wander if this dichotomy holds when considering their trophic functioning.

2. Material and methods

2.1. Study area and sampling strategy

This study took place in the Mont-Saint-Michel Bay (MSMB), a semi-diurnal macrotidal bay located in the western part of the English Channel, between Normandy and Brittany (France). The intertidal zone covers 250 km² where are present three *Sabellaria alveolata* reefs, in particular the Sainte-Anne reef in the central part of the MSMB (Desroy et al. 2011). Our two study sites were the Sainte-Anne reef (48°38'700N and 1°40'100W) and a control zone (control sediments: CS) located 1.5 km North-East of the reef and on the same bathymetric level (*i.e.* between the -2 and the -4 m isobaths, Noernberg et al., 2010). The reef is parallel to the coast and to the dominant tidal currents and composed of the previously defined engineered and associated sediments, hereafter indicated as ES and AS, respectively. In 2014, the maximal dimensions of the Sainte-Anne reef were 2.5 km in length for 1 km in width and the engineered sediments represented 32 ha (Jones et al., in prep). The area located in the central part of the bay and along the same isobaths as the reef is characterized by medium to muddy sands (Bonnot-Courtois et al. 2009) and by a species poor community typified by the bivalve *Limecola balthica*, previously known as *Macoma balthica* (Dubois et al. 2002). Field sampling took place over two consecutive spring tides in February and September 2015, hereafter referred to as winter and summer, to investigate the food webs over two contrasted seasons. Indeed, winter is characterized by low fauna metabolic rates and low pelagic phytoplankton productivity while in summer, fauna have higher metabolic rates and the different food sources are more abundant (Marín Leal et al. 2008). In each sediment type (ES, AS and CS), we randomly sampled ten stations, each separated by at least 75 m. During both sampling campaigns, every ES station was paired with an AS station.

2.2. Sample collection and laboratory processes

2.2.1. Macrofauna and megafauna

To investigate the trophic structure of each sediment type, we sampled the largest possible diversity of macrofaunal organisms at the 10 stations of each sediment type during the two seasons. Over-dispersed macrofauna, mainly composed of mollusks, was sampled using a 1 m² quadrat (3 replicates per station). For the AS and CS quadrat sampling, the first 5 cm of sediment was sieved through a 5-mm square mesh, while for the ES quadrat sampling, we collected by hand all the visible

macrofauna located on the reef and inside the reef interstices. Infauna and small macrofauna species were sampled using a 18.5 cm side corer (269 cm²) to a depth of 15 cm (1 replicate per station). On site, the soft sediment cores were sieved through a 1-mm square mesh and back at the lab, the resulting sediments were sorted. The ES cores were taken back to the lab where they were broken apart under water and the fauna retained on a 1-mm square mesh. All the sampled organisms were stored at -20°C until further processing. The biomass (wet weight) by m² of the species sampled by the cores and/or by the quadrats were estimated using the catch-per-unit-effort method, *i.e.* the ratio between the total catch biomass and the total amount of effort to harvest the catch biomass (Skalski et al. 2005). If a species was only collected by one sampling method, its biomass by m² was estimated using the corresponding sampling surface (1 m² for the quadrats and 269 cm² for the cores). For 17 species in winter and 15 species in summer sampled by both methods, their respective biomass by m² was calculated using the formula proposed by Jones et al. (2018) where the cumulated biomasses are divided by the sum of each gear's CPUE (1.0269 m²).

Mobile benthic and demersal megafauna was sampled using traditional set nets from the MSMB, called 'tézures' and analogous to fyke nets without wings (Secula 2011). In the control and reef sites, six nets were positioned at low tide with the opening landward and left to fish for two consecutive tidal cycles (24 h). In order to consider jointly the species sampled by the cores and/or the quadrats and by the set nets, we estimated the sediment surface sampled by each net. We used the annual mean bottom current speeds for the MSMB (Sainte-Anne reef zone in 2015, v = 0.188 $m.s^{-1}$) extracted from the MANGA500 model (Sextant 500 m spatial resolution), the mean width of the set nets (w = 1.45 m) and the mean fishing time of each net (t = 7 h), to estimate the instantaneous mean sediment surface sampled by the nets (S in m²). We used the following formula: $S = v \times w \times t \times 3600$ (1). S was estimated as 6869 m² and used to calculate the biomass by m² of the sampled species. Using the biomass by m² estimated with the cores, the quadrats and the set nets, we calculated the mean relative contribution of each species to the total biomass of the CS, AS and ES in winter and summer.

Prior to sample preparation, organisms were identified to the lowest taxonomic level (generally the species level). Isotopic analysis were performed on muscle tissue for fish, mollusks and shrimps. For smaller species, we used the whole body and removed the gut when possible. For very small species, several individuals were pooled to meet the minimum required weight for stable isotope analysis. All prepared samples were rinsed with Milli-Q water and then freeze-dried. As much as possible, a minimum of three replicates per species and per station were analyzed. For calcified organisms (crustaceans and echinoderms), a subsample was acidified (10% HCl) to remove any inorganic carbonates, then rinsed with Milli-Q water and freeze-dried for ^{13}C values, while a subsample was left untreated for ^{15}N value.

2.2.2. Primary producers

To estimate temporal variability in isotopic composition of primary producers, we sampled every month the different potential basal sources of organic matter (OM). In the control site, the OM available for benthic primary consumers was assumed to be mainly composed of suspended particulate organic matter (mainly phytoplankton, POM) and microphytobenthos (MPB). In the reef site, we considered green algae fragments of the genus *Ulva* (ULV) growing on the engineered sediments as a potential food source. The sediment organic matter (SOM) was assumed to be a mixture of the two or three aforementioned food sources depending on the site. Riverine terrestrial inputs of organic matter were not considered as potential food sources because they are very limited in the MSMB in general and even more so in the tidal dominated area of the bay where are located our two study sites (Riera 2007).

Every month from January 2015 to January 2016 and just before high tide, marine subsurface water (1 m below the surface) was collected, using a Niskin bottle, at one sampling point seaward of the Sainte-Anne reef, for POM analysis. We considered POM to be distributed homogeneously at the scale of the central part of the MSMB and consequently to have the same isotope composition at the reef and control sites. Water samples were prefiltered on a 200 µm square mesh, to remove macro detritus and zooplankton (Marín Leal et al. 2008), then filtered on three precombusted GF/F filters (4 h, 450°C) and finally rinsed with Milli-Q water (3 values per month). Filters were freeze-dried and half of each filter was acidified during 48 h with 32 M HCl fumes, to remove any traces of inorganic carbonates and used for ^{13}C values (Lorrain et al. 2003). After acidification, the half filters were dried at 30°C. The non-acidified halves were used for ^{15}N value. Every month from January 2015 to January 2016, the first centimeter of the AS was sampled using a 1-cm high plastic petri dish (57 cm^2), for MPB and SOM analysis. Every month except February and September 2015, the AS was sampled at two points inside the reef site, one located in an undisturbed section (3 replicates) and the other located in a disturbed section (3 replicates). In February and September 2015, we sampled three replicates of the sediment in each of the 10 stations of the reef (AS) and control sites. The samples were kept at -20°C until further analysis. To extract the MPB from the sediment we used the protocol in Marín Leal et al., (2008) which is a modified version of Blanchard et al., (1988) (see Appendix S1). For SOM samples, a subsample was acidified (10% HCl) to remove inorganic carbonates and the rest was left untreated. For ULV samples, every month from January 2015 to January 2016, green algae (*Ulva* spp.) was collected from the ES in a 10 m radius from the two points where the AS for MPB and SOM analysis were sampled. Back at the lab, epibionts were scraped off the green algae (ULV) using a clean scalpel and then the samples rinsed with Milli-Q water. For POM and SOM, we used the acidified subsamples for ^{13}C values and the untreated samples for ^{15}N values.

2.3. Stable isotope analysis

Each frieze-dried animal sample was ground to a homogeneous powder and 1 mg was weighted in a tin capsule for stable isotope analysis. For POM, every half filter was scraped with a clean scalpel and 10 mg of the resulting powder was placed in a tin capsule. Once cleaned and rinsed, the green algae was freeze-dried, grounded to powder and 3 mg was weighted in a tin capsule. Once extracted from the sediment and rinsed from the Ludox using Milli-Q water, MPB was freeze-dried, ground to a homogenous powder and 1 mg of powder was weighted in a tin capsule. Carbon and nitrogen isotope compositions were measured with a Thermo Delta V isotope mass spectrometer coupled via a Conflo IV to a Carlo Erba NC2500 elemental analyzer (Cornell University Stable Isotope Laboratory). Isotopic ratios of carbon and nitrogen were reported using the standard δ notation as units of parts per thousand (‰) relative to the international reference standards:

$$\delta X = \left[(R_{sample}/R_{reference}) - 1\right] \text{ x } 1000 \quad (2)$$

where X = ^{13}C or ^{15}N, and R = $^{13}C/^{12}C$ for carbon and $^{15}N/^{14}N$ for nitrogen. Vienna-Peed Dee Belemnite limestone and atmospheric nitrogen were used as reference standards for carbon and nitrogen respectively. The analytical precision was 0.09‰.

2.4. Data analysis

In the case of the reef and control zones, we used the monthly survey of the basal sources (MPB, POM and ULV) done in the reef zone to calculate the mean $\delta^{13}C$ and $\delta^{15}N$ (and associated standard deviations) used in the isotopic biplots (Figure 24) and in the mixing models. For the MPB, we used the data between April and September 2015. For the POM, we used the data from January 2015 to April 2015, June 2015 and October to January 2016. For the Ulva, we used the data from February 2015 to February 2016 excluding November and December 2015. Some monthly data could not be used because of analytical problems. These mean $\delta^{13}C$ and $\delta^{15}N$ values (± SD) were -22.92 ± 1.31 ($\delta^{13}C$) and 5.43 ± 0.91 ($\delta^{15}N$) for POM, -17.75 ± 1.57 ($\delta^{13}C$) and 5.54 ± 0.55 ($\delta^{15}N$) for MPB, -15.93 ± 0.75 ($\delta^{13}C$) and 8.93 ± 0.85 ($\delta^{15}N$) for ULV. In addition, the mean $\delta^{13}C$ and $\delta^{15}N$ of the different megafauna species sampled using the set nets deployed in the reef site were displayed on the AS and ES biplots. The species accounting for more than 1% of the total biomass of each sediment type were labelled (see section 2.2.1. for the calculation).

Overall, only three species were sampled in the three sediment types at both seasons (*Carcinus maenas*, *Lekanesphaera levii* and *Venerupis corrugata*). Most of the species occurred in only two sediment types and often at only one season. To test if a consumer had significant differences in isotopic composition linked to the sediment type (for winter or summer), we performed one-way unbalanced (weighted means) ANOVAS with the sediment type considered as a fixed factor. If the ANOVA revealed a significant difference between the three sediment types, a post-hoc Tukey honest-difference test (Tukey HSD) was performed to identify between which sediment types there was a significant

difference. Prior to running the ANOVAs, we tested the homogeneity of variance with a Levene test. If heteroscedasticity was present, Kruskal-Wallis non-parametric tests were run instead with the associated post-hoc test when the global test was significant.

To evaluate the use of basal resources in each community food web, we plotted the frequency distribution of the $\delta^{13}C$ and $\delta^{15}N$ values of all the primary consumers sampled in the CS, AS and ES in winter and summer. We considered as primary consumers species reported in the literature as being strictly suspension-feeders and/or deposit-feeders and/or grazers. Then, using the mean consumer stable isotope data, we calculated several community-wide metrics to estimate the overall size of each food web (CS, AS and ES), using the SIAR and SIBER packages in R. The total area of the convex hull encompassing the data (TA) developed by Layman et al. (2007), represents the overall isotopic niche space occupied by each consumer community but it is highly sensitive to sample size and extreme isotopic values (Brind'Amour and Dubois 2013). In order to limit the effect of sample size, Jackson et al. (2011) proposed a new metric, the standard ellipse area (SEA) which encompasses around 40% of the data. If the number of species per community is superior to 30, which was always our case (see Table 17), the SEA is not underestimated and a correction for small sample sizes is not necessary. A Bayesian estimate of the standard ellipse area (SEA_B) was also proposed by Jackson et al. (2011), to consider the uncertainty in the standard ellipse areas, hence allowing the computation of credible intervals. With this Bayesian method and using the posterior distributions, formal statistical comparison of the SEA of each isotopic food web is possible along with the calculation of the mean overlap in SEA between community pairs.

To quantify the relative contributions of OM sources to a species' diet, we used Bayesian mixing models based on Markov chain Monte Carlo (MCMC) and implemented in the simmr package in R (Parnell et al. 2010, 2013). This technique works by repeatedly guessing the values of the dietary proportions and finding the values, which fit the data best. The best estimates of the dietary proportions, given the data and the model, compose the posterior distribution (Parnell et al. 2013). We ran stable isotope mixing models for species known to feed at least partly on primary producers and for which we had at least three replicates in a given sediment type and at a given season. Two variables ($\delta^{13}C$ and $\delta^{15}N$) and two (POM and MPB in CS) or three (POM, MPB and ULV in AS and ES) sources were considered for the computation of the model, as *a posteriori* knowledge of isotopic signatures. SOM was not considered as a food source *per se*, rather as a mixture of MPB and POM in the CS and as a mixture of MPB, POM and ULV in the AS and ES. We used the mean source values and associated standard deviations presented at the beginning of this section to estimate the dietary proportions of the species sampled in the CS, AS and ES in winter and summer. An *a priori* estimate of the enrichment in $\delta^{13}C$ and $\delta^{15}N$ between primary producers and primary consumers is required to run mixing models. We used trophic enrichment factors (TEF) of 1‰ and 3.4‰ for carbon and nitrogen, respectively (McCutchan et al. 2003). We hypothesized that consumers were feeding *ad libitum* and had normal growth, hence having standard turnover for small invertebrates and standard TEF (Lefebvre and Dubois

2016). Bayesian mixing models allow the insertion of variability (SD) in the TEF values (Parnell et al. 2010). We set the SD to 1‰ for both the carbon and nitrogen TEF to take into account the known variability in the TEF values linked to multiple factors such as food quality, tissue turnover, environmental conditions and taxonomic group (Vander Zanden and Rasmussen 2001, McCutchan et al. 2003, Vanderklift and Ponsard 2003).

3. Results

3.1. General food web structure of the control, associated and engineered sediments

The $\delta^{13}C$ and $\delta^{15}N$ values measured for the consumers sampled in the three sediment types and during the two seasonal campaigns (winter and summer) are shown in Figure 24. As hypothesized, the SOM appears graphically to be a mixture of POM and MPB in the CS with the addition of ULV in the associated and engineered sediments. These two (POM and MPB) or three (POM, MPB and ULV) basal resources are likely to support the main primary consumers in the three sediment types. Furthermore, some species displayed extreme isotopic compositions. The isopods *Lekanesphaera levii* and *Lekanesphaera rugicauda a prior*i classified as deposit-feeders, systematically displayed $\delta^{15}N$-depleted values (*L. levii*: winter, CS: 6.19‰, AS: 7.40‰, ES: 6.91‰; summer, CS: 6.80‰, AS: 6.54‰, ES: 7.71‰ and *L. rugicauda*: summer, CS: 8.73‰, AS: 3.3‰). Collembolans sampled in summer in the ES also displayed $\delta^{15}N$-depleted values (6.98‰) along with relatively $\delta^{13}C$-enriched values (-14.27‰). The non-native ascidian *Styela clava*, a true suspension-feeder, displayed $\delta^{13}C$-depleted (summer, AS: -23.27‰ and ES: -23.56‰) and $\delta^{15}N$-enriched (summer, AS: 9.69‰ and ES: 10.74‰) isotopic ratios. *Sabellaria alveolata* displayed a relatively central position in the winter and summer ES biplots. In the CS, it was alternately the cockle *C. edule* or the Baltic tellin *L. balthica*, both suspension-feeders that represented the bulk of the biomass with 79.9% for the cockle in winter and 80.9% for the Baltic tellin in summer. They were associated with the deposit-feeding polychaete *Lanice conchilega*, which accounted for 7.2% and 12.3% of the total biomass in winter and summer respectively. The cockle and the Baltic tellin displayed very distinct mean $\delta^{13}C$ with respectively -18.03‰ and -15.35‰ in winter and -18.91‰ and -15.56‰ in summer. In the AS and ES, the "heavy" species in terms of biomass were less dominant than the CS ones since the "heaviest" species in the AS and ES taken together accounted for 61.95% of the total biomass. In the ES, the suspension-feeder *S. alveolata* was the dominant species in term of biomass in winter (57.85%) but not in summer, when the non-native Japanese oyster *M. gigas* accounted for most of the biomass (49.21%). In winter, *M. gigas* and *P. platycheles* represented respectively 31.95% and 4.49% of the total biomass while in summer *S. alveolata* and *P. platycheles* represented 22.66% and 19.38% of the total biomass, indicating a more equilibrated distribution of the biomass between the three dominant species in summer compared with winter. These three dominant species displayed closer mean $\delta^{13}C$ values than the CS ones, with -17.09‰ (winter) and -17.23‰

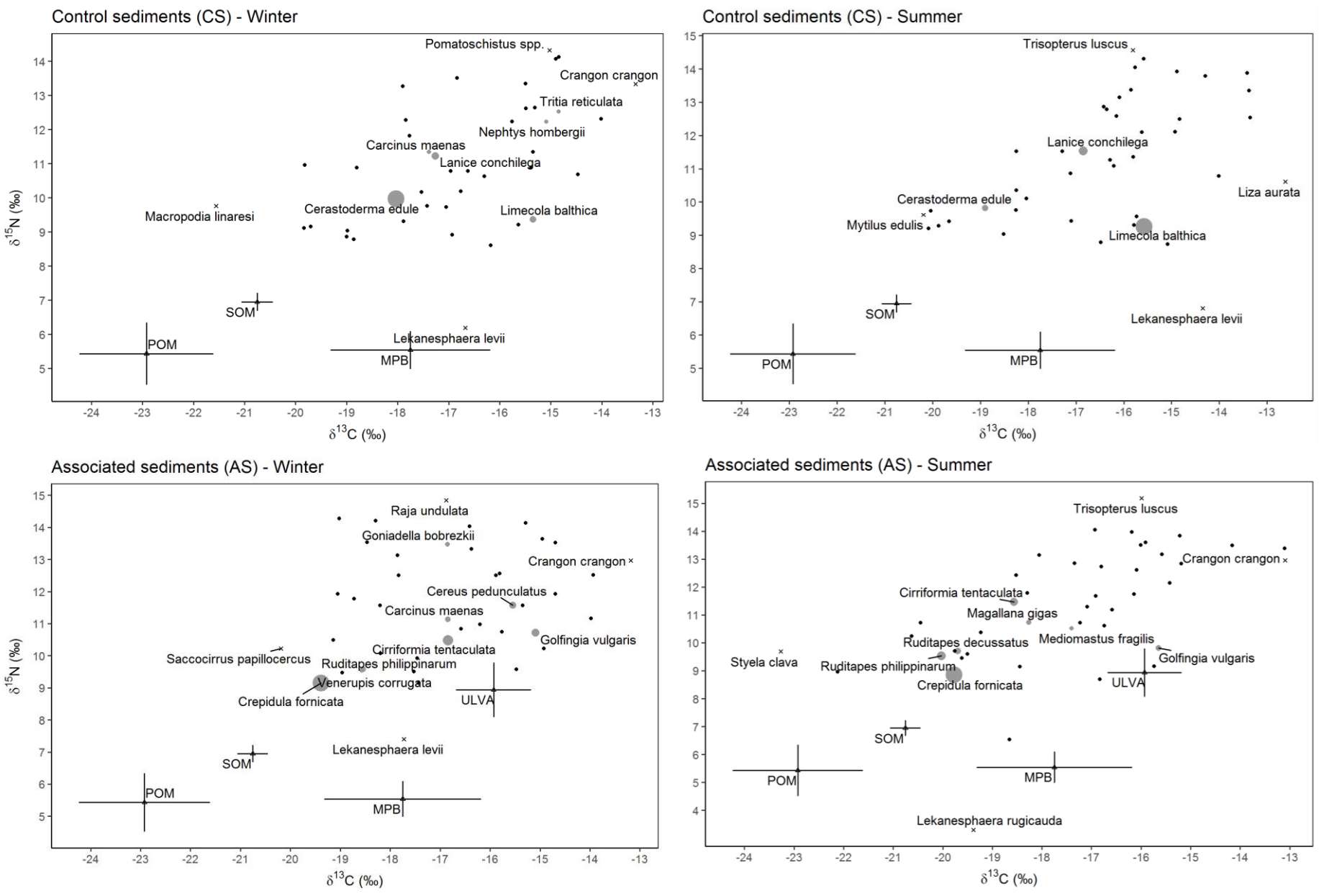
Control sediments (CS) - Winter
Pomatoschistus spp.
Crangon crangon
Tritia reticulata
Nephtys hombergii
Carcinus maenas
Lanice conchilega
Macropodia linaresi
Cerastoderma edule
Limecola balthica
SOM
POM
Lekanesphaera levii
MPB
δ15N (‰)
δ13C (‰)
Control sediments (CS) - Summer
Trisopterus luscus
Lanice conchilega
Liza aurata
Cerastoderma edule
Mytilus edulis
Limecola balthica
SOM
Lekanesphaera levii
POM
MPB
δ13C (‰)
Associated sediments (AS) - Winter
Raja undulata
Goniadella bobrezkii
Crangon crangon
Cereus pedunculatus
Carcinus maenas
Golfingia vulgaris
Cirriformia tentaculata
Saccocirrus papillocercus
Ruditapes philippinarum
Venerupis corrugata
Crepidula fornicata
ULVA
Lekanesphaera levii
SOM
POM
MPB
δ15N (‰)
δ13C (‰)
Associated sediments (AS) - Summer
Trisopterus luscus
Crangon crangon
Cirriformia tentaculata
Magallana gigas
Ruditapes decussatus
Mediomastus fragilis
Golfingia vulgaris
Styela clava
Ruditapes philippinarum
Crepidula fornicata
ULVA
SOM
POM
MPB
Lekanesphaera rugicauda
δ13C (‰)

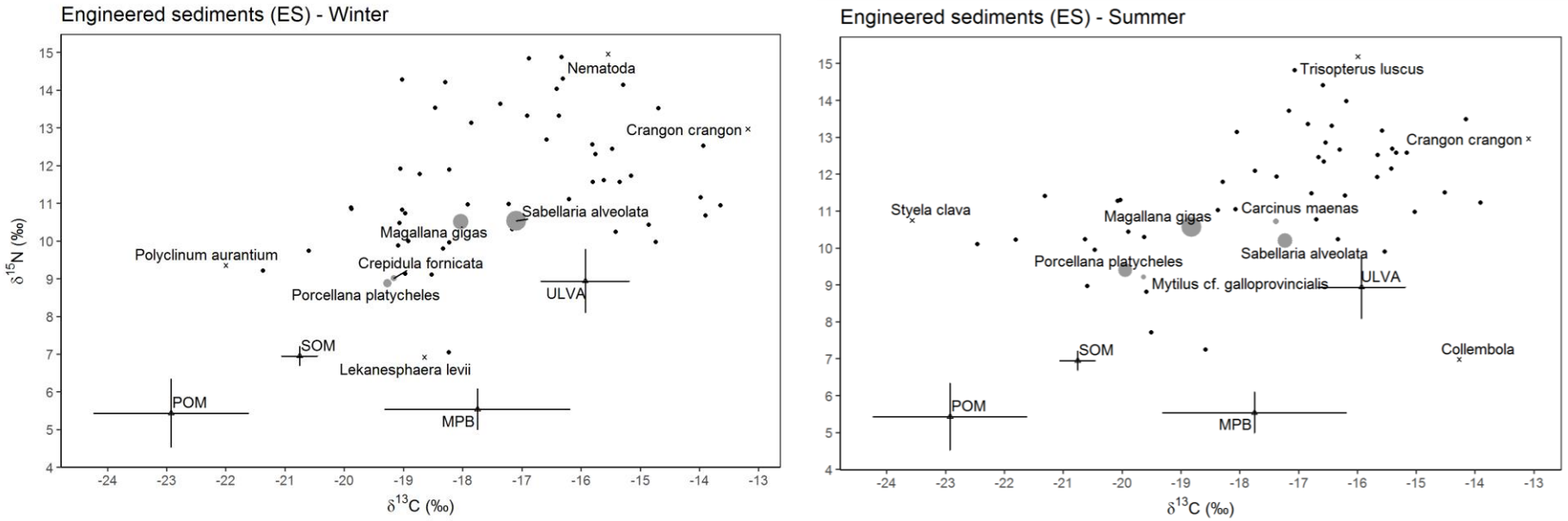

Figure 24. Carbon and nitrogen isotopic composition ($\delta^{13}C$ and $\delta^{15}N$) of the sampled species and organic matter sources during winter and summer in the control (CS), associated (AS) and engineered (ES) sediments. The mean and standard deviations of the sources (POM, SOM, MPB, ULV) are calculated as annual averages and used in the stable isotope mixing models. For consumers, mean $\delta^{13}C$ and $\delta^{15}N$ values are represented without error bars for clarity. The size of the grey bubbles is equal to the relative contribution of each species to the total biomass of each sediment type when this contribution is superior to 1% (see section 2.2.1). The other bubble values are equal to 1 (black bubbles). Species representing more than 1% of the total biomass are labelled (grey bubbles) along with the species displaying the most extreme $\delta^{13}C$ and $\delta^{15}N$ values (black crosses). Note that since the mean isotopic composition of *Venerupis corrugata* and *Ruditapes philippinarum* in the winter AS are almost identical, the grey circles representing the two species in the corresponding isotopic biplot are confounded.

(summer) for *S. alveolata*, -18.03‰ (winter) and -18.82‰ (summer) for *M. gigas* and -19.28‰ (winter) and -19.95‰ (summer) for *P. platycheles*. In the AS, the non-native gastropod *Crepidula fornicata*, reported as a suspension-feeder, represented over 50% of the total biomass with 59.00% (winter) and 61.95% (summer) accompanied by the mainly deposit-feeding polychaete *Cirriformia tentaculata*, which accounted for 15.11% (winter) and 7.14% (summer) of the total biomass. In summer, the rest of the biomass was accounted for by a suite of suspension-feeders (*Ruditapes decussatus* (3.95%), *Ruditapes philippinarum* (9.94%), *M. gigas* (1.86%)) and deposit-feeders (*Golfingia vulgaris* (2.63%), *Mediomastus fragilis* (1.30%)). In winter, predators (*Cereus pedunculatus*: 4.91%) and deposit-feeders (*G. vulgaris*: 5.99%) accounted for most of the remaining biomass.

The $\delta^{13}C$ and $\delta^{15}N$ of the species sampled in several sediment types are presented using boxplots in Appendix S2, hence showing inter-and intra-specific variations. For each species in winter and/or summer, the result of the ANOVA or the Kruskal-Wallis with the associated post-hoc test is presented. Overall, few species displayed significant inter-sediment $\delta^{13}C$ and $\delta^{15}N$ differences, with most of the time intra-sediment variations being the main source of variability. Significant inter-sediment differences were mainly observed between the control and engineered sediments or between the control and the two reef sediments (ES and AS). The only significant differences detected between the engineered and associated sediments concerned the $\delta^{15}N$ of the gastropod *Tritia reticulata* and the sedentary polychaete *Spirobranchus lamarckii*. For the $\delta^{13}C$, significant inter-sediment differences were detected for the green crab *Carcinus maenas* (summer: CS > ES, AS = CS and AS = ES), for *L. levii* (summer: CS > (AS = ES)), for the predatory polychaete *Glycera alba* (summer: CS > AS), for the anemone *Cereus pedunculatus* (winter: CS > (AS = ES)), for the mussel *Mytilus* cf. *galloprovincialis* (winter: CS < ES, AS = CS and ES = AS) and for *T. reticulata* (winter: CS > AS, ES = CS and AS = ES, summer: CS > AS). For the $\delta^{15}N$, significant inter-sediment differences were detected for the bivalves *Venerupis corrugata* (winter: CS < ES, AS = CS and ES = AS) and *Spisula solida* (summer: CS > AS), *S. lamarckii* (summer: AS < ES), *T. reticulata* (winter: (AS = CS) > ES), the shrimp *Crangon crangon* (summer: control < reef) and the benthic fish *Pleuronectes platessa* (summer: control > reef).

3.2. Isotopic composition of the primary consumers

The frequency distributions of $\delta^{13}C$ and $\delta^{15}N$ values displayed by all primary consumers sampled in the three sediment types in winter and summer are presented in Figure 25. In winter, the $\delta^{13}C$ frequency distribution in the control sediments spanned from -21.36 to -11.77‰, a range similar to the associated sediments (-22.33 to -12.56‰) and to the engineered sediments (-22.39 to -12.57‰). Furthermore, in the control sediments, primary consumers presented a range shifted ~1‰ towards $\delta^{13}C$-enriched values compared with the AS and ES. In summer, the engineered sediments exhibited the largest $\delta^{13}C$ range (-23.91 to -12.75‰) encompassing the range of the control sediments (-20.92 to -13.76‰) and almost the entire range of the associated sediments (-24.65 to -15.21‰). The range of the AS primary consumers was shifted towards $\delta^{13}C$-depleted values compared with the CS range.

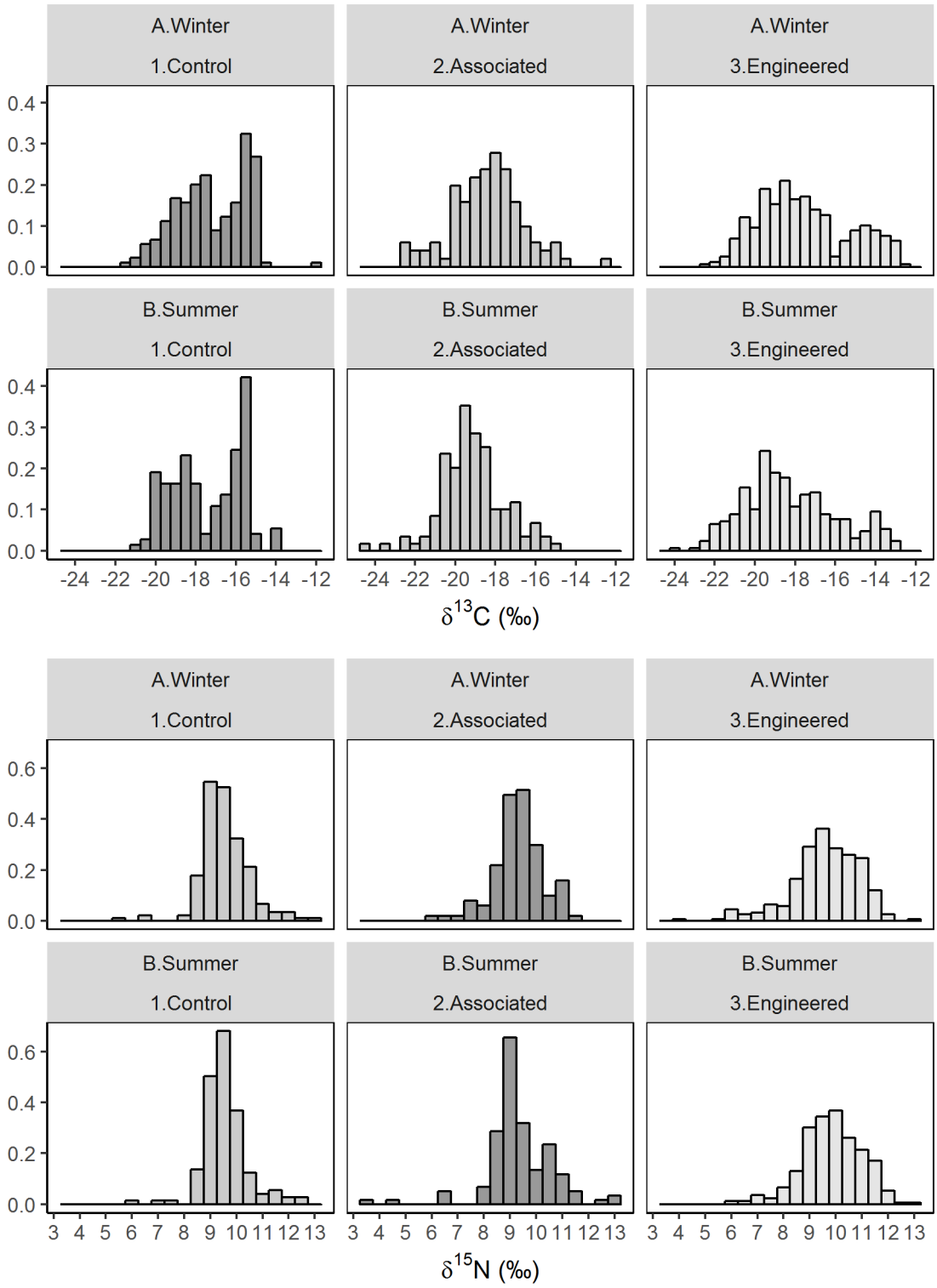

Figure 25. Frequency distributions of carbon (top) and nitrogen (bottom) isotopic compositions ($\delta^{13}C$ and $\delta^{15}N$) of all primary consumers sampled in the control, associated and engineered sediments for the two seasons (winter and summer). A size class of 0.5‰ was used for both $\delta^{13}C$ and $\delta^{15}N$.

Overall, the CS and AS $\delta^{13}C$ histograms have similar aspects with the notable exception that the CS primary consumer histogram displays two distinct modes (ca. -18.5‰ and -16‰). Regarding the engineered sediments $\delta^{13}C$ histograms, a secondary mode corresponding to $\delta^{13}C$-enriched values is

visible around -15‰ and -14‰ in winter and summer respectively, probably indicating a contribution of benthic microalgae. Furthermore, the $\delta^{15}N$ histograms of each sediment type have similar aspects at both seasons and inferior limits driven by the values of the isopods *L. levii* and *L. rugicauda* presenting $\delta^{15}N$-depleted isotopic compositions. An interesting feature of the $\delta^{15}N$ engineered sediments histograms is the presence of more individuals with $\delta^{15}N$-enriched isotopic compositions compared with the associated and control histograms, probably indicating a contribution of green macroalgae *(Ulva* spp.).

3.3. Integrative measurements of the isotopic food webs

Figure 26 represents the standard ellipse areas (SEA) and the convex hulls (TA) of the CS, AS and ES consumer communities. In general, the TA was driven by species presenting extreme isotopic compositions like *L. rugicauda* in the summer AS, highlighting the need for a less biased estimate of the total isotopic niche like the SEA. Overall, the SEA displayed a similar ellipsoid form when calculated for the three sediment types at both seasons, except the summer AS ellipse that displayed a larger eccentricity than the other ellipses. A general increase in the isotopic niches (TA) of all three communities between winter and summer is visible. Regarding the TA and SEA, this increase is particularly visible in the case of the engineered and associated sediments. In addition, the summer ellipse of the control sediments is shifted towards more $\delta^{13}C$-enriched values.

The values of the TA and SEA along with the 95% credible interval of the Bayesian SEA (SEA_B) calculated for the three sediment types in winter and summer are presented in Table 17. The community-wide metrics calculated for a global reef food web grouping the ES and AS are also presented in Table 17. Based on the TA, the ES had the largest isotopic niche width in winter (42.39), while the CS and the AS presented smaller isotopic niches of similar width (CS: 33.99, AS: 31.36). In summer, the picture changed with this time AS and ES having similarly large TA (AS: 54.93, ES: 53.19) and CS presenting a much smaller isotopic niche (34.80). In winter, the reef TA (AS+ES) was slightly inferior to the one calculated for ES (ES: 42.39 and ES+AS: 41.82). When considering the summer campaign, the reef TA was much larger than the other convex hulls (ES+AS: 71.60). Considering this time the SEA (Figure 27), the CS showed the smallest isotopic niche in winter (8.94) and summer (10.51), while ES displayed the largest in winter (ES: 11.02 and AS: 9.20) and AS the largest in summer (AS:12.09 and ES: 11.77). All three communities displayed larger SEA in summer than in winter. The global reef community showed an isotopic niche size (SEA) intermediate between the AS and ES isotopic niches in winter (10.11) and slightly larger than the AS isotopic niche in summer (summer: 12.45), displaying the same increase between winter and summer than the AS and ES ellipses.

Using the SEA_B, we tested whether the ellipse of one sediment type was smaller than another ellipse and looked into the mean overlap between two ellipses. The results are shown in Table 18. The winter CS ellipse respectively had a 54% and 83% probability of being smaller than respectively the winter AS and ES ellipses. In summer, the CS ellipse had a 75% and 70% probability of being smaller

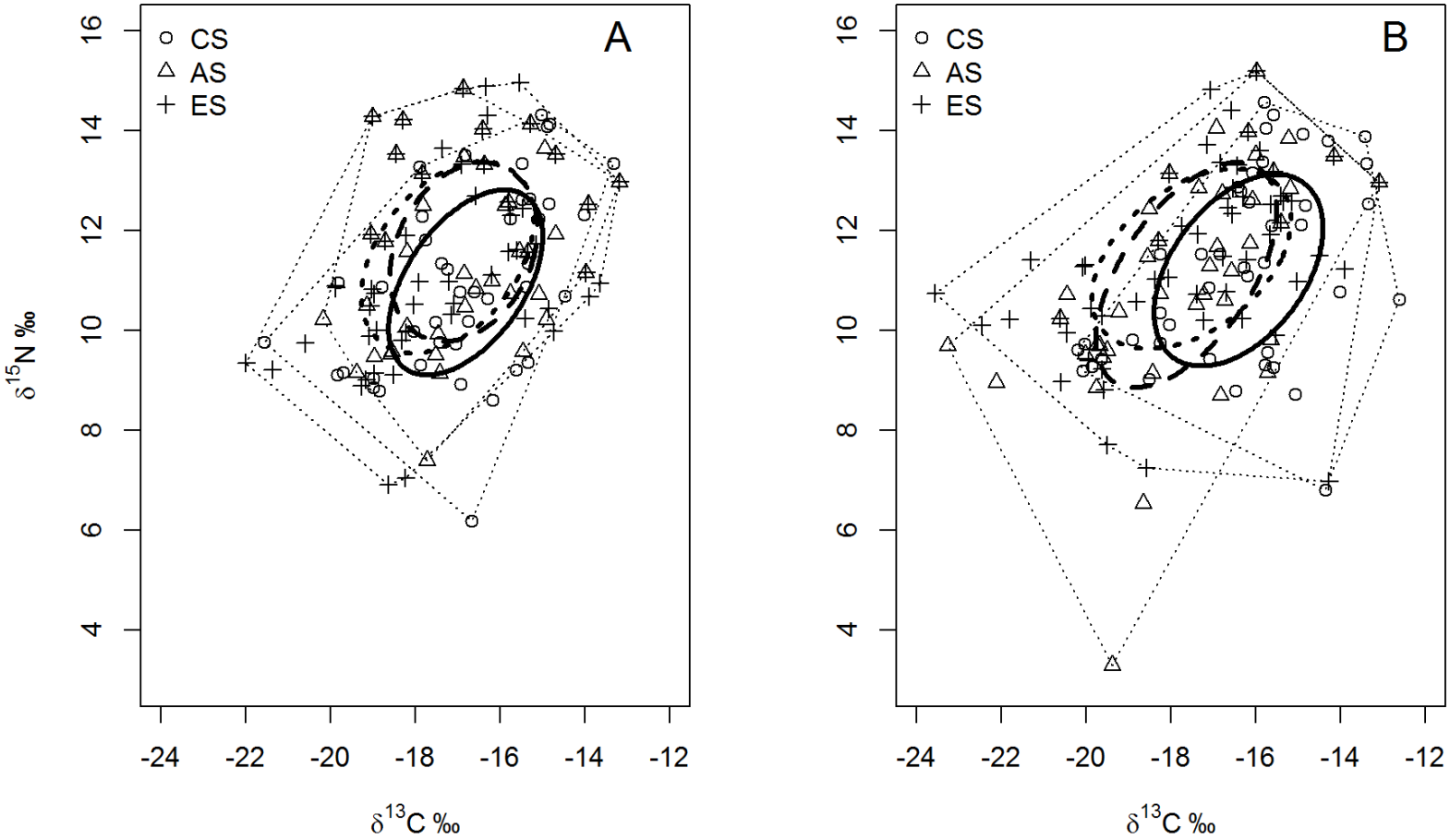

Figure 26. Biplot of the mean carbon and nitrogen isotopic compositions ($\delta^{13}C$ and $\delta^{15}N$) of the different consumers sampled in the control sediments (CS, circle), associated sediments (AS, triangle) and engineered sediments (ES, cross) in (A) winter and (B) summer. Solid ellipses enclose the standard ellipse area (SEA) of the control sediments, dashed ellipses the SEA of the associated sediments and dotted ellipses the SEA of the engineered sediments. The standard ellipse area represents the isotopic niche of the different consumer communities (AS, CS and ES) at the two seasons. Dotted lines represent the convex hulls, a proxy of the total niche width of the different consumer communities.

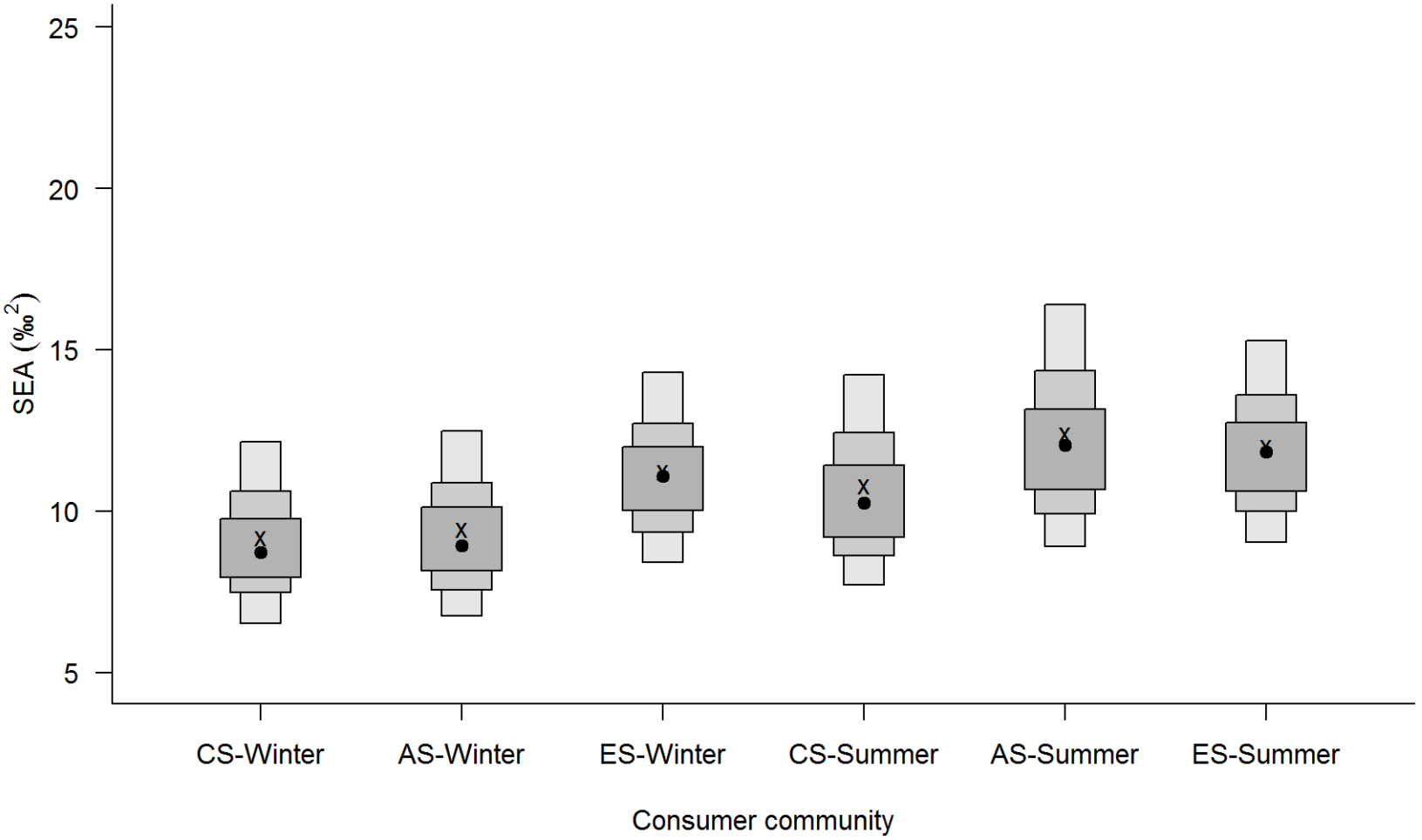

Figure 27. Density plots showing the credible intervals of the Bayesian Standard Ellipse areas (SEA_B) of consumers sampled in the three sediment types (control sediment: CS, associated sediment: AS and engineered sediment: ES) during winter and summer. Black dotes are the mode of the SEA (‰²) while the shaded boxes represent the 50% (dark grey), 75% (lighter grey) and 95% (lightest grey) credible intervals. The black cross represents the Standard Ellipse Area corrected for small sample sizes (SEA_C).

than respectively the summer AS and ES ellipses, stressing the overall size difference between the control and reef ellipses in summer. When considering the global reef ellipse (AS+ES), the CS ellipse had a 71% and 80% probability of being smaller than the AS+ES ellipse in winter and summer respectively. The AS ellipses had an 80.5% and 45% probability in winter and summer respectively, of being smaller than the respective winter and summer ES ellipses, confirming the summer increase of the isotopic niche of the AS compared with the ES. Regarding temporal differences, all three sediment types had probabilities higher than 60% of being smaller in winter than in summer (CS: 77%, AS: 90.5% and ES: 64%). The winter AS+ES ellipse had an 89% probability of being smaller than the summer one (winter < summer), a result similar to AS and ES.

In winter, the mean overlap between the CS ellipse and the two reef site ellipses was 46.54‰ and 51.52‰ for the AS and ES respectively. In summer, the mean overlap between the control sediments and the reef sediments increased, especially for the AS with almost a 10‰ increase (54.41‰) and a smaller increase for ES (54.88‰). The mean winter overlap between the CS and the AS+ES (49.88‰) was situated between the mean overlap with AS (46.54‰) and ES (51.52‰) respectively, while in summer, the mean overlap between CS and AS+ES was superior (56.80‰) than the respective mean overlap with AS (54.41‰) and ES (54.88‰). The mean overlap between the AS and ES ellipses in winter (52.06‰) was slightly larger than the other winter overlaps, while in summer the mean overlap between AS and ES was smaller (61.77‰) than the mean overlap between AS and AS+ES (66.20‰) and the mean overlap between ES and AS+ES (65.47‰).

3.4. Relative pelagic and benthic food source contributions

The mean and 97.5% confidence intervals of the contribution of the different food sources to the assimilated diet of the primary consumers present in winter and summer in the control (left part) and reef sediments (AS and ES, right part) are presented in Appendix S3. Some species' $\delta^{13}C$ and $\delta^{15}N$ were not located inside the space encompassing the two or three OM sources once corrected for the TEF (*e.g. L. levii* in the winter and summer CS), thus giving rise to very large uncertainties. When the number of replicate was limited (*e.g. R. philippinarum*, n = 3 in the winter ES) the ability of the model to estimate food source contributions with confidence is limited. Four mollusk species and one crustacean species were present (n > 3) in the three sediment types at both seasons (*L. levii*) or just in winter (*C. fornicata, M. cf. galloprovincialis, R. philippinarum, V. corrugata*) but because of the aforementioned limitations, we could not compare their relative dietary proportions with confidence. The calculation of the mean contribution of pelagic (POM) and benthic (MPB in CS and MPB + ULV in AS and ES) food sources to the diet of the different primary consumers showed that the CS food web relied by 1/3 on pelagic organic matter (31.7% in winter and 31.4% in summer) and 2/3 on benthic organic matter. Differently, pelagic OM contributed to a larger extent to the AS and ES food webs with a visible increase in contribution between winter (AS: 37.3% and ES: 35.18%) and summer (AS: 42.82% and ES: 42.46%).

Table 17 Community-wide metrics (total area of the convex hull, standard ellipse area and 95% credible interval of the Bayesian standard ellipse area) calculated for the three sediment types (control, associated and engineered) in winter and summer and for the overall reef site (AS+ES). The number of samples used to compute the metrics for each sediment type-season association is equal to n. The species sampled with the reef fixe nets are present in the AS and ES consumer communities and only once in the global reef community.

	Winter				**Summer**			
	CS	*AS*	*ES*	*AS+ES*	*CS*	*AS*	*ES*	*AS+ES*
n	42	42	57	67	42	43	54	69
TA	33.99	31.36	42.39	41.82	34.80	54.93	53.19	71.60
SEA	8.94	9.20	11.02	10.11	10.51	12.09	11.77	12.45
SEA_B	6.46-12.11	6.66-12.42	8.38-14.23	7.78-12.77	7.58-14.07	8.76-16.31	8.88-15.18	9.68-15.75

TA: total area of the convex hull, SEA: standard ellipse area and SEA_B: Bayesian standard ellipse area, CS: control sediments, AS: associated sediments, ES: engineered sediments

Table 18 Comparison of the standard ellipse area and mean overlap between pairs of consumer communities for each season, calculated using the Bayesian standard ellipse area. The upper part of the diagonal matrix shows the Bayesian probability that the ellipse of one consumer community is smaller than the ellipse of another. The bottom part of the diagonal matrix shows the mean overlap of the Bayesian standard ellipse area of pairs of consumer communities.

		Winter				**Summer**			
		CS	*AS*	*ES*	*AS+ES*	*CS*	*AS*	*ES*	*AS+ES*
Winter	*CS*	-	0.539	0.833	0.710	0.767			
	AS	46.54	-	0.805	0.678		0.905		
	ES	51.52	52.06	-	0.321			0.636	
	AS+ES	49.88	51.04	57.84	-				0.889
Summer	*CS*					-	0.748	0.698	0.804
	AS					54.41	-	0.446	0.542
	ES					54.88	61.77	-	0.614
	AS+ES					56.80	66.20	65.47	-

CS: control sediments, AS: associated sediments, ES: engineered sediments, AS+ES: global reef community (associated and engineered sediments

In the CS, MPB quantitatively represented 72% (± 3.5) and 96.4% (± 2.1) of the assimilated diet of respectively the dominant winter species *C. edule* and the dominant summer species *L. balthica*. In winter, MPB also accounted for 97.2% of the diet of *L. balthica* while in summer its contribution to the diet of *C. edule* decreased from 72 to 57% stressing the increased role of pelagic OM. Despite high uncertainties, the deposit-feeding polychaete *L. conchilega* relied more on MPB than POM with 76.1% (± 14.3) and 83.5% (± 9.3) contribution of MPB in winter and summer respectively. Unlike *C. edule*, there was an increase in the MPB contribution to the *L. conchilega* diet between winter and summer.

In the ES, benthic food sources represented similar proportions of the winter (75.9%) and summer (75.2%) diet of the engineer species *S. alveolata* with a strong contribution of ULV in winter (47.9 ± 3.2%) and summer (40.0 ± 2.6%). Benthic OM accounted for 61.8% (winter) and 50% (summer) of the diet of the *M. gigas* with a large contribution of ULV in winter (43.9 ± 4.2%) and summer (41.4 ± 3.2). MPB contributed more to the diet of *S. alveolata* (winter: 28.0 ± 4.7% and summer: 35.2 ± 3.8%) than to the diet of *M. gigas* (winter: 17.9 ± 6.1 and summer: 8.6 ± 3.9%). The crustacean *P. platycheles* clearly fed on POM (winter: 50.1 ± 5.9% and summer: 59.8 ± 4.5%) and MPB (winter: 44.3 ± 7.1% and summer: 25.8 ± 5.9%) with a weak contribution of ULV in summer (14.4 ± 3.3%). Some known grazers such as *Gibbula umbilicalis* and *Littorina littorea* had diets with an increase in the contribution of ULV between winter and summer and a reciprocal decrease in MPB contribution. *G. umbilicalis* mainly relied on ULV (winter: 55.1 ± 4.6 and summer: 71.6 ± 6.2%) and to a smaller extent on MPB (winter: 41.7 ± 4.9% and summer: 25.6 ± 6.3), especially in summer. *L. littorea* shifted from an MPB dominated diet in winter (MPB: 55.8 ± 9.4% and ULV: 34.9 ± 7.1%) to a more ULV dominated diet in summer (ULV: 64.0 ± 9.2% and MPB: 28.0 ± 10.1%) with less ULV in its diet than *G. umbilicalis*. *L. levii*, a relatively abundant deposit-feeder in the ES (mean density: 171 ind.m² and 358 ind.m² in respectively winter and summer), presented an MPB dominated diet in winter (56.6 ± 8.2%) followed by POM (38.2 ± 6.5%), with a shift towards a POM-dominated diet in summer (POM: 56.7 ± 9.0% and MPB: 37.6 ± 10.3%). The suspension-feeder *Venerupis corrugata* also displayed a seasonal dietary shift from a 50/50 benthic and pelagic diet in winter with a similar contribution of MPB (22.1 ± 9.4%) and ULV (26.6 ± 6.3%) to a pelagic dominated diet in summer (POM: 70.3 ± 3.9%, MPB: 8.7 ± 4.7% and ULV: 21.0 ± 4.1%). The winter and summer assimilated diet of the pycnogonida from the *Achelia* genus was evenly composed of benthic and pelagic (winter: 49.5 ± 5.5% and summer: 59.4 ± 6.9%) food sources with ULV contributing strongly to the benthic component (winter: 38.4 ± 6.6% and summer: 28.1 ± 6.9%). In winter and summer, the subsurface deposit-feeder *G. vulgaris* had a 95% benthic derived diet with a larger ULV contribution in winter (53.2 ± 8.5%) shifting to a larger MPB contribution in summer (56.1 ± 9.0%). Finally, green algae clearly dominated the winter and summer diet of the reported omnivorous polychaete *Perinereis cultrifera* present in the ES (winter: 77.1 ± 5.7% and summer: 70.1 ± 10.2%), while the relative contribution of POM and MPB was harder to tease out.

In the AS, the diet estimation of the gastropod *Crepidula fornicata* presented relatively low uncertainties and indicated a 50/50 contribution of benthic and pelagic food sources in winter (benthic: 49.3% and pelagic: 50.7%) and a higher POM contribution in summer (benthic: 56.7% and pelagic: 43.3%). Overall, the contribution of green algae to the diet of *C. fornicata* was low in winter (9.8%) and summer (4.9%). The diet estimation of the bivalve *R. philippinarum* presented very large uncertainties in winter but suggested a 50/50 contribution of benthic and pelagic food sources. In summer, the uncertainties were much smaller and the mixing model indicated a 36/64 contribution of benthic and pelagic OM with a similar contribution of MPB (19.5 ± 8.2%) and ULV (16.8 ± 5.6%). The same large winter uncertainties appeared when estimating the diet of *C. tentaculata* because of a low number of

replicates (3), nonetheless the model clearly indicated a larger contribution of benthic OM (78.3%) compared with pelagic OM (21.7%). In summer, the relative pelagic and benthic contributions were close to 50/50 (42.8 and 57.2%) with lower uncertainties and a stronger contribution of green alga (ULV: 43.0 ± 10.5% and MPB: 14.2 ± 10.5%).

Using mixing model outputs, we build a ternary plot (POM, MPB and ULV relative contributions) for the main ES primary consumers (Figure 28). Each set of points represents the realized isotopic niche of a primary consumer in winter or summer. Overall, the isotopic niches of all the consumers except *S. alveolata*, shifted towards an increased contribution of POM to their diets in winter. The engineer species displayed a very stable isotopic niche with a slight increase in MPB contribution between winter and summer. The two dominant species in terms of biomass (*S. alveolata* and *M. gigas*) displayed the most distinct isotopic niches relative to the other consumers. They did not present any overlap in their summer isotopic niches and a very small one in their winter isotopic niches. The other primary consumers (*Crepidula fornicata*, *Mytilus* cf. *galloprovincialis* and *Porcellana platycheles*) can account for relatively important portions of the total biomass and present in some locations very high abundances like *P. platycheles* (mean density: 712 ind. m² and 2680 ind.m² in winter and summer respectively). In winter, these species displayed very similar isotopic niches, especially *P. platycheles* and *C. fornicata*, which had almost identical niches. In summer, *P. platycheles* relied more on green algae and less on MPB while generally the POM contribution to their respective diets increased, leading to an overall decrease in the isotopic niche overlap.

4. Discussion

4.1. Food web modifications linked to the habitat modifier *S. alveolata*

Overall, our findings demonstrate that the establishment of the engineer species *S. alveolata* increases the consumer community isotopic niche, visible when comparing the non-engineered soft sediment community with the engineered sediment community. This result is also true when considering the summer associated sediment consumer community, indicating a difference between winter and summer regarding the trophic functioning of the two reef communities. Our summer results indicate that the trophic effect of *S. alveolata* is not limited to the strict habitat it engineers but extends to the neighboring soft sediments, stressing a longer distance effect than could have been expected (Van De Koppel et al., 2015). When comparing the engineered, associated and engineered+associated (reef) ellipses in winter and summer, the reef ellipse has an intermediate size between the engineered and associated sediments in winter, while in summer it is a larger than the two sediments taken independently. This result could indicate that a larger pool of resources is used in the engineered sediments in winter compared with the associated sediments, but that overall the species present in the two sediment types have similar trophic traits. Differently, the summer results seem to indicate a larger

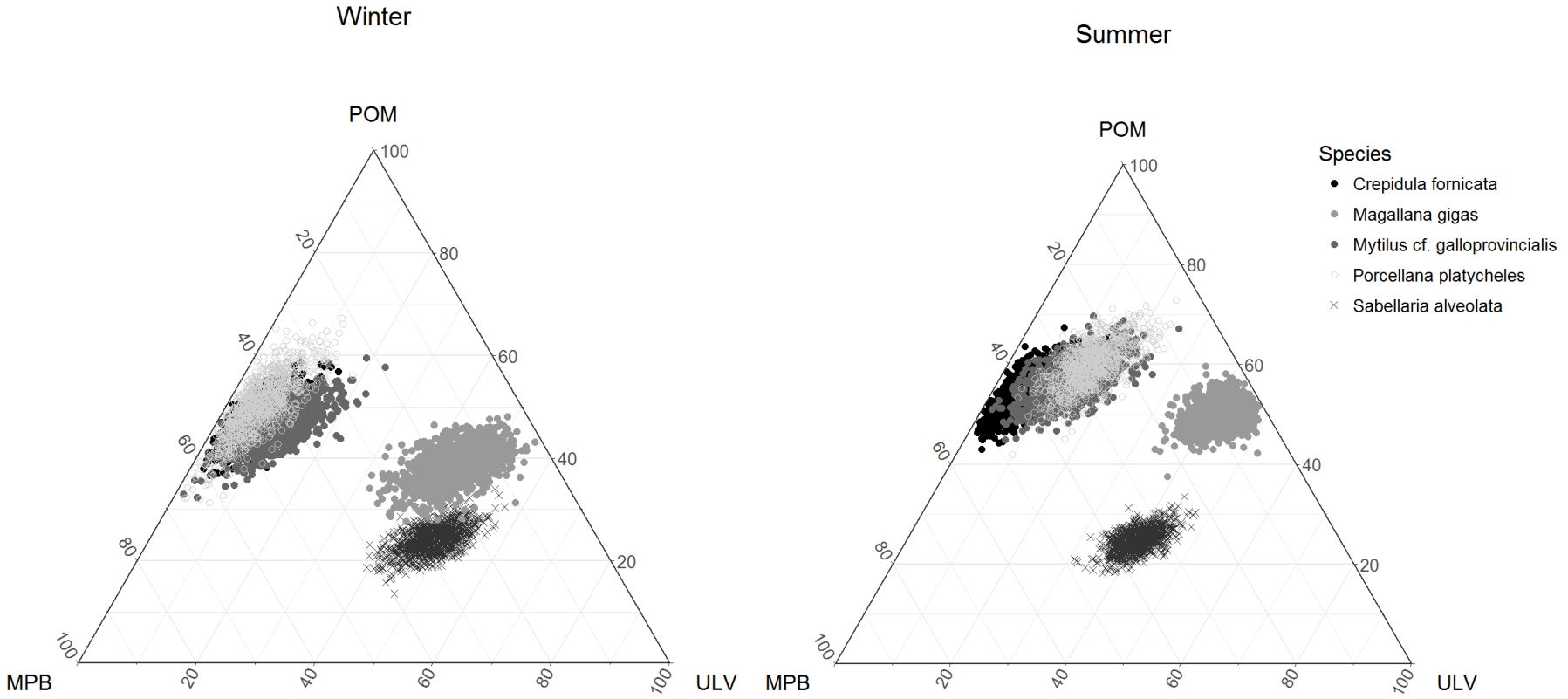

Figure 28. Ternary plots of the relative contributions of three food sources (Particulate organic matter: POM, Microphytobenthos: MPB, *Ulva* spp.: ULV) to the diet of the honeycomb-worm *Sabellaria alveolata* and four abundant suspension-feeders present in the engineered sediments (*Magallana gigas*, *Mytilus* cf. *galloprovincialis*, *Crepidula fornicata* and *Porcellana platycheles*), in winter and summer. Each point represents the posterior dietary proportions calculated by the Bayesian mixing model (see section 2.4.) using the $\delta^{13}C$ and $\delta^{15}N$ measured for each macrofauna sample. As an illustration, the assimilated summer diet of *S. alveolata* is composed of about 40% of ULV, 35% of MPB and 25% of POM. See Appendix S3 for the number of samples used to calculate the posterior dietary proportions for each species.

complementarity in term of resource use between the engineered and associated sediments, probably indicating sediment-specific trophic traits. Nonetheless, the mean isotopic overlap is higher between the two reef communities (AS and ES) than between each of them and the control community, indicating that the associated and engineered sediments have a more similar isotopic niche compared with the control sediments. Hence, the two reef communities have food web structures more similar than compared to a non-engineered sediment, despite their completely different structural nature and species composition (Jones et al. 2018). The quasi-absence of significant differences in the isotopic composition of species sampled in the engineered and associated sediments further indicates that overall a common pool of trophic resources is used by the consumers present in these two sediments. The presence of mobile species living in the associated and engineered sediments like *Pomatoschistus* spp. also contribute to increase the trophic link between the associated and engineer sediments.

The significant trophic effect of *S. alveolata* (engineered sediments) agrees with the theory developed by Sanders et al. (2014) linking habitat modifiers and food webs and with recent empirical studies on salt marsh and seagrass food webs (van der Zee et al. 2016). Interestingly, previous studies on marine habitats engineered by *Haploops nirae* (Rigolet et al. 2014a), *Lanice conchilega* (De Smet et al. 2015a) and *Zoostera noltei* (Baeta et al. 2009) did not detect effects of the ecosystem engineer on the isotopic food web structure of soft-bottom communities across seasons, despite drastic changes in the environmental conditions and consumer richness and composition (Rigolet et al. 2014b, De Smet et al. 2015b). These contrasted results resonate with the conclusions of Sanders et al. (2014) using a theoretical model, where the engineering effect on food chain structure and dynamics and associated food web stability, probably strongly depend on the trophic position of the engineer (primary producer or primary consumer) and complex feedbacks between engineering and trophic effects. Indeed, when the engineer is an intermediate consumer (*e.g. S. alveolata* or *H. nirae*) and affects resource carrying capacity (*e.g. S. alveolata* on microphytobenthos or *Ulva* sp. or *H. nirae* on epiphytic diatoms (Rigolet et al. 2014a)), a per capita increase of the engineering effect leads to cyclic dynamics of the other food web species and alternative stable states (Moore 1993 and Van De Koppel et al., 2015).

4.2. Basal node modulation in the reef site

The higher microphytobenthos biomass in the associated sediments compared with the control sediments (Jones et al. 2018) suggests an increased dietary contribution of benthic organic matter to the reef food web compared with the food web associated to non-engineered sediments. The opposite trend was actually observed, as the engineered and associated isotopic niches were $\delta^{13}C$-depleted compared with the control isotopic niche, especially in summer after the phytoplankton bloom (Figure 25). Hence, pelagic phytoplankton contributes more strongly to the trophic functioning of the reef, with an increasing role in the trophic functioning of the associated sediments. Indeed, the seasonal increase of the associated sediment consumer isotopic niche is caused by the consumption of more $\delta^{13}C$- and $\delta^{15}N$-depleted food sources (Figure 26), corresponding to pelagic organic matter consumed while suspended

in the water column or once deposited on the sediment. A similar conclusion is derived from the mixing models (Appendix S3) and from several primary (*L. levii*) and secondary consumers (*G. alba*, *C. pedunculatus*, *T. reticulata*) presenting δ^{13}C-depleted signatures in the reef sediments relative to the control sediments. In the Mont-Saint-Michel, benthic autotrophic biomass is high but productivity is low, which could indicate a sub-optimal use of this organic matter source (Davoult et al. 2008), a result we also detected at the scale of the reef habitat. Structurally complex engineered habitats such as oyster reefs, mussel beds or seagrass meadows alter boundary layer flow favoring local settlement of pelagic larvae (Commito et al. 2005, Donadi et al. 2013, 2014) and increasing particulate organic matter concentration just behind the engineered structure (González-Ortiz et al. 2014, Colden et al. 2016). This phenomenon combined with the reef's erected position above the local soft sediments could lead to a higher availability of particulate organic matter for the primary consumers living in the engineered and especially for the ones living in the associated sediments.

More specifically, in the engineered sediments the primary consumers displayed a broader spectrum of δ^{13}C values, a visible secondary mode around -15‰ in winter and -14‰ in summer and no peak in the frequency distribution (Figure 25). These results associated with mixing model outputs suggest the primary consumers associated with the engineered sediments rely on a diverse array of basal resources, have relatively restricted trophic niches and that some primary consumers rely on δ^{13}C-enriched food sources like microphytobenthos and green macroalgae. Overall, inter-specific competition for food is probably very limited in the engineered sediments, as found in *Haploops nirae* engineered habitats (Rigolet et al. 2014a). Indeed, Rigolet et al. (2014b) noted the development of benthic diatoms on *H. nirae* tubes that sustained the secondary production of both the engineered and the adjacent habitats and limited inter-specific food competition between the dominant primary consumers of the engineered habitat. Physically complex structures like polychaete or bivalve reefs are characterized by a wide diversity of organisms living in the numerous available microhabitats (Bruno et al. 2003), which could spatially limit inter-specific trophic competition by favoring the development of cryptic food sources like bacterial mats or photosynthetic communities present on oyster shells (Braeckman et al. 2011, Barillé et al. 2017). Judging by the isotope signatures of the Collembolans sampled in the engineered sediments (Fig. 1), bacterial mats developing on the mud present between the *S. alveolata* tubes could compose a significant part of their diet (Rossi et al. 2004, Kolasinski et al. 2016). Furthermore, the presence of *S. alveolata* reefs leads to the establishment of species typically found on rocky shores such as *Gibbula umbilicalis*, *Littorina littorea* and *Perinereis cultrifera*, presenting distinct diets composed of micro and macroalgae. The mixing models indicate that green macroalgae and microphytobenthos represented an important part of their assimilated diet, increasing the overall isotopic community niche. The microphytobenthic algae we sampled occur as extensive mats on the associated sediments, while the microalgae these species are grazing upon growth directly on the *S. alveolata* engineered structures and on small mud patches in between the tubes (pers. obs.). While we did not specifically investigated the isotope composition of the biofilm from the hard structures, other studies

showed that tubiculous reefs such as *Dendropoma* reefs (Colombo et al. 2013) supported a biofilm composed of diatom and cyanobacteria highly enriched in $\delta^{13}C$ and $\delta^{15}N$. This could further explain the large and enriched $\delta^{13}C$ and $\delta^{15}N$ range of the engineered sediment primary consumers (Figure 25).

In summer, species found in the associated sediments had a larger isotopic niche than the ones found in control soft sediments and engineered sediments, linked to an increase use of organic matter coming from the water column. Additional food sources like *Ulva* sp. growing on the reef structures, probably also contribute to the global increase of the isotopic niche. Indeed, the green macroalgae growing on the engineered sediments can fuel the associated sediments food web once detached and fragmented through the microbial loop. Green algae represented a significant portion of the assimilated diet of deposit-feeders living in the associated sediments like *Lanice conchilega*, *Cirriformia tentaculata* and *Mediomastus fragilis*. Furthermore, because of high feeding- and building-activity, the suspension-feeders present in the engineered sediments produce feces and pseudofeces and an important part of these biodeposits end up in the associated sediments, enriching them in organic matter compared with the control sediments (*i.e.* two-fold increase, Jones et al. (2018)). This organic matter increase is probably one of the cause of the observed shift from pelagic to benthic consumers, a change also evidenced in the context of oyster farming where the benthic community present under oyster bags presented more predators than the adjacent "control" community (Dubois et al. 2007c). Consequently, the inter-specific trophic competition could be higher in the associated sediments compared with the engineered sediments. Nonetheless, the low macrofauna abundance recorded in these sediments (Jones et al. 2018) and the relatively plastic diets many deposit-feeders can display (Dubois et al. 2007c, b, Lefebvre et al. 2009), should limit this inter-specific competition.

4.3. Trophic resource partitioning in the control and engineered sediments

In the control sediments, two basal resources fuel the food web, POM and MPB. The isotopic biplots (Figure 24) strongly suggested that the sediment bulk organic matter (SOM) was a mixture of sedimented POM and MPB with probably a small contribution of heterotrophic micro or meiofauna or rare macroalgae fragments leading to the slightly enriched $\delta^{15}N$ (Dubois et al. 2012). The Baltic tellin *L. balthica*, a facultative deposit-feeder, fed exclusively on MPB at both seasons, as reported by Christianen et al., (2017) at the scale of the Wadden Sea. This species can present dietary shifts linked to size and to conspecific density (Marinelli and Williams 2003, Rossi et al. 2004). We sampled individuals ranging from a maximum shell length of 7.9 to 23.7 mm in winter and from 9.2 to 22.5 mm in summer, and no significant correlation between the size and the $\delta^{13}C$ or $\delta^{15}N$ was detected, whatever the season ($p > 0.05$). The cockle *C. edule*, a strict suspension-feeder, fed for 2/3 to half on MPB. The Wadden Sea isoscape revealed spatial variability in the benthic contribution to the cockle's diet with contributions reaching ~ 95% in some intertidal muddy areas (Christianen et al. 2017). An important contribution of MPB to cockle growth and secondary production was also evidenced in the Marennes-Oléron Bay (Sauriau and Kang 2000). The diet partitioning for the sandmason-worm *Lanice conchilega*

was not as clear because of low sample sizes, but it also relied on MPB for ca. 75-80% of its diet, presenting an enriched $\delta^{15}N$ previously reported for this species and attributed to consumption of green algae fragments (Dubois et al. 2007b) or increased deposit-feeding (Dubois et al. 2007c). This polychaete, reported to switch from deposit- to suspension-feeding when densities become high (Buhr 1976), was locally present at maximal densities of ~ 1000 ind.m^{-2}, consistent with deposit-feeding. This feeding mode enables the consumption of a larger pool of organic matter than strict suspension-feeding, in the form of small heterotrophic meiofauna or bacterially processed organic matter from the sediment (Dubois et al. 2007c). Overall, our results indicated a partitioning of the trophic resource between the three dominant species and low intra-specific variability in the control sediments, not disregarding that there could be an intra-specific competition regarding the cockle in winter and the tellin in summer judging by the very high local densities (Jones et al. 2018), a hypothesis we could hardly verify. More generally, MPB represented at least 50% of the assimilated diet of the main primary consumers (*C. edule*, *L. balthica* and *L. conchilega*) with a stronger proportion in winter compared to summer, reflecting an increased use of benthic resources during late winter when phytoplankton biomass is low (Decottignies et al. 2007, Lefebvre et al. 2009, Dubois and Colombo 2014). The presence of MPB in the diet of *C. edule* also stresses the importance of resuspension (Orvain et al. 2012, Ubertini et al. 2012) in the provisioning of MPB to strict intertidal suspension-feeders.

Engineered sediments were dominated in terms of biomass by the tube builder *S. alveolata* in winter but in summer, the non-native Japanese oyster *Magallana gigas*, appeared as the dominant species because of the smaller biomass of the newly settled honeycomb-worms (Dubois et al. 2007a). Both species have been suspected to compete for food at the reef scale (Dubois et al. 2006a, Rollet et al. 2015), despite having different particle retention efficiencies (Dubois et al. 2003). The ternary plots based on the mixing model outputs (Figure 27) indicated a clear separation of their isotopic niche in summer when *M. gigas* consumed more POM and fed on less MPB. In winter, their realized isotopic niche were much closer with a very limited overlap, since the honeycomb-worm relied more on MPB and less on POM than *M. gigas*. Interestingly the relatively constant and high proportion of *Ulva* spp. (40-50%) to their diets in winter and summer stress the use of this additional food source originating from the engineered sediment by the two main consumers of the reef. Green macroalgae have previously been reported to represent up to 60% of the honeycomb-worm's diet on a rocky intertidal coast (Dubois and Colombo 2014). Furtermore, the isotopic niche of *S. alveolata* was small compared to the other primary consumers (Figure 27) indicating a low variability among individuals in the use of the different organic matter sources. Similarly, Jack et al. (2011) found low isotopic variability in the use of organic matter sources among red rock lobster individuals sampled inside kelp bed, while outside the engineered habitat; the lobster presented a broad trophic diversification. In the engineered sediment food web, the combination of trophic and engineering interactions result in a global positive trophic feedback between *S. alveolata* that engineers a large-scale habitat favoring the development of optimal trophic conditions for itself, with the presence of macroalgae and high local MPB biomass (Jones et al. 2018) resuspended

by tidal currents (Orvain et al. 2012). The gardening hypothesis was first outlined by Hylleberg, (1975) for the lugworms *Abarenicola pacifica*. This polychaete - via its digestion and feces production - stimulates the microbial loop in the sediment surrounding its burrow, microbes which can then be ingested by the worm. Since then, a similar mechanism has been evidenced for oysters (Cognie and Barille 1999, Echappé et al. 2017) and epiphytes growing on *Haploops nirae* tubes have been showed to contribute up to 50% to the diet of dominant species associated with this engineered habitat (Rigolet et al., 2014b). Our results indicating that MPB contributed up to 35% to the diet of *S. alveolata*, underline a notable gardening effect in the context of this engineered habitat and in favor of the ecosystem engineer.

The initial gardening hypothesis focused on the 'selfish' use by a species of a food source it promoted (Hylleberg 1975). A more 'altruist' gardening process can be considered where a species promotes a food source, which is then used by other species, a definition focusing on one component of ecosystem engineering, the modulation of the availability of trophic resources to other species (Jones et al. 1994). Such as process has been observed in the case of *H. nirea* tube mats, where the diatoms (*Navicula* spp.) growing on tubes were consumed by species living in the engineered habitat like the bivalve *Polititapes virgineus* but also exported and consumed by species living in the adjacent non-engineered habitat like the brittle star *Amphiura filiformis* (Rigolet et al. 2014a). In our case, microphytobenthos made up between 20% and 55% of the diet of other abundant primary consumers present in the engineered sediments (Figure 27: *P. platycheles*, *C. fornicata* and *M.* cf. *galloprovincialis*), stressing the importance of trophic resources promoted by the reefs, in the diet of associated species.

4.4. Mobile consumers and the *S. alveolata* reef

Inside engineered food webs, negative trophic feedbacks can affect the habitat modifier via the creation of refuge for its predator (Sanders et al. 2014, Agüera et al. 2015) while overall, the engineered habitat can increase predator foraging efficiency by reducing interference competition among them (Grabowski and Powers 2004). Mobile and abundant species like gobies from the genus *Pomatoschistus* and the green crab *Carcinus maenas* are potential predators of *S. alveolata*. *Carcinus maenas* presented $\delta^{13}C$ and $\delta^{15}N$ values very close to *S. alveolata* (Figure 24), indicating a primary-producer based diet and not a carnivorous diet. Overall, the green crabs sampled in the engineered sediments were juveniles (mean carapace width < 1 cm) consistent with ontogenic habitat shift. Indeed, smaller individuals would live in structured habitats like *S. alveolata* reef, with less predatory pressure and move towards soft sediments when they become larger. These smaller individuals very probably do not have the strength to carve the reef until reaching honeycomb-worms and feed primarily on green algae and detritus. Using the $\delta^{13}C$ and $\delta^{15}N$ values of *S. alveolata* as a baseline, one could identify the secondary consumers from the engineered sediments, that could be potential predator of this habitat modifier, such as the polychaetes *Phyllodoce laminosa* and *Eulalia viridis* and the demersal fish species *Pomatoschistus* spp.,

Lipophrys pholis, *Callionymus lyra* and *Scophthalmus rhombus*. *S. alveolata* opercular crowns were found in large quantity in the stomach content of the blennie *L. pholis* (Dubois et al. 2002), which lives inside the engineered sediments and remains there even at low tide. Hence, *S. alveolata* is both a probable food source and a habitat-provider. Such a predator-prey interaction between *S. alveolata* and a secondary consumer residing in the engineered sediments has the potential to lead to a negative trophic feedback that could alter the engineer density and reef-building activity.

Conclusion

All our results converge towards a general framework. For both seasons, the engineered sediment food web is dominated in terms of biomass by primary consumers, presenting small isotopic niches, suggesting a high trophic specialization linked to the engineered habitat. Indeed, several species had very specific diets based exclusively on engineered food sources (*e.g.* bacterial mats, *S. alveolata* tube microphytobenthos). Hence, there seems to be an optimal exploitation of the different food sources by the primary consumers, driven by abiotic consumable resources (space) and non-trophic interactions (facilitation). The associated sediment food web is dominated in terms of biomass by a more diversified set of species presenting various feeding modes such as suspension- and deposit-feeders along with predators, leading to a larger consumer community in summer when food sources are more diversified. Nonetheless, there appears to be a less even exploitation of the basal resources in this sediment type than in the engineered sediments. Finally, the control sediment food web is overall dominated in terms of biomass by very few suspension-feeding species. There is a distinct dietary segregation between the dominant species relying either exclusively on benthic food sources or more heavily on pelagic organic matter. This food web is turned towards benthic food sources while surprisingly the engineered and associated sediment food webs are turned towards more pelagic food sources especially in summer when pelagic primary production is higher. Overall, the engineering activity (reef construction) leads to the establishment of a species rich community in the engineered sediments while trophic effects (food source increase) leads to a diversification of trophic niches and potentially, to a more stable and resilient food web. Finally, the different results plead in favor of the consideration of a global reef food web.

Appendix

Appendix S1. Protocol used to extract the MPB from the sampled sediments.

To extract the MPB from the sediment, we used liquid silica (LUDOX HS-30). The sampled sediment was defrosted in a refrigerator, then 5 ml of homogenized sediment was placed into a 50 mL falcon (A) and 25 mL of LUDOX HS-30 were added. The flacon tubes were then mixed, placed into an ultrasound bath for 15 min and mixed again. After, they were centrifuged at 5000 rpm for 15 min at 10°C and the supernatant containing the MPB was placed into another falcon using a clean pipet (B). All the steps between A and B were repeated three times for each 50 ml falcon tube. In the end we had a new falcon tube containing a mix of MPB and liquid silica that we rinsed using MilliQ water and the dilution 3 MilliQ water for 1 supernatant. The falcon containing the supernatant and the MilliQ water was centrifuged at 3500 rpm for 10 min at 10°C, the resultant supernatant was removed and the rest was placed at -80°C until further processing.

Appendix S2. Boxplots of the carbon and nitrogen compositions ($\delta^{13}C$ and $\delta^{15}N$) of the consumers sampled in at least two sediment types (CS = control sediments, AS = associated sediments, ES = engineered sediments) during winter and/or summer and for which we had at least three replicate samples for each sediment type-season association. The results of the ANOVA or of the Kruskal-Wallis test are presented as stars indicating the p-value and the results of the associated post-hoc tests are presented as inferior, superior and equality symbols between the sediment types. If nothing is indicated, the ANOVA or the Kruskal-Wallis test revealed no significant difference between the sediment types. A level of significance of 0.05 was considered.

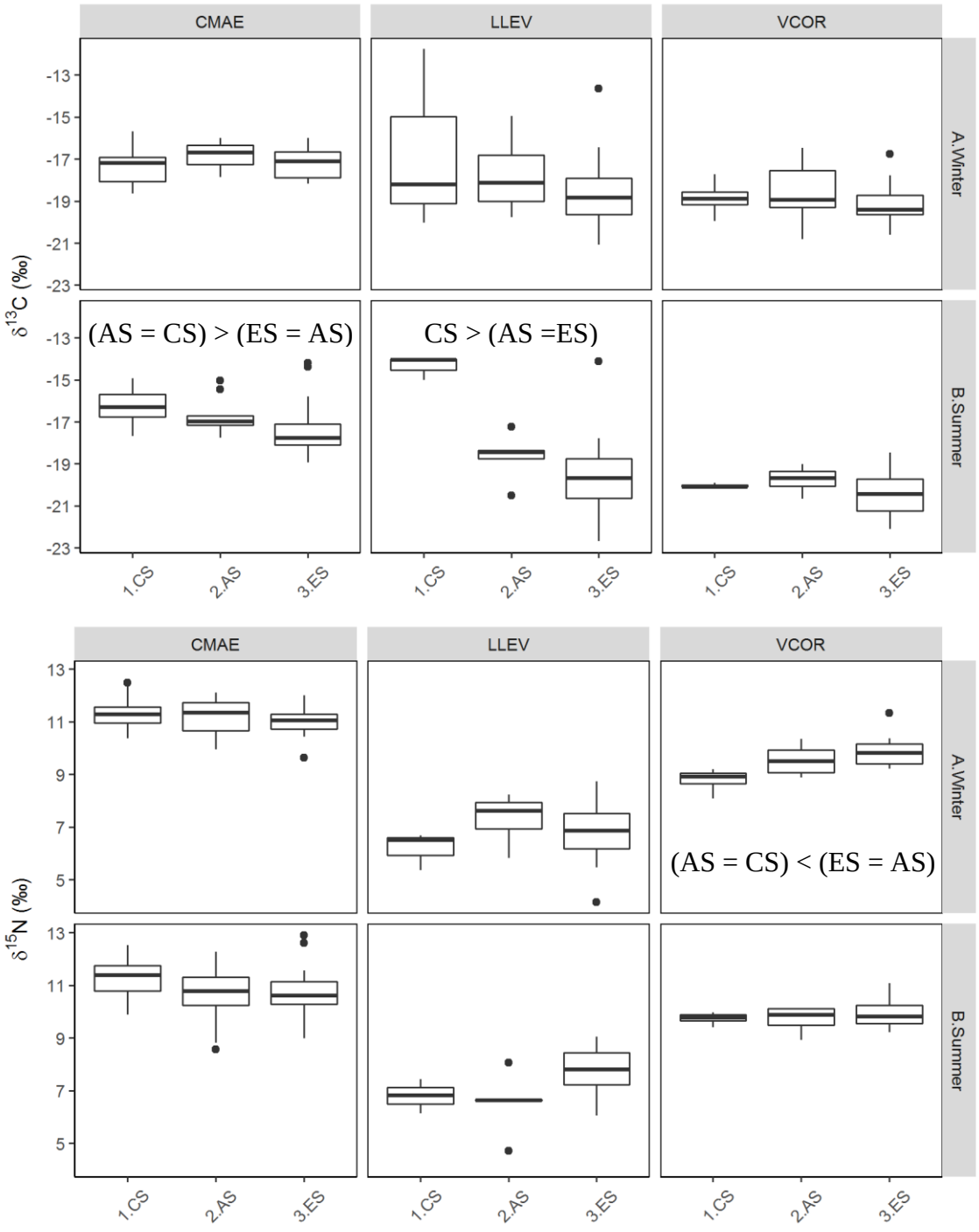

CMAE: *Carcinus maenas*, LLEV: *Lekanesphaera levii*, VCOR: *Venerupis corrugata*

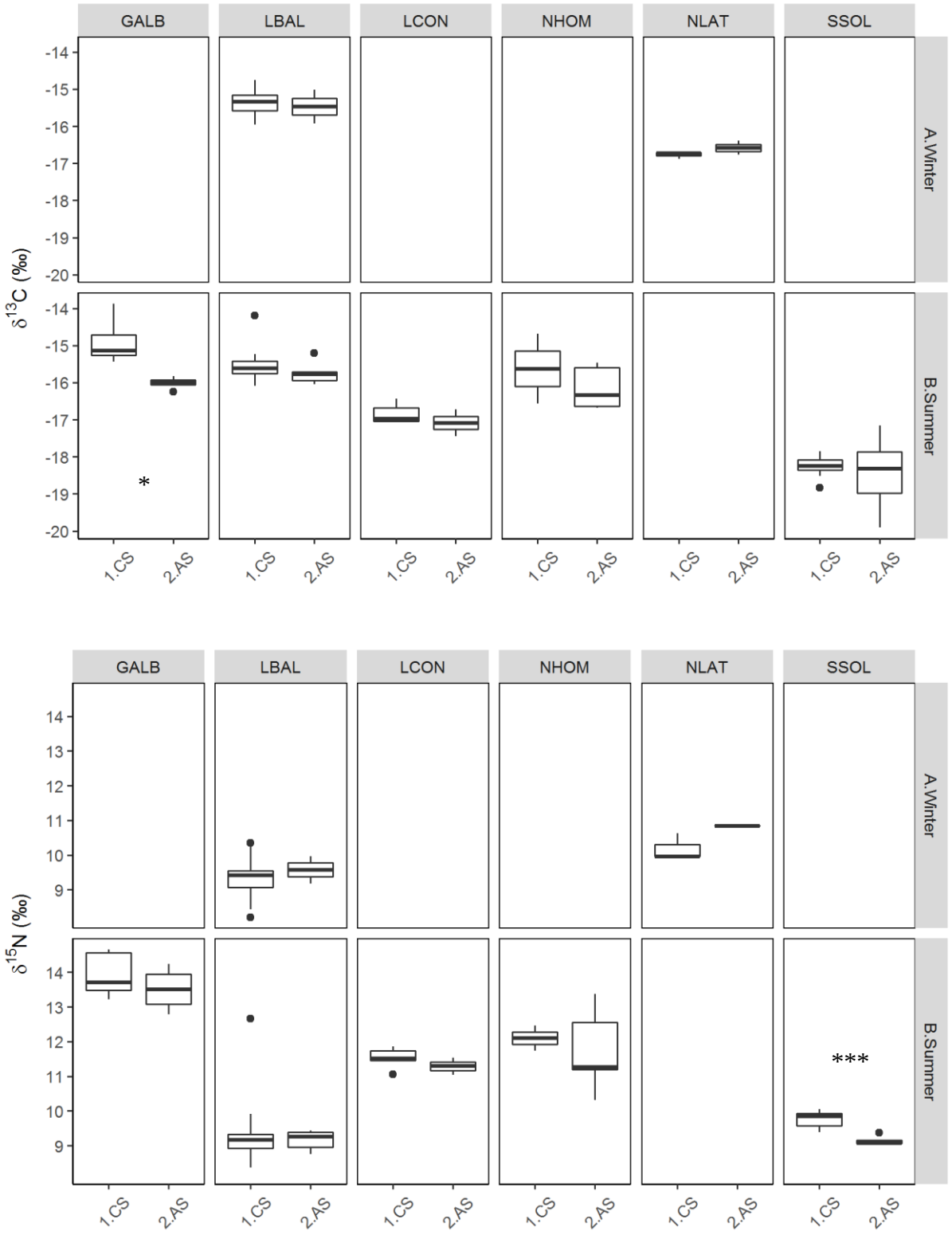

GALB: *Glycera alba*, LBAL: *Limecola balthica*, LCON: *Lanice conchilega*, NHOM: Nephtys hombergii, NLAT: *Notomastus latericeus*, SSOL: *Spisula solida*

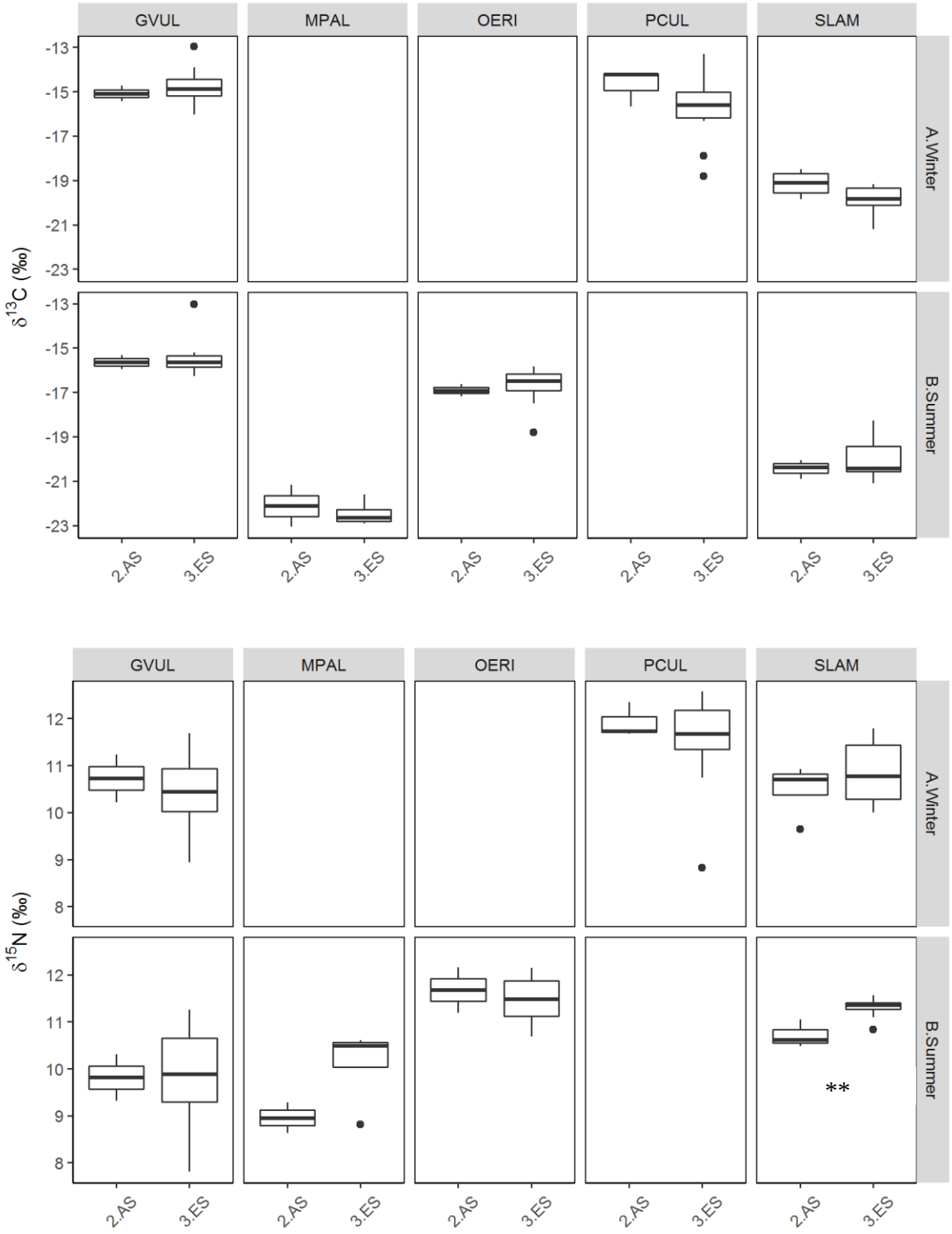

GVUL: *Golfingia vulgaris*, MPAL: *Melita palmata*, OERI: *Ocenebra erinaceus*, PCUL: *Perinereis cultrifera*, SLAM: *Spirobranchus lamarckii*

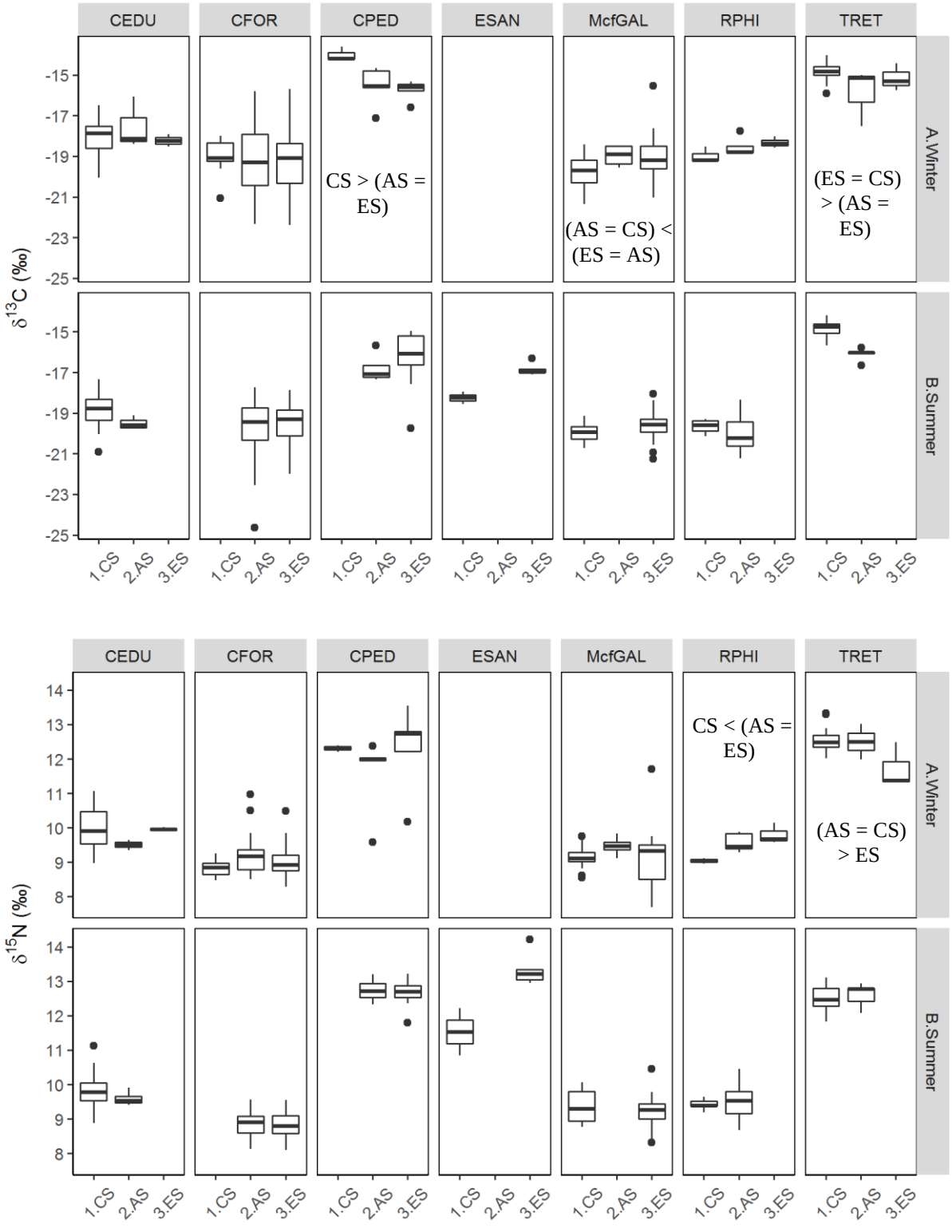

CEDU: *Cerastoderma edule*, CFOR: *Crepidula fornicata*, CPED: *Cereus pedunculatus*, ESAN: *Eumida sanguinea*, McfGAL: *Mytilus* cf. *galloprovincialis*, RPHI: *Ruditapes philippinarum*, TRET: *Tritia reticulata*

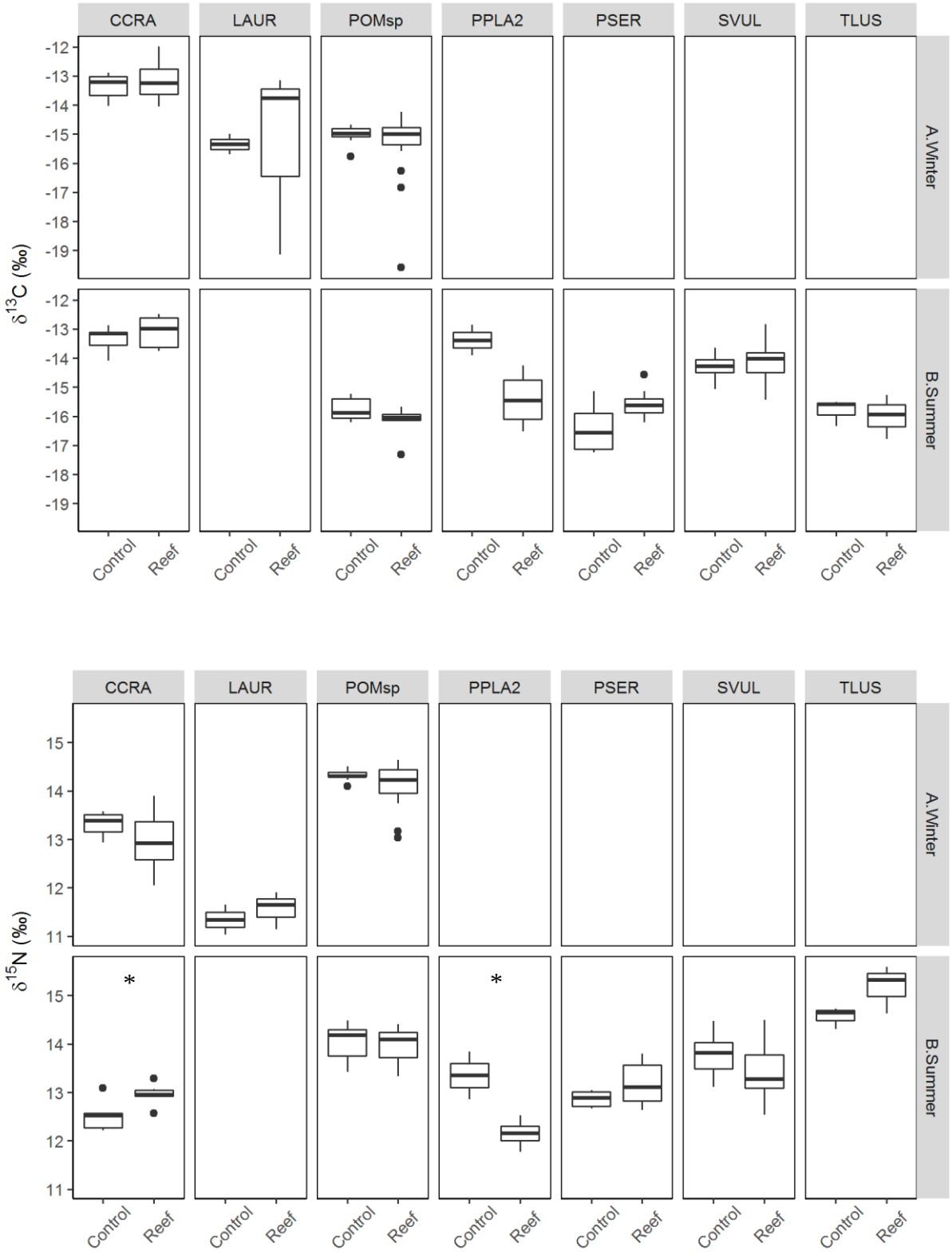

Species sampled in the set nets put in place in the control or reef zone. CCRA: *Crangon crangon*, LAUR: *Liza aurata*, POMsp: *Pomatoschistus* spp., PPLA2: *Pleuronectes platessa*, PSER: *Palaemon serratus*, SVUL: *Solea vulgaris*, TLUS: *Trisopterus luscus*

Appendix S3. Estimated contributions of the two (control site) or three (Reef site) main food sources, particulate organic matter (POM), microphytobenthos (MPB) and green algae from the genus *Ulva* (ULV), for the primary consumers present in the control, associated (AS) and engineered (ES) sediments in winter (W) and summer (S) using the Stable Isotope Mixing Model in R (simmr). The mean contribution ± the standard deviation of the mean contribution followed by the 97.5% confidence interval are indicated. The sum of the pelagic (POM) and benthic (MPB for the control site and MPB + ULV for the reef site) mean contributions is also indicated. The mixing model was run for species for which we had at least three replicate samples by sediment type and season, identified as n in the table. The species accounting for more than 1% of the total biomass in each sediment type (Sed) in winter and/or summer are designated by *.

Control site							Reef site							
Species	n	Sea	POM	MPB	Pelagic	Benthic	**Species**	n	Sea	Sed	POM	MPB	ULV	Pelagic	Benthic
CEDU*	51	W	28.0 ± 3.5 (20.9-34.7)	72.0 ± 3.5 (65.3-79.1)	28	72	**CEDU**	3	W	AS	29.3 ± 14.8 (5.3-62.6)	44.9 ± 19.7 (8.4-81.8)	25.8 ± 13.7 (4.8-56.8)	29.3	70.7
	41	S	42.9 ± 3.7 (35.6-50.0)	57.1 ± 3.7 (50.0-64.4)	42.9	57.1		5	S	AS	53.6 ± 10.2 (30.5-72.1)	26.2 ± 12.9 (5.2-55.5)	20.2 ± 8.1 (5.3-37.0)	53.6	46.4
CFOR	10	W	44.1 ± 7.6 (29.0-59.1)	55.9 ± 7.6 (40.9-71.0)	44.1	55.9	**CFOR***	39	W	AS	50.7 ± 4.8 (41.2-60.2)	39.5 ± 6.3 (26.8-51.6)	9.8 ± 3.3 (3.5-16.5)	50.7	49.3
								47	W	ES	47.4 ± 3.5 (40.3-54.2)	45.3 ± 4.9 (35.4-54.7)	7.3 ± 2.7 (2.6-13.1)	47.4	52.6
								47	S	AS	56.7 ± 3.8 (49.3-64.1)	38.4 ± 4.7 (28.8-47.3)	4.9 ± 2.3 (1.2-10.0)	56.7	43.3
								38	S	ES	54.6 ± 3.7 (47.3-61.8)	40.1 ± 4.9 (30.0-49.2)	5.3 ± 2.4 (1.5-10.7)	54.6	45.4
LCON*	4	W	23.9 ± 14.3 (3.7-59.7)	76.1 ± 14.3 (40.3-96.3)	23.9	76.1	**LCON**								
	6	S	16.5 ± 9.3 (2.9-37.2)	83.5 ± 9.3 (62.8-97.1)	16.5	83.5		3	S	AS	22.5 ± 10.3 (5.0-44.0)	24.9 ± 15.8 (3.4-65.4)	52.6 ± 14.7 (17.4-78.2)	22.5	77.5
LLEV	3	W	40.9 ± 24.8 (4.7-90.6)	59.1 ± 24.8 (9.4-95.3)	40.9	59.1	**LLEV**	10	W	AS	21.9 ± 10.7 (3.9-44.3)	68.6 ± 14.9 (33.6-91.9)	9.5 ± 7.7 (1.2-29.8)	21.9	78.1
								26	W	ES	38.2 ± 6.5 (25.3-51.0)	56.6 ± 8.2 (38.5-71.5)	5.2 ± 3.6 (0.9-14.4)	38.2	61.8
	3	S	34.2 ± 24.7 (3.0-88.7)	65.8 ± 24.7 (11.3-97.0)	34.2	65.8		5	S	AS	41.9 ± 14.2 (11.2-69.8)	38.9 ± 19.3 (6.4-78.9)	19.2 ± 12.1 (2.7-46.2)	41.9	58.1

								19	S	ES	56.7 ± 9.0 (39.2-74.7)	37.6 ± 10.3 (16.6-56.7)	5.7 ± 3.9 (1.0-15.7)	56.7	43.3
LBAL*	45	W	2.8 ± 1.6 (0.6-6.7)	97.2 ± 1.6 (93.9-99.4)	2.8	97.2	**LBAL**								
	37	S	3.6 ± 2.1 (0.7-8.5)	96.4 ± 2.1 (91.5-99.3)	3.6	96.4		5	S	AS	12.9 ± 9.7 (2.0-39.8)	62.5 ± 18.2 (18.8-90.1)	24.6 ± 16.1 (3.7-68.0)	12.9	87.1
McfGAL	21	W	54.6 ± 4.9 (45.6-64.3)	45.4 ± 4.9 (35.7-54.4)	54.6	45.4	**McfGAL***	4	W	AS	46.1 ± 12.2 (17.9-69.3)	33.1 ± 15.5 (6.2-67.3)	20.8 ± 9.3 (4.6-40.2)	46.1	53.9
								33	W	ES	46.5 ± 4.1 (38.5-54.3)	43.3 ± 6.2 (30.7-55.0)	10.2 ± 3.6 (3.5-17.7)	46.5	53.5
	8	S	58.9 ± 8.7 (41.0-75.8)	41.1 ± 8.7 (24.2-59.0)	58.9	41.1		26	S	ES	56.7 ± 4.0 (48.9-64.5)	30.6 ± 6.4 (17.9-42.8)	12.7 ± 4.0 (5.2-20.7)	56.7	43.3
RPHI	3	W	44.9 ± 17.1 (10.8-79.9)	55.1 ± 17.1 (20.1-89.2)	44.9	55.1	**RPHI***	5	W	AS	41.0 ± 10.2 (18.8-60.5)	35.5 ± 14.6 (8.9-66.1)	23.5 ± 9.0 (6.8-41.6)	41	59
								3	W	ES	37.1 ± 13.6 (9.5-63.1)	35.2 ± 17.8 (5.7-73.5)	27.7 ± 11.9 (5.9-51.9)	37.1	62.9
	6	S	54.1 ± 10.5 (32.5-74.5)	45.9 ± 10.5 (25.5-67.5)	54.1	45.9		14	S	AS	63.7 ± 5.5 (52.4-74.4)	19.5 ± 8.2 (5.0-36.4)	16.8 ± 5.6 (5.9-27.6)	63.7	36.3
SSOL							**SSOL**	11	W	AS	24.3 ± 6.5 (10.8-36.4)	58.7 ± 9.6 (40.1-77.3)	17.0 ± 6.3 (5.2-30.2)	24.3	75.7
	11	S	32.7 ± 7.5 (17.4-47.1)	67.3 ± 7.5 (52.9-82.6)	32.7	67.3		5	S	AS	38 ± 12.0 (12.8-61.0)	45.5 ± 15.8 (13.7-75.7)	16.5 ± 8.4 (3.4-36.1)	38	62
VCOR	4	W	42.6 ± 14.7 (13.4-73.6)	57.4 ± 14.7 (26.4-86.6)	42.6	57.4	**VCOR***	8	W	AS	40.6 ± 10.3 (19.3-59.8)	39.7 ± 14.0 (12.7-67.7)	19.7 ± 7.7 (6.0-35.7)	40.6	59.4
								12	W	ES	51.3 ± 6.3 (38.0-62.5)	22.1 ± 9.4 (5.8-42.2)	26.6 ± 6.3 (13.8-38.6)	51.3	48.7
	4	S	59.1 ± 14.9 (26.0-87.3)	40.9 ± 14.9 (12.7-74.0)	59.1	40.9		4	S	AS	54.8 ± 13.5 (21.3-77.8)	25.1 ± 14.5 (4.2-59.9)	20.1 ± 9.4 (4.5-40.1)	54.8	45.2
								23	S	ES	70.3 ± 3.9 (62.1-77.6)	8.7 ± 4.7 (1.8-19.5)	21.0 ± 4.1 (12.4-28.7)	70.3	29.7

AALB	9	W	12.7 ± 7.3 (2.4-30.2)	87.3 ± 7.3 (69.8-97.6)	12.7	87.3
	9	S	14.4 ± 7.3 (2.9-31.2)	85.6 ± 7.3 (68.8-97.1)	14.4	85.6
CALA	4	W	26.2 ± 14.8 (4.6-63.9)	73.8 ± 14.8 (36.1-95.4)	26.2	73.8
GZAD	6	W	56.8 ± 10.5 (36.0-77.5)	43.2 ± 10.5 (22.5-64.0)	56.8	43.2
MTEN	12	W	8.2 ± 5.2 (1.4-20.9)	91.8 ± 5.2 (79.1-98.6)	8.2	91.8
	9	S	10.6 ± 7.1 (1.8-28.3)	89.4 ± 7.1 (71.7-98.2)	10.6	89.4
NLAT	3	W	26.8 ± 19.1 (3.5-78.5)	73.2 ± 19.1 (21.5-96.5)	26.1	73.9
SARM	3	W	27.9 ± 22.6 (2.7-86.4)	72.1 ± 22.6 (13.6-97.3)	27.9	72.1
	3	S	26.8 ± 21.0 (3.1-82.5)	73.2 ± 21.0 (17.5-96.9)	26.8	73.2
UROsp	4	W	20.8 ± 18.9 (2.1-74.3)	79.2 ± 18.9 (25.7-97.9)	20.8	79.2
	4	S	23.3 ± 19.7 (2.4-78.1)	76.7 ± 19.7 (21.9-97.6)	23.3	76.7

ACHspp	9	W	ES	49.5 ± 5.5 (38.6-59.8)	12.1 ± 7.4 (2.2-30.7)	38.4 ± 6.6 (23.5-49.9)	49.5	50.5
	8	S	ES	59.4 ± 6.9 (43.8-71.7)	12.5 ± 7.5 (2.3-30.4)	28.1 ± 6.9 (13.4-40.9)	59.4	40.6
CTEN*	3	W	AS	21.7 ± 10.8 (4.6-46.0)	33.7 ± 17.2 (5.9-71.8)	44.6 ± 14.8 (14.2-72.8)	21.7	78.3
	8	S	AS	42.8 ± 7.5 (25.1-55.7)	14.2 ± 10.5 (2.0-42.2)	43.0 ± 10.5 (20.2-62.0)	42.8	57.2
CVOL	3	W	ES	36.4 ± 16.8 (6.8-72.4)	39.8 ± 21.6 (5.4-83.7)	23.8 ± 15.8 (2.8-59.4)	36.4	63.6
	5	S	ES	41.8 ± 12.1 (14.7-66.1)	39.2 ± 17.9 (6.7-76.5)	19.0 ± 11.7 (2.4-44.6)	41.8	58.2
GUMB	35	W	ES	3.2 ± 2.0 (0.6-8.2)	41.7 ± 4.9 (31.6-50.7)	55.1 ± 4.6 (46.5-64.8)	3.2	96.8
	30	S	ES	2.8 ± 1.8 (0.5-7.5)	25.6 ± 6.3 (12.0-36.6)	71.6 ± 6.2 (60.7-85.5)	2.8	97.2
GVUL*	16	W	ES	4.1 ± 2.7 (0.8-11.0)	42.7 ± 8.8 (23.1-58.7)	53.2 ± 8.5 (38.0-72.0)	4.1	95.9
	18	S	ES	4.4 ± 2.3 (1.0-10.0)	56.1 ± 9.0 (36.1-71.8)	39.5 ± 8.5 (24.5-58.4)	4.4	95.6
LLIT	13	W	ES	9.3 ± 6.6 (1.5-26.4)	55.8 ± 9.4 (35.5-72.9)	34.9 ± 7.1 (21.2-49.2)	9.3	90.7
	10	S	ES	8.0 ± 5.2 (1.3-20.8)	28.0 ± 10.1 (8.2-46.9)	64.0 ± 9.2 (47.7-83.5)	8	92
MGIG*	21	W	ES	38.2 ± 3.6 (31.1-45.3)	17.9 ± 6.1 (6.6-29.8)	43.9 ± 4.2 (35.5-52.2)	38.2	61.8
	3	S	AS	34.8 ± 12.7 (8.2-58.8)	26.4 ± 16.2 (3.9-65.0)	38.8 ± 13.7 (11.0-65.8)	34.8	65.2
	32	S	ES	50.0 ± 2.8 (44.5-55.4)	8.6 ± 3.9 (2.3-17.3)	41.4 ± 3.2 (34.8-47.4)	50	50

MFRA*	5	S	AS	27.5 ± 8.6 (9.8-44.1)	28.0 ± 13.9 (5.9-58.8)	44.5 ± 10.4 (21.3-62.9)	27.5	72.5
MPAL	16	W	ES	52.2 ± 4.0 (44.1-59.9)	10.7 ± 5.4 (2.4-23.2)	37.1 ± 4.6 (27.6-45.4)	52.2	47.8
	4	S	ES	60.7 ± 23.3 (10.8-93.2)	19.7 ± 16.9 (1.9-65.4)	19.6 ± 13.9 (2.0-51.5)	60.7	39.3
PCUL	19	W	ES	7.9 ± 3.7 (1.9-16.1)	15 ± 6.8 (3.3-29.1)	77.1 ± 5.7 (65.6-88.1)	7.9	92.1
	9	S	ES	19.5 ± 8.8 (3.8-38.4)	10.4 ± 7.5 (1.6-28.9)	70.1 ± 10.2 (47.0-86.8)	19.5	80.5
PPLA*	33	W	ES	50.1 ± 5.9 (38.1-61.8)	44.3 ± 7.1 (30.0-57.8)	5.6 ± 2.7 (1.3-11.6)	50.1	49.9
	51	S	ES	59.8 ± 4.5 (50.9-68.4)	25.8 ± 5.9 (13.8-37.4)	14.4 ± 3.3 (7.9-20.8)	59.8	40.2
SALV*	40	W	ES	24.1 ± 2.6 (18.8-29.2)	28.0 ± 4.7 (19.1-37.6)	47.9 ± 3.2 (41.8-54.0)	24.1	75.9
	54	S	ES	24.8 ± 2.2 (20.4-29.2)	35.2 ± 3.8 (27.6-42.6)	40.0 ± 2.6 (34.9-45.1)	24.8	75.2
SLAM	4	W	AS	46.5 ± 12.4 (15.8-67.9)	21.7 ± 13.7 (3.2-54.7)	31.8 ± 11.2 (9.4-54.0)	46.5	53.5
	7	W	ES	57.9 ± 10.2 (31.9-73.8)	12.7 ± 8.9 (1.9-35.1)	29.4 ± 10.4 (9.1-52.0)	57.9	42.1
	3	S	AS	49.2 ± 21.2 (7.4-83.1)	22.3 ± 15.9 (2.7-63.8)	28.5 ± 16.7 (3.7-65.3)	49.2	50.8
	8	S	ES	52.0 ± 16.0 (15.8-74.7)	11.8 ± 8.3 (1.7-32.9)	36.2 ± 15.7 (9.5-67.0)	52	48

Sea: season, CEDU: *Cerastoderma edule*, CFOR: *Crepidula fornicata*, LCON: *Lanice conchilega*, LLEV: *Lekanesphaera levii*, LBAL: *Limecola balthica*, McfGAL: *Mytilus* cf. *galloprovincialis*, RPHI: *Ruditapes philippinarum*, SSOL: *Spisula solida*, VCOR: *Venerupis corrugata*, AALB: *Abra alba*, CALA: *Caulleriella alata*, GZAD: *Gammarus zaddachi*, MTEN: *Macomangulus tenuis*, NLAT: *Notomastus latericeus*, SARM: *Scoloplos armiger*, UROsp: *Urothoe* sp., ACHspp: *Achelia* spp., CTEN: *Cirriformia tentaculata*, CVOL: *Corophium volutator*, GUMB: *Gibbula umbilicalis*, GVUL: *Golfingia vulgaris*, LLIT: *Littorina littorea*, MGIG: *Magallana gigas*, MFRA: *Mediomastus fragilis*, MPAL: *Melita palmata*, PCUL: *Perinereis cultrifera*, PPLA: *Porcellana platycheles*, SALV: *Sabellaria alveolata*, SLAM: *Spirobranchus lamarckii*.

Chapter III

The third chapter of this manuscript focuses on the evaluation for engineered sediments of key processes taking place in benthic ecosystems: biogeochemical fluxes and how these fluxes are linked to diversity changes taking place in more or less disturbed engineered sediments. This chapter is composed of one article ready to be submitted to Oikos.

The different biogeochemical fluxes (sediment oxygen demand, ammonium, nitrates and nitrites) were higher in the engineered sediments compared to non-engineered soft sediments, stressing the high functional value these habitats have in term of organic matter and nutrient cycling. These fluxes are mainly driven by the engineer via its abundance and biomass, conforming to the mass-ratio hypothesis. Notwithstanding, the use of functional diversity indices indicated a complementary diversity effect on the biogeochemical flxues observed with the functional dispersion index. In the end, the global biogeochemical functioning of the engineered sediments is maximal at intermediate disturbance levels.

Article 4 - Linking multiple facets of biodiversity and ecosystem function in a coastal engineered habitat

Auriane G. Jones [a,b,c], Lionel Denis[d], Jérôme Fournier [d,e], Nicolas Desroy [b], Gwendoline Duong [d], Stanislas F. Dubois [a]

Article ready to be submitted to Oikos

[a] IFREMER, Centre de Bretagne, DYNECO, Laboratoire d'Ecologie Benthique Côtière (LEBCO), 29280 Plouzané, France

[b] IFREMER, Laboratoire Environnement et Ressources Bretagne nord, 38 rue du Port Blanc, BP 80108, 35801 Dinard cedex, France

[c] CNRS, UMR 7208 BOREA, 61 rue Buffon, CP 53, 75231 Paris cedex 05, France

[d] Univ. Lille, CNRS, Univ. Littoral Côte d'Opale, UMR 8187, LOG, Laboratoire d'Océanologie et de Géosciences, F 62930 Wimereux, France

[e] MNHN, Station de Biologie Marine, BP 225, 29182 Concarneau cedex, France

1. Introduction

In the context of global change, terrestrial and aquatic systems are experiencing high rates of biodiversity loss and species composition changes (Sala et al. 2000, Hooper et al. 2005). The increasing awareness of the global scientific community on this exceptional biodiversity erosion, triggered in the 1990's a new line of work investigating the links between biodiversity and ecosystem functioning, known today as BEF studies (Schulze and Mooney 1994, Kunin and Lawton 1996). Focusing first on terrestrial autotrophic ecosystems, numerous work found that a decline in plant species richness lead to a decrease in functions like carbon and nutrient cycling, or production and decomposition (Balvanera et al. 2006, Cardinale et al. 2011). Nonetheless, species richness is not the unique driver of ecosystem functioning and the diversity of functions performed by the species, termed functional diversity, is also key in explaining the relationship between diversity and ecosystem functioning (Hooper et al. 2005, Díaz et al. 2007, Cadotte et al. 2011). Indeed, Mouillot et al. (2011) demonstrated that functional identity of species and functional diversity among grassland species, rather that species diversity per se, together promote key ecosystem functions such as decomposition and primary productivity.

In marine systems, biogeochemical fluxes are important ecosystem functions directly linked to processes such as organic matter mineralization and nutrient cycling. Sediments play a crucial role in these processes along with a range of benthic organisms from bacteria to macrofauna, which regulate them (Bolam et al. 2002, Stief 2013). More specifically, biogeochemical fluxes are influenced by benthic macrofauna able to rework sediments (bioturbation) and/or to transfer solutes (bio-irrigation) (Kristensen 1988, Aller and Aller 1998, Austen et al. 2002). When sediment-reworking species are present in important densities like in the case of fiddler crabs *Uca* spp. (Bertness 1985, Kristensen 2008), they are known as allogenic engineers (Jones et al. 1994) because they modify the resource - here the sediment - via their biological activity (*e.g.* feeding, burrowing and ventilation activities). As defined by (Jones et al. 1994), autogenic engineers "change the environment via their own physical structures" and common examples include forest trees or bog moss (Tansley 1968, Hedin et al. 1988, Jones et al. 1994). All these ecosystem engineers have the ability to maintain, modify, create or even destroy habitats (Jones et al. 1994, 1997, Bouma et al. 2009). These biogenic habitats are particularly present in the intertidal zone across the planet (Jones et al. 1997) and a wide range of organisms, like mollusks (*e.g. Crassostrea virginica, Modiolus modiolus(Kent et al. 2017)*), polychaetes (*e.g. Lanice conchilega, Phragmatopoma caudata*), cnidarians (*e.g.* scleractinian corals), algae (*e.g.* Laminariales) and plants (*e.g. Zostera marina*), can build such biogenic habitats (Goldberg 2013). In these habitats, local pressures such as predation and thermal stress are reduced, leading to the establishment of a high diversity of species (Jones et al. 2018). In the end, a particular context arises where the ecosystem engineer represents a very large part of the total abundance and biomass and at the same time, the local biodiversity is higher than in neighboring non engineered sediments (Jones et al. 1997, Bouma et al. 2009). In aquatic ecosystems, studies on the link between biodiversity and biogeochemical fluxes have

generally focused on soft sediment macrofauna and on the functional identity of bioturbating species in controlled experiments, often using densities much higher than observed *in situ* (Waldbusser et al. 2004, Mermillod-Blondin et al. 2005, Michaud et al. 2005, 2006, Ieno et al. 2006, Braeckman et al. 2010). These mesocosm experiments have the disadvantage of only representing a very small part of the actual biodiversity present in the studied sediment type, thus limiting interspecific interactions. In addition, since they are time-limited, processes such as environmental sorting or niche filtering cannot take place (Gamfeldt et al. 2015). In this context, observational studies can provide a complementary view on biodiversity-function relationships at larger spatial scales (Gamfeldt et al. 2015). Our aim was to start bridging this gap in the particular context of ecosystem engineering by reef-building macrofauna. Indeed, such correlational studies are particularly interesting in biogenic habitats where natural species richness gradients occur, but where the system is also dominated by one species, allowing scientists to investigate how these ecosystem engineers and their associated fauna considered in terms of identity and biological traits, influence a number of functions like biogeochemical fluxes.

Sabellaria alveolata - a.k.a. the honeycomb-worm - is an intertidal ecosystem engineer commonly found along the European Atlantic coast (Muir et al. 2016). This species is a gregarious polychaete that lives in a tube it builds using mainly bioclastic particles (Le Cam et al. 2011). When environmental conditions are favorable, *S. alveolata* can either form veneers on rocky substrates or reefs on sandflats (Gruet 1972, Holt et al. 1998, Dubois et al. 2002). In either case, these structures add three dimensional complexity to the original substrate (Noernberg et al. 2010), where many organisms can find food and shelter in holes, ponds and crevices engineered during the dynamic of the *S. alveolata* bioconstructions. Consequently, a very abundant and diverse reef-associated macrofauna community occurs in these biogenic habitats (Dias and Paula 2001, Dubois et al. 2002, Porta and Nicoletti 2009, Jones et al. 2018). *S. alveolata* reefs undergo natural cycles of growth and decline (Gruet 1972) forced by recruitment (Dubois et al. 2007a, Ayata et al. 2009), inter-specific competition (Dubois et al. 2007b, Dubois and Colombo 2014), bioclastic particle availability (Le Cam et al. 2011), sediment movements (Noernberg et al. 2010), low temperatures and strong hydrodynamic forces (storms and tidal currents) (Gruet 1986, Holt et al. 1998). Superimposed onto these natural cycles are a number of anthropogenic direct and indirect disturbances like trampling, coastal modifications and shellfish farming (Dubois et al. 2002, 2006a, Desroy et al. 2011, Plicanti et al. 2016). These growth and decline cycles are visible through morphological modifications of the reef's physical structure and changes in the associated fauna in terms of richness, abundance and composition (Dubois et al. 2002). Many studies have looked into the macrofauna inhabiting these reefs (Gruet 1986, Dias and Paula 2001, Porta and Nicoletti 2009, Schlund et al. 2016) and into the impacts of natural and anthropogenic disturbances on the associated fauna (Dubois et al. 2002, Plicanti et al. 2016, Jones et al. 2018), but to our knowledge very few studies have evaluated functions and processes performed by these biogenic habitats (Fournier et al. 2010).

In this context, different realized functions (*e.g.* sediment oxygen demand, total ammonium fluxes, nitrate and nitrite fluxes) were measured inside a *S. alveolata* reef and in control soft sediments.

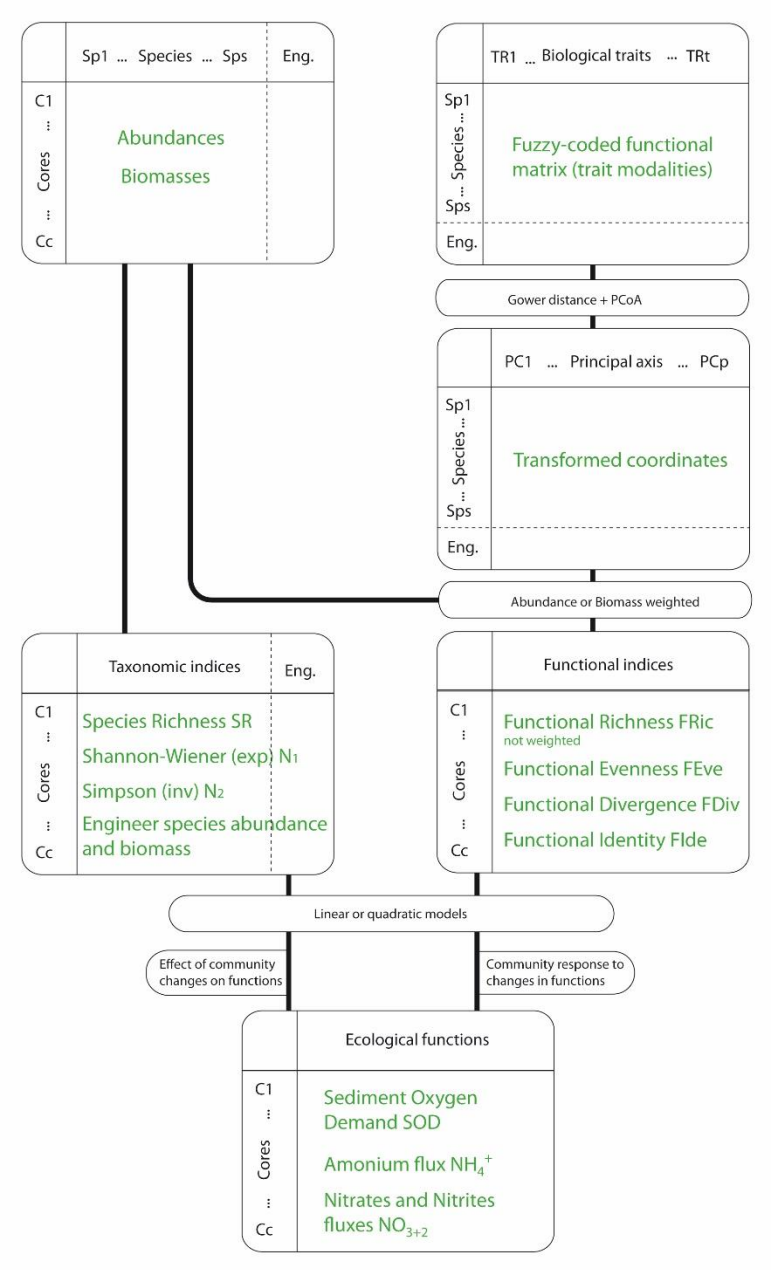

Figure 29. Conceptual framework to study the link between different facets of biodiversity and ecological functions in the context of a community influenced by an ecosystem engineer (Eng.). The link between biodiversity and measured functions can be seen both ways, either focusing on the effect of community changes on ecological functions or focusing on community response to changes in functions. In this article, the focus was made on how community changes in terms of taxonomic and functional changes can effect measured functions such as biogeochemical fluxes. Different taxonomic indices based on the identity of organisms were computed (species richness (SR), exponential of Shannon-Wiener (N1), inverse of Simpson's diversity (N2), engineer species abundance, biomass and mean biomass, associated fauna abundance, biomass and mean biomass) along with functional indices based on the species' biological traits (functional richness (FRic), functional evenness (FEve), functional divergence (FDiv), functional dispersion (FDis), functional identity (FIde)). All the functional indices (except functional richness) along with N1 and N2 were weighted by abundance or biomass. Figure adapted from Villéger et al. (2008).

Such measured functions are classically used to characterize an ecosystem, as done by Kellogg et al. (2013) in the context of a biogenic habitat. Then, using linear models, these realized functions were linked to a set of functional diversity and identity indices computed using the macrofauna associated with the reef, a functional approach more and more used to understand the impact of a disturbance on a system (Bremner 2008, Villéger et al. 2010). With this framework (Figure 98), we investigated the link between "theoretical" functional diversity estimated with synthetic indices based on biological traits and used as proxy of functions (Bremner 2008, Villéger et al. 2008) and measured ecosystem functions, a combined approach rarely investigated in the marine realm (Thrush et al. 2017).

2. Material and methods

2.1. Study area

The Mont-Saint-Michel Bay (MSMB) is a large macrotidal bay (about 500 km², 15.5 m maximal tidal range) located in the English Channel between Brittany and Normandy. In its central part is located the largest bioconstruction in Europe: the Sainte-Anne reef (48°38'700N and 1°40'100W) built by the gregarious polychaete worm *S. alveolata* (Gruet 1972, Holt et al. 1998). These fairly common biogenic reefs are mainly present in the intertidal zone from Scotland to Morocco (Muir et al. 2016) and they reach their maximal extension in the MSMB (France), located at a median latitude of their Atlantic distribution. Most *Sabellaria* reefs are present as hummocks or veneers on rocky shores and the Sainte-Anne reef is one of the rare reefs present on soft sediments (Holt et al. 1998). Consequently, the Sainte-Anne reef is formed by the actual structures built by the honeycomb-worm (engineered sediment, 32 ha) and by soft sediments present around these engineered structures (associated sediments, 128 ha). The Sainte-Anne reef, our study site, is located in the lower intertidal zone (between the -2 and -4 m isobaths), parallel to the coast and to the dominant tidal currents and about 3 km from the shoreline (Dubois et al. 2006a, Noernberg et al. 2010). This part of the MSMB is characterized by a high rate of bioclastic sediments (25% to 95%) presenting a decreasing medium grain size from the subtidal to the intertidal zone (Bonnot-Courtois et al. 2004, 2008). Natural and anthropogenic disturbances such as winter storms, tidal currents, trampling and mussel cultures, directly and indirectly affect the Sainte-Anne reef causing morphological modifications of the engineered sediment. This disturbed engineered sediment is characterized by a lower height, a higher fragmentation, a higher epibiont cover (*e.g. Ulva* spp. and *Magallana gigas*, formerly known as *Crassostrea gigas*) and a higher silt content (Dubois et al. 2002, 2006a, Desroy et al. 2011).

2.2. Field sampling and experimental set-up

To investigate the changes in the benthic biogeochemical fluxes linked to the presence of a *S. alveolata* reef, three sampling campaigns were carried out in spring (April 2015), summer (September 2015) and winter (February 2016). During each campaign, four stations were sampled; two control soft

sediment stations characterized by coarse sediment (CS) and muddy sediment (MS) and two engineered sediment stations located in an undisturbed section of the reef (UES) and in a disturbed section of the reef (DES). First, during high tide, bottom water was sampled close to the Sainte-Anne reef using inflatable bags (avoiding bubbles, total volume: 40L) which were brought back to the laboratory and placed in a dark room at *in situ* water temperature. Then at each station, four replicate cores were taken at low tide *(i.e.* total of 16 cores sampled during each sampling campaign). The engineered sediment cores were collected using a toothed metal corer (15 cm diameter) and then transferred into 35 cm-long perspex tubes of the same diameter as the corer. The control soft sediment cores were directly collected using the Perspex tubes. The tubes containing the cores were sealed, transported to the laboratory and placed inside a dark refrigerated room. After filling the Perspex tubes with bottom water previously sampled, incubations started ca. 2 hours after the sampling. During the incubations, the room temperature was similar to the *in situ* water temperature (8°C in winter, 12°C in spring and 17°C in summer).

The incubation set up was identical to the one previously detailed in Denis et al. (2001). In summary, just before the incubation started, the Perspex tubes were filled with bottom water, quickly sealed with caps equipped with small magnetic stirrers. Then, each core was connected by a tube to the inflatable reserve tank containing bottom water and every time overlaying water was sampled from a core, it was replaced by the same quantity of water from the reserve tank (*in situ* water was collected at high tide for this purpose). During an incubation period ranging from 3 to 15 hours (depending on the rate of oxygen depletion), the water overlying each core and the control water from the reserve tank were sampled 6 to 8 times using a 60 ml plastic syringe. These water samples were used to determine the oxygen, ammonium, nitrate and nitrite concentrations. The difference between concentration changes in the overlying water of each core and control bottom water allowed the calculation of sediment-water fluxes.

2.3. Flux measurements and calculations

The required volume for oxygen determination was gently transferred with a tubing from the syringe into a 10 ml glass flask, allowing overflow from the flask and avoiding air bubbles. Oxygen concentrations were measured using an oxygen Clark-type microsensor (Revsbech 1989) characterized by a 90% response time of <8s, a stirring sensitivity of <1.5% and a current drift of <1% h^{-1} (Unisense A/S, Aarhus, Denmark, 100µm tip diameter). Linear two-point calibration of each microelectrode was systematically performed before and after each series of measurements. Zero oxygen current was measured in the anoxic zone of an additional sediment core with fine muddy sediments while a 100% oxygen level was calibrated using air-bubbled water.

The remaining volume in the syringe was filtered through GF/F Whatman glass fiber filters and transferred into a 20ml polyethylene flask for ammonium analysis and a 10ml polyethylene tube for nitrate and nitrite analysis. Ammonium analyses were immediately carried out according to the

indophenol-blue method of (Solórzano 1969). Samples for the analysis of nitrate and nitrite were frozen for later analysis using a Seal autoanalyzer following the protocol of (Tréguer and Le Corre 1975). Fluxes were determined by regressing the change in overlying water concentration versus time. Non-significant regressions (Pearson correlation, $p > 0.05$) based on changes over time that were less than the analytical variability, were interpreted as zero fluxes. For all fluxes, a correction for water replacement was systematically applied. A multifunctionality variable was calculated for each engineered sediment core as the mean of the four fluxes after standardizing (mean of 0 and standard deviation of 1) each measured flux in order to give them the same weight (Mouillot et al. 2011).

2.4. Macrofauna

At the end of the incubation period, all engineered and soft sediment cores were fixed in a 5% formaldehyde solution and sieved through a 1-mm square mesh. The macrofauna was sorted, counted and identified to the species or genus level (except for Nemerteans, Nematodes and Tubificoides. For each core and for each taxonomic group, the abundance and the ash-free dry weight (AFDW – 4 hours at 550°C) were measured. Then, the fluxes, abundances and biomasses were standardized for a 1 m² surface. In the end, incubated cores by species matrixes were obtained for each sampling period using either abundance or biomass. The macrofauna was first considered on an identity basis using a set of taxonomic diversity indices, as detailed in Gray (2000); species richness (SR), exponential of Shannon-Wiener calculated using either the abundance ($N1_{ab}$) or the biomass ($N1_{biom}$) and the inverse of Simpson's diversity calculated using either the abundance ($N2_{ab}$) or the biomass ($N2_{biom}$). *S. alveolata* abundance ($SALV_{ab}$), biomass ($SALV_{biom}$) and mean biomass ($SALV_{mean\ biom}$) along with the associated fauna abundance (ASS_{ab}), biomass (ASS_{biom}) and mean biomass ($ASS_{mean\ biomass}$) were also calculated.

The species were then considered on a biological traits basis using a functional diversity approach. Biological traits can be of two types: effect or response traits. Effect traits are defined as determining an ecosystem function or process while response traits are defined as responding to environmental factors such as resources or disturbances (Lavorel and Garnier 2002). Since our goal was to investigate the link between functional macrofauna diversity and a specific function, here biogeochemical fluxes, we chose to consider five categorical traits (divided into modalities) that directly or indirectly determine the specific investigated function through processes like respiration, excretion or organic matter remineralization (Table 19). In order to take into account the intraspecific variability of the species for some traits like feeding mode (*e.g. Carcinus maenas* can be a grazer and a predator-scavenger), all the categorical traits were fuzzy coded (Chevenet et al. 1994). Each modality of a given trait is therefore assigned a value between 0 and 3, with 0 meaning no affinity of the species for the modality, 1 or 2 meaning an intermediate affinity and 3 meaning a strict affinity. The sum of the values attributed to all the modalities of a given trait were always equal to 3 except for the tidal position where it could be equal to 4 if the species had an equal affinity for intertidal (modality value = 2) and subtidal (modality value = 2). Furthermore, the two main components of the bioturbation potential defined by

(Queirós et al. 2013) were used: mobility and sediment reworking. Indeed, transferring bioturbation potential across space and time is only possible if the species body size is constant (Queirós et al. 2013) and it is not the case since macrofauna species were sampled over 3 seasons. Furthermore, reworking and mobility are both influenced by habitat structure as shown by Godbold et al. (2011), rendering the use of bioturbation potential inappropriate. A large part of the information on polychaete feeding mode and daily adult movement capacity was recovered from Fauchald and Jumars (1979) and Jumars et al. (2015), while the rest was found in peer-reviewed journals (Navarro-Barranco et al. 2013, Guerra-García et al. 2014), or biological trait databases (Biotic, Genus trait handbook).

Table 19 Biological traits used to calculate the functional diversity indices. For each trait, are indicated: the different modalities, the relevant definitions, the associated functions and processes and a selection of bibliographic references either on the actual trait or on the link between the trait and the associated functions and processes.

Trait	Modalities	Definition	Functions and processes	References
Maximum size	<10 [10-50[[50-100[[100-200[>200	Maximum size recorded in the litterature (mm)	respiration, excretion, carbon degradation	(Shumway 1979, Thrush et al. 2006)
Daily adult movement capacity	None Low Medium High	No movement 0-10 m daily 10-100 m daily >100 m daily	respiration, excretion, anaerobic mineralization, organic matter remineralization	(Solan et al. 2004, Queirós et al. 2013)
Sediment reworking	EpiF SurMod UpDown BioD ReG	Epifauna Surficial modifiers Upward and downward conveyors Biodiffusors Regenerators	anaerobic mineralization, organic matter remineralization	(Solan et al. 2004, Thrush et al. 2006, Janson et al. 2012, Queirós et al. 2013)
Feeding mode	SusP SurF SubS PreDScaV GraZ	Suspension feeder Surface deposit feeder Sub-surface deposit feeder Predator-scavenger Grazer	respiration, excretion, carbon degradation	(Shumway 1979, Thrush et al. 2006, Janson et al. 2012)
Bathymetric level	InterT SubT	Intertidal species Subtidal species	informs indirectly on the engineered sediment's thermal properties which can influence bacterial biogeochemical processes	(Gutiérrez and Jones 2006)

The biological traits matrix defined for all the species identified in the engineered sediment (all three seasons) was used to calculate the functional distances between species using Gower distance (Laliberté and Legendre 2010, Mouillot et al. 2014). A principal coordinate analysis (PCoA) was then performed on the functional distance matrix leading to the representation of each species in a multidimensional functional space, each dimension being a combination of traits. Finally, several functional indices were calculated for each core. We used four functional diversity indices (Table 20): functional richness (FRic, Villéger et al. 2008, Laliberté and Legendre 2010), functional evenness (FEve, Villéger et al. 2008, Laliberté and Legendre 2010), functional divergence (FDiv, Villéger et al. 2008) and functional dispersion (FDis, Laliberté and Legendre 2010). We also calculated the functional identity (Mouillot et al. 2013a) measured on the first four PCoA axis (FIde1 FIde2, FIde3 and FIde4, see Table 20 for details). We weighted all the aforementioned indices, except functional richness, using relative abundance (ab in subscript, *tal.* $FEve_{ab}$) or relative biomass (biom in subscript, *tal.* $FEve_{biom}$) and *S. alveolata* was always included in the data sets used to calculate the different indices. Functional divergence was calculated using the first four axes of the PCoA while functional evenness and functional dispersion were calculated using all the PCoA axis (here 31 axis). Functional richness is measured as the convex hull volume (Laliberté and Legendre 2010) and standardized by the 'global' functional richness (including all species recorded in the engineered sediment) in order to constrain it between 0 and 1 (Table 20, Laliberté and Legendre (2010)). Functional divergence represents the changes in the proportion of total abundance or biomass that is supported by species with the most extreme functional traits. Functional evenness measures how regularly is spaced the relative abundances and biomasses in the functional space. Finally, functional dispersion is calculated as the weighted average distance to the weighted average mean trait values of the community. If a species is very dominant in abundance or biomass, then the weighted average mean trait value will be very close to this species' position in the functional space and consequently the functional dispersion will be small. Since functional evenness and dispersion are calculated using all the dimensions of the functional space, they give an integrated view of the community in terms of functioning. The different R functions and packages used to calculate each functional index are presented in Table 20.

2.5. Statistical analysis

To investigate how the three seasons, the four stations and their interaction affected the functions (*i.e.* sediment oxygen demand (SOD), ammonium fluxes (NH_4^+) and nitrates + nitrites fluxes (NO_{2+3})), permutational multivariate analysis of variance (PERMANOVA) with a two-way crossed balanced design (9999 random permutations) were performed using the PRIMER v6 software with the PERMANOVA+ add-on (Anderson et al. 2008). Sediment type was considered as a fixed factor. If the interaction factor was significant for a flux, then pairwise tests were performed to disentangle the seasonal effect according to each station and the spatial effect according to each season.

Table 20 Functional indices (diversity and identity) used in this study with the corresponding abbreviation and definition. For each index, we indicated the type of data used to compute the index, if it is weighted by relative abundance or biomass or unweighted, the reference papers where the mathematical formulas can be found and the R functions and packages that can be used to compute the indices. The multidimFD function is available as a supplementary material in (Mouillot et al. 2013a). The * indicates the packages used in this study.

Functional indices	Name	Definition	Type of data used to compute the index	Unweighted or weighted	Key references	R function and packages
Functional identity	FIde	Weighted average position in the functional space	All the PCoA axes	Weighted by relative abundance or biomass	(Mouillot et al. 2013a)	multidimFD
Functional richness	FRic	Volume of multidimensional space filled by all species in a community within the functional space	Number of PCoA axes such as number of species > number of traits	Unweighted	(Villéger et al. 2008, Laliberté and Legendre 2010)	dbFD (FD package) * or multidimFD
Functional dispersion	FDis	Weighted average distance to the weighted average mean trait values of the community	Uncorrected species-species distance matrix	Weighted by relative abundance or biomass	(Laliberté and Legendre 2010)	dbFD
Functional divergence	FDiv	Proportion of total abundance or biomass supported by species with the most extreme trait values within a community – weighted average deviation of the Euclidian distance between the position of all the species in the functional space and the center of gravity of the vertices of the convex hull (unweighted center of gravity)	Number of PCoA axes such as number of species > number of traits	Weighted by relative abundance or biomass	(Villéger et al. 2008)	dbFD (FD package) * or multidimFD
Functional evenness	FEve	Regularity of abundance or biomass distributions in the functional space along the shortest minimum spanning tree linking all the species	All the PCoA axes	Weighted by relative abundance or biomass	(Villéger et al. 2008, Laliberté and Legendre 2010)	dbFD

According to Clough et al. (2005), macrofauna-normalized respiration (mmol $O_2.m^{-2}.g\ AFDW^{-1}$) was calculated for each incubated core by dividing the daily oxygen consumption measured for each core by the total macrofauna biomass present in the core. This value is indicative of the proportional effects of macro vs meio and microfauna processing of organic matter in the sediment. A value inferior to 1 indicates processes are predominantly driven by macrofauna while a value superior to 1 indicates processes are predominantly meio and microfauna driven.

Our aim was to understand which component(s) of the macrofauna (engineer species, associated fauna, taxonomic diversity, functional diversity and functional identity) explained the three fluxes and the multifunctionality variable. Relation between the four ecosystem functions (SOD, NH_4^+, NO_{2+3}, multifunctionality) and a set of explanatory variables composed of all the taxonomic and functional estimates previously described were first tested with simple linear regressions where each incubated core was considered as an independent replicate since different cores were taken at each season. All the taxonomic diversity indices along with the *S. alveolata* and associated fauna abundance, biomass and mean biomass were fourth-root transformed in order to meet homogeneity of variances hypothesis (Levene's test). The linear model assumptions were verified by inspection of residual distribution plots and normality of residuals was verified using the Shapiro-Wilks test. Visual inspections of plots of the fluxes against all the different explanatory variables led us to further test second degree polynomials leading to different functional forms (linear, convex and concave) (Thrush et al. 2017). A significance level of 0.05 was considered for all the tests.

3. Results

3.1. Effects of season and sediment type on the different fluxes

All the incubations resulted in a significant oxygen consumption by the soft sediment (SS) and the engineered sediment (ES) (Kruskal-Wallis, $p < 0.05$). Several cores did not show fluxes significantly different from zero (NH_4^+: two spring CS cores, for the nitrates, the four summer MS cores and for the nitrites, two spring MS cores, one summer MS core and one summer CS core). The results of the whole core incubations for the SOD, NH_4^+ fluxes and NO_{2+3} fluxes are presented in Table 21. The results of the two-way crossed PERMANOVA are presented in Table 22a and Table 22b. Sediment oxygen demand, NH_4^+ fluxes and NO_{2+3} fluxes were all three significantly different according to season ($p < 0.05$), station ($p < 0.05$) and the interaction between season and station ($p < 0.05$).

SOD ranged from a minimum of $105 \pm 33\ \mu mol.m^{-2}.h^{-1}$ in winter for the CS cores to a maximum of $10309 \pm 1939\ \mu mol.m^{-2}.h^{-1}$ in spring for the DES cores. Whatever the season, the ES cores had an SOD between 4 and 25 times that of the SS cores, with the MS cores having a higher SOD than the CS cores in spring and summer. Furthermore, for the two SS stations and for the DES station, the spring SOD was significantly higher than the summer and winter ones. In the case of the UES station, the spring and summer SOD were significantly higher than the winter ones.

Table 21 Mean (± SD, n = 4) sediment oxygen demand (SOD), total ammonium fluxes (NH_4^+) and the sum of nitrate and nitrite fluxes (NO_{2+3}) measured during the spring, summer and winter campaigns for the four different sediment types.

	Spring				**Summer**				**Winter**			
	CS	*MS*	*UES*	*DES*	*CS*	*MS*	*UES*	*DES*	*CS*	*MS*	*UES*	*DES*
SOD	414.74 ±	1445.44 ±	8032.65 ±	10308.92 ±	181.09 ±	693.80 ±	4294.58 ±	3083.76 ±	105.25 ±	178.47 ±	1276.05 ±	843.85 ±
(µmol.m^{-2}.h^{-1})	60.19	238.51	2426.51	1939.11	45.57	144.00	1259.16	718.79	33.26	62.86	166.90	429.31
NH_4^+	-0.82 ±	-2.40 ±	850.40 ±	653.86 ±	-4.36 ±	42.40 ±	698.25 ±	249.74 ±	-7.92 ±	32.83 ±	252.67 ±	65.26 ±
(µmol.m^{-2}.h^{-1})	1.00	0.62	121.79	269.02	1.22	67.25	359.19	49.08	1.28	8.81	62.06	31.03
NO_{2+3}	25.97 ±	-43.66 ±	381.87 ±	534.23 ±	35.60 ±	0.20 ±	1006.93 ±	322.81 ±	114.17 ±	42.78 ±	284.92 ±	170.57 ±
(µmol.m^{-2}.h^{-1})	13.44	20.30	108.61	166.24	8.79	0.75	463.81	89.03	51.34	17.27	14.16	64.29

CS: coarse sediments, MS: muddy sediments, UES: undisturbed engineered sediments and DES: disturbed engineered sediments.

Table 22 Results of the two-way crossed PERMANOVA on sediment oxygen demand (SOD), total ammonium fluxes (NH_4^+) and the sum of nitrate and nitrite fluxes (NO_{2+3}) according to the factors season and station and the interaction term season x station. Results of the (a) main test and (b) pairwise tests for the interaction term season x station according to pairs of level season and station. A significant level of 0.05 was considered.

(a)	**SOD**				**NH_4^+**				**NO_{2+3}**			
	df	*MS*	*Pseudo-F*	*P (perm)*	*df*	*MS*	*Pseudo-F*	*P (perm)*	*df*	*MS*	*Pseudo-F*	*P (perm)*
Season	2	8.23×10^7	81.95	**0.0001**	2	3.37×10^5	17.72	**0.0001**	2	1.45×10^5	6.41	**0.0021**
Station	3	6.91×10^7	68.83	**0.0001**	3	9.72×10^5	51.14	**0.0001**	3	8.09×10^5	35.89	**0.0001**
Season x Station	6	2.10×10^7	20.95	**0.0001**	6	1.38×10^5	7.26	**0.0001**	6	2.07×10^5	9.17	**0.0001**
Residuals	36	1.00×10^6			36	1.90×10^4			36	2.25×10^4		

(b)		**SOD**	**NH_4^+**	**NO_{2+3}**
Season x station	*Spring*	(UES = DES) > MS > CS	(UES = DES) > (CS = MS)	(UES = DES) > CS > MS
	Summer	(UES = DES) > MS > CS	(UES = DES) > (CS = MS)	(UES = DES) > CS > MS
	Winter	(UES = DES) > (MS = CS)	UES > (DES = MS) > CS	UES > ((MS = CS = DES (> MS))
Station x season	*CS*	spring > (summer = winter)	spring > summer > winter	spring = summer = winter (> spring)
	MS	spring > summer > winter	spring = summer = winter (> spring)	winter > summer > spring
	UES	(spring = summer) > winter	winter = summer = spring (> winter)	winter = spring = summer (> winter)
	DES	spring > summer > winter	(spring = summer) > winter	winter = summer = spring (> winter)

CS: coarse sediments, MS: muddy sediments, UES: undisturbed engineered sediments and DES: disturbed engineered sediments

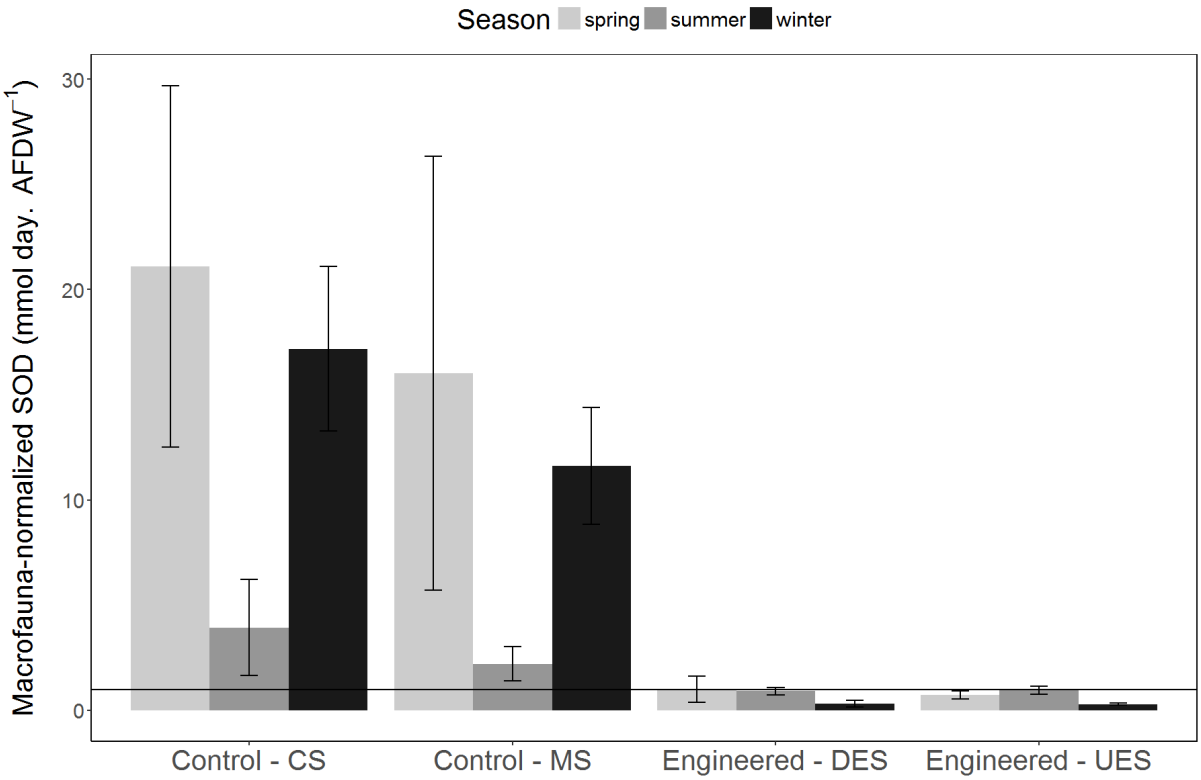

Figure 30. Macrofauna-normalized sediment oxygen demand (SOD) in mmol day.AFDWT^{-1} (mean ± SD, n = 4) calculated for each sediment type-season association. Sediment types include control coarse and muddy sediments (CS and MS respectively) and disturbed and undisturbed engineered sediment (DES and UES respectively). One winter coarse sediment core presenting a very high macrofauna-normalized SOD (140.5 mmol day.AFDW^{-1}) was removed to improve the readability.

Regarding the sediment type effect, the NH_4^+ fluxes presented a similar pattern to the one previously described for the SOD. For the seasonal effect, in spring, the SS cores presented negative NH_4^+ fluxes (*i.e.* from the water column into the sediment) while the ES cores presented fluxes around 700 µmol.m^{-2}.h^{-1}. In summer, the pattern was similar to spring, except the MS cores that presented positive NH_4^+ fluxes (42.40 ± 67.25 µmol.m^{-2}.h^{-1}). Finally, in winter the CS NH_4^+ fluxes were still negative but this time, the MS and DES NH_4^+ fluxes were not significantly different and were inferior to the UES ones. For the ES cores, the spring ammonium fluxes were always significantly higher than the winter ones and the summer fluxes were either similar to the spring ones (DES) or similar to the spring and winter ones (UES).

The NO_{2+3} fluxes were in a similar range as the NH_4^+ fluxes except for the CS cores that always presented positive NO_{2+3} fluxes. In spring and summer, the ES cores presented similar NO_{2+3} fluxes that were significantly higher than the soft sediment fluxes. In winter, only UES NO_{2+3} fluxes were higher than the three other sediment types. Except for MS cores, where a clear seasonal effect was visible (winter > summer > spring), the other sediment types presented similar NO_{2+3} fluxes between two seasons out of three.

Calculation of the macrofauna-normalized respiration for each incubated core (Figure 30) indicated that the oxygen fluxes measured in the soft sediment cores were under the control of the meio and microfauna (macrofauna-normalized respiration >> 1) rather than the macrofauna. Since we only had information on the macrofauna, the rest of the article focuses on the engineered sediments.

3.2. Functional diversity indices and functional identity

As an illustration, we calculated the different functional diversity and functional identity indices at the scale of a mean undisturbed and of a mean disturbed engineered core. Figure 31 illustrates the changes in the functional diversity metrics associated with these two "mean" engineered sediment types. In general, the functional richness was highest in the disturbed engineered sediments. Because of how the functional dispersion is measured (see section 2.4. and Table 20), if a species is very dominant in abundance or biomass (*e.g. S. alveolata* in an undisturbed engineered sediment), then the functional dispersion will be small (Figure 31: FDis for the UES). If another species is present, that is also dominant in terms of abundance or biomass, like the crustacean *Porcellana platycheles* in the DES cores, than the functional dispersion will increase and so on (Figure 31: FDis for the DES). Functional divergence was maximal (0.98 - 0.99) for various UES cores and decreased (< 0.8) for DES cores (Figure 30). In our case, functional evenness was not linked to the state of the engineered sediments and it was the only functional diversity index for which the index weighted by the biomass (range: 0.09-0.5) and the one weighted by the abundance (range: 0.4-0.8, Figure 31) were not significantly correlated ($p >$ 0.05). Functional identity was calculated for each selected PCoA axis (1 to 4), as the weighted average position in the functional space. In our case, the first PCoA axis was linked to movement capacity with negative values corresponding to species presenting none to low movement capacities and positive values corresponding to species presenting medium to high movement capacities (Figure 32). The second PCoA axis was linked to the sediment reworking trait with positive values corresponding to epifauna, intermediate values corresponding to biodiffusors and upward and downward conveyors and negative values corresponding to surficial modifiers. These two axis can also be considered in conjunction. In this case, negative values on the first axis associated with positive values on the second axis correspond to species presenting very similar characteristics to the ecosystem engineer regarding movement capacities and sediment reworking properties (Figure 32). Finally, the third axis can partially be linked to the feeding mode with positive values corresponding to predator-scavengers and values close to 0 corresponding to suspension feeders. Consequently, functional identity values on the first three PCoA axis are direct indications of which modalities are key in driving the different ecosystem processes.

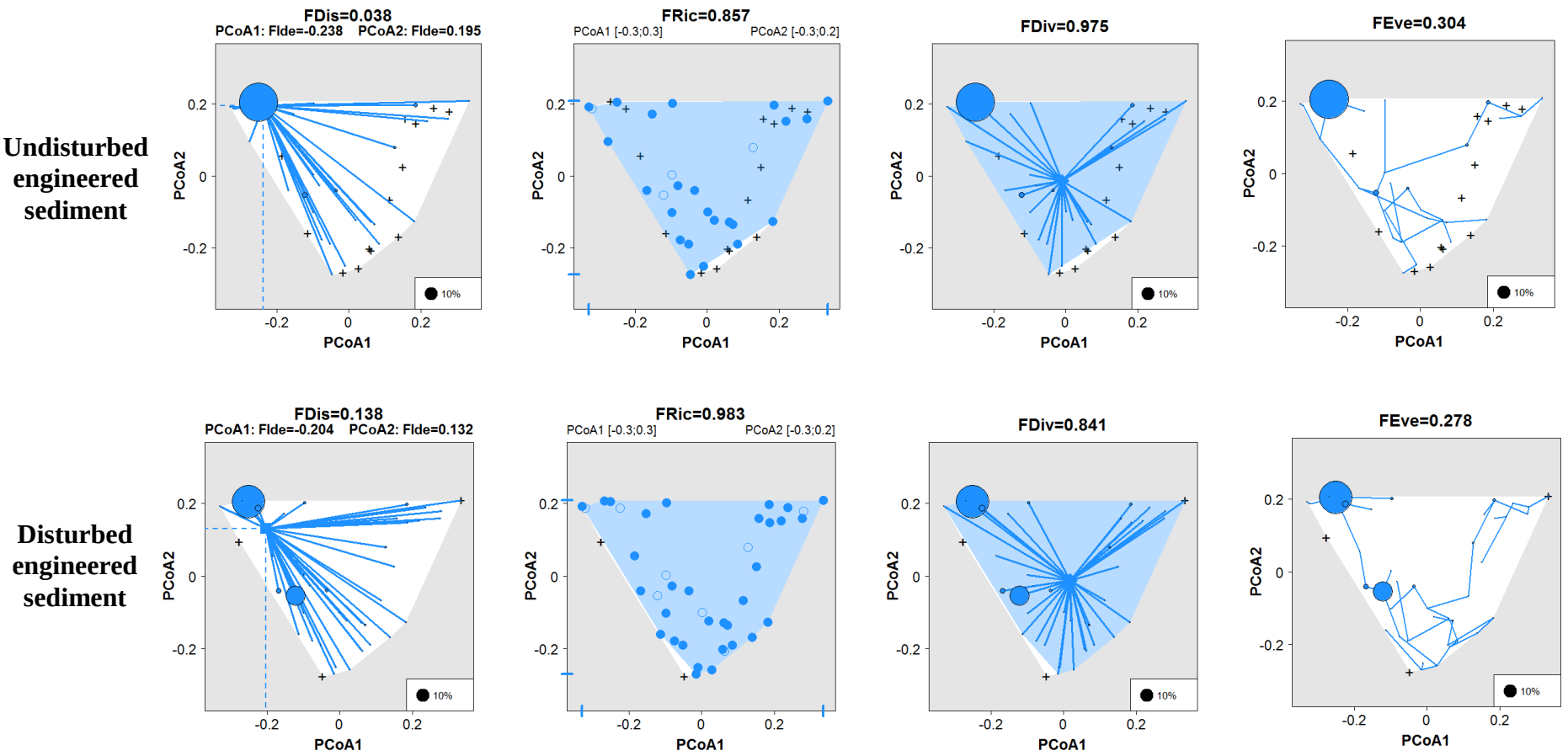

Figure 31. Two-dimensional (axis 1 and 2 of the PCoA) representation of the five functional diversity indices (Functional dispersion = FDis, functional identity = FIde, functional richness = FRic, functional divergence = FDiv, functional evenness = FEve) computed using all the species identified in the undisturbed (top) and disturbed (bottom) engineered sediment cores. Except for FRic, the dots represent the relative mean biomass of the recorded species. In the FDis panels, the square represents the weighted-mean position of the species in the multidimensional space. The vertical and horizontal dashed lines represent the weighted-mean positions of the species on the first and second PCoA axis respectively (Fide1 and Fide2). In the FRic panels, the colored convex polygon is a projection of the multidimensional convex hull in 2D and the filled symbols are species being vertices in the multidimensional space. The bold bars on the axis represent

the minimum and maximum values on each axis. In the FDiv panels, the diamond represents the center of gravity of the vertices and the lines represent all the distances to it. In the FEve panels, the blue lines represent the minimum spanning tree linking all species in the multidimensional space. Finally, the black crosses indicate species present in the global pool of species recorded at the engineered sediment level but absent at the sediment type level (UES or DES). Note that *Porcellana platycheles*, the second most important species in the DES, is represented by the second largest dot in the bottom panels. See Table 20 for the definition of each functional diversity index.

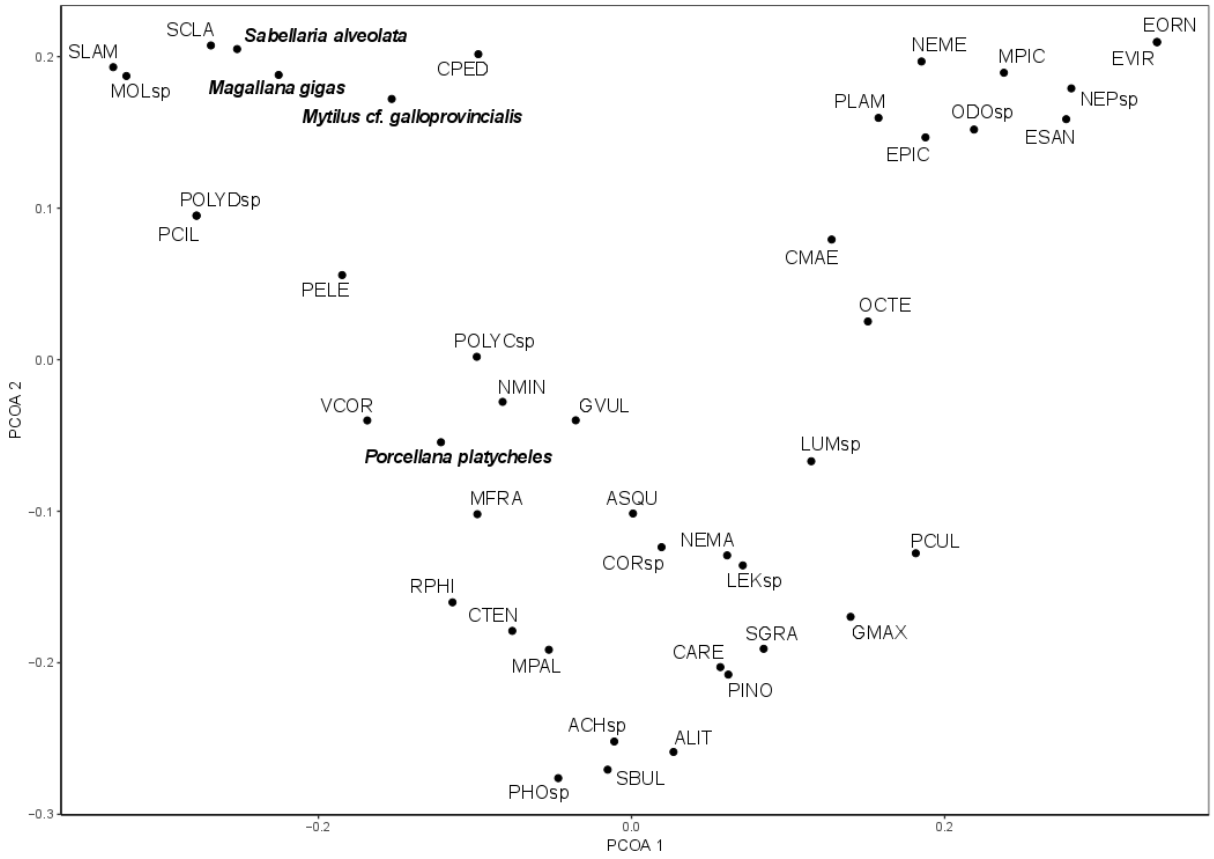

Figure 32. Position on the first two axis of the functional space of all the species present at the global engineered sediment level and identified by their abbreviated names (see Appendix for the corresponding full name). *Sabellaria alveolata*, the ecosystem engineer, *Porcellana platycheles*, the second most important species in terms of abundance and biomass in the disturbed engineered cores, are both identified by their full names. *Magallana gigas* and *Mytilus* cf. *galloprovincialis*, two important epibiont species are also identified by their full names. The first PCoA axis corresponds to a daily adult movement capacity gradient. Species presenting "none" and "low" movement capacities have negative values and the ones presenting "medium" and "high" movement capacities have positive values. Negative values on axis 2 are associated to predominantly "surficial modifiers" while the group of species close to *Sabellaria alveolata* are "epifauna" and the one in the top right corner are predominantly "biodiffusers".

3.3. Effect of the environment and the macrofauna defined according to its identity and biological traits on the biogeochemical fluxes of the engineered sediments

On each plot (Figure 33), the association of a color and of symbol correspond to a specific season-engineered sediment type (undisturbed or disturbed) combination allowing the visualization of specific patterns.

3.2.1. Linear effects

Water temperature only had a significant and positive effect on the NO_{2+3} fluxes and multifunctionality (Table 23). *S. alveolata* biomass explained over 50% of the variability of three functions out of four (SOD, NH_4^+ fluxes and multifunctionality) and was the variable with the highest explanatory power in these three cases (Table 23, Figure 33). *S. alveolata* abundance was the variable with the highest explanatory power ($adjR^2 = 0.40$) for the NO_{2+3} fluxes (Table 23, Figure 33). Other macrofauna variables had significant effects on biogeochemical fluxes. *S. alveolata* mean biomass had a positive effect on SOD and explained over 50% of the flux variability (Table 23). *S. alveolata* abundance also had a significant and positive effect on the NH_4^+ fluxes and multifunctionality (Table 23), explaining respectively 15 and 14% of the total variability. None of the taxonomic diversity indices had a significant effect on either the SOD or the NO_{2+3} fluxes ($p > 0.05$), while they explained between 20 and 40% of the NH_4^+ fluxes and 15-20% of multifunctionality ($p < 0.05$, Table 23, Figure 33). In all these cases, they had negative effects on the functions, with the strongest negative effect being the species richness on the NH_4^+ fluxes ($adjR^2 = 0.39$, Table 23, Figure 33).

None of the functional diversity indices had a significant effect on the SOD. FRic and $FDis_{biom}$ both had negative effects on the NH_4^+ fluxes and multifunctionality. They explained respectively 30% and 20% of the NH_4^+ flux variability and only explained, respectively 15% and 14% of the multifunctionality variability (Table 23). $FDis_{ab}$ also had a significant and negative effect on the NH_4^+ fluxes ($adjR^2 = 0.18$). The $FEve_{ab}$ explained 24% of the NO_{2+3} fluxes and it had a negative effect on the flux. Finally, the functional identity indices had significant effects on the NH_4^+ fluxes and multifunctionality. FIde1 and FIde3, weighted by abundance or biomass, always had negative effects on the NH_4^+ fluxes and the multifunctionality while FIde2 (weighted by abundance) had an effect only on the NH_4^+ fluxes and it was positive. $FIde1_{biom}$ and $FIde3_{biom}$ explained respectively 23% and 21% of the NH_4^+ flux variability (Table 23). Similar proportions of this flux were explained by the $FIde1_{ab}$ ($adjR^2 =$ 24%, Figure 33) and $FIde3_{ab}$ ($adjR^2 = 23\%$) while $FIde2_{ab}$ only explained 13% of the flux variability (Table 23). $FIde1_{biom}$ and $FIde3_{biom}$ explained around 20% of the multifunctionality (Table 23, Figure 33) while the equivalent indices calculated using the abundances explained a smaller proportion of the multifunctionality variable ($adjR^2 = 15\%$ in both cases).

3.2.2. Quadratic effects

Two concave quadratic functions with $N1_{ab}$ ($adjR^2 = 0.25$) and $FDis_{ab}$ ($adjR^2 = 0.43$) significantly explained the SOD (Table 23, Figure 33). Regarding the NH_4^+ fluxes, the only variable which explained a higher proportion of the flux when modelled using a quadratic function (concave functional form) rather than a linear one, was $FDis_{ab}$ ($adjR^2$ quadratic = 0.38 and $adjR^2$ linear = 0.18, Table 23). Around 20% of the NO_{2+3} fluxes variability was also explained by two concave quadratic functions with *S. alveolata* biomass and species richness respectively (Figure 33) and by a convex

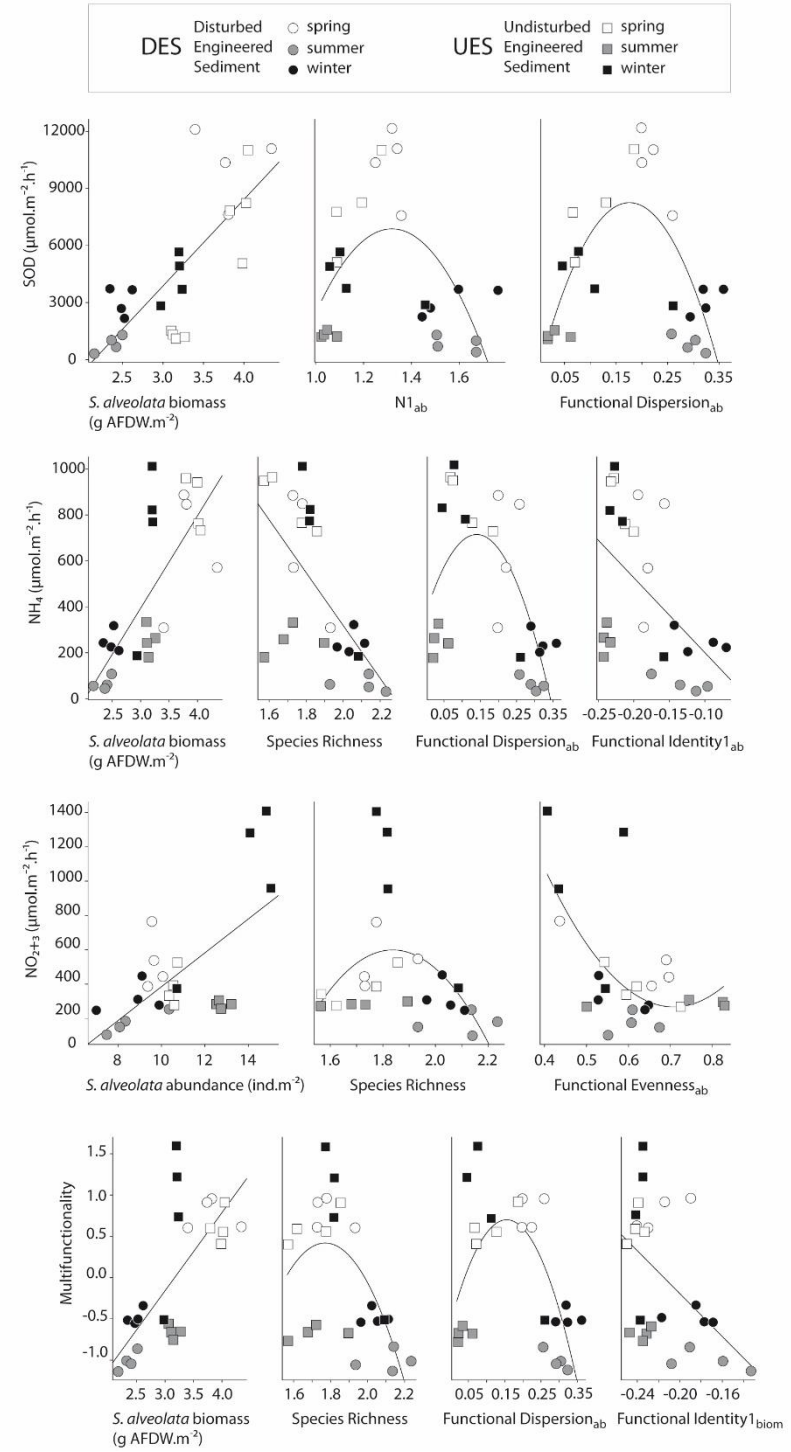

Figure 33. Sediment oxygen demand (SOD), ammonium fluxes (NH_4^+), nitrate + nitrite fluxes (NO_{2+3}) and multifunctionality as linear or quadratic functions of the variables significantly explaining the most of each ecosystem process (adjusted R^2, see Table 23) and belonging to each category of variables: macrofauna (*Sabellaria alveolata* and associated fauna), taxonomic diversity, functional diversity and functional identity (see Table 23). N1 is the exponential Shannon-Wiener and functional identity1 is the functional identity calculated on the first axis of the functional space. See Table 20 for the definition of each functional index. The subscript ab indicates that the index was weighted by the abundance. *S. alveolata* abundance and biomass, $N1_{ab}$ and the species richness were fourth-root transformed. The color and symbol codes are presented at the top of the figure.

quadratic function with *S. alveolata* mean biomass (Table 23). The convex quadratic function with $FEve_{ab}$ explained a higher proportion of the NO_{2+3} fluxes (adjR^2 quadratic = 0.36, Table 23 and Figure 33) than its linear equivalent (adjR^2 linear = 0.24, Table 23). Finally, two concave quadratic functions with taxonomic indices (species richness and $N1_{ab}$) and functional diversity indices ($FDis_{ab}$) significantly explained multifunctionality (Table 23, Figure 33). These models explained around one third of the multifunctionality variability (28% for $N1_{ab}$ to 39% for $FDis_{ab}$).

3.2.3. Ecosystem functions – macrofauna indices plots

The observation of the different plots (Figure 33) revealed that the cores sampled in the different sediment types and at the different seasons had similar dispersions regarding all the explanatory variables with one exception. The winter UES cores were much more homogenous in terms of mean *S. alveolata* biomass, *S. alveolata* biomass, N1, FIde1 and FIde2 than the cores sampled at the other season – sediment type combinations. One core of the summer UES sampling was atypical regarding several variables. It was characterized by higher $SALV_{mean\ biom}$, SR, N1, FDis and FIde1 and lower $SALV_{ab}$ compared to the other three cores sampled at the same time and in the same station. Nonetheless, the fluxes of this atypical core were perfectly in line with the linear or quadratic models presented above. The different plots also indicate that considering all the engineered sediments as independent was a correct assumption.

4. Discussion

Studying the link between taxonomic diversity, functional diversity and ecosystem functions is not an easy task but is crucial if we wish to understand in a more integrative way how ecosystems work and how they might be affected by increasing disturbances. These links were first studied in terrestrial autotrophic ecosystems using controlled experiments (Tilman et al. 1997, Díaz and Cabido 2001, Lavorel and Garnier 2002, Hooper et al. 2005, Mouillot et al. 2011). Then, they were extended in the context of benthic infauna species (Ieno et al. 2006, D'Andrea and DeWitt 2009, Braeckman et al. 2010, Janson et al. 2012). In the meanwhile, the functioning of biogenic habitats built by structural engineers like mussels and oysters (Berke 2010), was also investigated (*e.g.* respiration, calcification, benthо-pelagic coupling) but without any consideration for the role played by biodiversity in regulating it (Newell et al. 2002, Lejart et al. 2012, Kellogg et al. 2013, Smyth et al. 2015, 2016). Nonetheless, these habitats are biodiversity hotspots where structural and functional diversity changes could play a role in modulating functions such as biogeochemical fluxes. In the present study, we have started to fill this gap relative to the role played by biodiversity in the functions performed by marine structural engineers (Berke 2010) by building upon a number of studies that have focused on biogeochemical fluxes in bivalve reefs (mainly oyster and mussel reefs) in coastal ecosystems (see Stief (2013) and references therein).

Table 23. Significant ($p < 0.05$) linear and quadratic functions for the sediment oxygen demand (SOD), total ammonium fluxes (NH_4^+), the sum of nitrate and nitrite fluxes (NO_{2+3}) and the multifunctionality as a function of taxonomic indices, functional diversity indices and functional identity considering all the engineered sediment cores (n = 24). The type of explanatory variable is mentioned as E for environmental, M for macrofauna (*S. alveolata* and associated fauna), TD for taxonomic diversity, FD for functional diversity and FI for functional identity. For each type of explanatory variable, the variable explaining the most of the ecosystem process variability is in bold (highest adjusted R^2). All the M and TD explanatory variables were fourth-root transformed.

Ecosystem process		Explanatory variable	Slope	adjR^2	*p*
SOD (µmol.m^{-2}.h^{-1})	M	$SALV_{mean\ biom}$ (g AFDW)	+	0.52	<0.001
	M	**$SALV_{biom}$ (g AFDW.m^{-2})**	**+**	**0.58**	**<0.001**
	TD	**$N1_{ab}$**	**Quadratic concave**	**0.25**	**0.020**
	FD	**$FDis_{ab}$**	**Quadratic concave**	**0.43**	**0.0010**
NH_4^+ (µmol.m^{-2}.h^{-1})	M	$SALV_{ab}$ (ind.m^{-2})	+	0.15	0.035
	M	**$SALV_{biom}$ (g AFDW.m^{-2})**	**+**	**0.56**	**<0.001**
	TD	**SR**	**-**	**0.39**	**<0.001**
	TD	$N1_{ab}$	-	0.30	0.0034
	TD	$N2_{ab}$	-	0.26	0.0069
	TD	$N1_{biom}$	-	0.27	0.0053
	TD	$N2_{biom}$	-	0.19	0.018
	FD	FRic	-	0.30	0.0036
	FD	$FDis_{biom}$	-	0.20	0.018
	FD	$FDis_{ab}$	-	0.18	0.023
	FD	**$FDis_{ab}$**	**Quadratic concave**	**0.38**	**0.0027**
	FI	$FIde1_{biom}$	-	0.23	0.010
	FI	$FIde3_{biom}$	-	0.21	0.014
	FI	**$FIde1_{ab}$**	**-**	**0.24**	**0.0091**
	FI	$FIde2_{ab}$	+	0.13	0.048
	FI	$FIde3_{ab}$	-	0.23	0.010
NO_{2+3} (µmol.m^{-2}.h^{-1})	**E**	**Temp (°C)**	**+**	**0.26**	**0.0061**
	M	**$SALV_{ab}$ (ind.m^{-2})**	**+**	**0.40**	**<0.001**
	M	$SALV_{biom}$ (g AFDW.m^{-2})	Quadratic concave	0.21	0.035
	M	$SALV_{mean\ biom}$	Quadratic convex	0.22	0.027
	TD	**SR**	**Quadratic concave**	**0.18**	**0.047**
	FD	$FEve_{ab}$	-	0.24	0.0093
	FD	**$FEve_{ab}$**	**Quadratic convex**	**0.36**	**0.0033**
Multifunctionality	**E**	**Temp (°C)**	**+**	**0.17**	**0.026**

M	$SALV_{ab}$ (ind.m^{-2})	+	0.14	0.040
M	**$SALV_{biom}$ (g AFDW.m^{-2})**	**+**	**0.51**	**0.001**
TD	SR	-	0.22	0.013
TD	**SR**	**Quadratic concave**	**0.35**	**0.0042**
TD	$N1_{ab}$	-	0.19	0.021
TD	$N1_{ab}$	Quadratic concave	0.28	0.013
TD	$N2_{ab}$	-	0.16	0.029
TD	$N1_{biom}$	-	0.21	0.015
TD	$N2_{biom}$	-	0.15	0.033
FD	FRic	-	0.15	0.034
FD	$FDis_{biom}$	-	0.14	0.041
FD	**$FDis_{ab}$**	**Quadratic concave**	**0.39**	**0.0021**
FI	**$FIde1_{biom}$**	**-**	**0.21**	**0.014**
FI	$FIde3_{biom}$	-	0.17	0.025
FI	$FIde1_{ab}$	-	0.15	0.033
FI	$FIde3_{ab}$	-	0.15	0.033

Temp: in situ water temperature, $SALV_{ab}$: *S. alveolata* abundance, $SALV_{biom}$: *S. alveolata* biomass, $SALV_{mean\ biom}$: *S. alveolata* mean biomass, N1: exponential Shannon-Wiener, N2: inverse of Simpson's diversity, FRic: functional richness, FDiv: functional divergence, FEve: functional evenness, FDis: functional dispersion, FIde1, FIde2 and FIde3: functional identity on the 1st, 2nd and 3rd axis of the functional space respectively. The subscripts ab and biom indicate that the index was weighted using species abundance and biomass, respectively.

4.1. The role of structural engineers in community biogeochemical fluxes

Globally, community respiration, ammonium and NO_{2+3} fluxes were systematically higher in the engineered sediments compared to the muddy and sandy sediments, agreeing with previous studies that indicated an enhanced organic matter mineralization, nitrification and ammonium release in temperate reef habitats compared to bare non engineered soft sediments (Norling and Kautsky 2007, Kellogg et al. 2013, Stief 2013). In bivalve reefs, two mechanisms are put forward to explain the increased biogeochemical fluxes. First, the structures built by the reef-building bivalves extend the surface area available for colonization by nitrifying and denitrifying microorganisms (Gutiérrez et al. 2003, Stief 2013, Heisterkamp et al. 2013) which also benefit from the metabolic waste products excreted by the bivalves (ammonium and carbon dioxide). Second, the important production of biodeposits (feces and pseudofeces) by the bivalves represents an important source of labile organic matter used by microorganisms.

In sediments engineered by *S. alveolata*, the main factor explaining community respiration increasing across seasons is the engineer's biomass, a positive relation also evidenced in the case of the

bioirrigating shrimp *Upogedia pugettensis* (D'Andrea and DeWitt, 2009). We expected temperature to have a significant effect on respiration rates according to the Q10 of 2 relation stating that respiration rates are anticipated to double when the water temperature increases by 10°C (Franco et al. 2010, Charbonnier et al. 2016). Such a temperature effect was not observed since the maximal respiration rates were not reached for maximal water temperatures, as it was evidenced in the case of subtidal soft sediments (Janson et al. 2012) and subtidal oyster reefs (Kellogg et al. 2013). Another relation positively links an organism's weight to its respiration rate (Mahaut et al. 1995, Bosch et al. 2015), a relation observed in this study since the engineer species' biomass and mean biomass, both maximal in spring, explained over 50% of the community oxygen demand using a linear regression (positive effect). The mean *Sabellaria* biomass in spring was two to five times higher than in summer and winter, clearly overriding the temperature effect. This high spring biomass is likely due to very mature and ripe males and females ready to spawn (Dubois et al. 2007a). Another cause of the unobserved temperature effect on the respiration rates is suggested by Gutiérrez and Jones (2006). They introduced a concept where physical ecosystem engineers act as agents of biogeochemical heterogeneity *via* the structural changes they cause, which often affect heat transfer processes and consequently temperature dependent microbial activity. Temperature loggers placed inside the reefs have shown that the engineered sediments present lower heat transfer values than the surrounding coarse sediments (unpublished data), indicating that seasonal temperature variations could be buffered inside the engineered sediments, potentially limiting the seasonal variations in microbial activity and therefore changes in the measured respiration rates. In addition, Dubois et al. (2002) evidenced that subtidal species inhabit intertidal *S. alveolata* reefs, most likely because of low changes in temperatures within the reefs.

Furthermore, we evidenced a clear biomass-dependent effect of *S. alveolata* on the ammonium fluxes, a relation also evidenced by D'Andrea and DeWitt (2009) for *Upogedia pugettensis*. A double phenomenon, increased in spring, probably explains the high ammonium fluxes we recorded. First, the honeycomb-worm could present higher excretion rates in spring, as recorded for the none-native gastropod *Crepidula fornicata* in the Rade de Brest (Martin et al. 2006). Indeed, excretion by benthic macrofauna can account for 10 to 70% of ammonium fluxes from the sediment (Blackburn and Henriksen 1983, Kristensen 1988). Second, the honeycomb-worm could also present higher biodeposition rates, linked to the spring diatom bloom, as recorded by Navarro and Thompson (1997) for the horse mussel (*Modiolus modiolus*). Indeed, *S. alveolata* is capable of pre-ingestive particle selection and produces large quantities of feces and pseudofeces (Dubois et al. 2006a), biodeposits which can rapidly be remineralized by bacteria, producing ammonium (Stief 2013).

Finally, the transformation of ammonium into nitrites and then nitrates requires mineralized nitrogen (ammonium), oxygen and the presence of an aerobic nitrifying community. Nitrifying microbes can be directly associated with the surfaces of living organisms like polychaetes, amphipods and bivalve soft tissues (Welsh and Castadelli 2004) and it could very well be the case for *Sabellaria alveolata*. *S. alveolata* density reported in this study is also an indirect measure of tube density. These tubes probably

have a double role in promoting nitrification: as habitats for nitrifying microbes (D'Andrea and DeWitt 2009) and as vectors allowing oxygen to penetrate deeper into the engineered sediment consequently allowing nitrification to take place. The strong positive linear relation found between the NO_{2+3} fluxes and the *Sabellaria alveolata* density is evidence towards this hypothesis. Density-dependent effects on nitrogen cycling have previously been reported in *in situ* controlled experiment on a burrowing ecosystem engineer (D'Andrea and DeWitt 2009). The nitrification activity inside the *S. alveolata* tubes is probably enhanced by oxygen made more available to microorganisms *via* the animal's vertical movement in its tube.

4.2. Biogeochemical fluxes in engineered habitats: a comparison

Other studies have measured biogeochemical fluxes for engineered habitats like for a reef built by the invasive serpulid polychaete *Ficopomatus enigmaticus* (previously known as *Mercierella enigmatica*, (Keene 1980), for a restored subtidal *Crassostrea virginica* reef (Kellogg et al. 2013) and for a mudflat colonized by the bioirrigating shrimp *U. pugettensis* (D'Andrea and DeWitt 2009), allowing a comparison. The two polychaete reefs have very similar respiration rates (this study in spring and Keene (1980) in March: ~ 0.30 g $O_2.m^{-2}.h^{-1}$) and maximal NO_{2+3} fluxes (this study: ~ 1.01 mmol.$m^{-2}.h^{-1}$, Keene (1980): 1.05 mmol.$m^{-2}.h^{-1}$ in November) while maximal ammonium fluxes were two folds higher in our study (~ 0.85 mmol.$m^{-2}.h^{-1}$ in spring, Keene (1980): 0.40 mmol.$m^{-2}.h^{-1}$ in November). Furthermore, for similar water temperatures (~ 13°C), the respiration rates measured for the *S. alveolata* and *C. virginica* reefs were very similar (~ 11 mmol $O_2.m^{-2}.h^{-1}$). Regarding ammonium and nitrates + nitrites fluxes, the maximal values measured in the *S. alveolata* reef (~ 0.9 mmol.$m^{-2}.h^{-1}$) were also comparable to the ones measured in late spring-early summer at the restored oyster reef (Kellogg et al. 2013). Finally, maximal sediment oxygen demand and ammonium fluxes measured in this study were similar to the ones reported for high densities of the engineering mud shrimp (SOD: ~ -225.7 mmol $m^{-2}.d^{-1}$ and: NH_4^+~16.37 mmol $m^{-2}.d^{-1}$) by (D'Andrea and DeWitt 2009). Differently, maximal NO_{2+3} fluxes measured in the reefs were two folds greater than the ones recorded in high mud shrimp density plots (~11.38 mmol $m^{-2}.d^{-1}$).

This comparison highlights a few interesting points on biogeochemical fluxes and ecosystem engineers. First, the level of coalescence of the engineered structures seems to effect the ammonium effluxes via the amount of organic matter trapped inside the engineered habitat. Second, structural engineers that build coalescent structures enhance in similar ways sediment oxygen demand, ammonium and nitrates + nitrites fluxes. Third, reef-building ecosystem engineers also have density- and biomass-dependent effects on biogeochemical fluxes as do infaunal ecosystem engineers, suggesting this could be a general property of marine ecosystem engineers. Finally, reef-type engineered structures could have a higher potential as organic nitrogen recyclers than soft sediment engineered by infaunal species.

4.3. Biogenic habitats, mass-ratio and diversity hypothesis

Two major hypothesis link biodiversity and ecosystem functioning: the diversity hypothesis and the mass ratio hypothesis. The diversity hypothesis states that the diversity of species in a community along with their functional traits influence ecosystem functioning through mechanisms such as resource partitioning and niche complementarity and increase insurance regarding disturbances, through compensatory dynamics in space and time (Tilman 1997). This hypothesis supposes a positive relationship between evenness indices (N1 and N2) or diversity, either in terms of species richness (SR) or functional richness (FRic), and ecosystem functioning (Mokany et al. 2008). The mass ratio hypothesis states that the ecosystem's functioning is predominantly explained by the functional traits of the dominant species in that ecosystem and is relatively unaffected by the diversity of less abundant species (Grime 1998, Mokany et al. 2008). This hypothesis is linked to a selection effect influenced by competitive differences (Cadotte 2017). The diversity and mass ratio hypothesis have previously been found to both influence ecosystem functioning in secondary subtropical forests (Ali et al. 2017), depending on the functional trait considered.

4.3.1. The diversity hypothesis

Hill's indices (SR, N1 and N2) along with functional richness are relevant to test the 'diversity hypothesis' (Mokany et al. 2008). The effect of these indices on the fluxes were best explained either by negative linear models (SR, N1, N2 and FRic for NH_4^+; $N1_{biom}$, $N2_{ab}$ and $N2_{biom}$ for multifunctionality) or by concave quadratic models ($N1_{ab}$ for SOD; SR for NO_{2+3}; SR and $N1_{ab}$ for multifunctionality), indicating a general negative effect of diversity on biogeochemical fluxes, a result coherent with (Gamfeldt et al. 2015). Indeed, they found that benthic macrofauna polycultures showed significantly lower or similar levels of functioning compared to the monoculture with the highest functioning. Since honeycomb-worm reefs are exclusively built by one species, the habitat's environmental conditions are likely optimal for the ecosystem engineer. Hence, there is a very good chance *S. alveolata* is the best performing species for a majority of ecosystem functions performed by honeycomb-worm reefs, particularly biogeochemical fluxes.

In this context, the increase in species and functional richness enhances spatial and trophic competition potentially leading to a lower metabolic activity of the engineer species (*i.e.* lower respiration and excretion). It could also disrupt the local conditions created by the engineer (*i.e.* decrease in sediment oxygenation and microorganisms habitat via tube loss) leading to a lower nitrogen cycling. Nonetheless, diversity does not appear to be all-bad in view of the quadratic concave models, indicating an intermediate diversity effect, a result in accordance with (Thrush et al. 2017). They found a similar relation between intertidal benthic species richness and ammonium efflux during a controlled experiment (sandy sediments) where nitrogen had been added to the sediment (600 g $N.m^{-2}$). Multifunctionality was highest for intermediate levels of species richness and $N1_{ab}$ corresponding to the

middle of the disturbance continuum and characterizing slightly disturbed reefs. This effect of diversity on ecosystem functioning is probably linked to mechanisms such as facilitation or other forms of non-additive interactions among species (Stachowicz 2001, Bruno et al. 2003) such as an insurance effect where a few newly added species limit functional loss due to increasing disturbance and even enhance global functioning.

4.3.2. The mass-ratio hypothesis

Functional identity indices can only be associated to the mass ratio hypothesis since they are influenced by the dominant species in terms of abundance or biomass (Mokany et al. 2008). In our case, functional identity had significant linear effects on the ammonium fluxes (FIde1 and 3 negative effects, FIde2 positive effect) and multifunctionality (FIde1 and 3 negative effects) validating this hypothesis for the ammonium fluxes and multifunctionality. (Mokany et al. 2008) found that the mass-ratio hypothesis was strongly supported in a temperate native grassland since functional identity was more important than diversity in driving ecosystem functions. This hypothesis is regularly mentioned in the case of autotrophic terrestrial systems (Garnier et al. 2004, Díaz et al. 2007, Mokany et al. 2008, Ali et al. 2017) but to our knowledge, it is the first time it is evidenced in the context of structural ecosystem engineering (Berke 2010). As previously mentioned, the first three PCoA axis are directly linked to specific biological traits, with the values on these axes (FIde1 to 3) associated to specific modalities of the given trait. Consequently, ammonium fluxes are higher when species present none to low movement capacities, no sediment reworking abilities (epifauna) and are suspension-feeders, which correspond to a 'type' species very close to the engineer *S. alveolata*. Interestingly, FIde1 and 3 in terms of both abundance and biomass explained similar percentage of the ammonium flux variations (~ 20%) while FIde2 only had an influence on the ammonium flux when calculated using abundance. This result indicates that the density of species with specific reworking abilities more than their volume, estimated through biomass, influence part of the nitrogen cycle. Biomass is often considered as more functionally relevant than abundance or density (Mouillot et al. 2011), but for specific functions such as biogeochemical fluxes, it is not the case. Indeed previous studies have shown that density either in terms of species (Braeckman et al. 2010) or in terms of biogenic structures such as burrows (D'Andrea and DeWitt 2009), significantly and positively affect a number of biogeochemical fluxes. The importance of density associated to specific biological traits, here sediment reworking, is also visible in the case of a "hard" three-dimensional engineered habitat like a *S. alveolata* reef.

Multifunctionality is promoted when species presenting none to low movement capacities and suspension-feed are dominant in the system, in terms of both biomass and abundance, with $FIde1_{biom}$ explaining a higher part of the variation. Consequently, in terms of multifunctionality, the most important functional trait is movement capacity and species presenting none to low movement capacities promote the global biogeochemical functioning of the reef. In soft sediments, a species' bioturbation potential is the number one functional trait considered when looking into biogeochemical fluxes

(Braeckman et al., 2010; Ieno et al., 2006; Mermillod-Blondin et al., 2005; Michaud et al., 2005) and according to (Queirós et al. 2013), a species bioturbation potential is dependent of its sediment reworking abilities and its movement capacities. In the case of a *S. alveolata* reef, actual sediment reworking (excluding epifauna) is limited to more disturbed zones of the reef where soft sediments are present, or to few but abundant infaunal species like *Golfingia vulgaris* (Dubois et al. 2002). Consequently, it is not surprising that sediment reworking did not come out as a key functional trait, but its complementary trait in evaluating bioturbation did.

4.3.3. Complementary effects

Functional evenness, dispersion and divergence are relevant to both the diversity and the mass-ratio hypothesis (Mokany et al. 2008, Cadotte 2017). Functional dispersion (abundance weighted) is an important driver in SOD, ammonium fluxes and multifunctionality (~ 40% variability explained). These three functions are maximal for functional dispersion values of 0.15, which corresponds to the limit between the disturbed and undisturbed engineered sediments. Consequently, there is a small diversity effect, as previously identified for SOD and NO_{2+3} fluxes using richness and evenness indices, which is only detected when using abundance. These results highlight the importance of considering multiple metrics and both abundance and biomass to fully capture BEF relationships (Thrush et al. 2017), even in an ecosystem strongly dominated by one species like biogenic habitats. Finally, functional evenness (abundance weighted), an index informing on the regularity of the abundance distribution in the functional space, had a general negative effect on the NO_{2+3} fluxes. A high value indicates a homogenous distribution of the species and of their abundance in the functional space with similar distance separating them (Villéger et al. 2008). NO_{2+3} fluxes seem to be promoted when there are several packs of species presenting similar traits present in the reef, indicating that a certain level of biological trait complementarity associated to a certain level of species richness (~10 species), is necessary for an optimal nitrogen cycling in the reef.

4.4. Ecosystem consequences of increasing disturbance

In terms of associated fauna, an increasingly disturbed *S. alveolata* is characterized by a higher species richness and a more diverse species assemblage benefiting from the microhabitats made available by the decrease in honeycomb-worm abundance (Dubois et al. 2002, Jones et al. 2018). If we consider the diversity hypothesis, disturbed engineered sediments would be predicted to function better than undisturbed engineered sediments because of their higher diversity, a conclusion we did not clearly observe. Rather we evidenced that the ecosystem engineer in terms of biomass and abundance plays a key role in the reef's overall biogeochemical functioning, estimated with the multifunctionality variable; a key role complemented by the associated fauna biological trait diversity and identity estimated with respectively the functional dispersion and the functional identity 1 (*i.e.* proxy for mobility). This result highlights the importance of considering multiple taxonomic and functional indices in order to have the

most complete understanding of the functioning of a complex habitat like a biogenic reef and of the consequences of increasing disturbances (Thrush et al. 2017). Hence, it is of prime importance to protect the Sainte-Anne reef in order to maintain a high abundance and biomass of the engineer, which will enable this biogenic habitat to keep performing key ecosystem processes like organic matter remineralization and nitrogen cycling. Furthermore, localized disturbances enhancing functional diversity are not detrimental in terms of biogeochemical fluxes, they even seem beneficial, but they should be limited as much as possible. Indeed, monitoring of the Sainte-Anne reef (Desroy et al. 2011, Rollet et al. 2015) has shown that local disturbances tend to spread quickly over large sections of the reefs even if rapid recovery is also possible (*i.e.* between 2007 in 2011 in the North reef section) but strongly under the control of larval supply and recruitment (Ayata et al. 2009).

Finally, one winter undisturbed sediment core presented atypical values of the predictor variables compared to the three other replicates but conformed with the linear and quadratic models, indicating that macrofauna indices (taxonomic and functional), and especially the engineer biomass and functional dispersion, are good predictors of the biogeochemical functioning of a *S. alveolata* reef. In this study, functional dispersion appeared as the most promising functional index to predict biogeochemical fluxes. Further investigations on other functions such as primary and secondary production or consumption are needed to test if functional dispersion could be used as a global functioning index in the context of *Sabellaria alveolata* reefs. Indeed, preliminary field observations and studies of several *S. alveolata* reefs point towards a higher secondary and benthic primary production in more disturbed engineered sediments characterized by a higher functional dispersion, which could indicate a complex response of the reef in terms of functioning, to increasing disturbance.

Appendix

Mean (n = 12) abundance and biomass (ash-free dry weight in mg) of all the species identified in the undisturbed and disturbed engineered sediments. The mean was calculated over the three seasons and the four sampled cores for each engineered sediment type.

Species name	**Abbreviated name**	**Undisturbed engineered sediment**		**Disturbed engineered sediment**	
		Density (ind .m^{-2})	Biomass (AFDW mg.m^{-2})	Density (ind .m^{-2})	Biomass (AFDW mg.m^{-2})
***Achelia* sp.**	ACHsp	38	4	599	61
Axelsonia littoralis	ALIT	0	0	47	0
Amphipholis squamata	ASQU	9	5	156	32
Corophium arenarium	CARE	0	0	5	0
Carcinus maenas	CMAE	71	858	61	631
***Corophium* sp.**	CORsp	33	5	207	34
Cereus pedunculatus	CPED	439	67	104	846
Cirriformia tentaculata	CTEN	5	1	28	8
Eulalia ornata	EORN	170	65	0	0
Eteone picta	EPIC	0	0	5	1
Eumida sanguinea	ESAN	24	17	24	38
Eulalia viridis	EVIR	71	168	52	517
Gnathia maxilaris	GMAX	0	0	5	20
Golfingia vulgaris	GVUL	85	813	156	1 369
***Lekanesphaera* sp.**	LEKsp	179	313	269	541
***Lumbrinereis* sp.**	LUMsp	0	0	5	1
Magallana gigas	MGIG	0	0	9	4 347
Mytilus* cf. *galloprovincialis	McfGAL	47	89	132	251
Mediomastus fragilis	MFRA	24	1	85	15
***Molgula* sp.**	MOLsp	14	80	5	32
Melita palmata	MPAL	28	5	137	47
Mysta picta	MPIC	0	0	5	1
***Nematoda* spp.**	NEMA	726	185	1 151	103
Nemertean	NEME	231	1 637	278	1 311

***Nephtys* sp.**	NEPsp	0	0	5	2
Nephasoma minutum	NMIN	250	71	189	47
Odontosyllis ctenostoma	OCTE	0	0	118	28
***Odontosyllis* sp.**	ODOsp	42	9	42	5
Polydora ciliata	PCIL	9	9	0	0
Perinereis cultrifera	PCUL	47	207	141	209
Pygospio elegans	PELE	0	0	28	12
***Photys* sp.**	PHOsp	24	0	0	0
Pholoe inornata	PINO	0	0	9	6
Phyllodoce laminosa	PLAM	0	0	38	269
***Polycirrus* sp.**	POLYCsp	5	1	38	8
***Polydora* sp.**	POLYDsp	5	1	0	0
Porcellana platycheles	PPLA	236	3 916	2 415	35 303
Ruditapes philippinarum	RPHI	0	0	9	325
Sabellaria alveolata	SALV	25 734	151 178	7 036	99 177
Sphaerosyllis bulbosa	SBUL	0	0	9	1
Styela clava	SCLA	0	0	19	130
Syllis gracilis	SGRA	5	4	14	4
Spirobranchus lamarcki	SLAM	5	11	52	76
Venerupis corrugata	VCOR	14	30	52	3 004
Total macrofauna including *S. alveolata*		28 532	159 746	13 140	148 751
Total macrofauna excluding *S. alveolata*		2 798	8 568	6 104	49 574
Percentage of total abundance and biomass accounted for by *S. alveolata*		90.19	94.64	53.55	66.67

Chapter IV

The last chapter of this manuscript focuses on the combined use of trait-based functional diversity indices and isotopic diversity indices in the context of disturbances affecting an engineered habitat. This chapter is composed of one article in preparation to be submitted to Functional Ecology.

The calculation of these different indices and the observation of their variations along a disturbance gradient affecting the reef, revealed that two indices were affected in winter and summer by increasing disturbances: the functional dispersion, which can be linked to the reef's biogeochemical functioning and the isotopic richness, which could be linked to the diversity of available food sources and their use by the macrofauna.

Finally, the use of the functional diversity indices as a proxy of the fundamental niche of the reef community and the use of the isotopic diversity indices as a proxy of the realized niche of the reef community revealed that facilitation was the dominant process shaping the reef habitat.

Article 5 - Ecological niche estimated with functional and isotopic community-wide metrics: complementary or redundant pictures when investigating marine engineered habitat?

Auriane G. Jones [a,b,c], Stanislas F. Dubois [a], Nicolas Desroy [b], Jérôme Fournier [c,d]

Article in preparation (submission to Functional Ecology)

[a] IFREMER, Laboratoire Centre de Bretagne, DYNECO LEBCO, 29280 Plouzané, France

[b] IFREMER, Laboratoire Environnement et Ressources Bretagne nord, 38 rue du Port Blanc, BP 80108, 35801 Dinard cedex, France

[c] CNRS, UMR 7208 BOREA, 61 rue Buffon, CP 53, 75231 Paris cedex 05, France

[d] MNHN, Station de Biologie Marine, BP 225, 29182 Concarneau cedex, France

1. Introduction

Ecosystems worldwide are experiencing increasing disturbances linked directly or indirectly to human activities (Rockström et al. 2009). Direct anthropogenic disturbances are numerous and include for example habitat fragmentation and modification (*e.g.* trawling, urban development, coastal modification) and organic enrichment of rivers, lakes and coastal waters (Howarth et al. 2000, Fahrig 2003). Climate change linked to human activity also leads to various environmental disruptions such as sea and atmosphere temperature rise, ocean acidification and increase in extreme weather events (floods, storms and hurricanes) (IPCC 2014). In this context, understanding how ecosystems are affected by these various disturbances is a key part of ecological research (Sala et al. 2000, Hooper et al. 2005). Indeed, natural ecosystems perform a broad range of functions such as primary and secondary production, organic matter recycling, water filtering (*e.g.* oyster reefs) and extreme weather event buffering (*e.g.* coral reefs and tsunamis). Some also have high patrimonial (*e.g.* sacred lands and animals) and economical value (*e.g.* eco-tourism) (Costanza et al. 1997). Disturbances to these ecosystems affect their overall functioning and the different functions they perform, one example being the over-exploitation of tropical forests and the associated decrease in CO_2 sequestration (Pan et al. 2011).

Traditionally, the taxonomic diversity and structure of communities has been considered as direct measurements of ecosystem functioning (Hooper et al. 2005) or as reacting to various disturbance such as organic matter enrichment (Pearson and Rosenberg 1978). More recently, ecologists have started to focus on the roles played by species present in ecosystems. Measuring the distribution and range of what organisms do in a system is widely known as functional diversity (Tilman 2001) and it has been shown to be a driver of ecosystem functioning (Tilman et al. 1997, Lavorel and Garnier 2002, Díaz et al. 2007). For example, the functional identity of species and the functional diversity among grassland species promote key ecosystem functions such as decomposition and primary productivity (Mouillot et al. 2011). Consequently, ecosystem functioning can be apprehended directly by measuring the functions of interest or indirectly, via the biological traits of the species present in the system, which can be considered as proxies of their functional roles (Petchey and Gaston 2006). In addition, it is of central importance to detect disturbances affecting ecosystems as early as possible in order to anticipate potential functional changes and to set relevant conservation measures (Mouillot et al. 2013a). In this context, measures based on species' biological traits such as functional diversity indices developed by Petchey and Gaston (2002), Villéger et al. (2008) and Laliberté and Legendre (2010) and more recently extended by Mouillot et al. (2013b) can be useful tools.

Functional diversity metrics are based on biological traits assumed to be directly linked to functions such as size to secondary production or leaf surface area to primary production (Lavorel and Garnier 2002). When these traits come from the literature, they inform on the potential of a species to perform certain functions. When they are measured on sampled organisms, they are linked to ecosystem

processes performed by species that have passed abiotic and biotic filters (environment filtering and biotic interactions). Consequently, trait-based indices can not only provide early warning signals regarding disturbances or help predict ecosystem functioning, they can also inform on the fundamental niche of a community (Devictor et al. 2010a). Other indices based on measured markers for example – such as stable isotopes – provide information on what is integrated in animals tissues over time (*i.e.* integration time) and rely not only on their assimilated diet (Peterson and Fry 1987) but also on resources and habitat use (Newsome et al. 2007). Stable isotopes then provide information on a complex set of biological traits classically considered when calculating trait-based metrics (*i.e.* diet, habitat use, mobility, biotic interactions). As a result, they can inform of the realized niche of a community considered from a trophic point of view (Newsome et al. 2007, Devictor et al. 2010a, Rigolet et al. 2015).

Many metrics have been developed to quantify community structure and functioning based on stable isotopic compositions of species. Among them, the metrics investigated by Layman et al. (2007a) and the standard ellipse area developed by Jackson et al. (2011). One major drawback of these metrics is that they do not take into account the biomass of the different species, a key component of ecosystem structure and functioning (Grime 1998, Cardinale et al. 2013). More recently, Rigolet et al. (2015) and Cucherousset and Villéger (2015) have extended the trait-based functional diversity framework developed by Mouillot et al. (2013) to stable isotopes. These new isotopic diversity indices can be weighted by abundance or biomass, are mathematically independent from species richness (Brind'Amour and Dubois 2013, Cucherousset and Villéger 2015) and could be used as complementary tools to existing functional diversity metrics as suggested by Rigolet et al. (2015) for coastal marine macrobenthic communities or Cucherousset and Villéger (2015) for freshwater fish communities.

Furthermore, Devictor et al. (2010) suggest investigating ecological specialization according to the Grinellian (Grinnell 1917) or the Eltonian (Elton 1927) niches. The Grinellian niche refers to a species' requirements in terms of environmental conditions (habitat and resources) and it can be directly linked to what functional ecologist call response traits, defined as traits responding to environmental factors such as resources or disturbances (Lavorel and Garnier 2002). The Eltonian niche refers to the role of a species in a system, and it can be directly linked to effect traits, defined as traits determining an ecosystem function or process (Lavorel and Garnier 2002). When studying functional diversity of benthic communities like a *S. alveolata* reef, the majority of biological traits used can be considered either as effect or as response traits, depending on the question asked. As a result, niche will not be considered here as Grinellian or Eltonian but as defined by Chase and Leibold (2003). They proposed an alternative view where the ecological niche could be considered as an irreducible product of the species-environment interactions resulting from both species' impacts and requirements (Chase and Leibold 2003, Devictor et al. 2010a). This definition is particularly relevant for species that depend on niche construction, the process whereby organisms through their impact on habitat or on other species modify their own niche (Odling-Smee et al. 2003). Such a process strongly resonates with the concept

of ecosystem engineers, defined as organisms capable of modifying their local environment through their physical presence and/or their biological activity, directly or indirectly affecting the availability of resources to other species (Jones et al., 1994).

Sabellaria alveolata (Annelida: Polychaete) is a reef-building ecosystem engineer. Indeed, this sedentary polychaete transforms soft sediment into hard rock-looking three-dimensional structures (engineered sediment) by gluing together sand grains to build a tube in which it lives (Dubois et al. 2002). These engineered structures form new intertidal biodiversity hotspots where the environmental conditions are modified and where an original species assemblage is present (Dubois et al. 2002, Jones et al. 2018). In this habitat, biogeochemical fluxes are particularly high (Jones et al., in prep) and local benthic primary production enhanced (Jones et al. 2018), two key ecosystem functions. The modification of the local trophic resources (benthic microalgae and green macroalgae) lead to a potential larger trophic niche of this engineered habitat compared to a non-engineered soft sediment (Jones et al., in prep). Many natural and anthropogenic disturbances (*e.g.* storms, human trampling) can affect these habitats leading to fragmentation, establishment of epibionts, changes in the associated fauna (Dubois et al. 2006a, Plicanti et al. 2016) and in biogeochemical fluxes (Jones et al., in prep). The importance of engineered habitat as actors in key functions (*e.g.* primary production, coastal protection, water filtering) and the many threats affecting them worldwide (Bellwood et al. 2004, Pan et al. 2011, Kellogg et al. 2013), call for an increasing understanding of their functioning and how it is affected by disturbances. In this context, jointly using functional and isotopic diversity metrics could provide new information. Our study is a first step in this direction using the case of an increasingly studied European biogenic habitat built by the polychaete *S. alveolata*, known to perform key ecosystem functions and for which we can measure disturbance via mud content (Jones et al. 2018) or engineer density (Dubois et al. 2002).

To our knowledge, no study has coupled measured functional (trait-based) and isotopic diversity metrics. In this study, we investigated an increasingly disturbed ecosystem, in order to answer three key questions: (1) Are these different metrics complementary or redundant? (2) How do they vary along a disturbance gradient? (3) What information could they provide regarding the fundamental and realized niches of the ecosystem? Here we propose to investigate these three questions in the context of a marine engineered habitat built by the common and widespread honeycomb-worm *Sabellaria alveolata*.

2. Materials and methods

2.1. Study area and field sampling

The study took place in the Mont-Saint-Michel bay where is located, in the center of the bay, the most extensive *S. alveolata* reef in Europe, the Sainte-Anne reef (48°38’700N and 1°40’100W) (Desroy et al. 2011) covering 31.7 ha (engineered sediments). This bay is situated between Brittany and Normandy and in the western part of the English Channel. It is a semi-diurnal megatidal system with a

maximal tidal amplitude of 15.5 m (average: 10-11 m) and a large intertidal zone (250 km²) where is located the Sainte-Anne reef (Noernberg et al. 2010). The Sainte-Anne reef is parallel to the coast and to the dominant tidal currents and located in the lower intertidal zone, *i.e.* between the - 2 and the - 4 m isobaths (Noernberg et al. 2010). Since this reef is built on soft sediment, two distinct entities compose it: (1) the actual reefs built by *S. alveolata* (engineered sediments) and (2) the soft sediment present between the bioconstructions and under their direct influence, hereafter called the associated sediment.

Sampling was carried out in late February 2015 (hereafter winter) and late September 2015 (hereafter summer), in order to investigate functional and isotopic diversity metrics over two contrasted times of the year. Indeed, winter and summer are contrasted in terms of environmental conditions (hydro-sedimentary features, temperatures), food supply (benthic and pelagic phytoplankton productivity), population dynamics (recruitment patterns and species turnover) and biological activity (metabolic and growth rates) (Arbach Leloup et al. 2008, Marín Leal et al. 2008, Cugier et al. 2010). Our disturbance continuum comprised 10 stations located in the Sainte-Anne reef (reef stations). These ten reef stations were at 100 m apart minimum and composed of one engineered sediment (ES) station plus one associated sediment (AS) station. Indeed, the reef was considered as the entity composed of the actual bioconstruction (ES) and the adjacent soft sediment under the direct influence of the engineered sediment (AS) (Jones et al. 2018).

To calculate the functional indices and estimate the species' abundance and biomass, at each reef station six ES samples and six AS samples, separated by at least 5 m were randomly taken at low tide (see Jones et al., (2018) for more details). For the ES and AS, the first three samples were done using a 18.5 cm side corer (269 cm²) to a depth of 15 cm (macrofauna core samples). The other three samples were done using a 1 m² quadrat in order to estimate the over dispersed macrofauna (quadrat samples). The AS macrofauna core samples were sieved through a 1-mm square mesh on site while the ES macrofauna core samples were taken back to the laboratory where they were broken apart under water and the fauna retained on a 1-mm square mesh was collected. Associated quadrat samples were done by sieving on site the first 5 cm of sediment through a 5-mm square mesh. For the ES quadrats, we sampled by hand all the visible macrofauna located on the reef and inside the reef interstices. All macrofauna core samples were fixed in a 5% formaldehyde solution and the quadrat samples were stored at -20°C until further processing.

To calculate the isotopic indices, the previously defined quadrat samples (three replicates stored at -20°C) were used along with one ES isotopic core and one AS isotopic core (one replicate). The isotope cores were sampled the same way as the macrofauna cores. On site, the AS isotope cores were sieved through a 1-mm square mesh and back at the lab, the resulting sediments were sorted. The ES isotope cores were taken back to the lab where they were broken apart under water and the fauna retained on a 1-mm square mesh. All the sampled organisms were stored at -20°C until further processing.

2.2. Macrofauna: measurements and stable isotope analysis

All the macrofauna preserved in formaldehyde was counted and identified to the species or genus level (except for nemerteans, oligochaetes and nematodes, see Appendix in (Jones et al. 2018)). For each core, a maximal number of 10 randomly chosen individuals from each species identified were measured. Maximal shell length was measured for mollusks. For annelids, nematodes, nemerteans, peracarida, ascidians, sipunculids (metasoma only), vertebrata and insecta, total body length was measured on complete individuals only. For brachyuran and porcellanid crabs, carapace width was measured and for caridea, the length between the rostrum and the telson was used. For hermit crabs, the cephalothorax length was used. For ophiuroids, disk diameter was measured. For anthozoan, foot diameter was used and for ascidians, body width was used. For *S. alveolata*, the diameter of the opercular crown of a minimum of 50 randomly sampled individuals from each macrofauna core was measured as a proxy of the individual size and age (Dubois et al. 2006a). Then, for each macrofauna core, all the individuals from each identified species were weighted (total wet weight). For mollusks, the shell was removed before weighing.

All the individuals sampled using the quadrats and kept at -20 °C were identified to the species level, counted, weighted (wet weight) and measured as well (see above). For the different mollusks species, the wet weight was estimated using allometric relations linking wet weight with shell and no-shell wet weight for the sampled species ($R^2 > 0.83$). For *Littorina littorea, Littorina saxatilis*, *Tritia reticulata, Nucella lapillus* and *Ocenebra erinaceus*, not enough data was available to build allometric relations and data provided by (Brey 2001) was used to estimate the no-shell wet weight. Using the data gathered from the core and quadrat samples, a list of species present in each station along with their respective biomass by m^2 was obtained. The biomass of each species by m^2 were calculated using the catch-per-unit-effort (CPUE, *i.e.* the ratio between the total catch biomass and the total amount of effort to harvest the catch biomass (Skalski et al. 2005)) of each sampling gear (269 cm^2 for the core and 1 m^2 for the associated quadrat). If a species was sampled by both methods (core and quadrat), its biomass by m^2 was calculated using the formula in (Jones et al. 2018), where the cumulated biomasses are divided by the sum of each gear's CPUE (1.0269 m^2). Then, using the three macrofauna core + three quadrat replicates sampled in each station, an average station by species matrix was built using average biomasses. These stations by species biomass matrices were used to calculate the weighted functional and isotopic indices.

Individuals sampled using quadrats and cores (one additional replicate per station) were also extracted for stable isotopic analysis (SIA). SIA were performed on muscle tissue for fish, mollusks and shrimps. For smaller species, we used the whole body and removed the gut when possible. Several individuals were pooled to meet the minimum required weight for stable isotope analysis for very small species. All prepared samples were rinsed with Milli-Q water and then freeze-dried. As much as possible, a minimum of three replicates per species and per station were analyzed. For calcified

organisms (crustaceans and echinoderms), a subsample was acidified (10% HCl) to remove any inorganic carbonates, then rinsed with Milli-Q water and freeze-dried for ^{13}C values, while a subsample was left untreated for ^{15}N value. Each frieze-dried animal sample was ground to a homogeneous powder and 1 mg was weighted in a tin capsule for stable isotope analysis. Carbon and nitrogen isotope compositions were measured with a Thermo Delta V isotope mass spectrometer coupled via a Conflo IV to a Carlo Erba NC2500 elemental analyzer (Cornell University Stable Isotope Laboratory). Isotopic ratios of carbon and nitrogen were reported using the standard δ notation as units of parts per thousand (‰) relative to the international reference standards:

$$\delta X = \left[(R_{sample}/R_{reference}) - 1\right] \text{ x } 1000 \quad (1)$$

where X = ^{13}C or ^{15}N, and R = $^{13}C/^{12}C$ for carbon and $^{15}N/^{14}N$ for nitrogen. Vienna-Peed Dee Belemnite limestone and atmospheric nitrogen were used as reference standards for carbon and nitrogen respectively. The analytical precision was 0.09 ‰.

2.3. Functional and isotopic diversity indices

To calculate the functional diversity indices, the species were considered on a biological traits basis. Eight categorical traits (divided into modalities) were chosen (Table 24). The size ratio was calculated as the ratio between the mean recorded size and the maximal literature size. This trait was created to take into account a key function of the engineered habitat, previously discussed (Jones et al. 2018): its role in recruitment and as a potential nursery. This continuous trait was categorized into four modalities to inform on the proportion of "small" individuals present in the reef habitat relative to their maximal potential size. The maximal size trait did not refer to literature data but to our recorded data, in order to evaluate more closely the fundamental niche of each assemblage present along the disturbance continuum. For these two traits, all the size data previously presented, was computed into a mean and a max size for each recorded species. Since the mean and maximal recorded size of each species was different between the two seasons, a winter and a summer biological trait matrix were built and used to calculate the respective winter and summer functional diversity indices. The chosen traits are proxies for key ecosystem functions such as secondary production (maximal size and longevity), biogeochemical fluxes (daily adult movement capacity, living habit, feeding mode and sediment reworking), bentho-pelagic coupling (feeding mode and living habit) and trophic dynamics (maximal size, daily adult movement capacity, living habit and feeding mode). All these traits are likely to respond to reef habitat disturbance and/or be key in its resilience from disturbance. Indeed, when the reef habitat becomes increasingly disturbed, *S. alveolata* density decreases and space is freed, potentially allowing the establishment of larger species (maximal size) and/or larger individuals on average (size ratio). Oppositely, size and longevity are predicted to decrease with increasing disturbance (Pearson and Rosenberg 1978). Daily adult movement capacity and living habit can both inform on the capacity of adults to evade disturbance and if necessary recolonize the disturbed habitat, participating in its recovery. Similarly, the capacity of species to recover from a disturbance via reproduction and a

Table 24 Biological traits used to calculate the functional diversity indices. For each trait, are indicated: the different modalities, the relevant definitions, the main associated functions and processes and how they can be linked to disturbance. All the biological traits used were categorical and they were either fuzzy coded (#) or not (*).

Trait	Modalities	Definition	Main functions and processes	Link with disturbance
Size ratio *	<0.25 [0.25-0.50[[0.50-0.75[>0.75	Ratio between the mean recorded size and the maximal literature size [0-1]	Recruitment potential, nursery function, space utilization	Expected to increase with the decrease in spatial competition
Maximal size *	<10 [10-50[[50-100[>100	Maximal recorded size (mm)	Biogeochemical fluxes, secondary production, trophic dynamics	Expected to decrease with increasing disturbance
Longevity #	<1y 1-2y 2-5y >5y	Longevity recorded in the literature	Secondary production	Expected to decrease with increasing disturbance
Daily adult movement capacity #	none 0-1m 1-10m >10m	Daily adult movement capacity in non-disturbed conditions	Biogeochemical fluxes, trophic dynamics	Recovery and evasion potential
Living habit #	tdw bdw att fl	Tube-dweller Burrow-dweller Attached Free living	Biogeochemical fluxes, trophic dynamics	Recovery and evasion potential
Feeding mode #	SusP SurF SubS PreDScaV GraZ	Suspension feeder Surface deposit feeder Sub-surface deposit feeder Predator-scavenger Grazer	Biogeochemical fluxes, bentho-pelagic coupling, trophic dynamics	Dietary plasticity and utilization of new resources
Reproduction #	asx bsp ind dir	Asexual reproduction (budding) Sexual broadcast-spawner Sexual egg layer or brooder with a larval phase Sexual egg layer or brooder with no larval phase (direct development)	Colonisation, recolonisation and recovery potential	Recovery potential after a disturbance
Sediment reworking #	EpiF SurMod UpDown BioD ReG	Epifauna Surficial modifiers Upward and downward conveyors Biodiffusors Regenerators	Biogeochemical fluxes	Changes in community functioning linked to disturbance (see Jones et al., in prep)

* indicates that these traits were not fuzzy coded, which means that each species was characterized by one modality and not several like in fuzzy coding. When calculating the Gower distance, the modalities of these two traits were coded as numeric values.

# indicates that these traits were fuzzy coded and indicated as ordered factors when calculating the Gower distance.

potential larval phase is estimated by the synthetic reproduction trait. Feeding mode can also inform on the dietary plasticity of a species and its capacity to use new resources. Finally, the increasing presence of mud inside the more disturbed engineered sediments (Jones et al. 2018) can allow the establishment of species presenting more diversified sediment reworking modes and hence modify biogeochemical fluxes (Queirós et al. 2013).The two components of the bioturbation potential defined by (Queirós et al. 2013) – *i.e.* mobility and sediment reworking – were used instead of bioturbation potential, because reworking and mobility are both influenced by habitat structure (Godbold et al. 2011). Furthermore, transferring sediment reworking across space and time is only possible if the species body size is constant (Queirós et al. 2013) which is not the case since macrofauna species were sampled in winter and summer.

In order to take into account the intraspecific variability of the species for some traits like feeding mode (*e.g. Carcinus maenas* can be a grazer and a predator-scavenger), all the traits except the two size traits, were fuzzy coded (Chevenet et al. 1994) and considered as ordered factors for the distance calculation. A large part of the information on polychaete feeding mode and daily adult movement capacity was recovered from (Fauchald and Jumars 1979) and (Jumars et al. 2015), while the rest was found in peer-reviewed journals, biological trait databases (Biotic, Genus trait handbook) or informed using expert knowledge. The winter and summer biological traits matrix defined for all the species identified in the 10 stations were used to calculate the winter and summer functional distances between species using Gower distance (Laliberté and Legendre 2010). A principal coordinate analysis (PCoA) was then performed on the functional distance matrix leading to the representation of each species in a multidimensional functional space, each dimension being a combination of traits. Finally, five functional diversity indices were calculated for each station (Table 25): functional richness (FRic) (Villéger et al. 2008, Laliberté and Legendre 2010), functional evenness (FEve) (Villéger et al. 2008, Laliberté and Legendre 2010), functional divergence (FDiv) (Villéger et al. 2008), functional dispersion (FDis) (Laliberté and Legendre 2010) and functional originality (FOri) (Mouillot et al. 2013a). These indices were chosen because they have mathematical equivalents calculated using stable isotope compositions (Cucherousset and Villéger 2015), allowing straightforward comparisons. The first seven PCoA axis were used to calculate all the aforementioned indices. The quality of the multidimensional functional space was estimated using the "quality_funct_space_fromdist" R function (modified after Maire et al. (2015). This function calculates the mean squared deviation between the initial distance between species (Gower distance) and the Euclidian distance between species computed from the functional space composed of the chosen number of dimensions (from one to ten). For seven dimensions, the mean squared deviation was 0.0012 and 0.001 for the winter and summer functional space respectively (Appendix S1), values inferior to the recommended threshold of 0.01 (Maire et al. 2015). With seven dimensions, 43.39 and 42.68% of the total winter and summer PCoA inertia were accounted for, respectively. Using more dimensions led to an overestimation of the distance between species in the functional space compared to the initial distance (Appendix S1), which could mean an overestimation

Table 25 Functional and isotopic diversity indices used in this study with the corresponding abbreviation and R functions and packages used to compute them. Each functional diversity index is associated to its isotopic equivalent. This association is based on their mathematical formula (presented in the reference papers mentioned in this table) and on their interpretation, presented in part 2.3. For each group of indices (functional diversity and isotopic equivalent) is mentioned if they are weighted or unweighted.

Functional indices (FD)	**Name**	**R function and packages**	**Isotopic indices (ID)**	**Name**	**R function and packages**	**Common definitions**	**Weighted**
Functional richness (Villéger et al. 2008, Laliberté and Legendre 2010)	FRic	multidimFD function *	**Convex hull area or isotopic richness** (Layman et al. 2007a)	IRic	si_div_CR function **	Convex hull volume (FRic) or area (IRic) of filled by all species in a community within the functional or isotopic multidimensional space (number of dimensions depends on the number of PCoA axis or isotopes used)	x
Functional divergence (Villéger et al. 2008)	FDiv	multidimFD function *	**Isotopic divergence** (Cucherousset and Villéger 2015)	IDiv	si_div_CR function **	Weighted average deviation of the Euclidian distance between the position of all the species in the functional (FDiv) or isotopic space (IDiv) and the center of gravity of the convex hull vertices (unweighted center of gravity)	✓
Functional dispersion (Laliberté and Legendre 2010)	FDis	multidimFD function *	**Isotopic dispersion** (Cucherousset and Villéger 2015)	IDis	si_div_CR function **	Weighted deviation to the average position of species in the functional (FDis) or isotopic space (IDis) divided by the maximal distance to the center of gravity	✓
Functional evenness (Villéger et al. 2008, Laliberté and Legendre 2010)	FEve	multidimFD function *	**Isotopic evenness** (Cucherousset and Villéger 2015)	IEve	si_div_CR function **	Regularity of abundance or biomass distributions in the functional (FEve) or stable isotope space (IEve) along the shortest minimum spanning tree linking all the species	✓
Functional originality (Mouillot et al. 2013a)	FOri	multidimFD function *	**Isotopic uniqueness** (Cucherousset and Villéger 2015)	IUni	si_div_CR function **	Weighted average distance to nearest neighbor in the functional (FOri) or stable isotope space (IUni) divided by the maximal distance between two nearest neighbors	✓

***** available as supplementary data in Mouillot et al. (2013)**,** ** available as supplementary data in (Cucherousset and Villéger 2015)

of the fundamental niche estimated using the different functional diversity indices. Seven dimensions represented a good comprise between calculation time, quality of the resulting functional space and percentage of the total inertia accounted for.

Different facets of isotopic diversity were measured at the station scale (10 stations) for both seasons (winter and summer), using the convex hull area (Layman et al. 2007a) also called isotopic richness and four indices defined by (Cucherousset and Villéger 2015); the isotopic divergence (IDiv), dispersion (IDis), evenness (IEve) and uniqueness (IUni) (Table 25). These five indices were measured in the two-dimensional isotopic space defined by the carbon (^{13}C) and nitrogen (^{15}N) stable isotope compositions. Prior to computing the isotopic diversity (ID) indices, the multidimensional isotopic space was standardized in order for each axis to have similar importance in the index calculation. This standardization procedure scales each axis to have the same range (*e.g.* 0-1) for each stable isotope, a procedure similar to functional diversity metric calculation where values on the PCoA axis have similar ranges (-1 to 1). Following recommendations of (Cucherousset and Villéger 2015), the standardization procedure was done for the global winter and the global summer data sets containing all the mean stable isotope values of all the species present in each station. Scaling after pooling the stable isotope values gives the same weight to each isotope and guarantees that the diversity of basal resources is accounted for in the computation of the different indices. The calculation of these indices was done for each station in winter and in summer using the average $\delta^{13}C$ and $\delta^{15}N$ of all the species sampled in a station. The isotopic diversity indices were computed with species accounting for at least 93% of the total station biomass.

All the functional and isotopic diversity indices (Table 25) are constrained between 0 and 1 (Villéger et al. 2008, Mouillot et al. 2013a) and all of them - except the functional and isotopic richness - are mathematically independent from the species richness. The functional and isotopic richness are influenced by the number of species because of the relationship between the number of points and the probability of having extreme values and therefore higher multidimensional convex hull volume (FRic) or area (IRic). All the indices - except functional and isotopic richness- were weighted using relative biomass. Biomass is directly related to secondary production, a key ecosystem function (Grime 1998). The functional and isotopic indices chosen for this study have similar interpretation either in the multidimensional functional space or in the bi-dimensional isotopic space. Functional/isotopic richness represents the amount of functional/isotopic space filled by a community. Functional/isotopic divergence represents the changes in the proportion of total biomass that is supported by species with the most extreme functional traits or stable isotope values. Functional/isotopic evenness measures how regularly the relative biomasses of the species is spaced in the functional/isotopic space. Functional/isotopic dispersion is calculated as the weighted average distance to the weighted average mean trait value/stable isotope value of the community. Hence, if a species is very dominant in abundance or biomass, then the weighted average mean trait value/stable isotope value will be very close to this species' position in the functional/isotopic space and consequently the functional/isotopic

dispersion will be small. Finally, functional originality/isotopic uniqueness quantifies how changes in species biomasses modify the closeness of species in the functional/isotopic space. Functional and isotopic indices provide two different visions of the community niche since trait-based indices inform on the fundamental niche of the community, while isotope-based indices inform on the realized niche of the community (Bearhop et al. 2004, Newsome et al. 2007, Devictor et al. 2010a). The different R functions and packages used to compute the different indices are presented in Table 25.

2.4. Disturbance proxy

We considered the abundance of *S. alveolata* adults to be a relevant proxy for the disturbance and the degradation of the reef (Dubois et al. 2002, 2006a, Jones et al. 2018). The *S. alveolata* adult abundance was preferred to the mean mud content as used in Jones et al. (2018) because across seasons, the *S. alveolata* adult abundance presented lower intra-station variability than the mud content. The *S. alveolata* adult abundance also presented lower intra-station variability than the *S. alveolata* adult biomass. Based on Dubois et al. (2006), an opercular crown diameter of 2 mm was set as the inferior limit to consider an individual as an adult. Using the total number of *S. alveolata* and the number of adults counted in each macrofauna core, a percentage of adults was calculated, allowing the computation of the mean *S. alveolata* adult abundance at the station level (3 replicates).

2.5. Data analysis

Our first objective was to investigate the link between the different functional and isotopic diversity indices and if they provided redundant or complementary information about the functioning of the engineered habitat across two contrasted seasons. Using the winter and summer matrix crossing the different indices and the stations, a winter and summer typology of the functional and isotopic indices was built on a Principal Component Analysis (PCA). Additionally, since all the indices were normally distributed (Shapiro-Wilk test, p-value < 0.05), the relationship between each pair of indices was investigated using Pearson correlations and the significance of the relationship using correlation tests (cor.test). The relationship with the species richness (SR) was also investigated and tested (see Appendix S2).

Our second objective was to investigate how the functional and isotopic diversity indices changed along a disturbance gradient at the scale of a biogenic habitat composed of engineered and associated sediments. We investigated this link in winter and in summer using the ten reef stations sampled for both season. The mean *S. alveolata* adult abundance was used as the disturbance proxy and hence as the explanatory variable in several models. Two functional forms were tested using the "lm" function in R: linear and quadratic. The linear model assumptions were verified by inspection of residual distribution plots and normality of residuals was verified using the Shapiro-Wilks test. The best model linking a disturbance proxy and a diversity index was selected based the adjusted R^2 and confirmed by the calculation of the Akaike Information Criterion (AIC).

For our third objective, the ten reef stations were displayed in a multidimensional space using their coordinates on the first three axis of the PCoA based either on a station by functional diversity (FD) indices matrix or on a station by isotopic diversity (ID) indices matrix. To produce the PCoAs, the Euclidian distance was calculated between pairs of stations characterized by their five functional diversity indices or their five isotopic diversity indices. The first three PCoA axis based on the FD or the ID indices calculated in winter or summer accounted for at least 78% of the total inertia. For both seasons, using the ten reef stations displayed using either their FD coordinates or their ID coordinates, the corresponding convex hull volume (CHV) was calculated and displayed on the axis 1-2 and axis 1-3. The convex hull based on the FD indices was considered as a proxy of the fundamental niche of the reef community, while the convex hull based on the ID indices was considered as a proxy of the realized niche of the reef community. The two convex hulls were displayed simultaneously for either winter or summer in order to visualize the overlap between the fundamental and realized niche of the reef at both seasons and the potential changes between winter and summer. The R function available in Bowes et al. (2017) was used to calculate the different convex hull volumes.

3. Results

3.1. Graphical representations of the different indices

Functional and isotopic diversity indices were computed for the ten reef stations sampled in winter and summer. As an example, Figure 34 illustrates the five functional diversity indices calculated for reef station 7 and 3 in winter and displayed on the first two PCoA axis (PC1 and PC2) and figure 35 illustrates the five isotopic diversity indices calculated for the same two stations in winter and displayed on the scaled isotopic biplot ($\delta^{13}C$ and $\delta^{15}N$). A clear shift in the dominant species in term of biomass is visible. Indeed, reef station 7 is dominated by one species, the engineer *S. alveolata* (92.2% of the total biomass) while in reef station 3, four species dominate in terms of biomass, the Japanese oyster *Magallana gigas* (57.0%), *S. alveolata* (25.1%), the porcellanid crab *Porcellana platycheles* (8.5%) and the slipper-limpet *Crepidula fornicata* (4.0%). Furthermore, the engineer species is located at the center of the isotopic space (white diamond in panel IDiv of Figure 35) while it is at the periphery of the functional space, as one of the convex hull vertices. The position of the key species relative to the center of gravity of the functional and isotopic space (peripheral position *vs* central position) directly influences the value of the functional and isotopic divergence (see section 2.3 and Table 25). Indeed, these indices are calculated as the weighted average deviation of the Euclidian distance between the position of all the species in the functional or isotopic space and the center of gravity of the convex hull vertices. It is worth noticing that *S. alveolata* and *M. gigas* are close in the functional and isotopic spaces. However, *P. platycheles* and *C. fornicata* are close to *S. alveolata* and *M. gigas* in the isotopic space but more distant in the functional space. The influence of the weighting when computing the indices is obvious

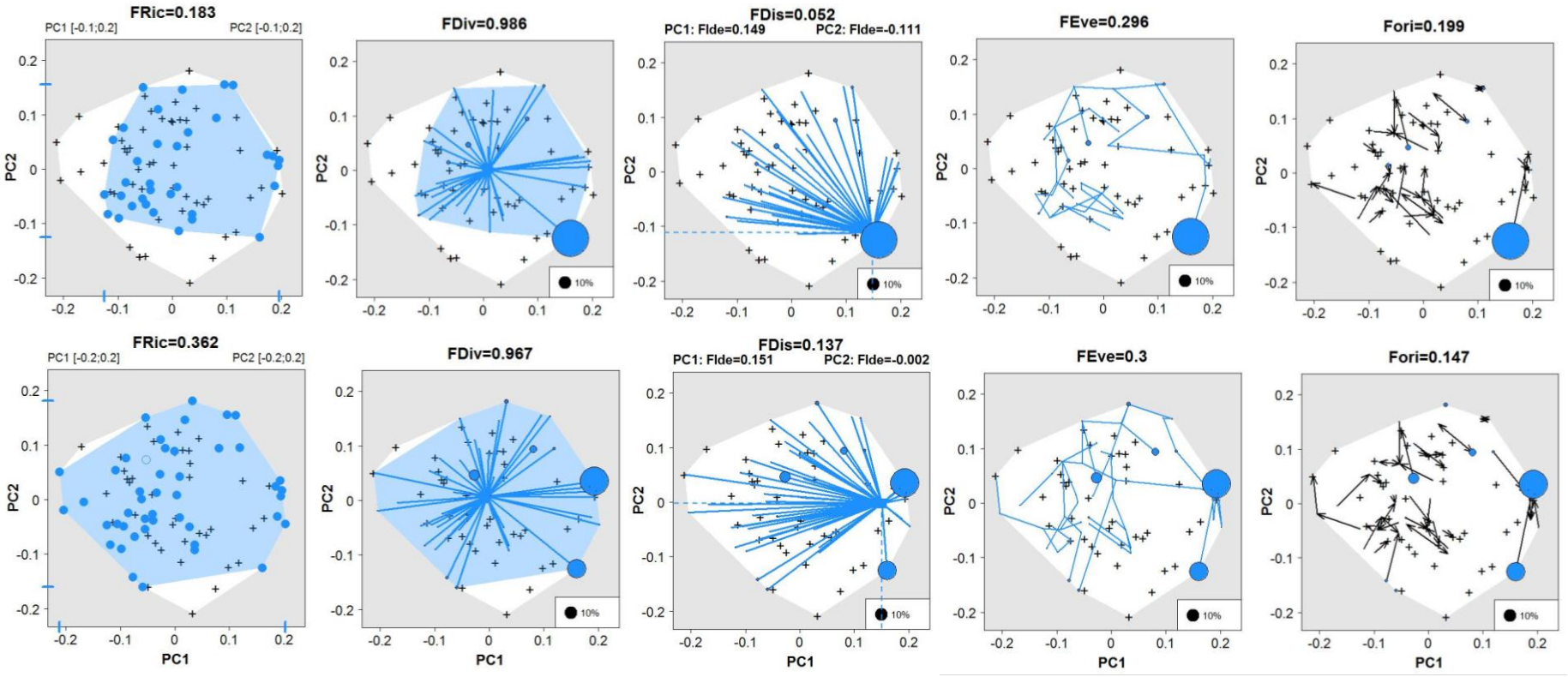

Figure 34. Two-dimensional (axis 1 and 2 of the PCoA) representation of the five functional diversity indices (Functional dispersion = FDis, functional richness = FRic, functional divergence = FDiv, functional evenness = FEve and functional originality = FOri) computed using the species identified in reef station 7 (top) and 3 (bottom) sampled in winter. Except for FRic, the dots represent the relative mean biomass of the species. In the FRic panels, the colored convex polygon is a projection of the multidimensional convex hull in 2D and the filled symbols are species being vertices in the multidimensional space. In the FDiv panels, the diamond represents the center of gravity of the vertices and the lines represent all the distances to it. In the FDis panels, the square represents the weighted-mean position of the species in the multidimensional space. In the FEve panels, the blue lines represent the minimum spanning tree linking all species in the multidimensional space. In the FOri panels, the black arrows represent the nearest species distances (black arrows). Finally, the black crosses indicate species present in the global pool of species recorded in the ten winter reef stations but absent of station 3 or 7. See Table 25 for the definition of each functional diversity index.

in the case of the functional dispersion (FDis) and isotopic dispersion (IDis). Indeed, this index is calculated based on the weighted-mean position of the species in the functional or isotopic space. In station 7, this position is confounded with the position of *S. alveolata* because of its very high biomass, while in station 3 the weighted-mean position is either shifted towards the center of gravity of the functional space or located between *M. gigas* and *S. alveolata* in the isotopic space, because the biomass is distributed between more species.

3.2. Typology of functional and isotopic diversity indices

The species richness was significantly correlated only to the functional richness and to the functional divergence in both winter (FRic: r = 0.956, p-value < 0.001, FDIv: r = -0.726, p-value = 0.017, Appendix S2) and summer (FRic: r = 0.962, p-value < 0.001, FDIv: r = -0.651, p-value = 0.042, Appendix S2). In winter, the first and second PCA axis explained 50.00% and 18.69% of the total variance, respectively, and the third axis accounted for an extra 13.42% (Figure 36). The isotopic divergence was significantly and positively associated with the first PCA axis (p-value = 0.048, r = 0.64) but did not display a clear grouping with the other indices which were significantly and positively associated with the first PCA axis (FRic, FDis, IRic, IDis, p-value < 0.04). This was confirmed by the Pearson correlations (Appendix S2), since the IDiv did not display any significant correlations with other indices (p-value > 0.05). The functional divergence and originality were also significantly associated to the first axis (p-value < 0.0015) but displayed negative correlations (|r| > 0.86). The isotopic evenness and uniqueness were significantly (p-value < 0.008) and oppositely associated to the second PCA axis (IEve: r = 0.84 and IUni: r^2 = -0.78) and significantly correlated (r = -0.774, Appendix S2). Finally, the only index significantly associated to the third axis was the functional evenness (p-value = 0.0012, r = 0.87), demonstrating an original behavior.

In summer, the first and second PCA axis accounted for 53.34% and 20.47% of the total inertia, respectively, while the third axis accounted for 9.87% (Figure 36b). As for winter, FDis, FDiv and IDis were all three strongly associated with the first PCA axis either positively (FDis and IDis, p-value < 0.014) or negatively (FDiv, p-value = 0.00014, r = -0.92). Contrary to winter, the isotopic divergence was also strongly associated to the first axis (p-value = 0.00017, r = 0.92). The indices based on the minimum spanning tree (FEve and IEve) or neighbor distances (FOri and IUni) displayed a different behavior than in winter. Indeed, IEve and IUni were this time significantly and negatively associated to the first PCA axis (p-value < 0.0072 and |r| > 0.78), FEve was significantly and positively associated to the second axis (p-value < 0.001 and r = 0.95) and FOri to the third axis (p-value = 0.0034 and r = 0.82). The two richness indices also showed a different pattern than in winter, since FRic correlated with the second axis (p-value = 0.036 and r = 0.66) while IRic did not significantly correlate with any axis. Overall, the functional divergence and dispersion were redundant but since FDis presents larger variations than FDiv (see Figures 34, 35 and 37), it could be more sensitive to changes and hence be a better divergence index in the case of an engineered habitat like a *S. alveolata* reef. In our case, FDis

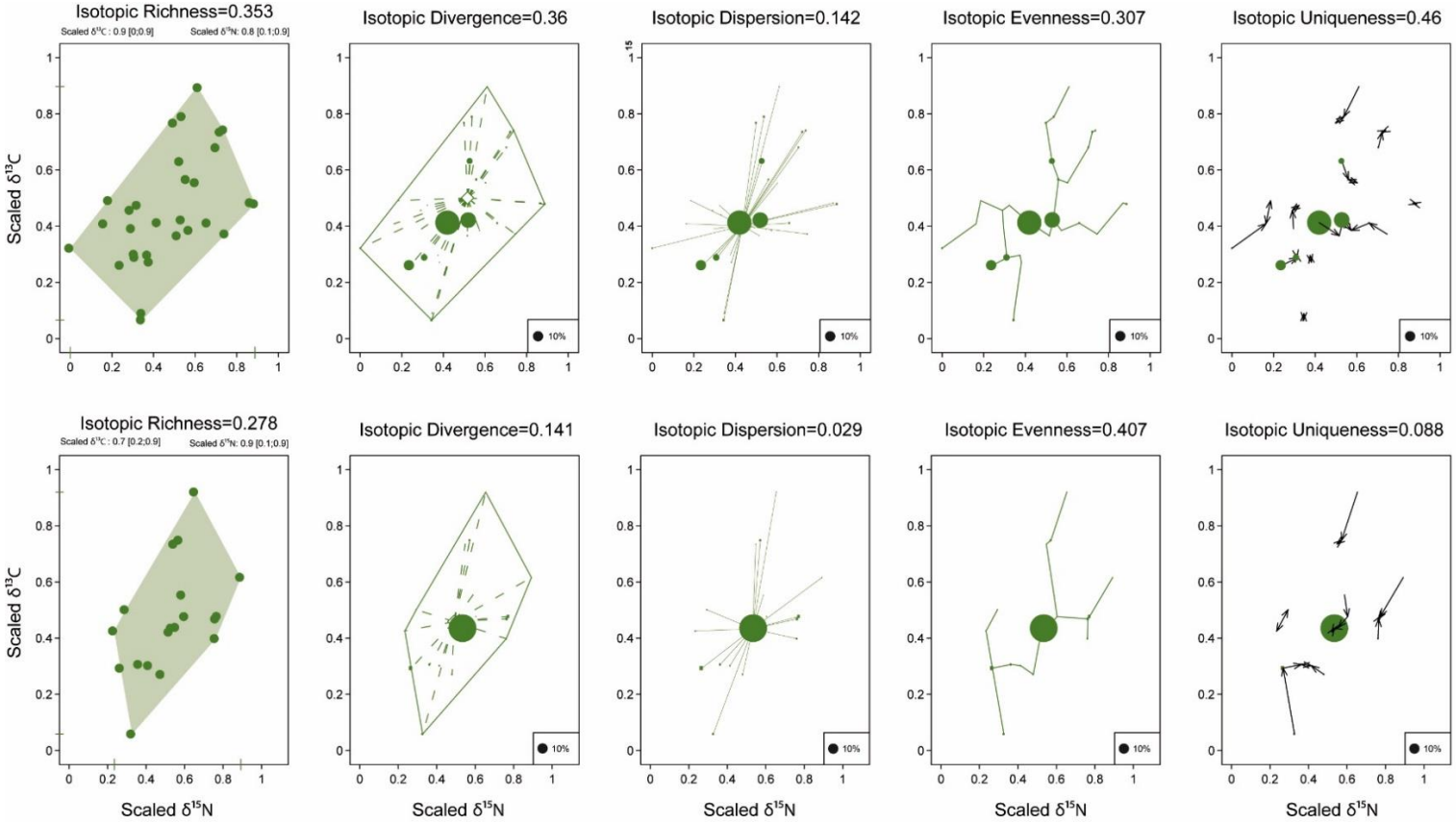

Figure 35. Isotopic biplot illustrating the five isotopic diversity indices computed for the reef station 7 (top) and 3 (bottom) sampled in winter. Prior to calculating the indices, the isotopic compositions of all species were standardized over the entire range of the measured winter values. In each panel, points represent the species' position (mean value measured at the station level) in the isotopic niche space and the point's size represents the species' relative biomass (mean value measured at the station level). The isotopic richness (colored area) measures the convex hull area, and the filled points are species being vertices in the bi-dimensional isotopic space. The isotopic divergence is illustrated through the center of gravity of the vertices (white diamond) and all the distances to it (dashed lines). The isotopic dispersion is illustrated with the weighted center of gravity of all points and all the distances to it (lines). The isotopic evenness is illustrated with the minimum spanning tree linking all points in the bi-dimensional isotopic space. The isotopic uniqueness is illustrated with all the nearest species distances (black arrows). See Table 25 for the definition of each isotopic diversity index.

and IDis also appeared as redundant. This pattern is caused by how the index is calculated and the relative positions of the dominant species in the functional and isotopic spaces, and very probably case specific. The other indices displayed variable grouping patterns according to season indicating they could be interesting to detect temporal changes.

3.3. Linking disturbance to functional and isotopic diversity indices

Using *S. alveolata* adult abundance as an indicator of perturbation, we investigated how the different indices changed when the reef became increasingly disturbed (Figure 37 and Table 26). In winter, the functional divergence and originality increased linearly with the increase of *S. alveolata* adult abundance (p-value < 0.01), meaning these two indices are lowest for a maximally disturbed reef. The *S. alveolata* adult abundance explained respectively 50% and 57% of the total variability of FDiv and FOri. On the other hand, the function dispersion and the isotopic richness both decreased linearly with the increase of *S. alveolata* adult abundance (p-value < 0.03), meaning these two indices are highest for a maximally disturbed reef. The disturbance proxy explained respectively 40% and 55% of the total variability of FDis and IRic.

In summer, a significant relationship was also found between the disturbance proxy and the isotopic richness (concave form: p-value = 0.03), the functional dispersion (concave form: p-value = 0.07) and the functional originality (linear model with a positive slope: p-value = 0.01). The *S. alveolata* adult abundance explained 52% of the IRic total variability, 40% of the FDis total variability and 52% of the FOri total variability. Two other significant relations were detected, both convex quadratic fits, between the disturbance proxy and the isotopic evenness (p-value = 0.08) and uniqueness (p-value = 0.09). The *S. alveolata* adult abundance explained 37% and 35% of the total variability of IEve and IUni respectively.

3.4. Functional and isotopic diversity indices as niche proxies

Using the functional and the isotopic diversity indices of each station and represented with a PCoA, the FD and ID convex hull volumes (CHV) were calculated based on the first three PCoA axis (Figure 38). The FD convex hull was considered as a proxy of the reef's fundamental niche while the ID convex hull was considered as a proxy of the reef's realized niche. The realized niche based on the species' carbon and nitrogen isotopic compositions was 16 and 3 times larger in winter and summer respectively, than the fundamental niche based on the species' biological traits (Figure 38). Overall, the realized niche became narrower between winter and summer, with the summer niche representing 0.67 of the winter niche, while the fundamental niche became larger between winter and summer, with the summer niche being 3.2 times bigger than the winter one. In winter, the fundamental niche was completely included in the realized niche whatever the axis considered (1-2 or 1-3) while in summer, the fundamental niche was completely included in the realized niche only when considering axis 1 and

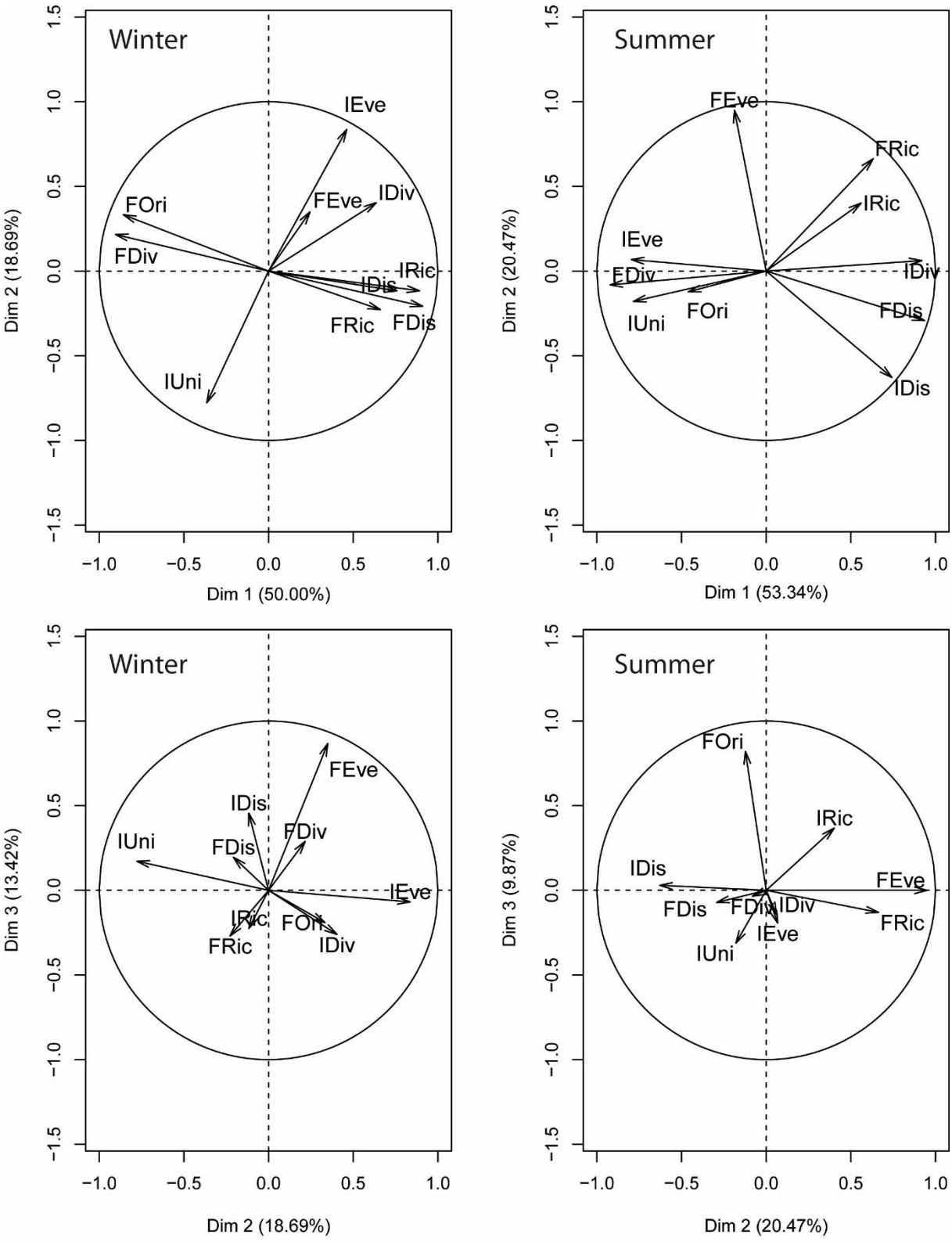

Figure 36. Principal Component Analysis (PCA) carried out on the ten reef stations sampled in winter (left panels) and summer (right panels). The five functional diversity indices and the five isotopic diversity indices are represented in the first two dimensions (top) and in the second and third dimensions (bottom). See Table 25 for the full names of the different indices.

3. When considering the axis 1 and 2 in summer, station 5 based on its FD indices caused the fundamental niche to have a small part not overlapping with the realized niche.

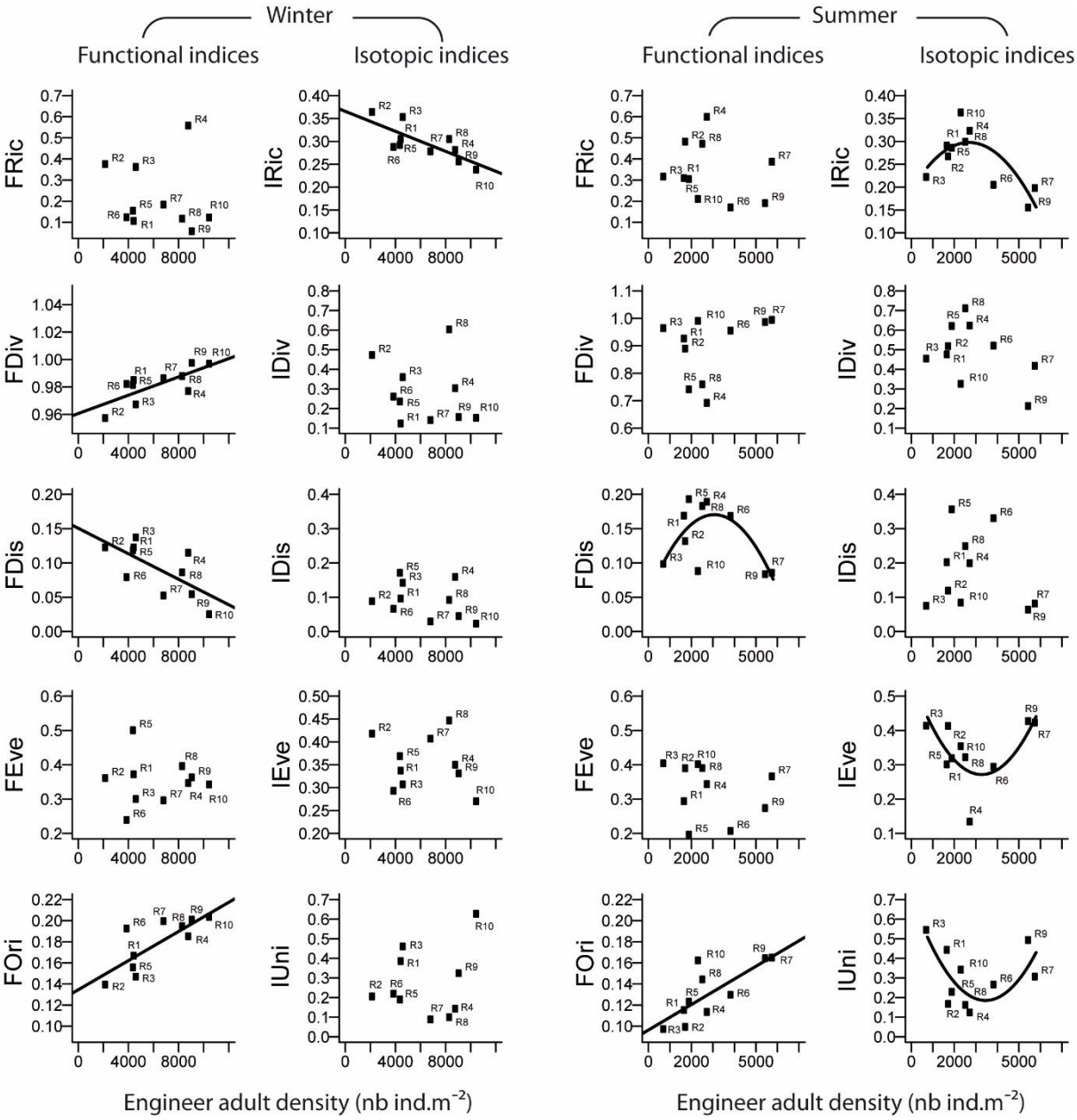

Figure 37. The five functional indices (FRic, FDiv, FDis, FEve, FOri) and the five isotopic indices (IRic, IDiv, IDis, IEve, IUni) plotted against the engineer adult density (number of adults m^{-2}), our disturbance proxy, in winter and summer using the ten sampled stations (R1 to R10). The best identified functional form (see Table 26) between linear and quadratic models is displayed on the corresponding graph. In some cases, no significant relationship was detected between the disturbance proxy and the investigated index, hence no functional form is displayed. All the indices except FRic and IRic are weighted using the relative biomass of each species. See Table 25 for the full names of the different indices.

Table 26 Best models significantly explaining the different community functional and isotopic diversity indices in winter and summer with the corresponding adjusted R^2 (R^2) and model p-value (p-value). Two models were tested to evaluate the relation between a community diversity index and a disturbance proxy: linear and quadratic. Only the best one is indicated. The *S. alveolata* adult abundance was used as the disturbance proxy and consequently as the explanatory variable. The sign of the slope for linear models or the form of the quadratic model are indicated. All the intercepts are significant at a p-value < 0.001 and the value of the intercept is indicated since it corresponds to a reef without any *S. alveolata*, potentially equivalent to a non-engineered sediment. All the indices are weighted by the biomass except the functional richness (FRic) and the isotopic richness (IRic). See Table 25 for the full names of the different indices. A significant level of 0.1 is considered.

Community indices	Best model	Slope	Intercept value	R^2	p-value
Winter					
FDiv	linear	+	0.96	0.50	0.01
FDis	linear	-	0.15	0.40	0.03
FOri	linear	+	0.13	0.57	0.007
IRic	linear	-	0.37	0.55	0.009
Summer					
FDis	quadratic	concave	0.14	0.40	0.07
FOri	linear	+	0.96	0.52	0.01
IRic	quadratic	concave	0.26	0.52	0.03
IEve	quadratic	convex	0.34	0.37	0.08
IUni	quadratic	convex	0.31	0.35	0.09

4. Discussion

This article represents a first attempt at understanding how functional and isotopic diversity indices behave in the context of an engineered habitat affected by increasing disturbances. Indeed, trait-based and isotopic-based indices are often used independently to understand the impact of disturbances (*e.g.* habitat degradation, non-native species, green tides) on either the trophic functioning of an ecosystem (Layman et al. 2007b, Sagouis et al. 2015, Quillien et al. 2016) or on the overall functioning of an ecosystem estimated using biological traits (Villéger et al. 2010, Villnäs et al. 2011, Hejda and de Bello 2013). Jointly using these two types of indices can inform on their potential redundancy or complementarity and help us detect indices more sensitive to habitat disturbance. These sensitive indices could inform early on, on potential functional changes of the ecosystem linked to increasing disturbances.

4.1. Complementary and redundant facets of functional and isotopic diversity

Our results first indicate that the functional dispersion and divergence are strongly linked and can be considered as redundant even if they are negatively correlated (r (winter) = -0.773 and r (summer) = -0.826). This strong correlation is not a general property of these indices.

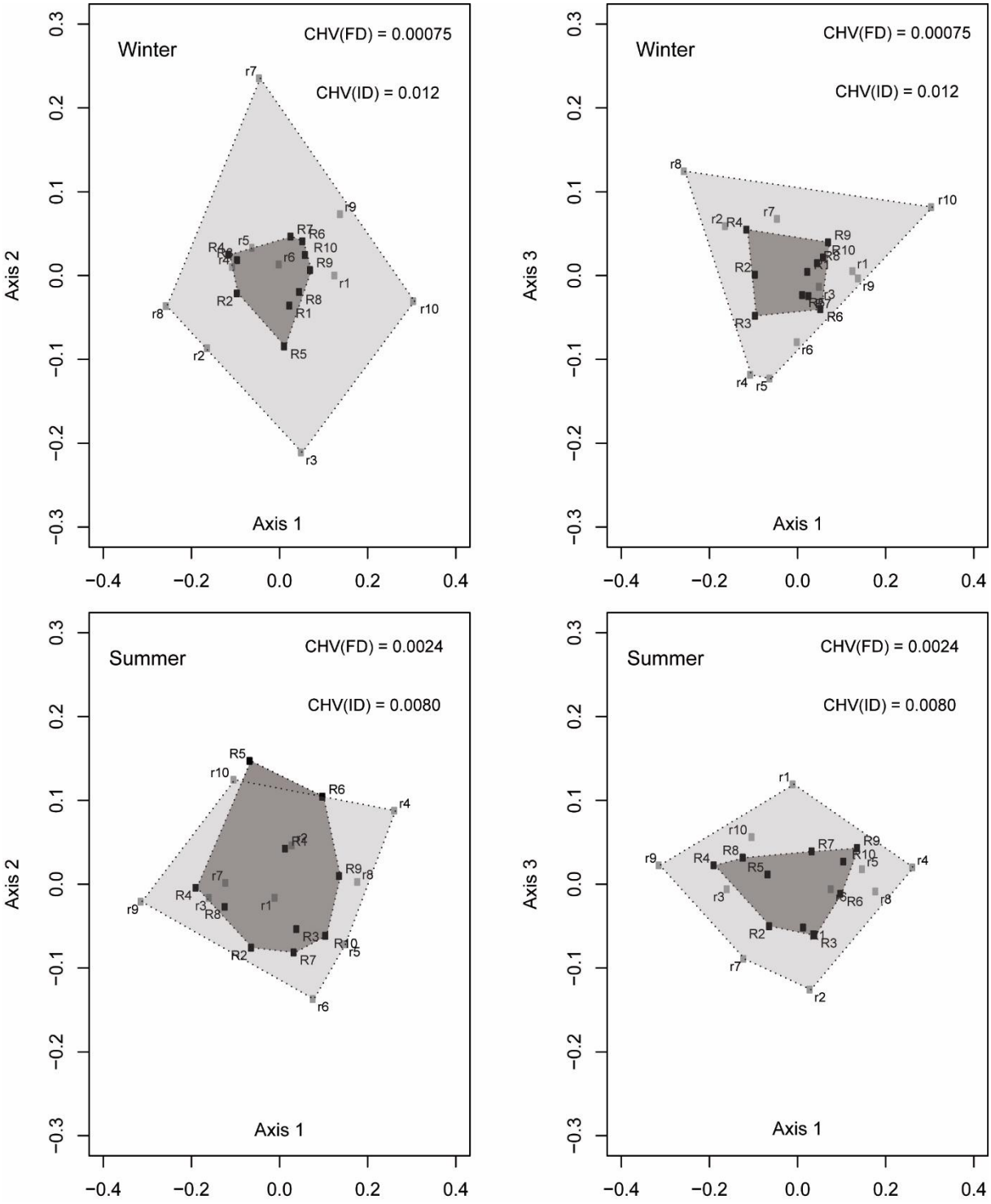

Figure 38. Winter (top) and summer (bottom) convex hulls displayed on the axis 1-2 and 1-3 of the PCoAs. The convex hulls are calculated using the position of the ten stations (sampled in winter or summer) in the first three dimensions of the PCoA based on either the stations by functional diversity (FD) indices matrix (dark grey area, black points) or the stations by isotopic diversity (ID) indices matrix (light grey area, light grey points). The values of each convex hull volume (CHV) based on the FD or the ID indices are displayed on the graphs along with the station number (1 to 10) and position based on the FD (*e.g.* R1) or ID (*e.g.* r1) indices.

Laliberté and Legendre (2010) demonstrated using *in silico* communities drawn randomly from a common pool, that these two indices were only moderately correlated (r = 0.457). In our case, their negative correlation comes from the strong dominance of the engineer species and its position in the functional space. Indeed, at both seasons *S. alveolata* is located on the edge of the functional space (as a convex hull vertex) and represents often over 50% of the station biomass (Figure 34). The functional divergence, which is measured relatively to the unweighted center of gravity of the functional space and informs on the proportion of the total abundance or biomass represented by species with extreme trait combinations, is hence very high and close to 1 whatever the disturbance level. Differently, the functional dispersion is measured relatively to the weighted-mean position of the species in the functional space, which in the case of a habitat over-dominated by a species, like a habitat structured by an ecosystem engineer, will be very close to the dominating species. Hence, the overall weighted-distance between the different species and this weighted-mean position a.k.a. the functional dispersion will be very small in stations where *S. alveolata* is over-dominant like station 7 in winter (Figure 34, FDis = 0.052). Interestingly, a similar redundancy between functional dispersion and divergence was found by (Mouchet et al. 2010), using theoretical species assemblages responding to different assembly processes. Functional dispersion *per se* was not used by Mouchet et al. (2010) but a very closely related index (Rao's quadratic entropy) showed high correlation with the functional dispersion (r = 0.966) developed in Laliberté and Legendre (2010). These different results seem to indicate that the coupled behavior of these two indices could be strongly linked to the ecological processes shaping the communities under investigation. Under random assembly, these two indices behave differently and can provide complementary information, while under limiting similarity they seem to be redundant, as indicated by our study case. Indeed, functional divergence (FDiv) values over 0.9 indicate that limiting similarity is the assembly process shaping the community (Mouchet et al., 2010) and we found FDiv values superior to 0.9 for all the reef stations except three in summer (stations R4, R5 and R8). Consequently, the main assembly process shaping the *S. alveolata* reef community is limiting similarity, with a few reef zones behaving differently in summer.

Furthermore, functional dispersion and isotopic dispersion behaved similarly and were positively correlated, at both seasons (r (winter) = 0.845 and r (summer) = 0.880). Even though no other study has jointly calculated these two indices, it is likely that the observed correlation is specific for engineered habitat and not a general property of these two indices. In our study, these two indices are redundant because of the relative proximity in the functional and isotopic space of the two dominant species in terms of biomass, *S. alveolata* and *Magallana gigas*, another suspension-feeder presenting an isotopic niche close to that of the honeycomb-worm (Jones et al., in prep). In a similar case-study, Rigolet et al. (2015) explored how multiple isotopic diversity metrics either previously developed (Layman et al. 2007a, Jackson et al. 2011) or newly adapted from functional diversity indices (Mouillot et al. 2013a), performed in the context of two benthic communities, a community engineered by the amphipod *Haploops nirae* and the surrounding non-engineered *Amphiura filiformis* community. They

found that isotopic divergence and dispersion behaved in a similar way and discriminated well the two communities while isotopic evenness and originality (equivalent to isotopic uniqueness) formed a second group of indices, less important in discriminating the two communities. We did not observe IDis and IDiv behaving similarly. Indeed, in our case isotopic divergence displayed a relatively atypical behavior in winter while in summer it grouped with isotopic dispersion and functional divergence along the first PCA axis, as observed by Rigolet et al. (2015). Between winter and summer, isotopic divergence increases overall (Figure 37), meaning that key species have more extreme isotopic compositions in summer than in winter. Since the isotopic compositions of the different food sources at the base of the reef food web are relatively constant in time (Jones et al., in prep), this increase indicates that in summer a larger resource pool is used by the reef species. Differently, in winter the dominant species rely on a smaller pool of resources, as expected because of the generally lower primary production in the water column. Consequently, isotopic divergence could be a good index to detect temporal shifts in the use of food resources by the dominant species of a community.

Mouchet et al. (2010) and Rigolet et al. (2015) revealed the relatively independent behavior of the functional and isotopic richness compared with other indices. A similar trend was observed in this study since they did not group with the same indices in winter and summer, indicating a temporally variable behavior when measured over two contrasted seasons. These two indices also provide complementary information about the functioning of the community as revealed by their low correlation (r (winter) = 0.452 and r (summer) = 0.372). In addition, since these two indices are unweighted, they also provide measures of community functioning unaffected by the dominance of the engineer species. Interestingly, the functional richness is very highly correlated with species richness while the isotopic richness is not. This indicates that the species pool associated to a *S. alveolata* reef present rare trait combinations, hence increasing the FRic (see Figure 34), while in terms of isotopic composition, these species have similar foraging behaviors, feeding movements or trophic relations with other species (*e.g.* competition and predator-prey interaction).

Finally, the indices based on the minimum spanning tree (FEve and IEve) or neighbor distances (FOri and IUni) displayed season-specific grouping patterns, either providing complementary information (winter) or displaying a more random behavior (summer). Functional evenness is known to be an independent component of functional diversity (Villéger et al. 2008, Mouchet et al. 2010) performing poorly when it comes to discriminating between assembly processes (Mouchet et al. 2010). In addition, Rigolet et al. (2015) recommended being cautious when interpreting isotopic evenness changes. In theory, functional and isotopic evenness inform on how evenly distributed species are in the functional or isotopic space. The weighting of this index by the abundance or the biomass seems to induce random responses, especially in communities with unbalanced species distributions, such as estuarine communities (van der Linden et al. 2016) or those structured by an ecosystem engineer (Rigolet et al. 2015). Our study points towards the risk of using this index to detect stable patterns. In this regard, the functional originality and isotopic uniqueness are more straightforward in their

calculation and inform on the redundancy in the functional and trophic strategies displayed by the dominant species. These indices also give a sense of the packing of species in the functional and isotopic space as do FEve and IEve. Despite easier interpretation, FOri and IUni displayed different behaviors between winter and summer, indicating they should be used with caution.

4.2. How do functional and isotopic diversity indices respond to disturbance?

According to Mouillot et al. (2013), functional richness, divergence, dispersion, evenness and originality are predicted to decrease following environmental disturbance. Along an increasing disturbance gradient, functional divergence and evenness could rapidly decrease providing an early warning signal of disturbance impacts. In their study, Cucherousset and Villéger (2015) give leads on how their different indices could change after a disturbance, but they focus on fish communities invaded by a non-native species, which is very far from our biological model. Nonetheless, using our knowledge of *S. alveolata* reefs and how they change under increasing disturbance, we can build some hypothesis. First, the presence of any engineered structure actually represents a form of disturbance relative to the non-engineered ecosystem, but since engineered habitats tend to increase the local biodiversity (Jones et al. 1997, Bouma et al. 2009) they are often considered positively and hence not considered as disturbances.

In this study, we investigated how functional and isotopic diversity indices vary when the reef changes because of multiple and concomitant disturbances linked to a decrease in the spatial pressure exerted by the engineer species. Multiple changes can be observed in reef parts qualified as more disturbed (Dubois et al. 2002, 2006a, Jones et al. 2018) and it is very hard to disentangle which disturbance came first and led to other disturbances. Indeed, both natural (storms) and anthropogenic (trampling) disturbances can physically damage the reef, generally leading to a decrease in the engineer species density, which can be counter-balanced by a higher recruitment since more space is available to new recruits. For the investigated reef, where space is freed, mud tends to deposit while forming new micro-habitat for normally muddy organic rich soft-sediment invertebrates (Jones et al. 2018). Meanwhile other suspension-feeding species like *M. gigas* establish because of available spaces. The establishment of *M. gigas* on the reef has been shown to increase the species richness and modify the species assemblages (Dubois et al. 2006a), a change linked to the oyster shells, which provide a secondary hard substratum and to the local increase in mud and organic content caused by the important quantities of feces and pseudofeces produced by oysters.

Jones et al. (2018) showed that increasing mud content leads to a higher species turnover and an increase in associated fauna abundance, in summer. This change in presence/absence- and abundance-based beta diversity was not observed in winter, indicating community changes are probably linked to spring and summer recruitment. Furthermore, in the more degraded reef sections, benthic primary production in the associated sediments is higher as detected using multispectral images (Jones et al., in prep). These different changes could lead to an increase of the trophic niche and a higher

diversity in diets (mixtures) for deposit-feeding species presenting original trait combinations, along with a new pool of species exploiting local food sources like bacteria. Overall, one can expect an increase of the functional and isotopic richness, along with an increase of the functional dispersion linked to a more even distribution of the biomass between species. A decrease in the isotopic uniqueness in summer is expected because of the higher abundance of species in the more disturbed reef sections leading to a potential higher trophic redundancy.

The investigated engineered habitat did not respond to increasing disturbances as predicted by Mouillot et al. (2013), which hints towards an original response of benthic habitats engineered by primary consumers like oyster reefs, mussel beds or amphipod tube mats, to increasing disturbances. The only index that did was the functional divergence in winter. Nonetheless, the very low variability in our habitat (often less than 0.1) and the absence of a significant relation with disturbance in summer does not make this metric a suitable early-warning signal of disturbance. The expected increase in functional dispersion and isotopic richness was only verified in winter, while in summer these two indices displayed a convex quadratic relation with disturbance. A closer look at the association of the winter and summer models reveals a peak of the isotopic richness and functional dispersion around a density of 4000 adult engineers in winter and between 2000 and 3000 in summer, corresponding to maximally disturbed stations in winter but to stations presenting an intermediate level of disturbance in summer. In these zones of the reef, trophic niche estimated by the isotopic richness is the largest indicating the exploitation of a larger pool of resources. Counterintuitively, in these same reef zones, the isotopic evenness and uniqueness are also minimal indicating higher inter-specific competition and an uneven distribution of food among organisms. Jones et al. (in prep) showed that at the scale of a whole reef, inter-specific competition between the two dominant suspension-feeders, *S. alveolata* and *M. gigas*, was virtually inexistent. Nonetheless, high trophic competition was observed between secondary suspension-feeders (biomass-wise) like *P. platycheles* and *C. fornicata*, which could led to the observed concave curve in summer.

Functional dispersion appears as a very promising index in the case of a *S. alveolata* reef. Indeed, functional dispersion weighted with abundance has proven to be a very good indicator of the reef's overall biogeochemical functioning measured using a multifunctionality index (Jones et al., in prep). Multifunctionality was maximal when functional dispersion was around 0.15-0.20 corresponding to the peak value reached in this study for an adult density of 2000-3000 in summer. Using the results of these two studies, we could consider a reef presenting an adult *S. alveolata* density of between 2000 and 4000 individuals.m^{-2} as functioning optimally at least in term of organic matter and nutrient cycling. Complementary studies focusing on the primary production measured inside the engineered sediments and on the reef's secondary production are necessary to generalize this finding, but it is already a first step towards a more integrated understanding of the reef's functioning. In this context, the isotopic richness could be an interesting index to consider in association with the functional dispersion in order to have a more trophic orientated vision of the reef's functioning.

4.3. *Sabellaria alveolata* reefs and facilitation

Building from the framework proposed by Devictor et al. (2010) to measure fundamental and realized niche, we considered our five functional diversity (FD) indices as a good representation of the potential or fundamental niche of each reef station and our five isotopic diversity (ID) indices as informing on the actual or realized niche of each reef station considered from a trophic point of view. The convex hull based on the ID indices, proxy for the realized niche, was 3 (summer) to 16 (winter) times larger than the FD convex hull, proxy for the fundamental niche. Until recently, the fundamental niche of a species was always considered to be larger than its realized niche because mechanisms such as dispersal limitation, negative biotic interactions (*e.g.* competition, predation) or disease prevented the species from arriving and/or surviving in certain locations where the environmental conditions were nonetheless suitable (Hutchinson, 1957). Extending this concept to communities meant that the realized niche of a community was always smaller than its fundamental niche because of competitive exclusion, hence completely excluding positive biotic interactions such as facilitation (Bruno et al. 2003), that have the potential to drastically increase a community's realized niche. Indeed, facilitation leads to the survival of species in physical or niche space they could not occupy if they were alone and not benefiting from positive interspecific interactions. Our results are clearly in line with ecological models including facilitation where realized niche is larger than the spatial range predicted by the fundamental niche (Bruno et al. 2003). Many intertidal engineer species like mussels, macroalgae or cordgrass, create complex habitats that reduce local pressures such as predation or thermal stress, whilst increasing biodiversity (Bouma et al. 2009). Ultimately, these favorable environmental changes can lead to a larger realized niche compared to the fundamental niche, as reported for mussels and barnacles in *Ascophyllum nodosum* canopies by (Bertness et al. 1999).

There are different mechanisms considered under the global term of facilitation such as habitat amelioration, predation refuge, resource enhancement and recruitment enhancement. In the case of *S. alveolata* reefs, habitat amelioration, resource enhancement and recruitment enhancement are very probably acting in synergy leading to the large realized niche, as suggested by previous studies (Jones et al. 2018). Indeed, *S. alveolata* reefs are composed of many micro-habitats like ponds, holes and unoccupied tubes were normally subtidal species can survive like the gastropod *Crepidula fornicata* (Jones et al. 2018). Furthermore, the presence of green algae growing on the reefs and of benthic microalgae growing on the associated sediments and on the mud present between the engineer tubes, are examples of resource enhancement leading to an increase of the reef's trophic niche compared with a control non-engineered soft sediment (Jones et al., in prep). Finally, the reef habitat has a strong recruitment potential enhanced in more disturbed reef sections, which shapes the associated fauna composition and abundance especially in summer (Jones et al. 2018).

The increase of the fundamental niche between winter and summer further supports the theory that the reef has a strong recruitment potential, and even more so for species presenting unique trait

combination compared with the winter community. This seems to indicate that functional rarity is high in the reefs in summer potentially supporting vulnerable and probably disregarded functions because of how estimate functioning and the overwhelming dominance of a few species. For example, Mouillot et al. (2013a) revealed that in high-diversity ecosystems like coral reefs, alpine plants and tropical trees, the most distinct combinations of traits were predominantly supported by rare species, indicating a very likely functional loss if these species became extinct. Finally, the decrease of the realized niche between winter and summer is probably linked to the variability in food sources available to the reef macrofauna. Since phytoplankton production is low in winter (Arbach Leloup et al. 2008), benthic primary production is particularly important for both suspension- and deposit-feeders during these months (Lefebvre et al. 2009). In addition, *S. alveolata* reef has been shown to enhance benthic primary production in its vicinity in both winter and summer (Jones et al. 2018), as do other engineered habitats like oyster reefs (Echappé et al. 2017) and mussels beds (Engel et al. 2017). When phytoplankton production increases in spring, it becomes a very abundant and accessible food sources for both suspension- and deposit-feeders. Consequently, during the spring and summer months, the reef macrofauna will rely mostly on pelagic-derived organic matter, leading to an overall decrease in its isotope-based realized niche. In comparison, during the colder months the macrofauna has to really on a more diverse array of food sources like benthic microalgae or green macroalgae (Jones et al. 2018) visible through the larger winter realized niche.

Conclusion

This study investigates for the first time coupled approaches between trait-based and isotope-based indices in the context of an engineered habitat like *S. alveolata* reefs. The main goal was to detect indices responding to disturbances, which could also be linked to measured ecosystem functions like biogeochemical fluxes (Jones et al., in prep). This study revealed the strong potential of functional dispersion as an index responding to disturbances and predicting ecosystem multifunctionality. The combined use of this index either as an explanatory variable in biodiversity-ecosystem functioning models or as a response variable along a disturbance gradient indicated that reef functioning could be maximal for adult engineer densities ranging from 2000 to 4000 individuals.m^{-2}. It would be interesting to see if other functions like secondary production are maximal for functional dispersion values around 0.15-0.20 (Jones et al. in prep) and what is the corresponding disturbance level. In a more global perspective, following other *S. alveolata* reefs in terms of engineer density, functional dispersion and functions like biogeochemical fluxes, could lead to the formulation of an integrative health index for these key European habitats. Finally, the joint use of functional and isotopic diversity indices as proxies of the fundamental and realized niche of the reef respectively, revealed that facilitation was the dominant mechanism shaping the reef community, as previously hypothesized (Jones et al. 2018) and demonstrated for other intertidal engineered habitats (Bertness et al. 1999, Bruno et al. 2003).

Appendix

Appendix S1. Winter (top) and summer (bottom) graphical outputs of the R function "quality_funct_space_fromdist", which is a simplified version of the R function available in (Maire et al. 2015) and is available at http://villeger.sebastien.free.fr/Rscripts.html. This function calculates the mean squared deviation between the initial distance between species (Gower distance) and the Euclidian distance between species computed from the functional space composed of two to ten dimensions. This function was run using the winter and the summer Gower distance matrix computed using the winter and summer species by traits matrices. The quality of the dendogram calculated using the unweighted pair group clustering method with arithmetic averages (UPGMA) and used to calculate the FD index of (Petchey and Gaston 2002) is also presented in red.

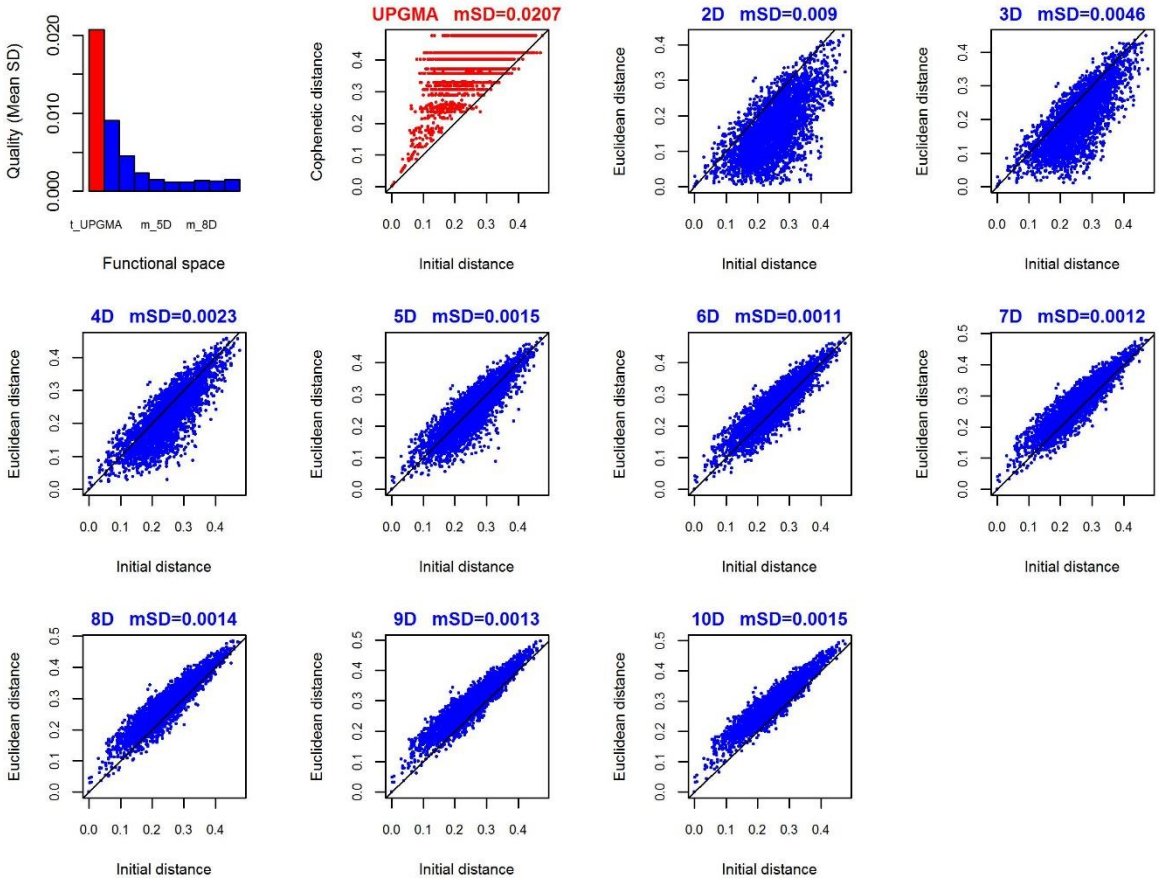

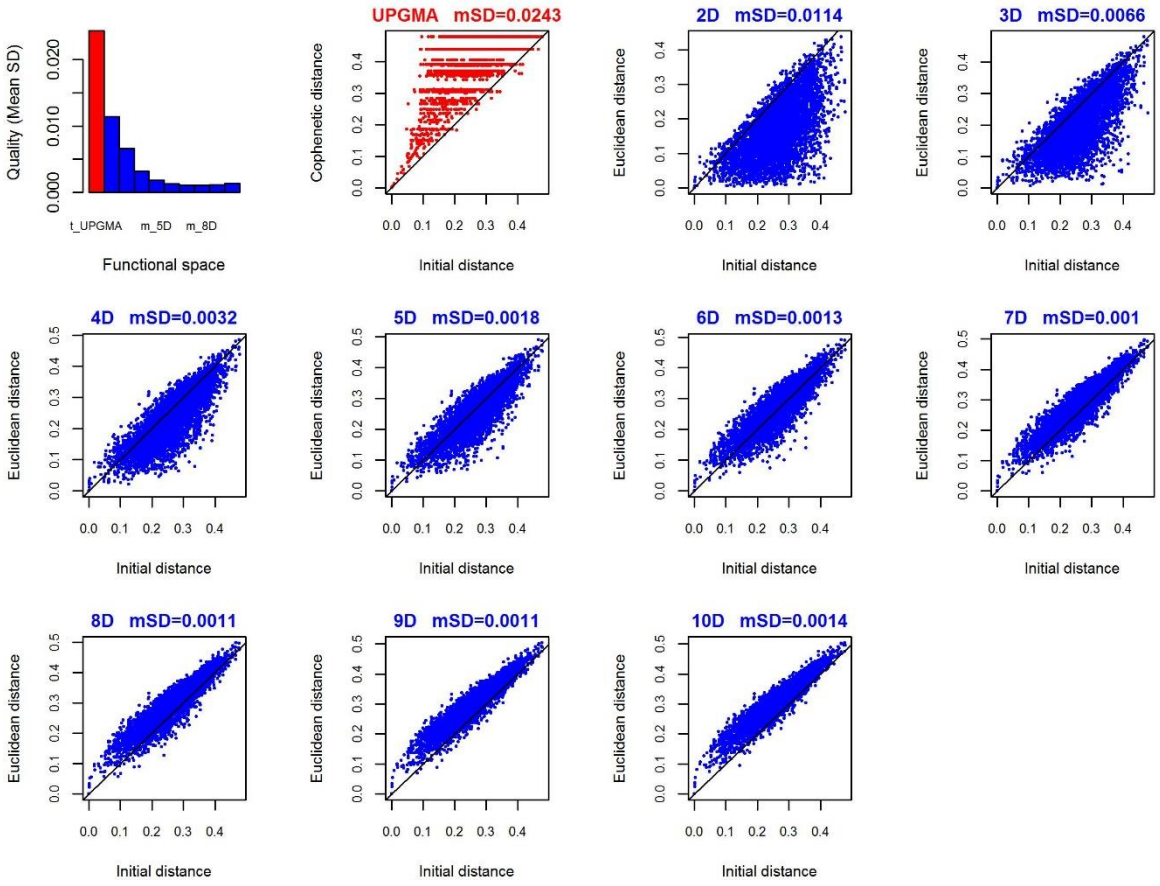
Quality (Mean SD)
0.000
0.010
0.020
t_UPGMA
m_5D
m_8D
Functional space
UPGMA mSD=0.0243
Cophenetic distance
Initial distance
2D mSD=0.0114
Euclidean distance
Initial distance
3D mSD=0.0066
Euclidean distance
Initial distance
4D mSD=0.0032
Euclidean distance
Initial distance
5D mSD=0.0018
Euclidean distance
Initial distance
6D mSD=0.0013
Euclidean distance
Initial distance
7D mSD=0.001
Euclidean distance
Initial distance
8D mSD=0.0011
Euclidean distance
Initial distance
9D mSD=0.0011
Euclidean distance
Initial distance
10D mSD=0.0014
Euclidean distance
Initial distance

Appendix S2. Pearson correlation coefficients between the species richness (SR) and the different functional and isotopic diversity indices (bottom half) and the result of the associated correlation test (upper half). The correlation coefficients and the tests were calculated using the ten reef stations sampled in (a) winter and (b) summer and the significant correlation coefficients (p-value < 0.05) are in bold. All the indices except SR, FRic and IRic are weighted using the relative biomass of each species. See Table 25 for the full names of the different indices.

(a)	SR	FRic	FEve	FDiv	FDis	FOri	IRic	IDiv	IDis	IEve	IUni
SR	1	***	NS	*	NS	NS	NS	NS	NS	NS	NS
FRic	**0.956**	1	NS	*	NS	NS	NS	NS	NS	NS	NS
FEve	-0.165	-0.121	1	NS	NS	NS	NS	NS	NS	NS	NS
FDiv	**-0.726**	**-0.709**	0.074	1	**	**	***	NS	NS	NS	NS
FDis	0.541	0.542	0.254	**-0.773**	1	**	**	NS	**	NS	NS
FOri	-0.447	-0.440	-0.291	**0.849**	**-0.861**	1	**	NS	*	NS	NS
IRic	0.538	0.452	-0.010	**-0.906**	**0.806**	**-0.859**	1	NS	NS	NS	NS
IDiv	0.436	0.331	0.121	-0.511	0.394	-0.318	0.612	1	NS	NS	NS
IDis	0.530	0.561	0.470	-0.519	**0.845**	**-0.638**	0.463	0.328	1	NS	NS
IEve	0.188	0.109	0.378	-0.278	0.219	-0.164	0.383	0.586	0.124	1	**
IUni	-0.184	-0.192	-0.128	0.218	-0.203	-0.026	-0.182	-0.388	-0.231	**-0.774**	1

(b)	SR	FRic	FEve	FDiv	FDis	FOri	IRic	IDiv	IDis	IEve	IUni
SR	1	***	NS	*	NS	NS	NS	NS	NS	NS	NS
FRic	**0.962**	1	NS	*	NS	NS	NS	*	NS	NS	*
FEve	0.552	0.458	1	NS	NS	NS	NS	NS	*	NS	NS
FDiv	**-0.651**	**-0.685**	0.133	1	**	NS	NS	**	NS	*	*
FDis	0.296	0.397	-0.437	**-0.826**	1	NS	NS	**	***	*	NS
FOri	-0.376	-0.393	-0.024	0.356	-0.448	1	NS	NS	NS	NS	NS
IRic	0.335	0.372	0.306	-0.495	0.409	-0.167	1	NS	NS	NS	NS
IDiv	0.611	**0.635**	-0.052	**-0.827**	**0.858**	-0.483	0.428	1	*	NS	*
IDis	-0.076	0.005	**-0.695**	-0.596	**0.880**	-0.238	0.206	**0.708**	1	NS	NS
IEve	-0.275	-0.426	0.234	0.707	-0.755	0.263	-0.541	-0.572	-0.553	1	NS
IUni	-0.514	**-0.642**	0.006	**0.712**	-0.616	0.102	-0.457	**-0.718**	-0.501	0.530	1

NS: non significant; * 0.01 < p < 0.05; ** 0.01 < p < 0.01 and *** p < 0.001

General conclusion and perspectives

One of the key features of the establishment of *Sabellaria alveolata* in a soft sediment environment is the development of two distinct physical entities: the actual three-dimensional structures that *S. alveolata* builds and in which it lives (engineered sediment) and the soft sediment present around those structures, potentially under the influence of the engineer. When walking between the engineered sediments, the feel of their influence on the adjacent soft sediments is very pregnant. Hence, it appears interesting to investigate the sphere of influence of the engineer on these sediments. Holt et al. (1998) defined reefs as "Solid, massive structures which are created by accumulations of organisms, usually rising from the seabed, or at least clearly forming a substantial, discrete community or habitat which is very different from the surrounding seabed. The structure of the reef may be composed almost entirely of the reef-building organism and its tubes or shells, or it may to some degree be composed of sediments, stones and shells bound together by organisms." What about the sediments or the mentioned seabed that could be under the direct influence of the so-called reef, what about the reef's "extended phenotype"? Indeed, in the case of *Sabellaria alveolata*, the engineer needs the input of external material in the form of mainly bioclastic sediment particles, to build its tube and build the huge reefs we can sometimes observe along our coasts. Is the action of the engineer on the local seabed merely in the form of extraction or do the engineer sediment also feedback to the local seabed? Could we integrate the so-called associated sediments to the reef definition? All along this discussion, I will try to stress certain results in favor of the consideration of *S. alveolata* reefs not just as being composed of the engineered sediments, but also of the seabed under its direct influence. In addition, a key aspect in the conservation of habitats such as biogenic reefs, is understanding their ecological roles, the functions they perform and how they can be affected by disturbances.

The establishment of *Sabellaria alveolata* modifies the macrofauna

In winter and summer, the species assemblage present in the engineered sediments and in the associated sediments are different and also differ from the one present in the control soft sediments (article 1). The environmental parameters responsible for these macrofaunal changes are the engineer biomass for the engineered sediment and the principal mode of the sediments (engineered or not) associated with the organic matter content of the sediments in winter, for the associated sediments. These last two environmental parameters are under the direct influence of the engineer as shown in the first part of this study (article 1). Consequently, *S. alveolata* directly structures the engineered sediments and the macrofauna associated to them, which is to be expected since it is a physical ecosystem engineer, but also indirectly structures the soft sediments immediately surrounding the engineer structures, a.k.a. the associated sediments. When looking at the species present in the three sediment types (engineered, associated and control), the associated sediments appear as highly variable in their taxonomic composition and either closer to the engineered sediments (winter) or to the control sediments (summer).

These sediments appear as a transitional zone between the engineered and control sediments, demonstrating how nature does not function in a black and white way but along gradients.

The species richness measured in the engineered sediments was in winter and summer significantly higher than the one measured in the associated and control sediments, both presenting similar species richness. If we consider the engineered and the associated sediments jointly, the reef in its extended definition promotes even more taxonomic diversity. Indeed, between 38% and 41% of species were only recorded in the engineered sediments and between 15% and 17% were only recorded in the associated sediments. Looking into the abundances present in the different sediments, the engineered and associated sediments appear as very different, with on average between 10,000 and 24,000 organisms in a square meter of engineered sediment against less than 1,500 organisms in the same surface of associated sediment. The high densities present in the engineered sediments is linked to their three dimensional complexity giving rise to many micro-habitats, a feature common to habitats built by structural engineers like mussels, oysters and seagrass (Duffy 2006, Bos et al. 2007, Lejart and Hily 2011, Arribas et al. 2014, Hollander et al. 2015, van der Zee et al. 2016). On the other hand, if we consider the associated sediments as a transitional zone between the engineered and control sediments it is not surprising to have a low species richness and abundances as observed in estuaries, which represent a transition between aquatic and marine systems (van der Linden et al. 2016).

Furthermore, a flux of material in the form of sediment particles was observed between the associated and engineered sediments, mediated by the tube-building activity of the engineer. Indeed, *S. alveolata* uses the local sediment particles to build its tube and when a tube is destroyed, the sediment particles return to their initial unconsolidated state (Desroy et al. 2011). There is also a probable flux of organisms between the two sediments, especially in winter and the use of stable isotopes can help us look into this flux. Indeed, storms break off parts of the biogenic structures, which end up in the associated sediments. This flux is probably anecdotal because many species associated to the engineered sediments have a preference for hard substratum and could not survive for extended periods in the associated sediments. Two other fluxes of organisms can link these two sediments: the transient use of the associated sediments by engineered sediment macrofauna to move from one patch to another and mobile species like shrimps (*Crangon crangon* and *Palaemon serratus*) and bentho-demersal fish (*Solea vulgaris* and *Pomatoschistus* spp.) that can feed on invertebrates present in both sediments (article 3). Finally, in the context of the high macrofauna abundances present in the engineered sediments, inter-specific negative trophic interactions like competition and predation could take place. Mechanisms that can limit negative trophic interactions between species include the increase in basal resources, trophic specialization and trophic plasticity.

Sabellaria alveolata reefs modulate basal resources

The establishment of a *S. alveolata* reef in a soft sediment environment increases the benthic primary production in the soft sediments under the influence of the biogenic structures (associated sediments) compared to non-engineered control soft sediments, measured as chlorophyll *a* concentration (article 1). A similar promotion of local benthic primary production has been associated to other structural engineers like the reef-building polychaete *Ficopomatus enigmaticus* (Bruschetti et al. 2011), the oysters *Magallana gigas* (Echappé et al. 2017) and *Crassostrea virginica* (Newell et al. 2002) and the mussel *Mytilus edulis* (Engel et al. 2017). The increased benthic primary production was hypothesized to be linked to two changes mediated by the ecosystem engineer. First, the reef built by *S. alveolata* represents a physical barrier in a normally soft sediment area, modifying the local hydrodynamic conditions and creating calmer depositional zones where mud can settle and accumulate. This is typically an example of a structural change causing an abiotic change, where the structural change is the engineer-mediated modification of a soft sediment into a hard rock looking three-dimensional substratum (engineered sediment). At the scale of the entire engineered habitat, these zones are located landward of the reef and visible as mudflats where microphytobenthos (MPB) growths, as revealed by the multispectral image and the calculation of the normalized vegetation index (NDVI) (article 2). Inside the engineered habitat, when the patches of engineered sediment are high and extensive enough to act as small-scale physical barriers, accumulation of pure mud can appear just behind the structures (Caline et al. 1988), where microphytobenthos is susceptible to grow (pers. obs.). The landscape metrics and the NDVI did not reveal such a link between engineered sediment patch size and MPB probably because of the mismatch between the scale at which the landscape metrics were calculated (75 x 75 m grid) and the small-scale process under investigation (a few meters). Second, the suspension-feeders living in the engineered sediments, mainly the engineer and a few associated species like the Japanese oyster *Magallana gigas* and the mussel *Mytilus* cf. *galloprovincialis*, produce large quantities of feces and pseudofeces via their biological activity. These biodeposits can end up in the associated sediments where they can be remineralized by bacteria and the resulting nutrients used by the benthic microalgae for their growth (van Broekhoven et al. 2015). These suspension-feeders also release inorganic nutrients such as carbon, nitrogen and phosphorus, stimulating MPB growth (van Broekhoven et al. 2014). At the scale of the entire engineered habitat, a positive and significant correlation between the abundance (measured as cover) of *M. gigas* and *M.* cf. *galloprovincialis* and the associated sediment NDVI, a proxy for MPB biomass was found, stressing the role of bivalves associated to the engineered sediments in promoting local benthic primary production (article 2).

Furthermore, green algae from the genus *Ulva* are present on the engineered sediments stressing the physical similarity between *S. alveolata* reefs and rocks on which macroalgae typically grow. The large-scale study of the *S. alveolata* reef revealed that macroalgae are more abundant where the engineered sediments are present as large continuous patches (article 2). This result is in contradiction

with previous studies and reports (Dubois et al. 2006a, Rollet et al. 2015) that associated green algae presence to disturbed and decaying reefs, which are highly fragmented. Overall, the establishment of a *S. alveolata* reef modulates two primary producers. It increases the local benthic primary production in the associated sediments (article 1) and the physical structure of the reef leads to the establishment of green macroalgae. These two basal resources are also heterogeneously distributed at the scale of the engineered habitat, partly driven by structural characteristics of the reef and biotic factors (associated bivalves) (article 2).

The trophic functioning of the reef habitat

First, the carbon isotopic ratio of the engineer and an associated suspension-feeder (*Mytilus* cf. *galloprovincialis*), measured every 75 m covering the entire engineered sediment (32 ha), presented low intra-specific variations (between 1.8 and 2 ‰) (article 2). The spatial patterns of variations (isoscapes) were explored in the light of spatial heterogeneity in primary production (MPB and green macroalgae), physical structuration of the engineered sediments (landscape metrics) and potential inter-specific trophic competition. The isoscapes were either interpreted at the global reef habitat scale or at different spatial scales ranging from 75 m to the entire reef (2.5 km long for 1 km width) using Moran Eigenvector Maps (MEMs). The main conclusion we can draw from this wide-scale spatial study is that the physical structuration of the reef habitat does not affect the isotopic composition of sessile species living in it but considering spatial heterogeneity in primary production, inter- and intra-specific spatial cover either at a global scale or at different spatial scales (MEMs) can help shed light on the sessile primary-consumer isoscapes. In this context, the stability in terms of isotopic ratio of two suspension-feeders at the scale of the entire engineered habitat, comforts the way marine ecologist tend to sample macrofauna to study habitat food webs, that is often with a limited integration of potential intra-habitat variability in the isotopic composition of the different species (De Smet et al. 2015a). Nevertheless, this affirmation should be considered in the context of an engineered habitat like a polychaete or a bivalve reef and for the engineer suspension-feeder or associated suspension-feeders. Our results also suggest that a suspension-feeder responds more or less strongly to high nutritional value food source spatial heterogeneity depending on its selection capacity (low for *Sabellaria alveolata* and high for *Mytilus* cf. *galloprovincialis)* as demonstrated by Dubois and Colombo (2014) at the scale of a rocky shore. Hence, similar studies at the scale of bivalve reefs could yield interesting complementary results regarding this aspect.

To gain a further understanding of the functioning of the reef habitat we explored its global food web. Since, two basal resources are modulated by the physical (reef structure), abiotic (mud) and biotic (biodeposits) components of the physical engineering effect, the question is: do they affect the food web functioning of this engineered habitat compared with a non-engineered soft sediment (article 3)? Overall, the ‘gardening hypothesis’ (Hylleberg 1975) was verified for the engineer species since *S.*

alveolata relied for 80% of its diet on the local benthic resources it promoted. The ecosystem engineer had a very limited trophic niche, agreeing with the low intra-habitat isotopic variability detected with the isoscapes (article 2) and no apparent trophic competitor. A form of 'altruistic gardening' was also revealed since microphytobenthos and green macroalgae were at the base of the diet of other macrofauna species living in the engineered and associated sediments. In the engineered sediments, the local benthic food sources exclusively composed the diet of a number of grazers (*Gibbula umbilicalis* and *Littorina littorea*) and deposit-feeders (*Golfingia vulgaris*) and represented a variable part of the diet of abundant suspension-feeders (*e.g. Porcellana platycheles*). In the end, the primary consumers present in the engineered sediments appeared as trophic specialists hence limiting inter-specific trophic competition. This result is linked to the numerous cryptic food sources present in the micro-habitats characterizing this sediment, like bacterial mats growing on the mud present between *S. alveolata* tubes and MPB growing on them. The macrofauna present in the associated sediments mainly relied on a diverse pool of resources linked to temporal variability in primary production (*e.g.* phytoplankton bloom). The associated sediments appeared as being mainly characterized by trophic generalists, agreeing with the many deposit-feeders identified in this sediment. Consequently, in terms of trophic functioning the associated and engineered sediments both benefit from the locally produced food sources but these food sources are not incorporated into the food web trough similar pathways (specialist *vs* generalist species).

The structure of the carbon isotopic ratios of the primary consumers is similar in the associated and control sediments. Nonetheless, the trophic niche of the associated sediments appears larger than the control sediment one especially in summer, stressing the temporal variability characterizing these sediments in terms of trophic functioning and the positive trophic feedback the engineered sediments have on the adjacent soft sediments. Differently, the engineered sediments appear very stable in their trophic functioning linked to the numerous cryptic food sources. Overall, the estimation of the diet of the primary consumers present in the three sediment types revealed that the food web characterizing the reef habitat (engineered and associated sediments) actually relied more on pelagic phytoplankton then the food web characterizing the control soft sediments. This is probably the direct consequence of the elevated position of the engineered sediments above the seafloor and the induced hydrodynamic modification leading to a deposition of pelagic particles in the engineered and associated sediments. Notwithstanding, the engineered and associated sediments can still be considered as being part of a global reef food web through the common pool of resources at the base of the trophic functioning and the higher-order consumers like shrimps (*e.g. Palaemon serratus*) and bentho-demersal fish (*e.g. Pomatoschistus* spp.), that probably feed on macrofauna present in both sediments.

Engineered habitat functioning in the context of increasing disturbances

Snelgrove et al. (2014) recognize many ecosystem functions that seafloor ecosystems can perform such as habitat/species diversity, productivity, decomposition, nutrient recycling, carbon

sequestration, resilience and sediment stability. Food web linkages are not explicitly accounted for in this list but are directly linked to carbon sequestration, resilience and decomposition. In the case of a *Sabellaria alveolata* reef habitat, considered as the biogenic structures and the soft sediment under their influence, several ecosystem functions are promoted compared to a non-engineered soft sediment. These reefs represent a new habitat in which a new species assemblage establishes (article 1) and where primary production is enhanced via the growth of benthic microalgae and the establishment of green macroalgae (article 1 and 2). The global reef food web relies on a larger pool of resources than a non-engineered sediment, exploited by specialists primary consumers leading to a stable trophic functioning of the engineered sediments or by generalists primary consumers leading to a temporally variable functioning of the associated sediments linked to allochthones food sources. Overall, the trophic niche of the engineered community is larger than the trophic niche of the non-engineered community hinting towards an increased resilience of this system (article 3).

To gain more insight on the overall functioning of the engineered habitat, biogeochemical fluxes were measured at the scale of engineered and soft sediment cores, fluxes that are linked to carbon and nutrient cycling (article 4). These fluxes are higher in the engineered sediments compared to muddy and coarse sediments, confirming the framework developed by Stief (2013) regarding the effects reef-building fauna (mussels and oysters) have on nitrogen cycling in aquatic ecosystems. Consequently, our findings show that in terms of carbon and nutrient cycling, coalescent reefs built by polychaetes like *S. alveolata* function similarly to bivalve reefs, stressing the need to recognize their ecological importance. Overall, *Sabellaria alveolata* reefs enhance many functions that could be modified when the reefs become increasingly disturbed. Indeed, multiple disturbances affect the reef and in this regard, functional and isotopic diversity indices can provide early warning signals on functional changes happening in the reef and provide valuable information on the role played by diversity in the reef's functioning. In the context of biodiversity-ecosystem functioning studies (BEF), diversity has been linked to ecosystem functioning according to two hypothesis: the diversity hypothesis (Tilman 1997) and the mass-ratio hypothesis (Grime 1998). The diversity hypothesis states that the diversity of species in a community along with their functional traits influence ecosystem functioning through mechanisms such as resource partitioning and niche complementarity and increase insurance regarding disturbances, through compensatory dynamics in space and time. The mass ratio hypothesis states that the ecosystem's functioning is predominantly explained by the functional traits of the dominant species in that ecosystem and is relatively unaffected by the diversity of less abundant species. In a *S. alveolata* reef, we detected a very strong effect of the engineer species (biomass and abundance) on all the fluxes measured, conforming to the mass-ratio hypothesis (article 4). Overall, these fluxes synthesized under a multifunctionality measure were maximal for a maximal biomass of the engineer species and for intermediate values of the functional dispersion, corresponding to intermediate levels of disturbance in the engineered sediment. The concave link detected between the functional dispersion and the biogeochemical multifunctionality reveals that adding a few functionally different species to the

engineered sediments dominated by the engineer leads to an optimal functioning of these biogenic structures in terms of organic matter remineralization and nitrogen cycling. Combining the engineered and associated sediments, functional and isotopic diversity indices were calculated along a disturbance gradient to detect indices that could be used as early warning signals of functional changes occurring at the engineered habitat scale (article 5). Functional dispersion was one of the few indices with isotopic richness that changed along our disturbance gradient in winter and summer. These two indices were maximal for an adult engineer density of ca. 4,000, corresponding to maximal biogeochemical fluxes (article 4), potentially setting a new conservation objective for these engineered habitats.

Finally, an interesting feature of increasingly disturbed engineered sediments is their role as recruitment promoters, revealed by the beta diversity changes measured along a disturbance gradient in winter and summer (article 1). *S. alveolata* reefs are zones where recruitment is high because of boundary-layer flow changes and of the hard nature of the engineered sediments, which acts as an attractant for some pelagic larvae and as a support for egg capsules. In this context, when engineered sediments become increasingly disturbed, space is freed where organic-rich mud can settle, especially in summer after the phytoplankton bloom. Consequently, space availability and the different chemical cues associated with mud deposition act as recruitment promoters. Hence, this function of the engineered sediment is increased by disturbance and the newly recruited organisms could play an important trophic role as prey for secondary consumers.

Facilitation at the scale of a *Sabellaria alveolata* reef

Facilitation is expected to be high in physically engineered habitats like coral reefs or mussel beds. One of the manifestations of facilitation is a larger realized community niche relative to its fundamental niche (Bruno et al. 2003). Following Devictor et al. (2010), we considered the functional diversity indices measured in the engineered habitat as a proxy of the fundamental niche of the reef community, while the isotopic diversity indices measured at the same scale, were considered as a proxy of the realized niche of the reef, seen from a trophic point of view (article 5). Indeed, stable isotopes are an integrated measure that informs on the foraging behavior, the feeding movements and the trophic relations of an organism (Newsome et al. 2007). The comparison of the reef's fundamental and realized niche revealed that facilitation was the dominant mechanism shaping the reef community, as previously hypothesized in article 1 and demonstrated for other intertidal engineered habitats (Bertness et al. 1999). Furthermore, there are different trophic and non-trophic interactions considered under the global term of facilitation such as habitat amelioration, predation refuge, resource enhancement and recruitment enhancement. In the case of the engineered habitat, facilitation appears mainly driven by habitat amelioration, resource enhancement (articles 2 and 3) and recruitment promotion (article 1).

Perspectives

This work is a first step towards an integrated evaluation of the functioning of an engineered habitat built by a sedentary polychaete. Indeed, many studies looking into the functioning of marine temperate engineered habitats focus on habitats built by economically valuable species like mussels and oysters (*e.g. Crassostrea virginica*, *Magallana gigas*, *Mytilus edulis*) (Green and Crowe 2013, Kellogg et al. 2013, Green et al. 2013, Echappé et al. 2017, Engel et al. 2017). This work indicates that other engineered habitats like *S. alveolata* reefs have a functional role similar too bivalves reefs and should be truly integrated into conservation programs like the European Union's Habitats Directive 92/43/EEC (habitat type 1170 'Reef'). Concerning, *S. alveolata* reefs at least partly established in a soft sediment environment, the reef definition should be extended to include the soft sediments present between the engineered structures. In these sediments, commercial species like the Japanese carpet shell *Ruditapes philippinarum* can be present in large quantities and many locals repeatedly come to the reefs to dig up these bivalves, disturbing the associated sediments and creating small-scale spatial heterogeneity. We did not directly evaluate this anthropogenic disturbance but it could be one of the causes of the low abundances found in the associated sediments (Watson et al. 2017) and it could potentially increase the spatial heterogeneity in benthic primary production. This disturbance to one of the components of the reef habitat deserves attention buts it seems very hard to investigate this question because of the high natural spatial and temporal variability of the associated sediments and the need for precise surveys of the anthropogenic pressure exerted by the locals, a very time consuming task. Hydrodynamic forces like storms physically disturb only the fore reef while trampling can affect any part of the reef. It would be interesting to look into the macrofauna specifically present in the fore reef to see if these organisms present biological traits linked to resistance and/or resilience to this cyclic disturbance such as size, mobility and reproduction. These fore reef zones are rarely visited by anglers hence studying them could help tease out diversity changes linked to natural disturbances from those associated to trampling.

Furthermore, *Magallana gigas* oysters growing on the engineered sediments are considered as being bad for the reef by the locals and many people that harvest them think they are helping the reef by doing so. Indeed, spatial and trophic competition between the engineer and this epibiont has been supposed, meaning this non-native species could have a negative effect on the engineer. In addition, this epibiont has been shown to increase the species richness and modify the macrofauna assemblage (Dubois et al. 2006a) relative to non-colonized engineered sediments, hence having a positive effect on the global reef diversity. In this context, our results show that there is virtually no trophic competition between these two suspension-feeders, but there could be a spatial competition. After observing the Sainte-Anne reef during three years and talking with researcher investigating wild *Magallana gigas* reefs, I have come to the following framework of interactions. First, forces like storms and trampling by anglers looking for mussels affect the physical structure of the engineered sediments, releasing the spatial competition exerted by the engineer. The physically damaged engineered sediments represent an

ideal support for the recruitment of oyster larvae coming from the oyster farms located in the Western part of the Mont-Saint-Michel Bay. Once settled, the oysters can represent a spatial competitor for the engineer species but the oyster do not negatively affect the engineer through trophic competition. I have observed newly recruited *S. alveolata* on reef patches colonized by oysters, meaning the recovery of the reef in term of engineer density is probably linked to external factors affecting the retention and distribution of *S. alveolata* larvae at the scale of the Mont-Saint-Michel Bay. In the reef part colonized by oysters, alternative states of *M. gigas* dominance followed by a potential recovery to the initial *S. alveolata* densities could take place over 4 year cycles as revealed by successive surveys of the reef's health status in 2007, 2011 and 2015 (Rollet et al. 2015). Hence, it could be interesting to study in well chosen engineered sediment patches and over several years the dynamic interaction between these two suspension-feeders. In this context, I would greatly advise conservationist to take measure in order to limit the harvesting of oysters at the scale of the Sainte-Anne reef. Indeed, the harvesting of oysters is generally accompanied by the removal of a part of engineered sediment, meaning less substrate and chemical cues for recruiting *S. alveolata* larvae. In the first article, we looked into beta diversity changes along a disturbance gradient characterized using the reef mud content. The measured beta diversity was based on the taxonomic identity of species and revealed a homogenization of the associated macrofauna with increasing disturbance. Overall, the association of more or less disturbed engineered sediment patches leads to a high habitat-scale species richness but if the entire habitat was to become highly disturbed a decrease of the landscape species richness would probably be observed. In this context, investigating functional beta diversity changes (Villéger et al. 2013) along the same mud content disturbance gradient could yield a functional vision of the impact disturbances have on the reef macrofauna.

As a way of combining our different results into a causal framework, it could be very interesting to build Structural Equation Models (SEM) as done in many studies investigating the link between diversity and ecosystem functioning in controlled field experiments (Mokany et al. 2008, Mouillot et al. 2011, Ali et al. 2017). Indeed, SEM is a powerful technique that can combine complex path models with latent external variables (factors). This general statistical modeling technique would allow use to test different models linking complementary forms of diversity (taxonomic, functional, isotopic) and the engineer abundance or biomass to different ecosystem functions like primary production or biogeochemical fluxes and to find models that best fits our data. In order to go further in the understanding of the functioning of a *S. alveolata* reef and comfort functional dispersion as a good functional health index, other functions and processes should be measured at the habitat scale and along a disturbance gradient. A very promising function to measure or estimate using for example the models developed by Brey (2012) is the secondary production. Indeed, preliminary work estimating the secondary production (Brey 2012), based on the over-dispersed megafauna sampled in the quadrats (see article 1), revealed a much higher secondary production in the engineered sediments compared to the associated and control sediments and that this production was higher in highly disturbed engineered

sediments than in less disturbed engineered sediments. In a similar context, surveying the engineered sediment every month using multispectral images could provide more information on the spatial and temporal heterogeneity in the reef primary production and could help detect stable primary production hotspots.

Finally, to get a finer insight on the fate of the locally produced microphytobenthos and its incorporation by the associated and engineered sediment bacteria, meio and macrofauna, we could perform in situ ^{13}C- and ^{15}N-labeling experiments of the MPB (Middelburg et al. 2000, Galván et al. 2008, Evrard et al. 2010). More generally, transplanting a small engineered structure void of macroalgae to the control soft sediments and following the carbon and nitrogen isotopic ratios of the sources and macrofauna could provide an estimation of the trophic engineering effect. Indeed, we could see how the assimilated diet of the different primary consumers along with their trophic interactions are modified by the removal of the green macroalgae and the lower microphytobenthos biomass.

Bibliographic references

-A-

Achary, P. K. 1974. Polychaete of the family Sabellariidae with special referecne to their intertidal habitat. - Proceedings of the Indian Science Academy: 442–455.

Agüera, A. et al. 2015. Beyond food: a foundation species facilitates its own predator. - Oikos 124: 1367–1373.

Ali, A. et al. 2017. Community-weighted mean of leaf traits and divergence of wood traits predict aboveground biomass in secondary subtropical forests. - Science of The Total Environment 574: 654–662.

Aller, R. C. and Aller, J. Y. 1998. The effect of biogenic irrigation intensity and solute exchange on diagenetic reaction rates in marine sediments. - Journal of Marine Research 56: 905–936.

Anderson, M. et al. 2008. PERMANOVA+ for PRIMER: Guide to Software and Statistical Methods. - PRIMER-E, Plymouth.

Arbach Leloup, F. et al. 2008. Interactions between a natural food web, shellfish farming and exotic species: The case of the Bay of Mont Saint Michel (France). - Estuarine, Coastal and Shelf Science 76: 111–120.

Arribas, L. P. et al. 2014. Intertidal mussels as ecosystem engineers: their associated invertebrate biodiversity under contrasting wave exposures. - Mar Biodiv 44: 203–211.

Audouin, J. V. and Milne-Edwards, H. 1832. Recherches pour servir à l'histoire naturelle du littoral de la France, ou Recueil de mémoires sur l'anatomie, la physiologie, la classification et les mœurs des animaux des nos côtes: Voyage à Granville, aux îles Chausey et à Saint Malo. - Crochard.

Austen, M. C. et al. 2002. Biodiversity links above and below the marine sediment–water interface that may influence community stability. - Biodiversity and Conservation 11: 113–136.

Ayata, S.-D. et al. 2009. Modelling larval dispersal and settlement of the reef-building polychaete *Sabellaria alveolata*: Role of hydroclimatic processes on the sustainability of biogenic reefs. - Continental Shelf Research 29: 1605–1623.

-B-

Baeta, A. et al. 2009. Eutrophication and trophic structure in response to the presence of the eelgrass Zostera noltii. - Mar Biol 156: 2107–2120.

Balvanera, P. et al. 2006. Quantifying the evidence for biodiversity effects on ecosystem functioning and services. - Ecology letters 9: 1146–1156.

Barillé, L. et al. 2017. Photosynthetic epibionts and endobionts of Pacific oyster shells from oyster reefs in rocky versus mudflat shores. - PLOS ONE 12: e0185187.

Barnes, C. et al. 2008. The importance of quantifying inherent variability when interpreting stable isotope field data. - Oecologia 155: 227–235.

Bascompte, J. 2010. Structure and dynamics of ecological networks. - Science 329: 765–766.

Bearhop, S. et al. 2004. Determining trophic niche width: a novel approach using stable isotope analysis. - Journal of Animal Ecology 73: 1007–1012.

Beck, M. W. et al. 2011. Oyster reefs at risk and recommendations for conservation, restoration, and management. - BioScience 61: 107–116.

Belley, R. and Snelgrove, P. V. R. 2017. The role of infaunal functional and species diversity in short-term response of contrasting benthic communities to an experimental food pulse. - Journal of Experimental Marine Biology and Ecology 491: 38–50.

Bellwood, D. R. et al. 2004. Confronting the coral reef crisis. - Nature 429: 827–833.

Ben-David, M. et al. 1997. Annual and seasonal changes in diets of martens: evidence from stable isotope analysis. - Oecologia 111: 280–291.

Berke, S. K. 2010. Functional groups of ecosystem engineers: a proposed classification with comments on current issues. - Integr. Comp. Biol. 50: 147–157.

Bertness, M. D. 1985. Fiddler crab regulation of *Spartina alterniflora* production on a New England salt marsh. - Ecology 66: 1042–1055.

Bertness, M. D. and Callaway, R. 1994. Positive interactions in communities. - Trends in Ecology & Evolution 9: 191–193.

Bertness, M. D. et al. 1999. Testing the relative contribution of positive and negative interactions in rocky intertidal communities. - Ecology 80: 2711–2726.

Blackburn, T. H. and Henriksen, K. 1983. Nitrogen cycling in different types of sediments from Danish waters. - Limnol. Oceanogr. 28: 477–493.

Blanchard, G. et al. 1988. Méthode simplifiée pour l'extraction du microphytobenthos des sédiments marins par le gel de silice Ludox. - Comptes rendus de l'Académie des sciences. Série 3, Sciences de la vie 307: 569–576.

Blanchet, F. G. et al. 2008. Forward selection of explanatory variables. - Ecology 89: 2623–2632.

Blanchet-Aurigny, A. et al. 2012. Tissue-diet discrimination factors of isotopic ratios (Δδ13C and Δδ15N) in two brittle star species: Effect of reproductive state, diet and tissue composition. - Journal of Experimental Marine Biology and Ecology 426: 68–77.

Bolam, S. G. et al. 2002. Diversity, biomass, and ecosystem processes in the marine benthos. - Ecological Monographs 72: 599–615.

Bonnot-Courtois, C. et al. 2004. Recent morphodynamics of shell banks in the western part of the Bay of Mont-Saint-Michel (France) / Morphodynamique actuelle des bancs coquilliers dans la partie occidentale de la baie du Mont-Saint-Michel (France). - Géomorphologie : relief, processus, environnement 10: 65–79.

Bonnot-Courtois, C. et al. 2008. Remaniements sédimentaires superficiels sur l'estran occidental de la baie du Mont-Saint-Michel. - European Journal of Environmental and Civil Engineering 12: 51–65.

Bonnot-Courtois, C. et al. 2009. Carte morpho-sédimentaire de la baie du Mont Saint-Michel (Ille-et-Vilaine et Manche) échelle 1/25 000. - Ifremer.

Borcard, D. and Legendre, P. 2002. All-scale spatial analysis of ecological data by means of principal coordinates of neighbour matrices. - Ecological Modelling 153: 51–68.

Bos, A. R. et al. 2007. Ecosystem engineering by annual intertidal seagrass beds: Sediment accretion and modification. - Estuarine, Coastal and Shelf Science 74: 344–348.

Bosch, J. A. et al. 2015. Short-term effects of nereid polychaete size and density on sediment inorganic nitrogen cycling under varying oxygen conditions. - Marine Ecology Progress Series 524: 155–169.

Bouma, T. J. et al. 2009. Ecosystem engineering and biodiversity in coastal sediments: posing hypotheses. - Helgoland Marine Research 63: 95–106.

Bowes, R. E. et al. 2017. Multidimensional metrics of niche space for use with diverse analytical techniques. - Scientific Reports in press.

Braeckman, U. et al. 2010. Role of macrofauna functional traits and density in biogeochemical fluxes and bioturbation. - Marine Ecology Progress Series 399: 173–186.

Braeckman, U. et al. 2011. Biological vs. physical mixing effects on benthic food web dynamics. - PLOS ONE 6: e18078.

Bremner, J. 2008. Species' traits and ecological functioning in marine conservation and management. - Journal of Experimental Marine Biology and Ecology 366: 37–47.

Bremner, J. et al. 2003. Assessing functional diversity in marine benthic ecosystems: a comparison of approaches. - Mar Ecol Prog Ser 254: 11–25.

Bremner, J. et al. 2006. Methods for describing ecological functioning of marine benthic assemblages using biological traits analysis (BTA). - Ecological Indicators 6: 609–622.

Brey, T. 2001. Population dynamics in benthic invertebrates. A virtual handbook. Version 01.2.

Brey, T. 2012. A multi-parameter artificial neural network model to estimate macrobenthic invertebrate productivity and production. - Limnol. Oceanogr. Methods 10: 581–589.

Brind'Amour, A. and Dubois, S. F. 2013. Isotopic diversity indices: how sensitive to food web structure? - PLOS ONE 8: e84198.

Brind'Amour, A. et al. 2005. Multiscale spatial distribution of a littoral fish community in relation to environmental variables. - Limnol. Oceanogr. 50: 465–479.

Bruno, J. F. 2000. Facilitation of cobble beach plant communities through habitat modification by spartina alterniflora. - Ecology 81: 1179–1192.

Bruno, J. F. et al. 2003. Incorporating facilitation into ecological theory. - Trends in Ecology and Evolution 18: 119–125.

Bruschetti, M. et al. 2011. Effect of biodeposition of an invasive polychaete on organic matter content and productivity of the sediment in a coastal lagoon. - Journal of Sea Research 66: 20–28.

Buhr, K.-J. 1976. Suspension-feeding and assimilation efficiency in Lanice conchilega (Polychaeta). - Mar. Biol. 38: 373–383.

Burnett, M. R. et al. 1998. The influence of geomorphological heterogeneity on biodiversity I. A patch-scale perspective. - Conservation Biology 12: 363–370.

-C-

Cadotte, M. W. 2017. Functional traits explain ecosystem function through opposing mechanisms. - Ecol Lett 20: 989-996.

Cadotte, M. W. et al. 2011. Beyond species: functional diversity and the maintenance of ecological processes and services. - Journal of applied ecology 48: 1079–1087.

Caline, B. et al. 1988. Les récifs à annélides (Hermelles) en Baie du Mont Saint-Michel: écologie, géomorphologie, sédimentologie, implications géologiques. - BRGM.

Cardinale, B. J. et al. 2011. The functional role of producer diversity in ecosystems. - American journal of botany 98: 572–592.

Cardinale, B. J. et al. 2013. Biodiversity simultaneously enhances the production and stability of community biomass, but the effects are independent. - Ecology 94: 1697–1707.

Carlier, A. et al. 2009. Spatial heterogeneity in the food web of a heavily modified Mediterranean coastal lagoon: stable isotope evidence. - Aquatic Biology 5: 167–179.

Carlisle, A. B. et al. 2012. Using stable isotope analysis to understand the migration and trophic ecology of northeastern pacific white sharks (*Carcharodon carcharias*). - PLOS ONE 7: e30492.

Ceballos, G. et al. 2015. Accelerated modern human–induced species losses: Entering the sixth mass extinction. - Science Advances 1: e1400253.

Charbonnier, C. et al. 2016. Role of macrofauna on benthic oxygen consumption in sandy sediments of a high-energy tidal beach. - Continental Shelf Research 120: 96–105.

Chase, J. M. and Leibold, M. A. 2003. Ecological niches: linking classical and contemporary approaches.

Chevenet, F. et al. 1994. A fuzzy coding approach for the analysis of long-term ecological data. - Freshwater Biology 31: 295–309.

Christianen, M. J. A. et al. 2017. Benthic primary producers are key to sustain the Wadden Sea food web: stable carbon isotope analysis at landscape scale. - Ecology 98: 1498–1512.

Clough, L. M. et al. 2005. Impacts of water depth, sediment pigment concentration, and benthic macrofaunal biomass on sediment oxygen demand in the western Arctic Ocean. - Can. J. Fish. Aquat. Sci. 62: 1756–1765.

Cognie, B. and Barille, L. 1999. Does bivalve mucus favour the growth of their main food source, microalgae? - Oceanologica Acta 22: 441–450.

Colden, A. M. et al. 2016. Sediment suspension and deposition across restored oyster reefs of varying orientation to flow: implications for restoration. - Estuaries and Coasts 39: 1435–1448.

Colombo, F. et al. 2013. Trophic structure of vermetid reef community: High trophic diversity at small spatial scales. - Journal of Sea Research 77: 93–99.

Commito, J. A. et al. 2005. Mussels matter: postlarval dispersal dynamics altered by a spatially complex ecosystem engineer. - Journal of Experimental Marine Biology and Ecology 316: 133–147.

Como, S. et al. 2012. Spatial variations in δ13C and δ15N values of primary consumers in a coastal lagoon. - Estuarine, Coastal and Shelf Science 115: 300–308.

Costanza, R. et al. 1997. The value of the world's ecosystem services and natural capital. - Nature 387: 253–260.

Crisp, D. J. 1964. The effects of the severe winter of 1962-63 on marine life in britain. - Journal of Animal Ecology 33: 165–210.

Cucherousset, J. and Villéger, S. 2015. Quantifying the multiple facets of isotopic diversity: New metrics for stable isotope ecology. - Ecological Indicators 56: 152–160.

Cugier, P. et al. 2010. Assessing the role of benthic filter feeders on phytoplankton production in a shellfish farming site: Mont Saint Michel Bay, France. - Journal of Marine Systems 82: 21–34.

-D-

D'Andrea, A. F. and DeWitt, T. H. 2009. Geochemical ecosystem engineering by the mud shrimp *Upogebia pugettensis* (Crustacea: Thalassinidae) in Yaquina Bay, Oregon: Density-dependent effects on organic matter remineralization and nutrient cycling. - Limnol. Oceanogr. 54: 1911–1932.

Davoult, D. et al. 2008. Spatio-temporal variability of intertidal benthic primary production and respiration in the western part of the Mont Saint-Michel Bay (Western English Channel, France). - Hydrobiologia 620: 163–172.

Dawkins, R. 1982. The extended phenotype. - Oxford University Press.

De Smet, B. et al. 2015a. Integrating ecosystem engineering and food web ecology: testing the effect of biogenic reefs on the food web of a soft-bottom intertidal area. - PLOS ONE 10: e0140857.

De Smet, B. et al. 2015b. Biogenic reefs affect multiple components of intertidal soft-bottom benthic assemblages: the *Lanice conchilega* case study. - Estuarine, Coastal and Shelf Science 152: 44–55.

Decottignies, P. et al. 2007. Exploitation of natural food sources by two sympatric, invasive suspension-feeders: *Crassostrea gigas* and *Crepidula fornicata*. - Marine Ecology Progress Series 334: 179–192.

DeNiro, M. J. and Epstein, S. 1978. Influence of diet on the distribution of carbon isotopes in animals. - Geochimica et Cosmochimica Acta 42: 495–506.

Denis, L. et al. 2001. Temporal variability in dissolved inorganic nitrogen fluxes at the sediment–water interface and related annual budget on a continental shelf (NW Mediterranean). - Oceanologica Acta 24: 85–97.

Denslow, J. S. 1995. Disturbance and diversity in tropical rain forests: the density effect. - Ecological Applications 5: 962–968.

Desroy, N. et al. 2011. The conservation status of *Sabellaria alveolata* (L.) (Polychaeta: Sabellariidae) reefs in the Bay of Mont-Saint-Michel. - Aquatic Conservation: Marine and Freshwater Ecosystems 21: 462–471.

Devictor, V. et al. 2010a. Defining and measuring ecological specialization. - Journal of Applied Ecology 47: 15–25.

Devictor, V. et al. 2010b. Spatial mismatch and congruence between taxonomic, phylogenetic and functional diversity: the need for integrative conservation strategies in a changing world. - Ecology Letters 13: 1030–1040.

Dias, A. S. and Paula, J. 2001. Associated fauna of *Sabellaria alveolata* colonies on the central coast of Portugal. - Journal of the Marine Biological Association of the United Kingdom 81: 169–170.

Díaz, S. et al. 2007. Incorporating plant functional diversity effects in ecosystem service assessments. - PNAS 104: 20684–20689.

Díaz, S. and Cabido, M. 2001. Vive la différence: plant functional diversity matters to ecosystem processes. - Trends in Ecology & Evolution 16: 646–655.

Donadi, S. et al. 2013. Cross-habitat interactions among bivalve species control community structure on intertidal flats. - Ecology 94: 489–498.

Donadi, S. et al. 2014. The bivalve loop: Intra-specific facilitation in burrowing cockles through habitat modification. - Journal of Experimental Marine Biology and Ecology 461: 44–52.

Dray, S. et al. 2006. Spatial modelling: a comprehensive framework for principal coordinate analysis of neighbour matrices (PCNM). - Ecological Modelling 196: 483–493.

Dubois, S. 2003. Ecologie des formations récifales à *Sabellaria alveolata* (L.) : valeur fonctionnelle et patrimoniale.

Dubois, S. F. and Colombo, F. 2014. How picky can you be? Temporal variations in trophic niches of co-occurring suspension-feeding species. - Food Webs 1: 1–9.

Dubois, S. et al. 2002. Biodiversity associated with *Sabellaria alveolata* (Polychaeta: Sabellariidae) reefs: effects of human disturbances. - Journal of the Marine Biological Association of the United Kingdom 82: 817–826.

Dubois, S. et al. 2003. Efficiency of particle retention and clearance rate in the polychaete *Sabellaria alveolata* L. - Comptes Rendus Biologies 326: 413–421.

Dubois, S. et al. 2005. Particle capture and processing mechanisms in *Sabellaria alveolata* (Polychaeta: Sabellariidae). - Marine Ecology Progress Series 301: 159–171.

Dubois, S. et al. 2006a. Effects of epibionts on *Sabellaria alveolata* (L.) biogenic reefs and their associated fauna in the Bay of Mont Saint-Michel. - Estuarine, Coastal and Shelf Science 68: 635–646.

Dubois, S. et al. 2006b. Feeding mechanism of the polychaete *Sabellaria alveolata* revisited:: reply to Riisgard & Nielsen (2006). - Marine Ecology Progress Series 328: 307–311.

Dubois, S. et al. 2007a. Distribution and retention of *Sabellaria alveolata* larvae (Polychaeta: Sabellariidae) in the Bay of Mont-Saint-Michel, France. - Marine Ecology Progress Series 346: 243–254.

Dubois, S. et al. 2007b. Small-scale spatial variability of food partitioning between cultivated oysters and associated suspension-feeding species, as revealed by stable isotopes. - Marine Ecology Progress Series 336: 151–160.

Dubois, S. et al. 2007c. Effects of oyster farming on macrofaunal assemblages associated with *Lanice conchilega* tubeworm populations: A trophic analysis using natural stable isotopes. - Aquaculture 271: 336–349.

Dubois, S. et al. 2009. Feeding response of the polychaete *Sabellaria alveolata* (Sabellariidae) to changes in seston concentration. - Journal of Experimental Marine Biology and Ecology 376: 94–101.

Dubois, S. et al. 2012. Origin and composition of sediment organic matter in a coastal semi-enclosed ecosystem: An elemental and isotopic study at the ecosystem space scale. - Journal of Marine Systems 94: 64–73.

Duffy, J. E. 2006. Biodiversity and the functioning of seagrass ecosystems. - Mar Ecol Prog Ser 311: 233–250.

Duffy, J. E. et al. 2007. The functional role of biodiversity in ecosystems: incorporating trophic complexity. - Ecology Letters 10: 522–538.

-E-

Echappé, C. et al. 2017. Satellite remote sensing reveals a positive impact of living oyster reefs on microalgal biofilm development. - Biogeosciences Discuss. 2017: 1–30.

Eckman, J. E. 1983. Hydrodynamic processes affecting benthic recruitment. - Limnol. Oceanogr. 28: 241–257.

Eldridge, D. J. et al. 2016. Mammalian engineers drive soil microbial communities and ecosystem functions across a disturbance gradient. - J Anim Ecol 85: 1636–1646.

Elton, C. 1927. Animal Ecology.

Engel, F. G. et al. 2017. Mussel beds are biological power stations on intertidal flats. - Estuarine, Coastal and Shelf Science 191: 21–27.

Estes, J. A. and Palmisano, J. F. 1974. Sea otters: their role in structuring nearshore communities. - Science 185: 1058–1060.

Evrard, V. et al. 2010. Carbon and nitrogen flows through the benthic food web of a photic subtidal sandy sediment. - Marine Ecology Progress Series 416: 1–16.

-F-

Fabricius, K. E. 2005. Effects of terrestrial runoff on the ecology of corals and coral reefs: review and synthesis. - Marine Pollution Bulletin 50: 125–146.

Fahrig, L. 2003. Effects of habitat fragmentation on biodiversity. - Annual Review of Ecology, Evolution, and Systematics 34: 487–515.

Fauchald, K. and Jumars, P. A. 1979. The diet of worms: a study of polychaete feeding guilds. - Aberdeen University Press.

Flockhart, D. T. T. et al. 2013. Tracking multi-generational colonization of the breeding grounds by monarch butterflies in eastern North America. - Proceedings of the Royal Society of London B: Biological Sciences 280: 20131087.

Fournier, J. et al. 2010. Inter- and intraspecific variability in the chemical composition of the mineral phase of cements from several tube-building polychaetes. - Geobios 43: 191–200.

France, R. I. 1995. Carbon-13 enrichment in benthic compared to planktonic algae: foodweb implications. - Marine Ecology Progress Series 124: 307–312.

Franco, M. de A. et al. 2010. Respiration partitioning in contrasting subtidal sediments: seasonality and response to a spring phytoplankton deposition. - Marine Ecology 31: 276–290.

Fry, B. and Sherr, E. B. 1989. δ13c measurements as indicators of carbon flow in marine and freshwater ecosystems. - In: Stable Isotopes in Ecological Research. Ecological Studies. Springer, New York, NY, pp. 196–229.

Fry, B. et al. 1978. Grasshopper food web analysis: use of carbon isotope ratios to examine feeding relationships among terrestrial herbivores. - Ecology 59: 498–506.

-G-

Galván, K. et al. 2008. Stable isotope addition reveals dietary importance of phytoplankton and microphytobenthos to saltmarsh infauna. - Marine Ecology Progress Series 359: 37–49.

Gamfeldt, L. et al. 2015. Marine biodiversity and ecosystem functioning: what's known and what's next? - Oikos 124: 252–265.

Garnier, E. et al. 2004. Plant functional markers capture ecosystem properties during secondary succession. - Ecology 85: 2630–2637.

Gharajehdaghipour, T. et al. 2016. Arctic foxes as ecosystem engineers: increased soil nutrients lead to increased plant productivity on fox dens. - Sci Rep in press.

Gillis, L. G. et al. 2014. Potential for landscape-scale positive interactions among tropical marine ecosystems. - Marine Ecology Progress Series 503: 289–303.

Godbold, J. A. et al. 2011. Habitat structure mediates biodiversity effects on ecosystem properties. - Proceedings of the Royal Society of London B: Biological Sciences 278: 2510–2518.

Goldberg, W. M. 2013. The biology of reefs and reef organisms.

Golubski, A. J. and Abrams, P. A. 2011. Modifying modifiers: what happens when interspecific interactions interact? - Journal of Animal Ecology 80: 1097–1108.

González-Ortiz, V. et al. 2014. Interactions between seagrass complexity, hydrodynamic flow and biomixing alter food availability for associated filter-feeding organisms. - PLOS ONE 9: e104949.

Grabowski, J. H. and Powers, S. P. 2004. Habitat complexity mitigates trophic transfer on oyster reefs. - Marine Ecology Progress Series 277: 291–295.

Graham, B. S. et al. 2010. Using isoscapes to trace the movements and foraging behavior of top predators in oceanic ecosystems. - In: Isoscapes. Springer, pp. 299–318.

Grall, J. et al. 2006. Community structure and food web based on stable isotopes (δ15N and δ13C) analysis of a North Eastern Atlantic maerl bed. - Journal of Experimental Marine Biology and Ecology 338: 1–15.

Green, D. S. and Crowe, T. P. 2013. Physical and biological effects of introduced oysters on biodiversity in an intertidal boulder field. - Marine Ecology Progress Series 482: 119–132.

Green, D. S. et al. 2013. Effects of non-indigenous oysters on ecosystem processes vary with abundance and context. - Ecosystems 16: 881–893.

Grime, J. P. 1998. Benefits of plant diversity to ecosystems: immediate, filter and founder effects. - Journal of Ecology 86: 902–910.

Grinnell, J. 1917. The niche-relationships of the california thrasher. - American Ornithological Society 34: 427–433.

Gruet, Y. 1972. Aspects morphologiques et dynamiques de constructions de l'Annelide polychete *Sabellaria alveolata* (Linne). - Revue des Travaux de l'Institut des Pêches Maritimes 36: 131–161.

Gruet, Y. 1984. Granulometric evolution of the sand tube in relation to growth of the polychaete Annelid *Sabellaria alveolata* (Linné) (Sabellariidae). - Ophelia 23: 181–193.

Gruet, Y. 1986. Spatio-temporal changes of sabellarian reefs built by the sedentary polychaete *Sabellaria alveolata* (Linne). - Marine Ecology 7: 303–319.

Gruet, Y. et al. 1987. Composante biominérale du ciment du tube chez *Sabellaria alveolata* (L.), Annélide Polychète. - Canadian Journal of Zoology 65: 837–842.

Guerra-García, J. M. et al. 2014. Dietary analysis of the marine Amphipoda (Crustacea: Peracarida) from the Iberian Peninsula. - Journal of Sea Research 85: 508–517.

Gutiérrez, J. L. and Jones, C. G. 2006. Physical ecosystem engineers as agents of biogeochemical heterogeneity. - BioScience 56: 227–236.

Gutiérrez, J. L. et al. 2003. Mollusks as ecosystem engineers: the role of shell production in aquatic habitats. - Oikos 101: 79–90.

Gutiérrez, J. L. et al. 2012. Physical ecosystem engineers and the functioning of estuaries and coasts. - Treatise on Estuarine and Coastal Science 7: 53–81.

-H-

Hacker, S. D. and Gaines, S. D. 1997. Some implications of direct positive interactions for community species diversity. - Ecology 78: 1990–2003.

Hamilton, S. L. et al. 2011. Extensive geographic and ontogenetic variation characterizes the trophic ecology of a temperate reef fish on southern California (USA) rocky reefs. - Marine Ecology Progress Series 429: 227–244.

Hastings, A. et al. 2007. Ecosystem engineering in space and time. - Ecology Letters 10: 153–164.

Hedin, L. O. et al. 1988. The effect of deforestation on organic debris dams. - Verein Limnology: 1135–1141.

Heisterkamp, I. M. et al. 2013. Shell biofilm-associated nitrous oxide production in marine molluscs: processes, precursors and relative importance. - Environmental Microbiology 15: 1943–1955.

Hejda, M. and de Bello, F. 2013. Impact of plant invasions on functional diversity in the vegetation of Central Europe. - J Veg Sci 24: 890–897.

Hemminga, M. and Mateo, M. 1996. Stable carbon isotopes in seagrasses: variability in ratios and use in ecological studies. - Mar Ecol Prog Ser 140: 285–298.

Hemminga, M. A. et al. 1999. Leaf nutrient resorption, leaf lifespan and the retention of nutrients in seagrass systems. - Aquatic Botany 65: 141–158.

Hill, J. M. et al. 2008. Temporal and spatial variability in stable isotope ratios of SPM link to local hydrography and longer term SPM averages suggest heavy dependence of mussels on nearshore production. in press.

Hobson, K. A. 2005. Stable isotopes and the determination of avian migratory connectivity and seasonal interactions. - The Auk 122: 1037–1048.

Hobson, K. A. and Wassenaar, L. I. 1997. Linking breeding and wintering grounds of neotropical migrant songbirds using stable hydrogen isotopic analysis of feathers. - Oecologia 109: 142–148.

Hollander, J. et al. 2015. Effects of the alien Pacific oyster (*Crassostrea gigas*) on subtidal macrozoobenthos communities. - Mar Biol 162: 547–555.

Holt, T. J. et al. 1998. Biogenic reefs. An overview of dynamic and sensitivity characteristics for conservation management of marine SACs.: 170.

Hooper, D. U. et al. 2005. Effects of biodiversity on ecosystem functioning: a consensus of current knowledge. - Ecological Monographs 75: 3–35.

Houghton, R. A. 1990. The global effects of tropical deforestation. - Environ. Sci. Technol. 24: 414–422.

Howarth, R. W. et al. 2000. Issues in ecology: nutrient pollution of coastal rivers, bays, and seas.: 1–16.

Hutchinson, G. E. 1957. Concluding remarks. - Cold Spring Harb Symp Quant Biol 22: 415–427.

Hylleberg, J. 1975. Selective feeding by Abarenicola pacifica with notes on *Abarenicola vagabunda* and a concept of gardening in lugworms. - Ophelia 14: 113–137.

Hyndes, G. A. et al. 2013. The magnitude of spatial and temporal variation in δ15N and δ13C differs between taxonomic groups: Implications for food web studies. - Estuarine, Coastal and Shelf Science 119: 176–187.

Hyndes, G. A. et al. 2014. Mechanisms and ecological role of carbon transfer within coastal seascapes. - Biological Reviews 89: 232–254.

-I-

Ieno, E. N. et al. 2006. How biodiversity affects ecosystem functioning: roles of infaunal species richness, identity and density in the marine benthos. - Mar Ecol Prog Ser 311: 263–271.

IGN 2015. Guide utilisateur Pléiades.

IPCC 2014. Climate Change 2014: Synthesis Report. Contribution of Working Groups I, II and III to the Fifth Assessment Report of the Intergovernmental Panel on Climate Change.: 151.

-J-

Jackson, A. L. et al. 2011. Comparing isotopic niche widths among and within communities: SIBER – Stable Isotope Bayesian Ellipses in R. - Journal of Animal Ecology 80: 595–602.

Janson, A. L. et al. 2012. Macrobenthic biodiversity and oxygen uptake in estuarine systems: The example of the Seine estuary. - Journal of Soils and Sediments 12: 1568–1580.

Jones, C. G. et al. 1994. Organisms as ecosystem engineers. - Oikos 69: 373–386.

Jones, C. G. et al. 1997. Positive and negative effects of organisms as physical ecosystem engineers. - Ecology 78: 1946–1957.

Jones, C. G. et al. 2006. Linking ecosystem engineers to soil processes: a framework using the Jenny State Factor Equation. - European Journal of Soil Biology 42: S39–S53.

Jones, C. G. et al. 2010. A framework for understanding physical ecosystem engineering by organisms. - Oikos 119: 1862–1869.

Jones, A. G. et al. 2018. Interplay between abiotic factors and species assemblages mediated by the ecosystem engineer *Sabellaria alveolata* (Annelida: Polychaeta). - Estuarine, Coastal and Shelf Science in press.

Jumars, P. A. et al. 2015. Diet of worms emended: an update of polychaete feeding guilds. - Annual Review of Marine Science 7: 497–520.

-K-

Keene, W. C. 1980. The importance of a reef-forming polychaete, Mercierella enigmatica fauvel, in the oxygen and nutrient dynamics of a hypereutrophic subtropical lagoon. - Estuarine and Coastal Marine Science 11: 167–178.

Kéfi, S. et al. 2012. More than a meal… integrating non-feeding interactions into food webs. - Ecology Letters 15: 291–300.

Kellogg, M. L. et al. 2013. Denitrification and nutrient assimilation on a restored oyster reef. - Marine Ecology Progress Series 480: 1–19.

Kent, F. E. A. et al. 2017. In situ biodeposition measurements on a *Modiolus modiolus* (horse mussel) reef provide insights into ecosystem services. - Estuarine, Coastal and Shelf Science 184: 151–157.

Koh, C.-H. et al. 2006. Tidal resuspension of microphytobenthic chlorophyll a in a Nanaura mudflat, Saga, Ariake Sea, Japan: flood–ebb and spring–neap variations. - Marine Ecology Progress Series 312: 85–100.

Kolasinski, J. et al. 2016. Stable isotopes reveal spatial variability in the trophic structure of a macro-benthic invertebrate community in a tropical coral reef. - Rapid Commun. Mass Spectrom. 30: 433–446.

Kraan, C. et al. 2009. Patchiness of macrobenthic invertebrates in homogenized intertidal habitats:: hidden spatial structure at a landscape scale. - Marine Ecology Progress Series 383: 211–224.

Kramer, D. L. and Bryant, M. J. 1995. Intestine length in the fishes of a tropical stream: 2. Relationships to diet — the long and short of a convoluted issue. - Environ Biol Fish 42: 129–141.

Kristensen, E. 1988. Benthic fauna and biogeochemical processes in marine sediments: microbial activities and fluxes. - In: Nitrogen cycling in coastal marine environments. Wiley. Blackburn, T.H., Sørensen, J., pp. 275–299.

Kristensen, E. 2008. Mangrove crabs as ecosystem engineers; with emphasis on sediment processes. - Journal of sea Research 59: 30–43.

Kunin, W. E. and Lawton, J. H. 1996. Does biodiversity matter? Evaluating the case for conserving species. - In: Biodiversity: a biology of numbers and differences. Blackwell Science. Gaston KJ, pp. 396.

-L-

Laliberté, E. and Legendre, P. 2010. A distance-based framework for measuring functional diversity from multiple traits. - Ecology 91: 299–305.

Larkin, D. J. et al. 2008. Topographic heterogeneity influences fish use of an experimentally restored tidal marsh. - Ecological Applications 18: 483–496.

Lavorel, S. and Garnier, E. 2002. Predicting changes in community composition and ecosystem functioning from plant traits: revisiting the Holy Grail. - Functional Ecology 16: 545–556.

Layman, C. A. et al. 2007a. Can stable isotope ratios provide for community-wide measures of trophic structure? - Ecology 88: 42–48.

Layman, C. A. et al. 2007b. Niche width collapse in a resilient top predator following ecosystem fragmentation. - Ecology Letters 10: 937–944.

Le Cam, J.-B. et al. 2011. The strength of biogenic sand reefs: Visco-elastic behaviour of cement secreted by the tube building polychaete *Sabellaria alveolata*, Linnaeus, 1767. - Estuarine, Coastal and Shelf Science 91: 333–339.

Lefebvre, S. and Dubois, S. F. 2016. The stony road to understand isotopic enrichment and turnover rates : insight into the metabolic part. - Vie et Milieu 66: 305–314.

Lefebvre, S. et al. 2009. Seasonal dynamics of trophic relationships among co-occurring suspension-feeders in two shellfish culture dominated ecosystems. - Estuarine, Coastal and Shelf Science 82: 415–425.

Legendre, P. and Legendre, L. 2012. Numerical ecology. - Elsevier.

Legendre, P. and Gauthier, O. 2014. Statistical methods for temporal and space–time analysis of community composition data. - Proc Biol Sci in press.

Legendre, P. et al. 2009. Partitioning beta diversity in a subtropical broad-leaved forest of China. - Ecology 90: 663–674.

Lejart, M. and Hily, C. 2011. Differential response of benthic macrofauna to the formation of novel oyster reefs (*Crassostrea gigas*, Thunberg) on soft and rocky substrate in the intertidal of the Bay of Brest, France. - Journal of Sea Research 65: 84–93.

Lejart, M. et al. 2012. Respiration and calcification of *Crassostrea gigas*: contribution of an intertidal invasive species to coastal ecosystem co2 fluxes. - Estuaries and Coasts 35: 622–632.

Lorrain, A. et al. 2003. Decarbonation and preservation method for the analysis of organic C and N contents and stable isotope ratios of low-carbonated suspended particulate material. - Analytica Chimica Acta 491: 125–133.

Lucas, G. and Lefevre, P. 1956. Contribution à l'étude de quelques sédiments marins et de récifs d'hermelles du mont Saint-Michel. - Revue des Travaux de l'Institut des Pêches Maritimes 20: 85–112.

-M-

MacKenzie, K. M. et al. 2011. Locations of marine animals revealed by carbon isotopes. - Scientific Reports 1: srep00021.

Mahaut, M.-L. et al. 1995. Weight-dependent respiration rates in deep-sea organisms. - Deep Sea Research Part I: Oceanographic Research Papers 42: 1575–1582.

Maire, E. et al. 2015. How many dimensions are needed to accurately assess functional diversity? A pragmatic approach for assessing the quality of functional spaces. - Global Ecology and Biogeography 24: 728–740.

Marín Leal, J. C. et al. 2008. Stable isotopes (δ13C, δ15N) and modelling as tools to estimate the trophic ecology of cultivated oysters in two contrasting environments. - Mar Biol 153: 673–688.

Marinelli, R. L. and Williams, T. J. 2003. Evidence for density-dependent effects of infauna on sediment biogeochemistry and benthic–pelagic coupling in nearshore systems. - Estuarine, Coastal and Shelf Science 57: 179–192.

Martin, S. et al. 2006. Respiration, calcification, and excretion of the invasive slipper limpet, *Crepidula fornicata* L.: Implications for carbon, carbonate, and nitrogen fluxes in affected areas. - Limnol. Oceanogr. 51: 1996–2007.

Mason, N. W. H. et al. 2003. An index of functional diversity. - Journal of Vegetation Science 14: 571–578.

Matthew, M. W. et al. 2000. Status of atmospheric correction using a MODTRAN4-based algorithm. 4049: 199–207.

Maxwell, E. L. et al. 1982. Remote sensing as a biomass and insolation assessment tool.: 67.

McCutchan, J. H. et al. 2003. Variation in trophic shift for stable isotope ratios of carbon, nitrogen, and sulfur. - Oikos 102: 378–390.

McGarigal, K. et al. 2012. FRAGSTATS v4: Spatial pattern analysis program for categorical and continuous maps.

Méléder, V. et al. 2003. Cartographie des peuplements du microphytobenthos par télédétection spatiale visible-infrarouge dans un écosystème conchylicole. - Comptes Rendus Biologies 326: 377–389.

Menge, B. A. and Olson, A. M. 1990. Role of scale and environmental factors in regulation of community structure. - Trends in Ecology & Evolution 5: 52–57.

Mermillod-Blondin, F. et al. 2005. Biodiversity of benthic invertebrates and organic matter processing in shallow marine sediments: an experimental study. - Journal of Experimental Marine Biology and Ecology 315: 187–209.

Michaud, E. et al. 2005. The functional group approach to bioturbation: The effects of biodiffusers and gallery-diffusers of the *Macoma balthica* community on sediment oxygen uptake. - Journal of Experimental Marine Biology and Ecology 326: 77–88.

Michaud, E. et al. 2006. The functional group approach to bioturbation: II. The effects of the *Macoma balthica* community on fluxes of nutrients and dissolved organic carbon across the sediment–water interface. - Journal of Experimental Marine Biology and Ecology 337: 178–189.

Middelburg, J. J. et al. 2000. The fate of intertidal microphytobenthos carbon: An in situ 13C-labeling study. - Limnol. Oceanogr. 45: 1224–1234.

Mokany, K. et al. 2008. Functional identity is more important than diversity in influencing ecosystem processes in a temperate native grassland. - Journal of Ecology 96: 884–893.

Mortillaro, J. M. et al. 2014. Comparative study of isotopic trends in two coastal ecosystems of North Biscay: A multitrophic spatial gradient approach. - Estuarine, Coastal and Shelf Science 136: 149–156.

Mouchet, M. A. et al. 2010. Functional diversity measures: an overview of their redundancy and their ability to discriminate community assembly rules. - Functional Ecology 24: 867–876.

Mouillot, D. et al. 2005. Functional regularity: a neglected aspect of functional diversity. - Oecologia 142: 353–359.

Mouillot, D. et al. 2011. Functional structure of biological communities predicts ecosystem multifunctionality. - PloS one 6: e17476.

Mouillot, D. et al. 2013a. A functional approach reveals community responses to disturbances. - Trends in Ecology & Evolution 28: 167–177.

Mouillot, D. et al. 2013b. Rare species support vulnerable functions in high-diversity ecosystems. - PLOS Biology 11: e1001569.

Mouillot, D. et al. 2014. Functional over-redundancy and high functional vulnerability in global fish faunas on tropical reefs. - PNAS 111: 13757–13762.

Muir, A. P. et al. 2016. Lipid remodelling in the reef-building honeycomb worm, *Sabellaria alveolata*, reflects acclimation and local adaptation to temperature. - Scientific Reports 6: 35669

-N-

Naiman, R. J. 1988. Animal influences on ecosystem dynamics. - BioScience 38: 750–752.

Nature 2017. Why function is catching on in conservation. - Nature News 546: 7.

Navarro, J. M. and Thompson, R. J. 1997. Biodeposition by the horse mussel Modiolus modiolus (Dillwyn) during the spring diatom bloom. - Journal of Experimental Marine Biology and Ecology 209: 1–13.

Navarro-Barranco, C. et al. 2013. Feeding habits of amphipods (crustacea: malacostraca) from shallow soft bottom communities: comparison between marine caves and open habitats. - Journal of Sea Research 78: 1–7.

Neutel, A.-M. et al. 2007. Reconciling complexity with stability in naturally assembling food webs. - Nature 449: 599–602.

Newell, R. I. E. et al. 2002. Influence of simulated bivalve biodeposition and microphytobenthos on sediment nitrogen dynamics: A laboratory study. - Limnol. Oceanogr. 47: 1367–1379.

Newsome, S. D. et al. 2007. A niche for isotopic ecology. - Frontiers in Ecology and the Environment 5: 429–436.

Newsome, S. D. et al. 2010. Using stable isotope biogeochemistry to study marine mammal ecology. - Marine Mammal Science 26: 509–572.

Noernberg, M. A. et al. 2010. Using airborne laser altimetry to estimate *Sabellaria alveolata* (Polychaeta: Sabellariidae) reefs volume in tidal flat environments. - Estuarine, Coastal and Shelf Science 90: 93–102.

Nordström, M. C. and Bonsdorff, E. 2017. Organic enrichment simplifies marine benthic food web structure. - Limnol. Oceanogr. 62: 2179–2188.

Nordström, M. C. et al. 2015. Food web heterogeneity and succession in created saltmarshes. - J Appl Ecol 52: 1343–1354.

Norling, P. and Kautsky, N. 2007. Structural and functional effects of *Mytilus edulis* on diversity of associated species and ecosystem functioning. - Marine Ecology Progress Series 351: 163–175.

-O-

Odling-Smee, F. J. et al. 2003. Niche construction: the neglected process in evolution.

Olff, H. et al. 2009. Parallel ecological networks in ecosystems. - Philosophical Transactions of the Royal Society B: Biological Sciences 364: 1755–1779.

Orvain, F. et al. 2012. Spatial and temporal interaction between sediment and microphytobenthos in a temperate estuarine macro-intertidal bay. - Marine Ecology Progress Series 458: 53–68.

-P-

Paganelli, D. et al. 2012. Functional structure of marine benthic assemblages using Biological Traits Analysis (BTA): A study along the Emilia-Romagna coastline (Italy, North-West Adriatic Sea). - Estuarine, Coastal and Shelf Science 96: 245–256.

Paine, R. T. 1966. Food web complexity and species diversity. - The American Naturalist 100: 65–75.

Paine, R. T. 1969. A note on trophic complexity and community stability. - The American Naturalist 103: 91–93.

Pan, Y. et al. 2011. A large and persistent carbon sink in the world's forests. - Science 333: 988–993.

Parnell, A. C. et al. 2010. Source partitioning using stable isotopes: coping with too much variation. - PLOS ONE 5: e9672.

Parnell, A. C. et al. 2013. Bayesian stable isotope mixing models. - Environmetrics 24: 387–399.

Pawlik, J. R. 1988a. Larval settlement and metamorphosis of sabellariid polychaetes, with special reference to Phragmatopoma lapidosa, a reef-building species, and Sabellaria floridensis, a non-gregarious species. - Bulletin of Marine Science 43: 41–60.

Pawlik, J. R. 1988b. Larval settlement and metamorphosis of two gregarious sabellariid polychaetes: *Sabellaria alveolata* compared with *Phragmatopoma californica*. - Journal of the Marine Biological Association of the United Kingdom 68: 101–124.

Pearson, T. H. and Rosenberg, R. 1978. Macrobenthic succession in relation to organic enrichment and pollution of the marine environment. - Oceanography and Marine Biology: An Annual Review 16: 229–311.

Petchey, O. L. and Gaston, K. J. 2002. Functional diversity (FD), species richness and community composition. - Ecology Letters 5: 402–411.

Petchey, O. L. and Gaston, K. J. 2006. Functional diversity: back to basics and looking forward. - Ecology Letters 9: 741–758.

Peterson, B. J. and Fry, B. 1987. Stable isotopes in ecosystem studies. - Annual Review of Ecology and Systematics 18: 293–320.

Phillips, D. L. 2001. Mixing models in analyses of diet using multiple stable isotopes: a critique. - Oecologia 127: 166–170.

Phillips, D. L. 2012. Converting isotope values to diet composition: the use of mixing models. - Journal of Mammalogy 93: 342–352.

Pittman, S. J. et al. 2004. Linking fish and prawns to their environment: a hierarchical landscape approach. - Mar Ecol Prog Ser 283: 233–254.

Plicanti, A. et al. 2016. Human impacts on biogenic habitats: Effects of experimental trampling on *Sabellaria alveolata* (Linnaeus, 1767) reefs. - Journal of Experimental Marine Biology and Ecology 478: 34–44.

Polis, G. A. et al. 1997. Toward an integration of landscape and food web ecology: the dynamics of spatially subsidized food webs. - Annual Review of Ecology and Systematics 28: 289–316.

Porta, B. L. and Nicoletti, L. 2009. *Sabellaria alveolata* (Linnaeus) reefs in the central Tyrrhenian Sea (Italy) and associated polychaete fauna. - Zoosymposia 2: 527–536.

Post, D. M. 2002. Using stable isotopes to estimate trophic position: models, methods, and assumptions. - Ecology 83: 703–718.

Prado, P. et al. 2014. Influence of salinity regime on the food-web structure and feeding ecology of fish species from Mediterranean coastal lagoons. - Estuarine, Coastal and Shelf Science 139: 1–10.

-Q-

Queirós, A. M. et al. 2013. A bioturbation classification of European marine infaunal invertebrates. - Ecol Evol 3: 3958–3985.

Quillien, N. et al. 2016. Opportunistic basal resource simplifies food web structure and functioning of a highly dynamic marine environment. - Journal of Experimental Marine Biology and Ecology 477: 92–102.

-R-

R Core Team 2016. R: A Language and Environment for Statistical Computing. - R Foundation for Statistical Computing.

Rascher, K. G. et al. 2012. Community scale 15N isoscapes: tracing the spatial impact of an exotic N2-fixing invader. - Ecology Letters 15: 484–491.

Reise, K. 2002. Sediment mediated species interactions in coastal waters. - Journal of Sea Research 48: 127–141.

Revsbech, N. P. 1989. An oxygen microsensor with a guard cathode. - Limnol. Oceanogr. 34: 474–478.

Richoux, N. B. and Froneman, P. W. 2007. Assessment of spatial variation in carbon utilization by benthic and pelagic invertebrates in a temperate South African estuary using stable isotope signatures. - Estuarine, Coastal and Shelf Science 71: 545–558.

Ricklefs, R. E. 1984. Ecology, Second Edition.

Riemann, J. C. et al. 2017. Functional diversity in a fragmented landscape — Habitat alterations affect functional trait composition of frog assemblages in Madagascar. - Global Ecology and Conservation 10: 173–183.

Riera, P. 2007. Trophic subsidies of *Crassostrea gigas*, *Mytilus edulis* and *Crepidula fornicata* in the Bay of Mont Saint Michel (France): A δ13C and δ15N investigation. - Estuarine, Coastal and Shelf Science 72: 33–41.

Rigolet, C. et al. 2014a. Food web structures of subtidal benthic muddy habitats: evidence of microphytobenthos contribution supported by an engineer species. - Marine Ecology Progress Series 500: 25–41.

Rigolet, C. et al. 2014b. Benthic control freaks: Effects of the tubiculous amphipod *Haploops nirae* on the specific diversity and functional structure of benthic communities. - Journal of Sea Research 85: 413–427.

Rigolet, C. et al. 2015. Investigating isotopic functional indices to reveal changes in the structure and functioning of benthic communities. - Functional Ecology 29: 1350–1360.

Robert, K. et al. 2014. Megafaunal distribution and biodiversity in a heterogeneous landscape: the iceberg-scoured Rockall Bank, NE Atlantic. - Marine Ecology Progress Series 501: 67–88.

Rockström, J. et al. 2009. A safe operating space for humanity. - Nature 461: 472–475.

Rogerson, P. A. 2001. Statistical methods for geography. - Sage.

Rollet, C. et al. 2015. Suivi de l'état de conservation des récifs d'hermelles (*Sabellaria alveolata*).: 58.

Rooney, N. et al. 2008. A landscape theory for food web architecture. - Ecol. Lett. 11: 867–881.

Ropert, M. and Goulletquer, P. 2000. Comparative physiological energetics of two suspension feeders: polychaete annelid *Lanice conchilega* (Pallas 1766) and Pacific cupped oyster *Crassostrea gigas* (Thunberg 1795). - Aquaculture 181: 171–189.

Rossi, F. et al. 2004. Interspecific and intraspecific variation of δC and δN in deposit- and suspension-feeding bivalves (*Macoma balthica* and *Cerastoderma edule*): Evidence of ontogenetic changes in feeding mode of *Macoma balthica*. - Limnol. Oceanogr. 49: 408–414.

Rouse, J. W. et al. 1974. Monitoring the vernal advancement and retrogradation (green wave effect) of natural vegetation.: 93.

-S-

Sagouis, A. et al. 2015. Non-native species modify the isotopic structure of freshwater fish communities across the globe. - Ecography 38: 979–985.

Sala, O. E. et al. 2000. Global biodiversity scenarios for the year 2100. - Science 287: 1770–1774.

Salomon, J. P. 2000. Etude d'impact de la restructuration conchylicole en baie du Mont-Saint-Michel. Etude courantologique et sédimentologique.

Salomon, J.-C. and Breton, M. 2000. Mathematical model of mont saint michel bay.: 65.

Sanders, D. et al. 2014. Integrating ecosystem engineering and food webs. - Oikos 123: 513–524.

Sauriau, P.-G. and Kang, C.-K. 2000. Stable isotope evidence of benthic microalgae-based growth and secondary production in the suspension feeder Cerastoderma edule (Mollusca, Bivalvia) in the Marennes-Oléron Bay. - Hydrobiologia 440: 317–329.

Schlund, E. et al. 2016. Macrofauna associated with temporary *Sabellaria alveolata* reefs on the west coast of Cotentin (France). - SpringerPlus 5: 1260.

Schulze, E.-D. and Mooney, H. A. 1994. Ecosystem function of biodiversity: a summary. - In: Biodiversity and ecosystem function. Springer, pp. 497–510.

Secula, C. 2011. Acteurs et gestion du littoral. Une anthropologie de la baie du Mont-Saint-Michel.

Shumway, S. E. 1979. The effects of body size, oxygen tension and mode of life on the oxygen uptake rates of polychaetes. - Comparative Biochemistry and Physiology Part A: Physiology 64: 273–278.

Shumway, S. E. et al. 1985. Particle selection, ingestion, and absorption in filter-feeding bivalves. - Journal of Experimental Marine Biology and Ecology 91: 77–92.

Skalski, J. R. et al. 2005. Analysis of population indices. - In: Wildlife demography: analysis of sex, age, and count data. Academic Press, pp. 359–434.

Smyth, A. R. et al. 2015. Habitat context influences nitrogen removal by restored oyster reefs. - J Appl Ecol 52: 716–725.

Smyth, A. R. et al. 2016. Biological activity exceeds biogenic structure in influencing sediment nitrogen cycling in experimental oyster reefs. - Marine Ecology Progress Series 560: 173–183.

Snelgrove, P. V. R. et al. 2014. Real world biodiversity–ecosystem functioning: a seafloor perspective. - Trends in Ecology & Evolution 29: 398–405.

Solan, M. et al. 2004. Extinction and ecosystem function in the marine benthos. - Science 306: 1177–1180.

Solórzano, L. 1969. Determination of ammonia in natural waters by the phenolhypochlorite method. - Limnol. Oceanogr. 14: 799–801.

Stachowicz, J. J. 2001. Mutualism, facilitation, and the structure of ecological communities positive interactions play a critical, but underappreciated, role in ecological communities by reducing physical or biotic stresses in existing habitats and by creating new habitats on which many species depend. - BioScience 51: 235–246.

Stallins, J. A. 2006. Geomorphology and ecology: Unifying themes for complex systems in biogeomorphology. - Geomorphology 77: 207–216.

Stief, P. 2013. Stimulation of microbial nitrogen cycling in aquatic ecosystems by benthic macrofauna: mechanisms and environmental implications. - Biogeosciences 10: 7829–7846.

Stokes, M. D. et al. 2011. Temperature variability and algal isotopic heterogeneity on a Floridian coral reef. - Marine Ecology 32: 364–379.

Streitberger, M. et al. 2017. Contrasting response of vascular plant and bryophyte species assemblages to a soil-disturbing ecosystem engineer in calcareous grasslands. - Ecological Engineering 99: 391–399.

Suykerbuyk, W. et al. 2012. Suppressing antagonistic bioengineering feedbacks doubles restoration success. - Ecol Appl 22: 1224–1231.

-T-

Tansley, A. G. 1968. Britain's green mantle: Past, present and future. - Allen & Unwin.

Thayer, C. W. 1979. Biological bulldozers and the evolution of marine benthic communities. - Science 203: 458–461.

Thrush, S. F. et al. 2006. Functional role of large organisms in intertidal communities: community effects and ecosystem function. - Ecosystems 9: 1029–1040.

Thrush, S. F. et al. 2017. Changes in the location of biodiversity–ecosystem function hot spots across the seafloor landscape with increasing sediment nutrient loading. - Proc. R. Soc. B 284: 20162861.

Tilman, D. 1997. Community invasibility, recruitment limitation, and grassland biodiversity. - Ecology 78: 81–92.

Tilman, D. 2001. Functional diversity. - In: Levin, S. A. (ed), Encyclopedia of Biodiversity. Elsevier, pp. 109–120.

Tilman, D. and Downing, J. A. 1994. Biodiversity and stability in grasslands. - Nature 367: 363–365.

Tilman, D. et al. 1997. The influence of functional diversity and composition on ecosystem processes. - Science 277: 1300–1302.

Tilman, D. et al. 2014. Biodiversity and Ecosystem Functioning. - Annual Review of Ecology, Evolution, and Systematics 45: 471–493.

Tréguer, P. and Le Corre, P. 1975. Manuel d'analyse des sels nutritifs dans l'eau de mer. - Université de Bretagne Occidentale.

-U-

Ubertini, M. et al. 2012. Spatial variability of benthic-pelagic coupling in an estuary ecosystem: consequences for microphytobenthos resuspension phenomenon. - PLOS ONE 7: e44155.

Ubertini, M. et al. 2015. Impact of sediment grain-size and biofilm age on epipelic microphytobenthos resuspension. - Journal of Experimental Marine Biology and Ecology 467: 52–64.

Underwood, G. J. C. and Kromkamp, J. 1999. Primary production by phytoplankton and microphytobenthos in estuaries. - In: Advances in ecological research. Estuaries. Academic Press. D.B. Nedwell and D.G. Raffaelli, pp. 93–139.

-V-

van Broekhoven, W. et al. 2014. Nutrient regeneration by mussel *Mytilus edulis* spat assemblages in a macrotidal system. - Journal of Sea Research 88: 36–46.

van Broekhoven, W. et al. 2015. Nutrient regeneration from feces and pseudofeces of mussel *Mytilus edulis* spat. - Marine Ecology Progress Series 534: 107–120.

van de Koppel, J. et al. 2012. The influence of local- and landscape-scale processes on spatial self-organization in estuarine ecosystems. - Journal of Experimental Biology 215: 962–967.

van der Heide, T. et al. 2014. Predation and habitat modification synergistically interact to control bivalve recruitment on intertidal mudflats. - Biological Conservation 172: 163–169.

van der Linden, P. et al. 2016. The performance of trait-based indices in an estuarine environment. - Ecological Indicators 61: 378–389.

van der Zee, E. M. et al. 2016. How habitat-modifying organisms structure the food web of two coastal ecosystems. - Proc. R. Soc. B 283: 20152326.

Vander Zanden, M. J. and Rasmussen, J. B. 2001. Variation in δ15N and δ13C trophic fractionation: Implications for aquatic food web studies. - Limnol. Oceanogr. 46: 2061–2066.

Vanderklift, M. A. and Ponsard, S. 2003. Sources of variation in consumer-diet δ15N enrichment: a meta-analysis. - Oecologia 136: 169–182.

Villéger, S. et al. 2008. New multidimensional functional diversity indices for a multifaceted framework in functional ecology. - Ecology 89: 2290–2301.

Villéger, S. et al. 2010. Contrasting changes in taxonomic vs. functional diversity of tropical fish communities after habitat degradation. - Ecological Applications 20: 1512–1522.

Villéger, S. et al. 2013. Decomposing functional β-diversity reveals that low functional β-diversity is driven by low functional turnover in European fish assemblages. - Global Ecology and Biogeography 22: 671–681.

Villnäs, A. et al. 2011. Structural and functional shifts in zoobenthos induced by organic enrichment — Implications for community recovery potential. - Journal of Sea Research 65: 8–18.

Vizzini, S. and Mazzola, A. 2006. Sources and transfer of organic matter in food webs of a Mediterranean coastal environment: Evidence for spatial variability. - Estuarine, Coastal and Shelf Science 66: 459–467.

Volkenborn, N. et al. 2009. Sediment destabilizing and stabilizing bio-engineers on tidal flats: Cascading effects of experimental exclusion. - Helgoland Marine Research 63: 27–35.

-W -

Waldbusser, G. G. et al. 2004. The effects of infaunal biodiversity on biogeochemistry of coastal marine sediments. - Limnol. Oceanogr. 49: 1482–1492.

Wang, X. et al. 2014. Measuring habitat fragmentation: An evaluation of landscape pattern metrics. - Methods Ecol Evol 5: 634–646.

Wang, S. et al. 2015. Trophic dynamics of filter feeding bivalves in the yangtze estuarine intertidal marsh: stable isotope and fatty acid analyses. - PLOS ONE 10: e0135604.

Watson, G. J. et al. 2017. Assessing the impacts of bait collection on inter-tidal sediment and the associated macrofaunal and bird communities: The importance of appropriate spatial scales. - Marine Environmental Research in press.

Welsh, D. T. and Castadelli, G. 2004. Bacterial nitrification activity directly associated with isolated benthic marine animals. - Marine Biology 144: 1029–1037.

West, J. B. et al. 2009. Isoscapes: understanding movement, pattern, and process on Earth through isotope mapping. - Springer Science & Business Media.

Wilson, D. P. 1974. Sabellaria colonies at Duckpool, North Cornwall, 1971–1972, with a note for May 1973. - Journal of the Marine Biological Association of the United Kingdom 54: 393–436.

Wright, J. P. and Jones, C. G. 2006. The concept of organisms as ecosystem engineers ten years on: progress, limitations, and challenges. - BioScience 56: 203–209.

Wright, J. P. et al. 2002. An ecosystem engineer, the beaver, increases species richness at the landscape scale. - Oecologia 132: 96–101.

Wright, J. P. et al. 2004. Patch dynamics in a landscape modified by ecosystem engineers. - Oikos 105: 336–348.

Wright, J. P. et al. 2006. Predictability of ecosystem engineering effects on species richness across environmental variability and spatial scales. - Journal of Ecology 94: 815–824.

-Y-

Yallop, M. L. et al. 2000. Interrelationships between rates of microbial production, exopolymer production, microbial biomass, and sediment stability in biofilms of intertidal sediments. - Microb Ecol 39: 116–127.

Effect of an engineer species on the diversity and functioning of benthic communities: the *Sabellaria alveolata* reef habitat

Abstract:

Coastal zones worldwide are home to a large diversity of ecosystem engineers that perform key functions such as the recycling of organic matter and nutrients. The habitats resulting from the biological activity of these species are exposed to numerous disturbances such as over harvesting and trampling or via coastal modification. In this context, it is becoming key to understand the functioning of these engineered habitats and how they are affected by increasing disturbances. During my PhD, I used the reef habitat built by the gregarious tubiculous polychaete *Sabellaria alveolata* as a study case. First, the environmental and biotic changes associated with the establishment of a *S. alveolata* reef and its increasing disturbance were assessed, focusing on sediment characteristics (*e.g.* grain-size distribution, organic matter content) along with taxonomic diversity and species assemblage. In the same vain, the third article looks into the trophic functioning of the reef community and a control community to understand the effects of the establishment of the engineer species on carbon transfers, successively looking at the whole consumer community, the primary consumers and the importance of autochthonous (microphytobenthos and *Ulva* sp.) vs allochthone (phytoplankton) food sources. In this part, I used carbon and nitrogen stable isotopes and different analytical approaches such as isotopic niche metrics and mixing models. Article 2 aims towards understanding the interactions between reef habitat complexity, autochthonous food source heterogeneity and spatial scales in explaining the carbon isotopic ratio variations of *S. alveolata* and an associated suspension-feeder. In the last two chapters, I address the functioning of the engineered habitat either directly, using benthic core incubations to measure biogeochemical fluxes (*e.g.* oxygen demand) or indirectly, through the use of integrative functional and isotopic diversity indices. This last part reveals the existence of an optimum value of *S. alveolata* density, used as a disturbance proxy, where the trophic niche and the biogeochemical functioning of the reef are both maximal.

Key words: Ecosystem engineer – reef habitat – benthic macrofauna – functional and isotopic diversity – facilitation – benthic primary production – food web – biogeochemical fluxes – isoscape – biological traits

Effet d'une espèce ingénieur sur la diversité et le fonctionnement des communautés benthiques : l'habitat récifal à *Sabellaria alveolata*

Résumé :

A travers le monde, les zones côtières abritent une grande diversité d'ingénieurs de l'écosystème accomplissant des fonctions clés comme le recyclage de la matière organique et des nutriments. Les habitats résultants de l'activité biologique de ces espèces sont exposés à de nombreuses perturbations comme la surpêche, le piétinement ou via l'aménagement des côtes. Dans ce contexte, il est urgent de comprendre le fonctionnement de ces habitats ingénieurés et comment ils sont affectés par des perturbations croissantes. Pendant ma thèse, j'ai utilisé l'habitat récifal construit par le polychète grégaire tubicole *Sabellaria alveolata* comme cas d'étude. Tout d'abord, les changements environnementaux et biotiques associés à la mise en place d'un récif à *S. alveolata* et à sa perturbation croissante ont été évalué, se concentrant sur les paramètres du sédiment (*e.g.* granulométrie, contenu en matière organique) ainsi que la diversité taxonomique et les assemblages d'espèces. De manière similaire, le troisième article se penche sur le fonctionnement trophique de la communauté récifale et d'une communauté contrôle afin de comprendre les effets de la mise en place de l'espèce ingénieur sur les transferts de carbone, s'intéressant successivement à l'ensemble de la communauté des consommateurs, aux consommateurs primaires et à l'importance des sources de nourriture autochtones (microphytobenthos et *Ulva* sp.) vs allochtone (phytoplancton). Dans cette partie, j'ai utilisé les isotopes stables du carbone et de l'azote ainsi que différentes approches analytiques telles que des mesures de la niche isotopique et des modèles de mélange. L'article 2 a pour but de comprendre les interactions entre complexité de l'habitat récifal, hétérogénéité des sources de nourriture autochtones et échelles spatiales dans l'explication des variations du rapport isotopique du carbone de *S. alveolata* et d'un suspensivore associée. Dans les deux derniers chapitres, j'ai traité la question du fonctionnement de l'habitat ingénieuré de manière directe, en utilisant des incubations de carottes benthiques pour mesurer des flux biogéochimiques (*e.g.* demande en oxygène), ou indirecte, en utilisant des indices de diversité fonctionnelle et isotopique intégratifs. Cette dernière partie révèle l'existence d'un optimum de densité de *S. alveolata*, utilisée comme proxy des perturbations, où la niche trophique et le fonctionnement biogéochimique du récif sont tous les deux maximaux.

Mots-clés : Ingénieur de l'écosystème – habitat récifal – macrofaune benthique – diversité fonctionnelle et isotopique – facilitation – production primaire benthique – réseau trophique – flux biogéochimiques – isoscape – traits biologiques